**SANDIA REPORT**
SAND2017-4042
Unlimited Release
Printed April 2017

# Catalog of Window Taper Functions for Sidelobe Control

Armin W. Doerry

Prepared by
Sandia National Laboratories
Albuquerque, New Mexico 87185 and Livermore, California 94550

Sandia National Laboratories is a multi-program laboratory managed and operated by Sandia Corporation, a wholly owned subsidiary of Lockheed Martin Corporation, for the U.S. Department of Energy's National Nuclear Security Administration under contract DE-AC04-94AL85000.



Issued by Sandia National Laboratories, operated for the United States Department of Energy by Sandia Corporation.



Available to DOE and DOE contractors from

U.S. Department of Energy
Office of Scientific and Technical Information
P.O. Box 62
Oak Ridge, TN 37831

Telephone: (865) 576-8401
Facsimile: (865) 576-5728
E-Mail: reports@adonis.osti.gov
Online ordering: http://www.osti.gov/bridge

Available to the public from

U.S. Department of Commerce
National Technical Information Service
5285 Port Royal Rd.
Springfield, VA 22161

Telephone: (800) 553-6847
Facsimile: (703) 605-6900
E-Mail: orders@ntis.fedworld.gov
Online order: http://www.ntis.gov/help/ordermethods.asp?loc=7-4-0#online

SAND2017-4042
Unlimited Release
Printed April 2017

# Catalog of Window Taper Functions for Sidelobe Control

Armin W. Doerry
ISR Mission Engineering
Sandia National Laboratories
PO Box 5800
Albuquerque, NM 87185-0519

## Abstract

Window taper functions of finite apertures are well-known to control undesirable sidelobes, albeit with performance trades. A plethora of various taper functions have been developed over the years to achieve various optimizations. We herein catalog a number of window functions, and compare principal characteristics.

# Acknowledgements

This report was the result of an unfunded research and development activity.

Sandia National Laboratories is a multi-program laboratory managed and operated by Sandia Corporation, a wholly owned subsidiary of Lockheed Martin Corporation, for the U.S. Department of Energy's National Nuclear Security Administration under contract DE-AC04-94AL85000.

# Contents

*"It is a capital mistake to theorize before one has data."*
*-- Arthur Conan Doyle*

# Foreword

This report details the results of an academic study. It does not presently exemplify any modes, methodologies, or techniques employed by any operational system known to the author.

## Classification

The specific mathematics and algorithms presented herein do not bear any release restrictions or distribution limitations.

This report formalizes preexisting informal notes and other documentation on the subject matter herein.

# 1 Introduction

Fourier Transform relationships abound in endeavors dealing with signals where one domain is bounded by a finite aperture, and analysis needs to be examined in the other domain. Such endeavors include antenna beam analysis/design, radar and communication systems, optics and optical processing, data interpolation, spectral analysis, and general data analysis/processing.

In such systems, finite apertures inescapably cause the generation of undesirable sidelobes, or ringing, in the other domain. Sidelobes, however, may be reduced and/or somewhat controlled by the employment of window taper functions across the finite aperture, albeit at the expense of other signal degradations.

Finding or determining an optimum window taper function for some purpose has been the subject of much research over the years. Parzen[1] states that "The present period of research may be said to have commenced about 1945, when Bartlett[2] and Daniell pointed out that the periodogram needs to be smoothed if it is to form a consistent estimate of the spectral density." Today, many specific functions and function families exist as a result, and new ones periodically appear.

In various disciplines, a window taper function may go by other names, including any of the following.

Window, Window function,
Taper, Tapering function,
Shading,
Weight function,
Smoothing function, smoothing kernel,
Averaging kernel,
Apodization function,
Beamshaping, Beamshaping functions.

There are no doubt others. We will make use of several of these terms interchangeably.

Principal general references for this report include

A report by Harris detailing characteristics of a number of window taper functions.[3] Harris also wrote a paper on substantially the same analysis, albeit with additions.[4]

A text by Prabhu also details a number of different window taper functions.[5]

A paper by Anterrieu, et al., discusses a number of window functions for Synthetic Aperture Imaging Radiometers.[6]

We also suggest an excellent treatment of window functions is given in a pair of papers by Blackman and Tukey.[7,8] These were later collected into a book by Blackman and Tukey.[9] Blackman extended this work in a subsequent book.[10]

As previously stated, the literature on window functions is fairly extensive, which begs the question "Why does the world need yet another report on this topic?"

We offer as answer the observation that extensive catalogs of window functions are in fact somewhat sparse. As a consequence, this report attempts to be somewhat broader in scope than previous publications. We have furthermore attempted to place the various window taper functions discussed in this report into a common format, so that they may be easier to compare. We also suggest that the references may be of some value in cataloging original source material.

Finally, we have attempted to keep the discussion on a somewhat practical level, to facilitate ready employment by system analysts, designers, and engineers.

# 2 Background

## 2.1 Some Definitions

To set up the following discussion, we begin by defining a generic signal

$$x(t) \quad = \text{continuous function of time } t. \tag{1}$$

As we will be interested in the Fourier Transform of functions, we accordingly define

$$\begin{aligned} X(f) &= \int_{-\infty}^{\infty} x(t) e^{-j2\pi ft} dt \quad = \text{forward transform, and} \\ x(t) &= \int_{-\infty}^{\infty} X(f) e^{j2\pi ft} df \quad = \text{inverse transform,} \end{aligned} \tag{2}$$

where the Fourier Transform is in terms of frequency $f$. We may use shorthand to identify the transform pair as

$$x(t) \Leftrightarrow X(f). \tag{3}$$

While we have identified the Fourier Transform and its inverse in terms of time/frequency, we might just as easily have used other constructs, such as perhaps

frequency/time
space/wavenumber
wavenumber/space
current density / far-field pattern (for antennas)

We note that in radar signal processing, specifically Synthetic Aperture Radar image formation, we generally collect raw wavenumber data and therefrom calculate spatial information.

There are a multitude of variations for defining the forward and inverse transforms as well. Nevertheless, we will hereafter discuss in terms of time/frequency and use the definitions of Eq. (2). We further identify several particularly useful functions as follows.

The rectangle function is defined as

$$\text{rect}(z) = \begin{cases} 1 & |z| < 1/2 \\ 1/2 & |z| = 1/2 \\ 0 & |z| > 1/2 \end{cases}. \tag{4}$$

The particular value at $z = 1/2$ doesn't particularly matter for continuous-time calculations, but does lead to some subtleties for discrete-time systems.

We define the sinc function as

$$\text{sinc}(z) = \frac{\sin \pi z}{\pi z}. \tag{5}$$

We note that these constitute a transform pair, namely

$$\text{rect}(t) \Leftrightarrow \text{sinc}(f). \tag{6}$$

Hereafter we will also make use of a number of Fourier Transform properties and identities that can be found in any number of references.

## 2.2 The Need

Consider that we have knowledge of our time function over only a limited interval. Accordingly, the function segment available to us can then be described as the product of the complete function $x(t)$ and an observation interval, that is

$$x_a(t) = x(t)\,\text{rect}\left(\frac{t - t_0}{T}\right) \text{ = observed segment of the desired function,} \tag{7}$$

where Fourier Transform identities allow us to identify the Fourier Transform pair

$$\text{rect}\left(\frac{t - t_0}{T}\right) \Leftrightarrow T e^{-j2\pi t_0}\,\text{sinc}(Tf), \tag{8}$$

where we will employ the parameters

$$\begin{aligned} t_0 &= \text{center of observation interval, and} \\ T &= \text{length of the observation interval (presumed positive).} \end{aligned} \tag{9}$$

The observation interval in some fields is referred to as an "aperture." We will use this term herein as well. The "segment" is the portion of the function that falls within the aperture. We may then also identify the Fourier Transform pair

$$x_a(t) \Leftrightarrow X_a(f), \tag{10}$$

where we may relate the segment's Fourier Transform to the original function's Fourier Transform as

$$X_a(f) = X(f) * Te^{-j2\pi t_0} \operatorname{sinc}(Tf), \tag{11}$$

where "*" denotes convolution.

We observe that the spectrum of the segment is a smeared version of the spectrum of the original function, where the degree of smearing depends on the length of the observation interval, that is, the size of the aperture.

This smearing is actually a linear filtering of the spectrum, that is, a filtering in the spectral domain of the signal. Such smearing is sometimes referred to as "spectral leakage," or "frequency leakage."

***Example***

Consider as example the function where $x(t)$ is a constant modulus rotating vector, which we also refer to as a complex sinusoid,

$$x(t) = e^{j2\pi f_0 t}, \tag{12}$$

where

$$f_0 = \text{frequency of oscillation.} \tag{13}$$

We note that this function has spectrum

$$e^{j2\pi f_0 t} \Leftrightarrow \delta(f - f_0), \tag{14}$$

where

$$\delta(z) = \text{Dirac delta function.} \tag{15}$$

For our convenience, let the aperture be centered at zero with unit width, that is, the observed signal is

$$x_a(t) = x(t)\operatorname{rect}(t). \tag{16}$$

The observed signal's spectrum is then

$$X_a(f) = \delta(f - f_0) * \operatorname{sinc}(f) = \operatorname{sinc}(f - f_0), \tag{17}$$

Not only is the segment's spectrum smeared, but it is smeared over an infinite extent, albeit with diminishing effect away from its center.

In addition, the smearing comes in the form a main lobe with offset discrete "bumps" in the spectrum separated by nulls. These offset lobes are called "sidelobes" or "grating lobes." We also observe that the first sidelobes of the observed signal's spectrum are only 13 dB less than the mainlobe peak. Thereafter, sidelobes fall proportional at a $1/f$ rate. Figure 1 illustrates this example with $f_0 = -2$ Hz in a 1-second aperture.

***Example***

Now consider as example the function where $x(t)$ is the sum of two constant modulus rotating vectors

$$x(t) = A_0 e^{j2\pi f_0 t} + A_1 e^{j2\pi f_1 t}, \tag{18}$$

where

$f_0$ = frequency of oscillation of first vector,
$f_1$ = frequency of oscillation of second vector, $f_1 \neq f_0$,
$A_0$ = amplitude of first vector, and
$A_1$ = amplitude of second vector. (19)

With the same aperture as the previous example, the observed signal's spectrum then becomes

$$X_a(f) = A_0 \operatorname{sinc}(f - f_0) + A_1 \operatorname{sinc}(f - f_1). \tag{20}$$

Since this is a linear operation, superposition holds. That is, the spectrum of the sum of individual signals is the same as the sum of the spectrums of the individual signals.

What is important here is that if the two signal components have large disparate signal amplitudes, then the spectral contribution of the second lesser signal might be lost in the spectral sidelobes of the first, or dominant signal. This suggests that it would be useful to suppress sidelobes in cases when

1. Large dynamic ranges are expected, and

2. The signal spectrum is complex, with multiple or distributed frequency content.

Figure 2 illustrates this example with $f_0 = -2$ Hz, $f_0 = 3.5$ Hz, and $A_1$ less than $A_0$ by 30 dB, all in a 1-second aperture.

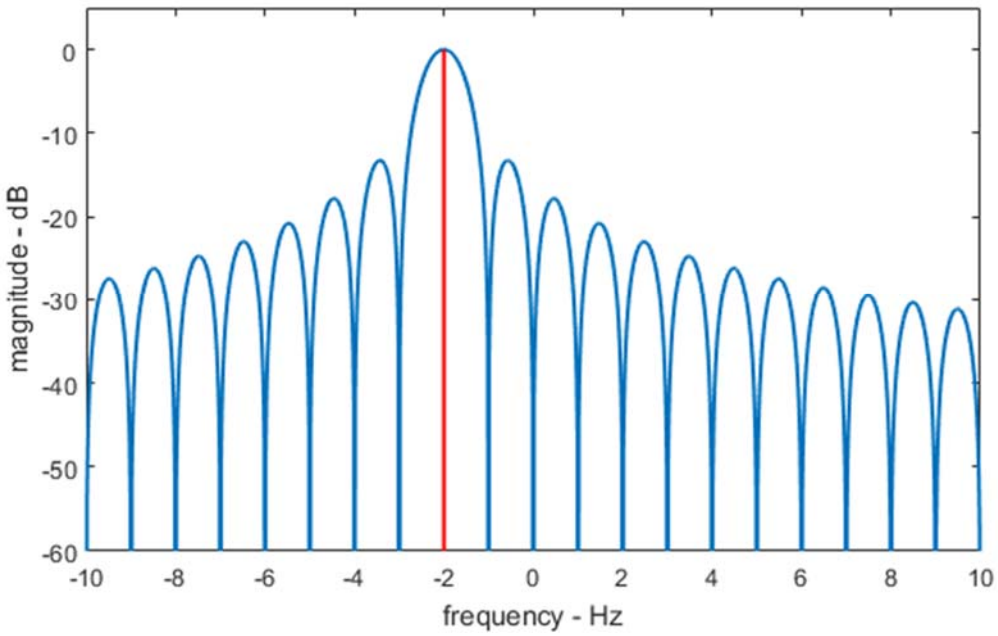


**Figure 1. The red plot denotes the location and amplitude of the original constant-frequency signal. The blue curve is the spectrum of the observed segment of the original signal. Note the generation of sidelobes due to the finite aperture employed to extract the observed signal segment.**

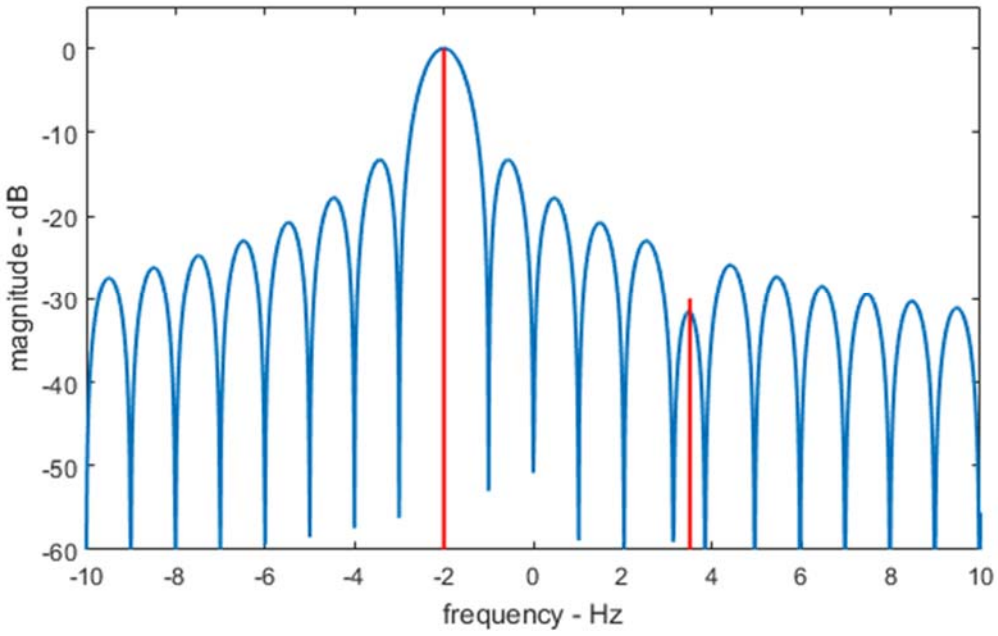


**Figure 2. The red plots denote the location and amplitude of the original sum of two constant-frequency signals. The blue curve is the spectrum of the observed segment of the composite original signal. Note how the lower-amplitude signal is buried in the sidelobe of the stronger signal.**

Note that in this example, the second signal is buried in the sidelobe of the first signal. While a perturbation of the sidelobe is observed that might seem to allow some degree of detection, we have thus far ignored noise and other data anomalies. The question then remains "Are any sidelobe perturbations due to noise, measurement errors, signal channel effects, or are they due to real signals?"

Therefore, it seems to become advantageous to employ signal processing techniques to lower sidelobes, even at the expense of other factors such as signal localization or resolution, i.e. mainlobe width.

## 2.3 Sidelobe Causes

It is a reasonable question to ask "What about a signal causes sidelobes?"

The short answer is "any sharp edges or data discontinuities." A longer answer is given with the following analysis.

We begin our analysis with a simple edge, namely a step function

$$x(t) = u(t) = \begin{cases} 0 & t < 0 \\ +1 & t \geq 0 \end{cases} = \text{ Heaviside unit step function.} \tag{21}$$

In this case, we identify the Fourier Transform pair

$$u(t) \Leftrightarrow \left[ \frac{\delta(f)}{2} + \frac{1}{j2\pi f} \right]. \tag{22}$$

From this we observe that spectral energy density exists out to $\pm\infty$, simply due to the edge itself. This is true even if we were to remove the DC bias, that is

$$\left[ u(t) - \frac{1}{2} \right] \Leftrightarrow \frac{1}{j2\pi f}. \tag{23}$$

This also means that to faithfully reproduce the sharp step, we need an infinite bandwidth of spectral information. Finite bandwidth will reduce the fidelity of the reproduced step. The reduced fidelity will manifest as ringing in the region of the intended discontinuity. This is the well-known Gibbs phenomenon. It in fact represents a sidelobe issue from a finite aperture in the other domain.

Now let us soften the edge by creating a more gradual transition than the abrupt step of the unit step function.

Before we proceed, it is useful to realize that

$$u(t) = \int_{-\infty}^{t} \delta(z)\,dz\,. \tag{24}$$

We create the gradual, or tapered, transition with the function

$$x(t) = \int_{-\infty}^{t} \frac{1}{\tau}\,\mathrm{rect}\left(\frac{z}{\tau}\right)dz\,. \tag{25}$$

This function transitions linearly from a value of 0 to a value of 1 over an interval of length $\tau$ centered at $t = 0$. The spectrum of this function can be calculated to be

$$X(f) = \left[\frac{\delta(f)}{2} + \frac{\mathrm{sinc}(\tau f)}{j2\pi f}\right]. \tag{26}$$

We immediately observe that Eq. (26) shows less spectral energy at higher frequencies than the spectrum indicated in Eq. (22). This is due to the additional frequency roll-off of the sinc function.

From this we learn

- A gradual transition means less high-frequency content to the spectrum.
- The more gradual the transition, the quicker is the frequency roll-off in the spectrum.
- We can only get rid of high-frequency content altogether if we have infinitely long transition regions.
- Finite transition regions guarantee infinite spectral widths, with generally non-zero spectral density out to infinity, nulls notwithstanding.
- With finite transition regions, the best we can do is to reduce high-frequency content, but never eliminate it entirely (except for discrete nulls).

We state without elaboration that other tapered transitional characteristics might have been chosen than indicated in Eq. (25), but would not have added substantively to the conclusions listed.

The bottom line is that more gradual transitions, or tapers, reduce high-frequency content, which manifests as reduced sidelobes away from the spectral feature of interest.

To repeat our assertion at the beginning of this section, the misplaced frequency content represented by sidelobes is caused by sharp edges or discontinuities in the data segment.

Of special concern to us are the discontinuities due to the edges of the aperture, even for an otherwise smooth signal.

A smooth signal, such as a sinusoid, with infinite aperture will not generally exhibit sidelobes. The moment an aperture becomes finite, sidelobes appear. The shorter the aperture, the farther in frequency higher sidelobes extend.

## 2.4 Window Tapers for the Aperture

In previous sections we have considered an aperture to the signal of interest to be a rectangular function as indicated in Eq. (7). We have noted that the abrupt edges of the signal segment from this aperture causes sidelobes that may interfere with detecting and/or characterizing signals buried within the sidelobes of larger nearby signals.

Here we now substitute the rect function in Eq. (7) with a more generic "window" function which we define as

$$w(z) = \text{window taper function,} \tag{27}$$

such that the observed signal segment is modified to

$$x_a(t) = x(t)\, w\left(\frac{t-t_0}{T}\right) = \text{observed segment of the desired signal function.} \tag{28}$$

In signal processing practice, we normally select an observation interval with a rect function, and then apply the window taper during signal analysis. In antenna pattern generation, however, the window taper is often built into the antenna electromechanical configuration. The antenna community generally calls these tapers "shading."

The window functions we shall consider with rare exception are stipulated to have the following convenient properties.

1. $w(z)$ is real, even, and positive.

2. $w(z)$ is of finite length, defined over the interval $[-1/2, 1/2]$, with

$$w(z) = w(z)\,\mathrm{rect}(z). \tag{29}$$

   We stipulate $w(z)$ is zero outside of the interval $[-1/2, 1/2]$.

3. $w(z)$ has unit DC gain. This means

$$\int_{-\infty}^{\infty} w(z)\,dz = 1. \tag{30}$$

This also means that if any part of $w(z)$, edges notwithstanding, is less than one, then $w(0) > 1$.

4. $w(z)$ is non-increasing with distance from its center. This means

$$w(z_1) \geq w(z_2) \text{ for } |z_1| < |z_2|. \tag{31}$$

Typically, $w(z)$ slopes towards zero away from its peak value at $w(0)$, but not necessarily at a constant rate. More often, they do so smoothly.

We caveat this discussion that the properties previously listed are typical of window taper functions employed in signal processing and other applications. However, we acknowledge that for special applications, or for special purposes, that nearly any of the properties might be violated.

Eq. (28) also implies that in the frequency domain, the segment has spectrum

$$X_a(f) = X(f) * Te^{-j2\pi t_0} W(Tf), \tag{32}$$

where the window taper function exhibits the transform pair

$$w(t) \Leftrightarrow W(f). \tag{33}$$

We observe that $W(f)$ is the spectrum of the window function $w(t)$. In radar signal processing, where the raw signal is typically frequency or wavenumber data, the spectral response of the window itself is often called the window's Impulse Response (IPR), or its Point Spread Function (PSF).

It is important to remember that window taper functions are essentially just linear filters in the frequency domain of the raw original signal. In fact, we may reap the sidelobe reduction effects of a window taper function by directly implementing the frequency-domain convolution of Eq. (32), although the infinite width of $W(f)$ would have to be dealt with, perhaps by truncation or cropping.

***Example***

The previous example that resulted in Figure 1 is repeated here, except that a window taper function is employed over the aperture of the original signal. The window taper function is plotted in Figure 3. The new spectral plot is given in Figure 4.

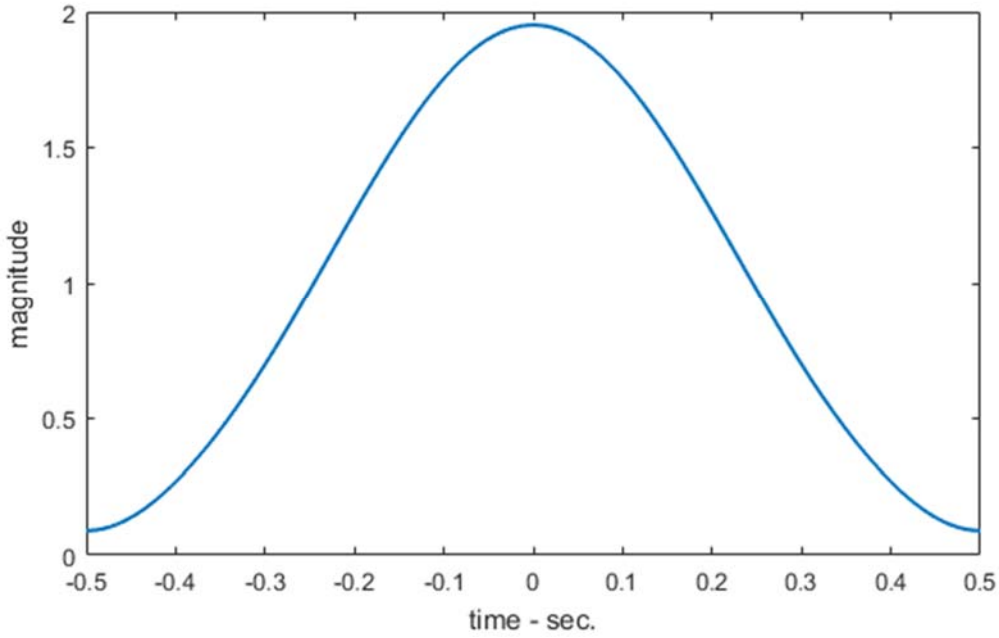


**Figure 3. The window taper function; specifically a –50 dB Taylor window (nbar=7).**

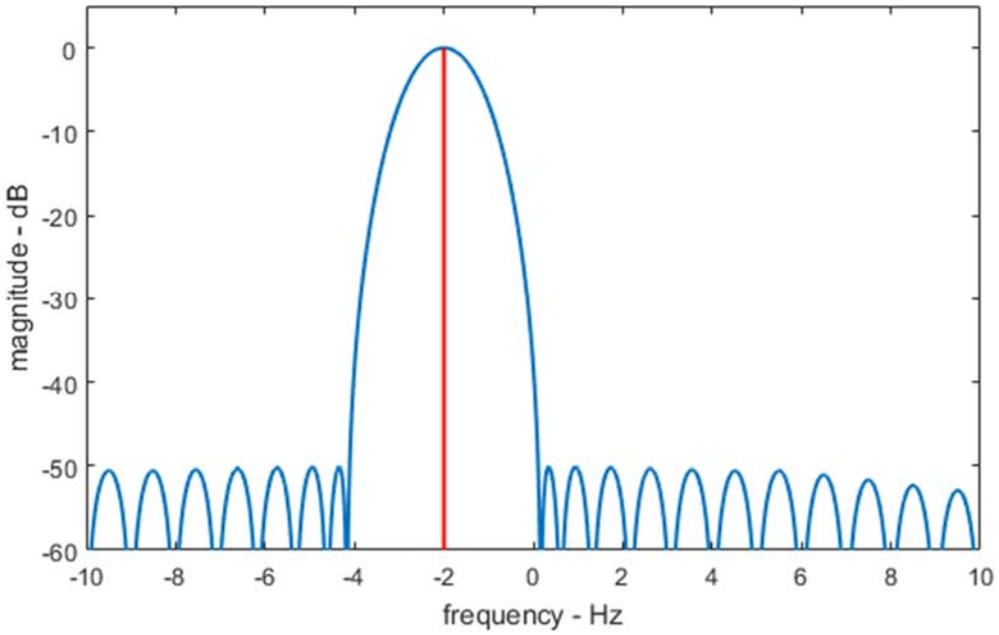


**Figure 4. Shown is the example of Figure 1, except that the segment has had applied a –50 dB Taylor window (nbar=7).**

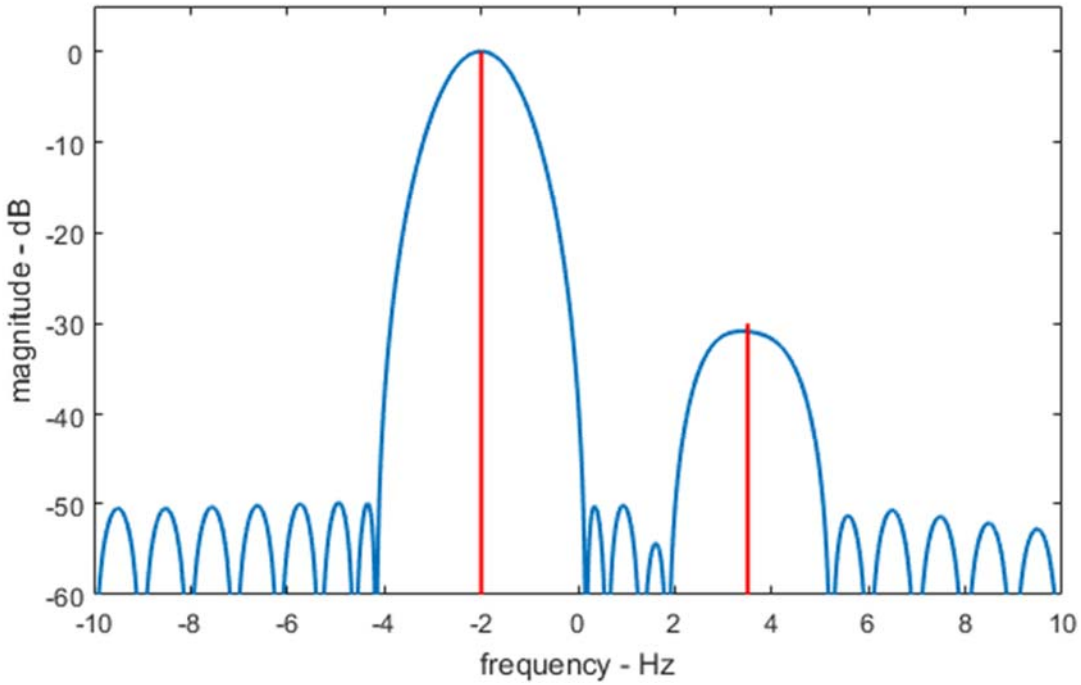


**Figure 5. Shown is the example of Figure 2, except that the segment has had applied a –50 dB Taylor window (nbar=7).**

We note that sharp discontinuities have been reduced in the aperture. In addition, we see that sidelobes are reduced in the spectrum but at the expense of a broader mainlobe. This is often considered a good trade.

***Example***

If we consider the two signals that yielded the spectrum of Figure 2, but now apply the window taper function of Figure 3 to the aperture, then the resulting spectrum is shown in Figure 5. Note that now there is no problem discerning the smaller second signal, even though it is 30 dB below the first signal, and relatively near in frequency.

## 2.5 Characteristics of Window Function Frequency Response

A window taper function with the properties listed previously in section 2.4 will generate a frequency response with the general characteristics that include

1. $W(f)$ will be real and typically even, but not always, and not always positive.
2. $W(f)$ will be of infinite length, defined over the interval $(-\infty, \infty)$.
3. $W(f)$ will have a distinct mainlobe.

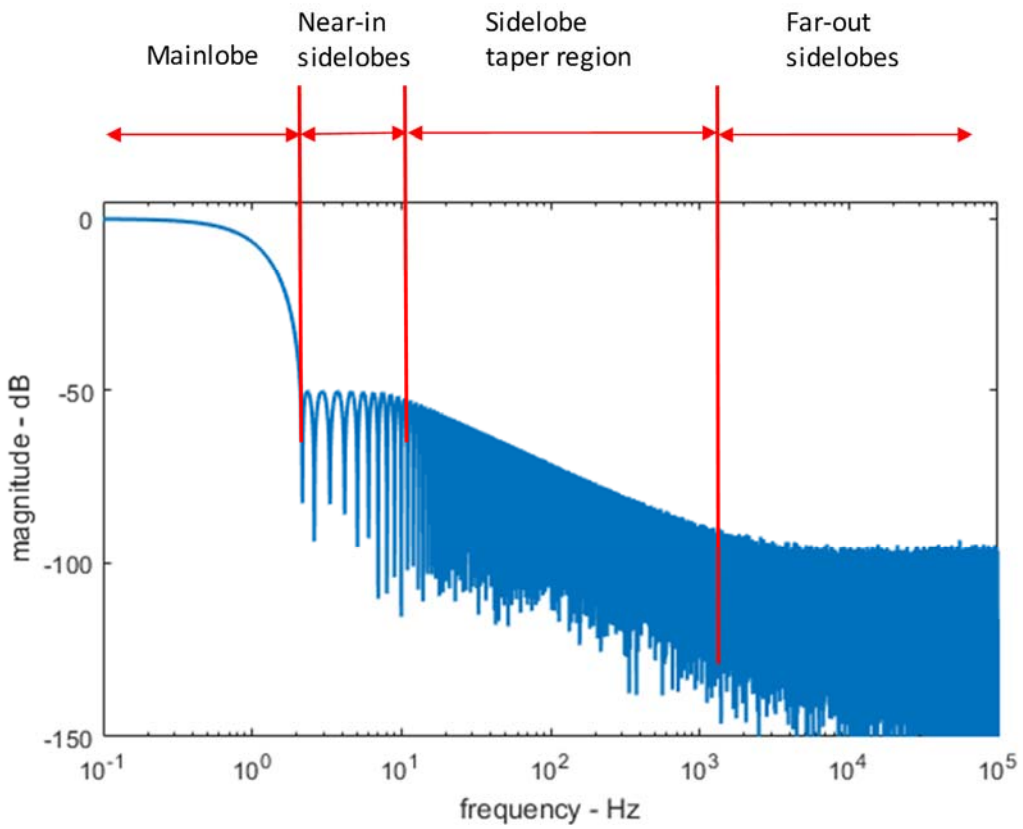


**Figure 6. Major regions of the frequency response of a window taper function. The window whose spectrum is displayed is the same –50 dB Taylor window (nbar = 7) displayed in Figure 3, but quantized in magnitude to about 200 different levels. Only the positive frequencies of the frequency response are displayed with a logarithmic frequency axis.**

Note that we are talking about continuous window taper functions, and not discrete-time window taper functions, whose properties might vary somewhat from these.

Figure 6 exemplifies a window taper function spectrum, and identifies several key regions to the spectrum. Different window functions trade between the characteristics of these various regions. In fact, not all window function spectra even exhibit all of these specific characteristics. Choosing a particular window function should be done with these trades in mind; with some assessment of which features are most important to the application at hand. We discuss these regions now.

***Mainlobe***

The peak of the frequency response is expected to be at $W(0)$, and $W(f)$ will attenuate with frequency offset from this, usually towards a null in the overall response. This region is the main lobe of $W(f)$. The mainlobe is typically characterized by various "width" measures, including one or more of the following:

–3 dB width

–*K* dB width, where *K* is some other arbitrary attenuation

half-power width, which is ever so slightly different than –3 dB width

noise-equivalent width, a measure of how much noise the window passes

Essentially, this is a bandwidth measure, so any specific bandwidth metric might also be used to characterize the mainlobe width of the window frequency response.

Note that the noise-equivalent width is often treated as a Signal-to-Noise Ratio (SNR) loss for using a window taper function, with the loss being with respect to using no window function at all.

***Near-in Sidelobes***

These are the sidelobes in the near vicinity of the mainlobe. For $W(f)$ being a sinc function, these are the sinc function sidelobes that are intolerably too high, and need to be suppressed, or at least reduced to acceptable levels.

One of the most important window design/selection trades is mainlobe widening at the expense of near-in sidelobe suppression.

***Sidelobe Taper Region***

Beyond the near-in sidelobes, we generally expect the sidelobes' magnitude to fall off as frequency offset increases. We define this as the sidelobe taper region. The rate of fall-off depends on the specific window taper function employed, and will generally be some low power of $|1/f|$. Note that $|1/f|$ corresponds to –6 dB per octave. If the actual window taper function endpoints do not smoothly arrive at zero, then generally the sidelobe taper will be no better than –6 dB per octave.

For a continuous window taper function, energy constraints require the sidelobe taper to ultimately be at a rate faster than $|1/\sqrt{f}|$, or –3 dB per octave (i.e. –10 dB/decade).

***Far-out Sidelobe Floor***

As sidelobes fall off in the taper region, they eventually reach a level at which they become inconsequential to our purposes, and can be tolerated at that level for an indefinite frequency offset from the peak response. Although not structural to the window taper function itself, system imperfections, and imperfections in arithmetic calculations such as due to quantization effects, might limit the floor that is in fact achievable. We of course generally desire the achievable floor to be below the

inconsequential level. Nevertheless, we must recognize that there are realistic limits to how well sidelobes can be suppressed, practically resulting in a far-out sidelobe floor.

## 2.6 Discrete-Time Window Taper Functions

When working with discrete data samples, a window taper function will also typically be a sampled version of the continuous-time function. Accordingly, we identify discrete window taper function sample values as

$$w_N(n) = w\left(\frac{n}{N-1} - \frac{1}{2}\right) = \text{discrete-time window taper function values,} \tag{34}$$

where the time index values of the discrete samples are integer values

$$0 \le n \le N-1\,. \tag{35}$$

A consequence of selecting discrete weights this way is that Eq. (30) now becomes

$$\sum_{n=0}^{N-1} w_N(n) \to N\ , \text{ for large } N. \tag{36}$$

While equality will not strictly hold, as $N$ increases, the sum of the weights gets closer to $N$. Of course, the weights may be scaled ever so slightly to force equality. Nevertheless, for all intents and purposes, for most windows and any reasonably sized $N$, equality may typically be presumed. Thus, the DC gain for a discrete-time window taper function as defined is effectively $N$.

While Eq. (34) describes how a continuous window taper function may be sampled to create a Discrete-Time window taper function, we stipulate that other sampling schemes might also be employed. For example, we might wish to divide the window into $N$ equal-sized segments and select the center of each segment to yield

$$w_N(n) = w\left(\frac{n}{N} - \frac{N-1}{2N}\right). \tag{37}$$

Otherwise, we may alternatively wish to select an average value over the individual segments by calculating

$$w_N(n) = N \int_{\left(\frac{n-N/2}{N}\right)}^{\left(\frac{n-N/2+1}{N}\right)} w(t)dt\,. \tag{38}$$

Other schemes can also be easily conjured. All converge to the same answer as $N \to \infty$. Hereafter, we will generally assume to employ Eq. (34) and its consequences out of convenience.

With this scheme, we identify

$$T_\Delta = \frac{T}{(N-1)} = \text{the time-sample spacing, and}$$

$$f_s = \frac{1}{T_\Delta} = \text{the time-sampling frequency.} \tag{39}$$

We note that for a unit-width aperture, where $T = 1$, then *N* samples spread from end to end over this aperture implies that

$$f_s = N - 1\ , \quad \text{for a unit-width aperture.} \tag{40}$$

The Discrete-time Fourier Transform (DFT) of the sampled window taper function data is calculated as

$$W_K(k) = \sum_{n=0}^{N-1} w_N(n) e^{-j2\pi \frac{k}{K} n}\ , \tag{41}$$

where the frequency index is nominally

$$0 \le k \le K - 1\ . \tag{42}$$

Although this is the nominal span for index *k*, with frequency itself mapped to

$$f = \frac{k}{K} f_s\ . \tag{43}$$

it should be appreciated that the nature of the spectra of sampled data is such that the spectra repeat so that we may in fact use indices outside the range specified in Eq. (42). This is the well-known phenomenon of sampled-data periodic spectra.[11] In fact, we may extend to an arbitrary integer index *k* by stipulating that

$$W_K(k + K) = W_K(k), \text{ for all } k. \tag{44}$$

As a consequence, any set of *K* contiguous DFT output samples will completely specify the frequency response of the time-sampled window taper function.

It is also convenient to recognize the frequency-sample spacing

$f_\Delta = \dfrac{f_s}{K}$ = frequency-sample spacing, and

$T_a = \dfrac{1}{f_\Delta}$ = time-interval represented by frequency-sample spacing. (45)

Another consequence of a periodic spectrum is that any particular frequency sample $W_K(k)$ contains energy not only from the desired nominal frequency associated to it by Eq. (43), but also from any frequencies aliased to it. As a practical matter, this will impact the degree to which far-out sidelobes can be suppressed, regardless of the characteristics of the corresponding continuous-time window taper function spectrum, often in a manner that depends somewhat on *N*.

It should be obvious from aliasing characteristics, that regardless of the specific window taper function, as frequency increases and crosses the $f_s/2$ mark, sidelobe levels cease declining, and necessarily begin growing again as we approach the duplicate mainlobe centered at frequency $f_s$.

Nevertheless, near the mainlobe peak, for $|k| << K$,

$$W_K(k) \approx N\,W\left(\frac{N-1}{K}k\right), \text{ for small } k. \tag{46}$$

***Example***

Consider the spectrum of a continuous window taper function, along with its sampled version with 128 samples. Figure 7 illustrates the frequency range between DC and the sampling frequency.

Note that while the spectrum of the continuous window keeps tapering to the right as we might desire and expect, the spectrum of the sampled window agrees closely only for a small fraction of the displayed frequency band near the mainlobe, and displays actually increasing spectral density after $f_s/2$ towards the replicated mainlobe at $f_s$.

### *Windowing Periodic Functions*

When a function is known to be periodic over *N* samples, we are given to understand that although our sample set is for indices $[0:N-1]$, index values outside this range yield

$$x_N(n+N) = x_N(n). \tag{47}$$

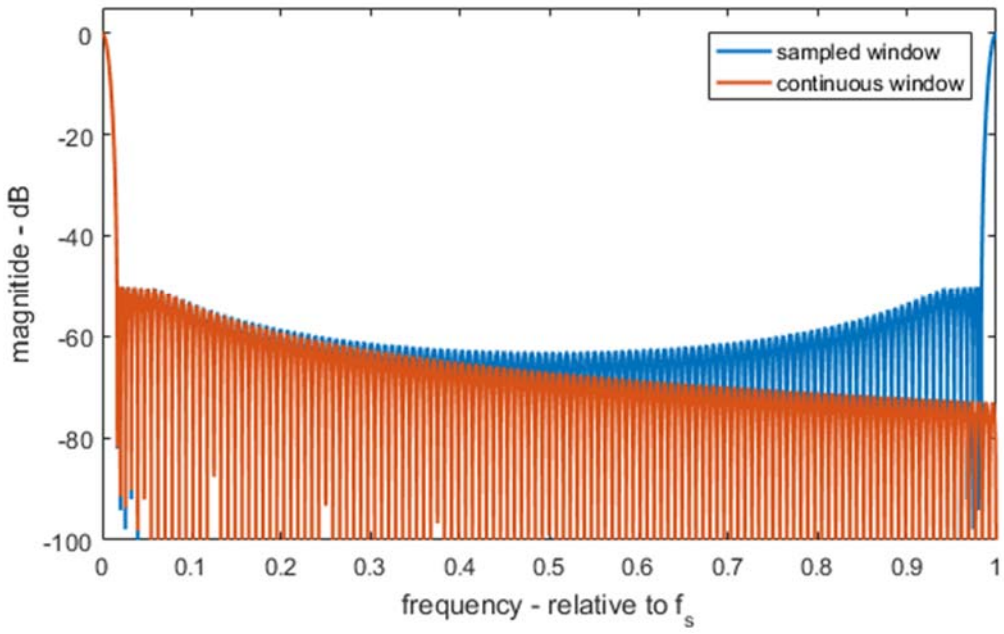


**Figure 7. Spectrum differences for sampled window versus continuous window. Both are a –50 dB Taylor window (nbar=7). Only positive frequencies are shown. Sampled window uses 128 samples.**

Specifically, we understand that

$$x_N(N) = x_N(0). \tag{48}$$

In this case, we would employ a discrete-time window taper function where

$$w_N(N-m) = w_N(0+m), \quad \text{for integer values of } m. \tag{49}$$

This suggests that Eq. (34) for such periodic signals becomes

$$w_N(n) = w\left(\frac{n}{N} - \frac{1}{2}\right). \tag{50}$$

In this case, we identify

$$T_\Delta = \frac{T}{N} \text{ = the time-sample spacing.} \tag{51}$$

This idea will come into play for those window taper functions that are specified by, and calculated from, their spectra. We refer the reader to Appendix A for details.

## 2.7 Window Taper Function Metrics

Here we address a number of different, but often related metrics for window taper functions and their spectra.

As prelude to this section, we identify Energy Spectral Density (ESD) of the continuous window taper function as

$$\left|W\left(f\right)\right|^2 = \text{Energy Spectral Density.} \tag{52}$$

From Parseval's theorem, we understand that

$$\int_{-\infty}^{\infty} \left|W\left(f\right)\right|^2 df = \int_{-\infty}^{\infty} \left|w(t)\right|^2 dt \,. \tag{53}$$

Recall that we have defined window taper functions such that

$$\int_{-\infty}^{\infty} w(t)\, dt = 1 \,. \tag{54}$$

Likewise, for the spectrum of the sampled window taper function,

$$\frac{1}{K}\sum_{k=0}^{K-1} \left|W_K\left(k\right)\right|^2 = \sum_{n=0}^{N-1} \left|w_N\left(n\right)\right|^2 \,. \tag{55}$$

Recall also that we have defined discrete-time window taper functions such that

$$\sum_{n=0}^{N-1} w_N\left(n\right) = N \,. \tag{56}$$

For the following discussions, we will normalize all width and frequency offset measurements to $1/T$ , where

$$T = \text{the window width,} \tag{57}$$

which we have heretofore assumed to be unity. To calibrate ourselves, among other things, $1/T$ is the distance from peak to first null for a sinc function frequency response.

### 2.7.1 Half-Power Mainlobe Width

This metric is the width of the mainlobe where

$$\left|W\left(f_1\right)\right|^2 = \frac{1}{2}\left|W\left(0\right)\right|^2. \tag{58}$$

Assuming symmetry, the width of the mainlobe is then calculated as

$$a_{w,hp} = 2\left|f_1\right|. \tag{59}$$

For a sampled window taper function, we interpolate to find the smallest fractional index where

$$\left|W_K\left(k_1\right)\right|^2 = \frac{1}{2}\left|W_K\left(0\right)\right|^2. \tag{60}$$

The width of the mainlobe is then calculated as

$$a_{w,hp} = 2\frac{N}{K}k_1. \tag{61}$$

For a sinc function, $a_{w,hp} \approx 0.88588$.

### 2.7.2 –3 dB Mainlobe Width

While –3 dB is often presumed to be half power, it isn't exactly so. Accordingly, this metric is the width of the mainlobe where

$$\left|W\left(f_1\right)\right|^2 = \left(10^{\frac{-3}{10}}\right)\left|W\left(0\right)\right|^2. \tag{62}$$

Assuming symmetry, the width of the mainlobe is then calculated as

$$a_{w,-3dB} = 2\left|f_1\right|. \tag{63}$$

For a sampled window taper function, we interpolate find the smallest fractional index where

$$\left|W_K\left(k_1\right)\right|^2 = \left(10^{\frac{-3}{10}}\right)\left|W_K\left(0\right)\right|^2. \tag{64}$$

The width of the mainlobe is then calculated as

$$a_{w,-3dB} = 2\frac{N}{K}k_1 . \tag{65}$$

For a sinc function, $a_{w,-3dB} \approx 0.88448$.

### 2.7.3 M dB Mainlobe Width

We often wish to find the mainlobe width farther down its sides, at perhaps some other power ratio. Accordingly, this metric is the width of the mainlobe for some arbitrarily relative power level *M*, where

$$\left|W\left(f_1\right)\right|^2 = \left(10^{\frac{M}{10}}\right)\left|W\left(0\right)\right|^2, \quad \text{for } M < 0 \text{ in units of dB.} \tag{66}$$

Assuming symmetry, the width of the mainlobe is then calculated as

$$a_{w,MdB} = 2\left|f_1\right| . \tag{67}$$

For a sampled window taper function, we interpolate find the smallest fractional index where

$$\left|W_K\left(k_1\right)\right|^2 = \left(10^{\frac{M}{10}}\right)\left|W_K\left(0\right)\right|^2 . \tag{68}$$

The width of the mainlobe is then calculated as

$$a_{w,MdB} = 2\frac{N}{K}k_1 . \tag{69}$$

A typical value for radar signal processing is $M = -18$ dB. We must be cognizant, however, that for very negative values of *M*, spectral sidelobes will pop up above this level. Therefore, some ambiguity exists in whether this metric applies to just the mainlobe, or also to the farthest sidelobe that meets this criterion.

For a sinc function, for the mainlobe only, and neglecting any sidelobes, $a_{w,-18dB} \approx 1.7721$.

### 2.7.4 Noise-Equivalent Mainlobe Width

This metric answers the question "What equivalent ideal-filter bandwidth will pass the same noise power as the window taper function spectrum, assuming White Gaussian Noise (WGN) is input?" That is, we wish to find two-sided bandwidth $a_{w,noise}$ such that

$$\left|W\left(0\right)\right|^2 a_{w,noise} = \int_{-\infty}^{\infty} \left|W\left(f\right)\right|^2 df \ . \tag{70}$$

This may be calculated as

$$a_{w,noise} = \frac{1}{\left|W\left(0\right)\right|^2} \int_{-\infty}^{\infty} \left|w(t)\right|^2 dt \, . \tag{71}$$

For a sampled window taper function, we may calculate this as

$$a_{w,noise} = \frac{N/K}{\left|W_K\left(0\right)\right|^2} \sum_{k=0}^{K-1} \left|W_K\left(k\right)\right|^2 \, . \tag{72}$$

For our window taper function definitions, this becomes

$$a_{w,noise} = \frac{1}{N} \sum_{n=0}^{N-1} \left|w_N\left(n\right)\right|^2 \, . \tag{73}$$

This number, for most window functions, will typically somewhat larger than the half-power, or –3 dB mainlobe widths.

For a sinc function, $a_{w,noise} = 1.0$.

### 2.7.5 SNR Gain/Loss

The noise-equivalent mainlobe width calculated in the previous section is often utilized as a loss in SNR of a signal. The loss is calculated as

$$L_{window} = a_{w,noise} \, . \tag{74}$$

In terms of dB, this becomes

$$L_{window,dB} = 10 \log_{10}\left(a_{w,noise}\right) . \tag{75}$$

For a sinc function, $L_{window,dB} = 0$.

### 2.7.6 First-Null Offset

The first null is the null nearest to the mainlobe peak. It is the smallest $f_1$ to yield

$$\left|W\left(f_1\right)\right|^2 = 0 . \tag{76}$$

Note that first nulls occur at both $\pm f_1$. Accordingly, we may also define a null-to-null mainlobe width to be

$$a_{w,null-to-null} = 2\left|f_1\right| . \tag{77}$$

For a sampled window taper function, we interpolate to find the smallest fractional index where

$$\left|W_K\left(k_1\right)\right|^2 = 0 . \tag{78}$$

We may correspond this fractional index to a frequency-offset for the null with the relationship

$$f_1 = \frac{N}{K} k_1 . \tag{79}$$

The width of the mainlobe is then calculated as

$$a_{w,null-to-null} = 2\left|f_1\right| = 2\frac{N}{K} k_1 . \tag{80}$$

For a sinc function, $f_1 =$ 1.0, and $a_{w,null-to-null}$ = 2.0.

### 2.7.7 Peak Sidelobe Level (PSL)

Sidelobes are by definition energy in the frequency response of the window taper function in the sidelobe regions located beyond the first null (both positive and negative).

The peak sidelobe level answers the question "What is the minimum attenuation achievable for an interfering narrow-band source not in the mainlobe?"

The peak sidelobe level for a frequency response may be found by looking for the peak frequency response beyond the first null. It is furthermore related to the mainlobe peak. Accordingly, for a continuous window function's spectrum

$$PSL = \frac{\max\left(W(f)\big|_{f>|f_1|}\right)}{W(0)}, \tag{81}$$

where $f_1$ is the first null. Since we have opted to define the DC gain of the continuous window taper function to be unity, we may identify $W(0)=1$.

For a sampled window taper function, we interpolate to find the peak value of the first sidelobe beyond the first null, but limited to frequencies corresponding to less than $f_s/2$, owing to the periodic nature of sampled signal spectra. This constrains the index to $k_1 < k < K/2$, where $k_1$ is the first null. Accordingly,

$$PSL = \frac{\max\left(W_K(k)\big|_{k_1<k<K/2}\right)}{W_K(0)}. \tag{82}$$

Since we have opted to specify the DC gain of the discrete-time window taper function to be *N*, we may identify $W(0)=N$.

For both continuous and discrete-time window taper functions, the PSL is typically expressed in dB. Consequently, we calculate

$$PSL_{dB} = 10\log_{10}(PSL). \tag{83}$$

For a sinc function, $PSL_{dB} \approx -13.26$ dB.

### *2.7.8 Integrated Sidelobe Level (ISL)*

The integrated sidelobe level answers the question "What fraction of the window taper function's spectrum's energy is in the sidelobes?"

It further answers the question "What minimum attenuation might we expect for a broadband white-spectrum interference source outside of the mainlobe response?"

In radar imaging systems, this is a source of multiplicative noise, and contributes to the Multiplicative Noise Ratio (MNR).

Accordingly, for a continuous window function's spectrum

$$ISL = \frac{2\int_{f_1}^{\infty} |W(f)|^2 \, df}{\int_{-\infty}^{\infty} |W(f)|^2 \, df}, \tag{84}$$

where $f_1$ is the first null. Using Eq. (53), this may also be written as

$$ISL = \frac{2\int_{f_1}^{\infty} |W(f)|^2 \, df}{\int_{-\infty}^{\infty} |w(t)|^2 \, dt}. \tag{85}$$

Using previous results, specifically Eq. (70), we may also write this as

$$ISL = \frac{2\int_{f_1}^{\infty} |W(f)|^2 \, df}{|W(0)|^2 \, a_{w,noise}}. \tag{86}$$

For a sampled window taper function, we may calculate

$$ISL = \frac{\sum_{k=k_1}^{K/2-1} |W_K(k)|^2}{\sum_{k=0}^{K/2-1} |W_K(k)|^2}, \tag{87}$$

where $k_1$ is the first null. Summation is limited to integer index values. Using Eq. (55), and symmetry properties, this may be calculated as

$$ISL = \frac{2\sum_{k=k_1}^{K/2-1} |W_K(k)|^2}{K\sum_{n=0}^{N-1} |w_N(n)|^2}. \tag{88}$$

Using also Eq. (73), this may also be written as

$$ISL = \frac{2\sum_{k=k_1}^{K/2-1} \left|W_K(k)\right|^2}{K\,N\,a_{w,noise}}. \tag{89}$$

For both continuous and discrete-time window taper functions, the ISL is typically expressed in dB. Consequently, we calculate

$$ISL_{dB} = 10\log_{10}(ISL). \tag{90}$$

For a sinc function, $ISL_{dB} \approx -9.68$ dB.

We offer that these relatively high levels for ISL and PSL render the sinc function unattractive as a frequency response, and the rect function thereby as deficient as a window taper function. This is the reason other taper functions were developed in the first place.

### *2.7.9 Sidelobe Asymptotic Taper Rate*

The sidelobes will fall off in the sidelobe taper region of the frequency response at a rate that depends on how continuous is the window function, including the transition to a constant zero at its edges.

Generally, a discontinuity in the $n^{\text{th}}$ derivative of the window taper function $w(t)$ will cause a $-6(n+1)$ dB per octave asymptotic roll-off of the sidelobes. A roll-off of $-6$ dB per octave equates to $-10$ dB per decade, which equates to a $1/|f|$ rate.

We see this from the following analysis.

Recall that for a transform pair

$$w(t) \Leftrightarrow W(f), \tag{91}$$

then if the $n^{\text{th}}$ derivative exists, basic Fourier Transform properties give us that

$$\frac{d^n}{dt^n} w(t) \Leftrightarrow (j2\pi f)^n W(f). \tag{92}$$

A discontinuity in the $n^{\text{th}}$ derivative, where the $n^{\text{th}}$ derivative is still finite, means that the right side of Eq. (92) still falls off at a $1/|f|$ rate, to keep the energy in the right-side function finite. This, of course, means that the spectrum $W(f)$ itself must fall off at a $1/|f|^{n+1}$ rate.

**Figure 8. Richard Wesley Hamming (February 11, 1915 – January 7, 1998), inventor and namesake of the Hamming window taper function, among many other achievements. (image courtesy Wikipedia)**

# 3 Picking a Window Taper Function

The selection of a particular window taper function is typically an exercise in making engineering trades with respect to window spectrum characteristics. That is, the "perfect" taper is generally not achievable, so the correct taper is one that is "good enough." The system designer must first ascertain acceptable limits of degradation with respect to the following characteristics

1. Mainlobe broadening, i.e., spectral resolution,
2. Noise bandwidth, or SNR loss,
3. Near-in PSL,
4. Spectral sidelobe taper rate,
5. Far-out sidelobe level,
6. ISL,
7. Length-limits of the window,
8. Ease of generation.

Often, the priority of the required characteristics will be driven by the application. i.e. whether the intended use is for spectral estimation, filter design, interpolation, etc.

In any case, there are a myriad of window taper functions from which to choose, and an infinite set of variations in their ability to be "tuned."

What follows is a catalog of some of the more popular window taper functions, and families of functions.

**Figure 9. Julius Ferdinand von Hann (23 March 1839 – 1 October 1921), Austrian meteorologist and namesake of the Hann window taper function. (image courtesy Wikipedia)**

# 4 Window Taper Functions

In the following we present characteristics of various window taper functions, specifically parameters of their spectral nature.

We stipulate that the measured parameters were for discrete-time window functions with the following common characteristics.

1. All window functions used $N = 16{,}384$ samples, unless otherwise noted.

2. All window spectra were calculated for $K = 256\,N$ frequency samples.

3. All discrete-time window functions were normalized to a DC signal gain of $N$, where the DC frequency yields a spectrum magnitude of $N$.

4. All frequency width and frequency offset values are normalized to a unit time interval $T$, that is a frequency increment of $1/T$. This is the distance from peak to first null for a sinc function frequency response.

5. Any interpolation uses linear interpolation between integer-index samples.

6. All frequency spectrum plots will be normalized to the peak value, and scaled in dB with respect to the peak value (dBc).

We stipulate that the following listing is incomplete. Essentially, any function that exhibits a mainlobe can be used as a window taper function. Many functions furthermore allow adjustments via parameter manipulation. Furthermore yet, many of these can be combined in an infinite set of relative scaling, yielding a further expansion of the universe of window taper functions.

The literature often describes the same window taper function with different names. In addition, we also find sometimes the same name get applied to fundamentally different window taper functions.

We suggest the reader wishing to select a window taper function practice “caveat emptor.”

## 4.1 Rectangle (a.k.a. Boxcar, Dirichlet, Uniform)

The Rectangle, or Rectangular, window taper function is equivalent to no window at all.

The continuous time window taper function is given as

$$w(t) = \text{rect}(t), \tag{93}$$

where the rect function is defined as in Eq. (4).

The Fourier Transform of the continuous time window taper function is given as

$$W(f) = \text{sinc}(f), \tag{94}$$

where the sinc function is defined as in Eq. (5).

The DFT of a sampled window taper function is calculated to be

$$W_K(k) \approx N \left[ \frac{\sin\left(\pi(N-1)\frac{k}{K}\right)\cos\left(\pi\frac{k}{K}\right)}{(N-1)\sin\left(\pi\frac{k}{K}\right)} \right], \tag{95}$$

where we have ignored the group-delay phase term. We note the cosine factor is a consequence of the rect function definition in Eq. (4).

Note that for small $k$, this can be approximated as

$$W_K(k) \approx N\,\text{sinc}\left(\frac{N-1}{K}k\right), \tag{96}$$

with the mainlobe region approaching the shape of Eq. (94). This is a consequence of Eq. (46).

Plots and characteristics are given in Figure 10. Note that sidelobes fall off at a rate of –6 dB per octave.

The Rectangle window taper function is the baseline to which all others are typically compared.

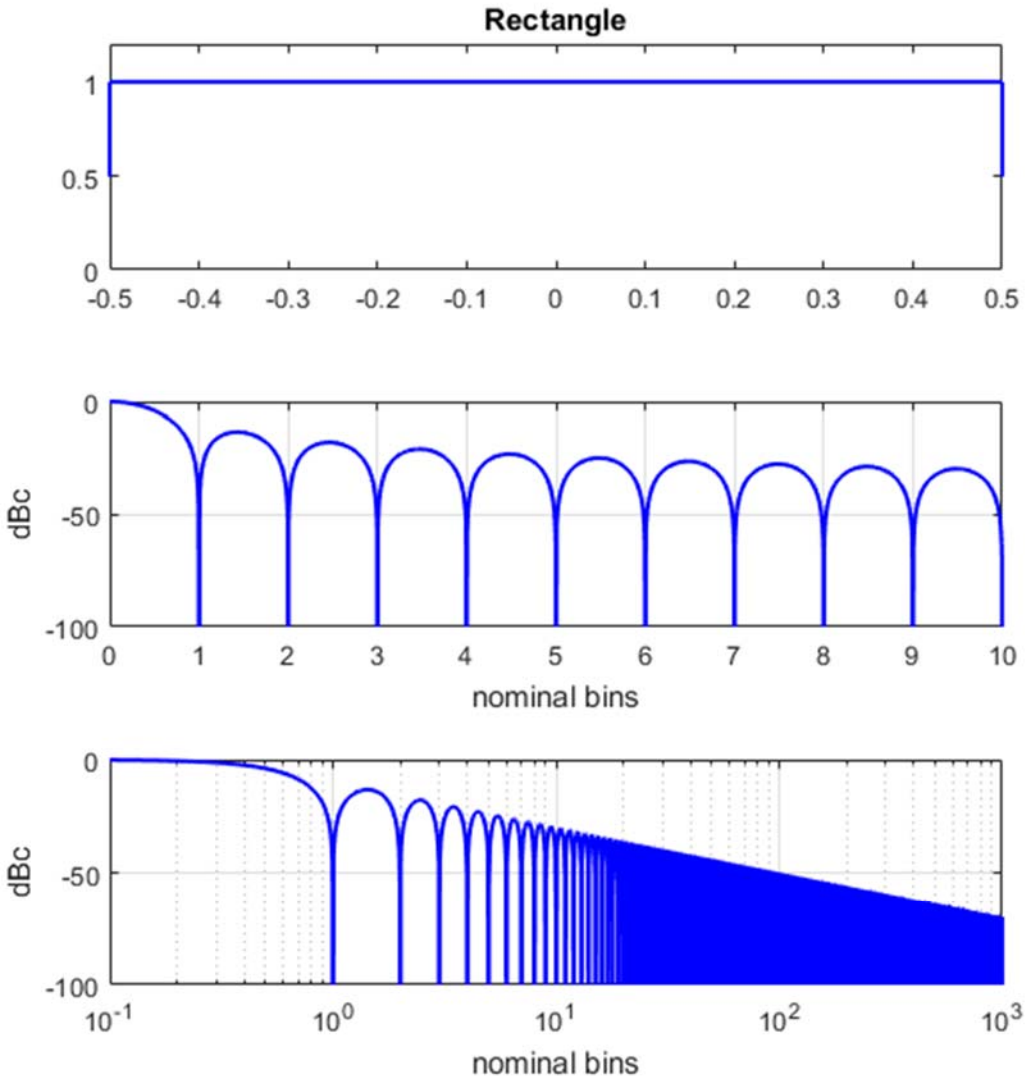


WINDOW SPECTRUM CHARACTERISTICS

half-power bandwidth = 0.88588 (normalized to 1/T)
-3 dB bandwidth = 0.88448 (normalized to 1/T)
-18 dB bandwidth = 1.7721 (normalized to 1/T)
noise bandwidth = 1 (normalized to 1/T)
SNR loss = 0 dB
first null = 1 (normalized to 1/T)
PSL = -13.2615 dBc
ISL = -10.1247 dBc from first null outward

**Figure 10.**

## 4.2 Triangle (a.k.a. Bartlett)

The Triangle, or Triangular, window taper function is defined with form scaled for unit DC gain as

$$w(t) = 2\left(1 - 2|t|\right)\text{rect}\left(t\right) = 2\Lambda\left(2t\right), \tag{97}$$

where the triangle function is defined as

$$\Lambda\left(x\right) = \left(1 - |x|\right)\text{rect}\left(\frac{x}{2}\right). \tag{98}$$

Bartlett described this window function in an early paper.[12]

The Fourier Transform of the continuous time window taper function is calculated as

$$W\left(f\right) = \text{sinc}^2\left(\frac{f}{2}\right). \tag{99}$$

Plots and characteristics are given in Figure 11. Note that sidelobes fall off at twice the rate of the Rectangle window, namely at a rate of −12 dB per octave.

The Triangle window is a member of a family of window taper functions known as "B-spline windows." These are functions that can be derived from convolving a $M$ identical rect functions together. Specifically, the Triangle window taper function is a 2nd order $\left(M = 2\right)$ B-spline window, suitably compressed in time and scaled in amplitude to meet the unit width and unit DC gain characteristics.

Harris[4] also identifies this as a Fejér window, but we will reserve this name for a different kernel based on an earlier source.

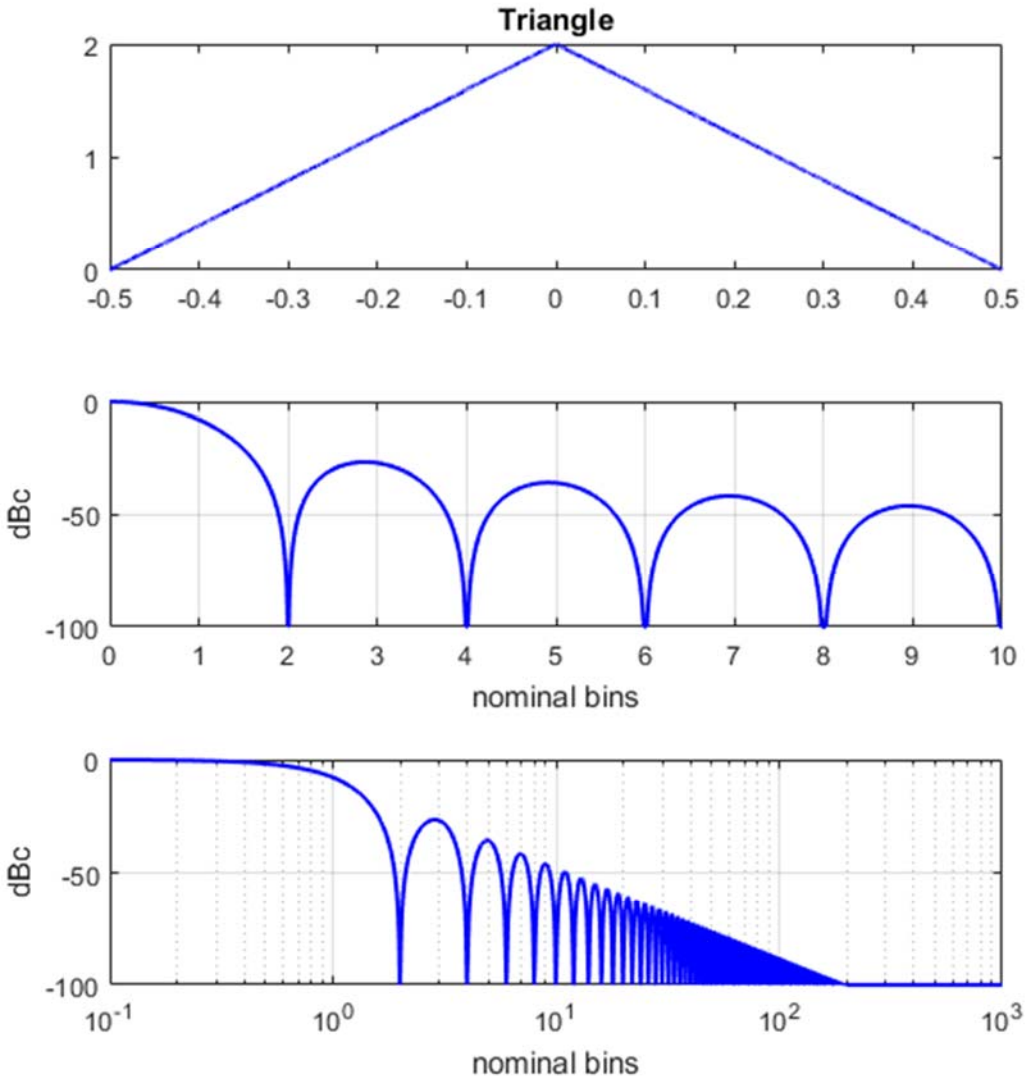


WINDOW SPECTRUM CHARACTERISTICS

half-power bandwidth = 1.2757 (normalized to 1/T)
-3 dB bandwidth = 1.2736 (normalized to 1/T)
-18 dB bandwidth = 2.8383 (normalized to 1/T)
noise bandwidth = 1.3333 (normalized to 1/T)
SNR loss = 1.2494 dB
first null = 2 (normalized to 1/T)
PSL = -26.523 dBc
ISL = -25.3097 dBc from first null outward

**Figure 11.**

## 4.3 Parzen

The Parzen[13] window taper function is defined with form scaled for unit DC gain as

$$w(t)=\begin{cases}\left(\frac{8}{3}\right)\left(1-24|t|^2+48|t|^3\right) & |t|\le 1/4\\ \left(\frac{8}{3}\right)\left(2-12|t|+24|t|^2-16|t|^3\right) & 1/4<|t|\le 1/2\\ 0 & \textit{else}\end{cases}. \tag{100}$$

This particular window characteristic was first suggested orally by Parzen at an Institute of Mathematical Statistics (I.M.S.) Annual Meeting in 1957.[13]

The Fourier Transform of the continuous time window taper function is calculated as

$$W(f)=\operatorname{sinc}^4\left(\frac{f}{4}\right). \tag{101}$$

Plots and characteristics are given in Figure 12. Note that sidelobes fall off at four times the rate of the Rectangle window, namely at a rate of –24 dB per octave.

The Parzen window is a member of a family of window taper functions known as "B-spline windows." These are functions that can be derived from convolving a $M$ identical rect functions together. Specifically, the Parzen window taper function is a 4th order $(M=4)$ B-spline window, suitably compressed in time and scaled in amplitude to meet the unit width and unit DC gain characteristics. It can also be formed by convolving two identical triangle functions together, suitably compressed in time and scaled in amplitude to meet the unit width and unit DC gain characteristics.

Harris[4] also identifies this as a de la Vallée Poussin, or Jackson, window, but we will reserve these names for a different kernel based on an earlier source.

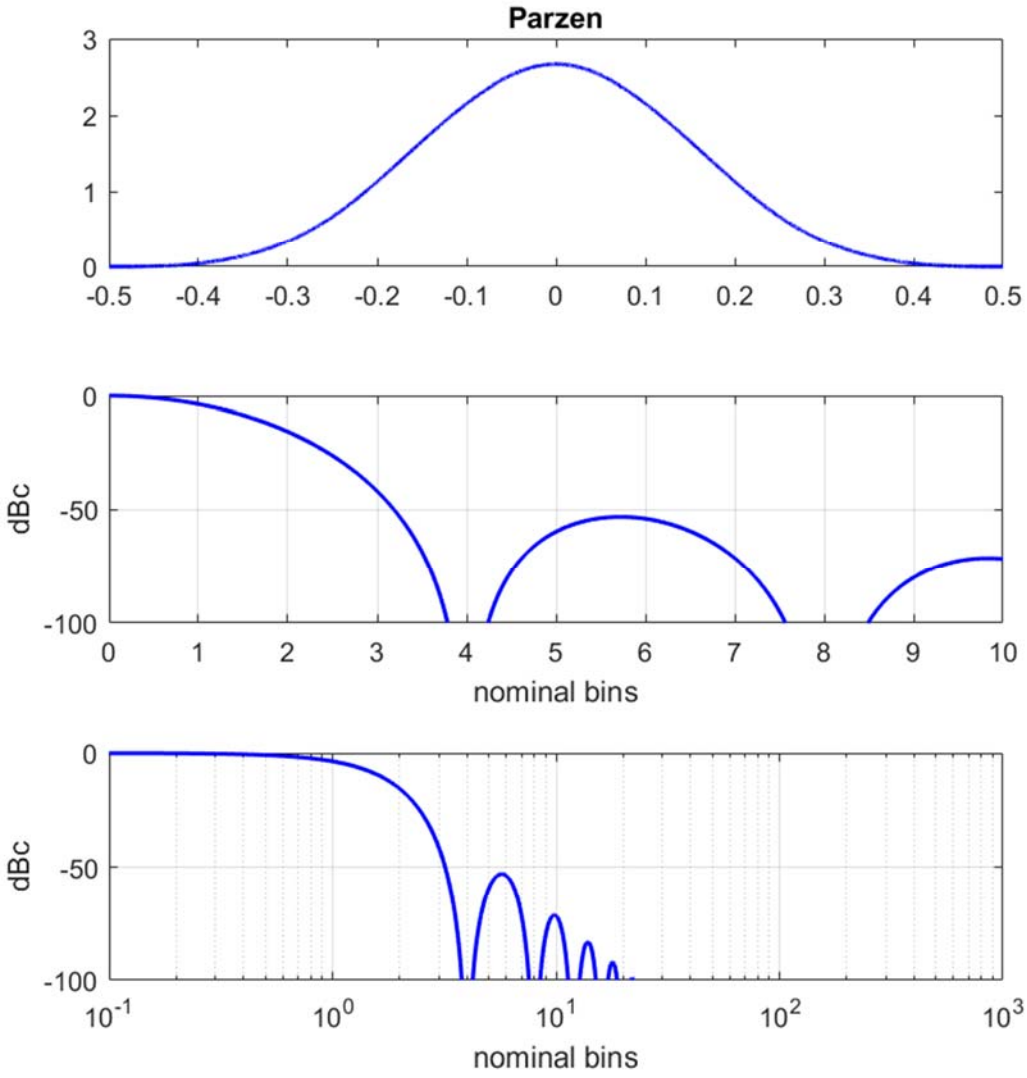


WINDOW SPECTRUM CHARACTERISTICS

half-power bandwidth = 1.8202 (normalized to 1/T)
-3 dB bandwidth = 1.8171 (normalized to 1/T)
-18 dB bandwidth = 4.2541 (normalized to 1/T)
noise bandwidth = 1.9176 (normalized to 1/T)
SNR loss = 2.8275 dB
first null = 4 (normalized to 1/T)
PSL = -53.0458 dBc
ISL = -52.408 dBc from first null outward

**Figure 12.**

## 4.4 General B-Spline

The B-spline family of window taper function is generated by convolving some $M$ number of identical rect functions together,

$$w(t) = \left( \text{rect}_1\left(\frac{t}{M}\right) * \text{rect}_2\left(\frac{t}{M}\right) * \quad ... \quad * \text{rect}_M\left(\frac{t}{M}\right) \right), \tag{102}$$

where we identify

$$M \text{ = the order, or number of rect functions convolved together.} \tag{103}$$

The Rectangle, Triangle, and Parzen window taper functions of the previous sections are just B-spline windows with $M$ = 1, 2, and 4, respectively.

For $M = 3$, the window is described by

$$w(t) = \begin{cases} \left(\frac{9}{8}\right)\left(2 - 24|t|^2\right) & |t| \le 1/6 \\ \left(\frac{9}{8}\right)\left(3 - 12|t| + 12|t|^2\right) & 1/6 < |t| \le 1/2 \\ 0 & \textit{else} \end{cases}. \tag{104}$$

For $M = 5$, the window is described by

$$w(t) = \begin{cases} \left(\frac{25}{384}\right)\left(46 - 1200|t|^2 + 12000|t|^4\right) & |t| \le 1/10 \\ \left(\frac{25}{384}\right)\left(44 + 80|t| - 2400|t|^2 + 8000|t|^3 - 8000|t|^4\right) & 1/10 < |t| \le 3/10 \\ \left(\frac{25}{384}\right)\left(125 - 1000|t| + 3000|t|^2 - 4000|t|^3 + 2000|t|^4\right) & 3/10 < |t| \le 1/2 \\ 0 & \textit{else} \end{cases}. \tag{105}$$

The Fourier Transform of the continuous time window taper functions are calculated as

$$W(f) = \mathrm{sinc}^M\left(\frac{f}{M}\right). \tag{106}$$

Plots and characteristics are given in Figure 13 and Figure 14, for $M = 3$ and $M = 5$ respectively. Note that sidelobes fall off at *M* times the rate of the Rectangle window.

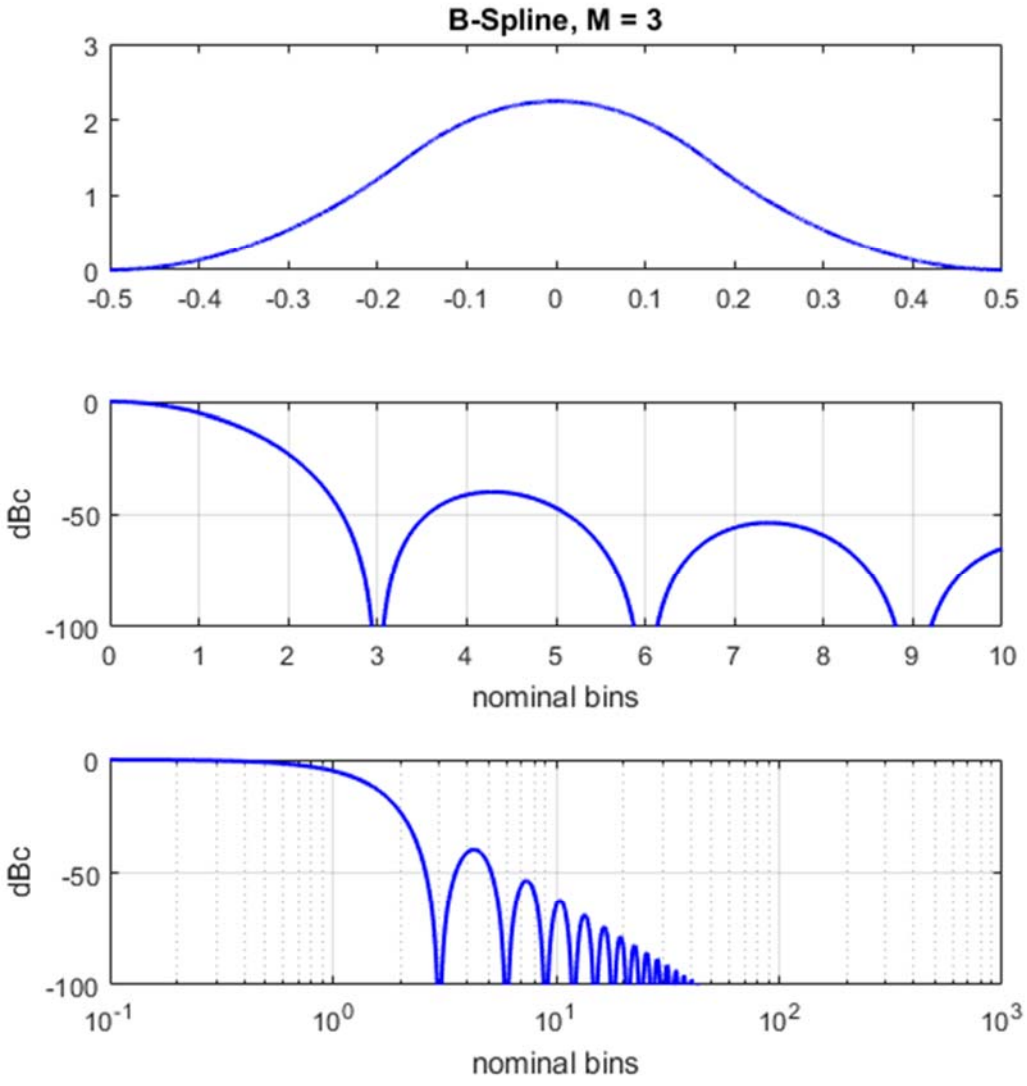


WINDOW SPECTRUM CHARACTERISTICS

half-power bandwidth = 1.5717 (normalized to 1/T)
-3 dB bandwidth = 1.5691 (normalized to 1/T)
-18 dB bandwidth = 3.6151 (normalized to 1/T)
noise bandwidth = 1.6501 (normalized to 1/T)
SNR loss = 2.1751 dB
first null = 3 (normalized to 1/T)
PSL = -39.7844 dBc
ISL = -39.0217 dBc from first null outward

**Figure 13.**

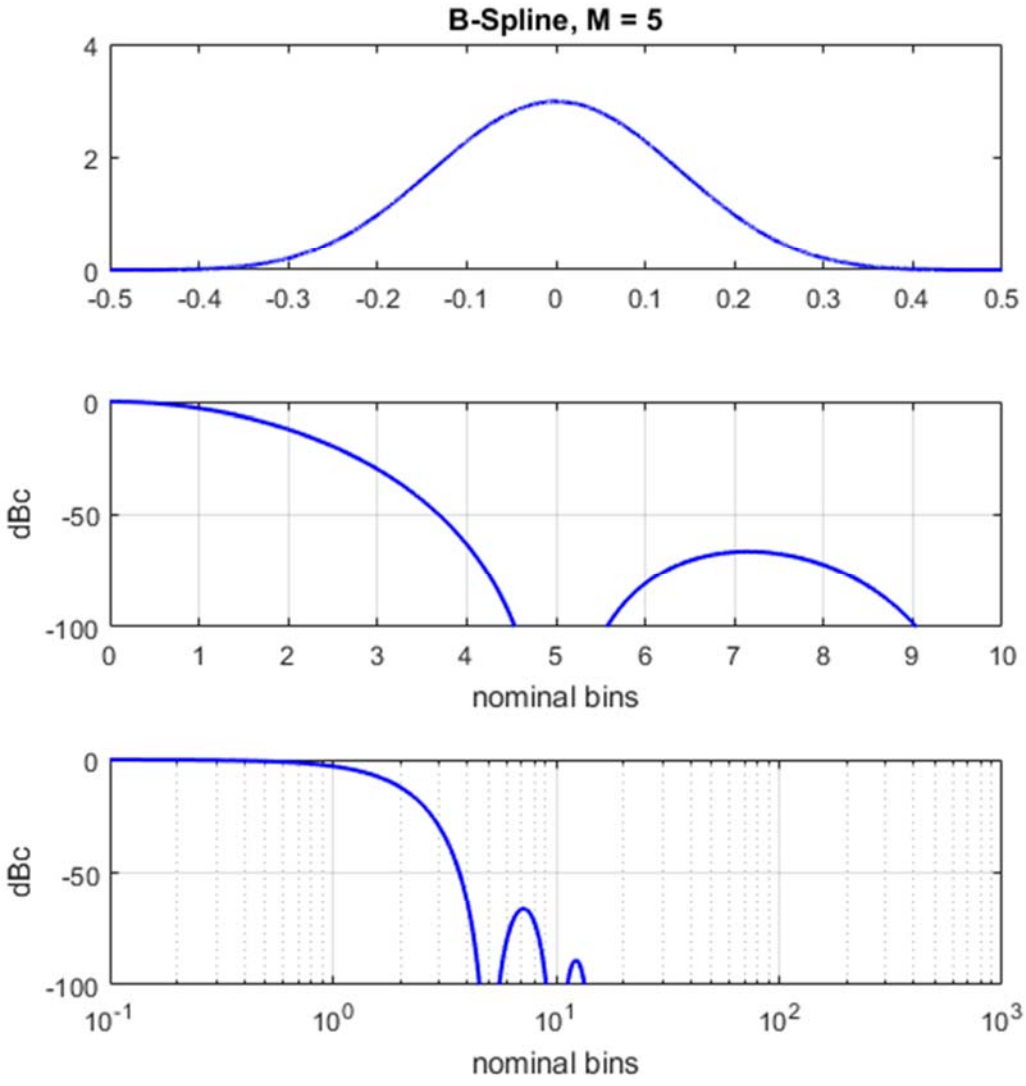


WINDOW SPECTRUM CHARACTERISTICS

half-power bandwidth = 2.0386 (normalized to 1/T)
-3 dB bandwidth = 2.0352 (normalized to 1/T)
-18 dB bandwidth = 4.8095 (normalized to 1/T)
noise bandwidth = 2.1522 (normalized to 1/T)
SNR loss = 3.3289 dB
first null = 5 (normalized to 1/T)
PSL = -66.3073 dBc
ISL = -65.7045 dBc from first null outward

**Figure 14.**

## 4.5 Welch (a.k.a. Riesz, Bochner, Parzen)

The Welch[14] window taper function is a member of a family of Polynomial window taper functions. Specifically, it is an inverted parabola with form scaled to provide unit DC response as

$$w(t) = \frac{3}{2}\left(1 - 4t^2\right)\mathrm{rect}(t). \tag{107}$$

The Fourier Transform of the continuous time window taper function is calculated as

$$W(f) = \frac{3\sin(\pi f) - 3\pi f\cos(\pi f)}{\pi^3 f^3}. \tag{108}$$

Plots and characteristics are given in Figure 15.

Harris[4] calls this a Riesz window, but references Parzen.[13]

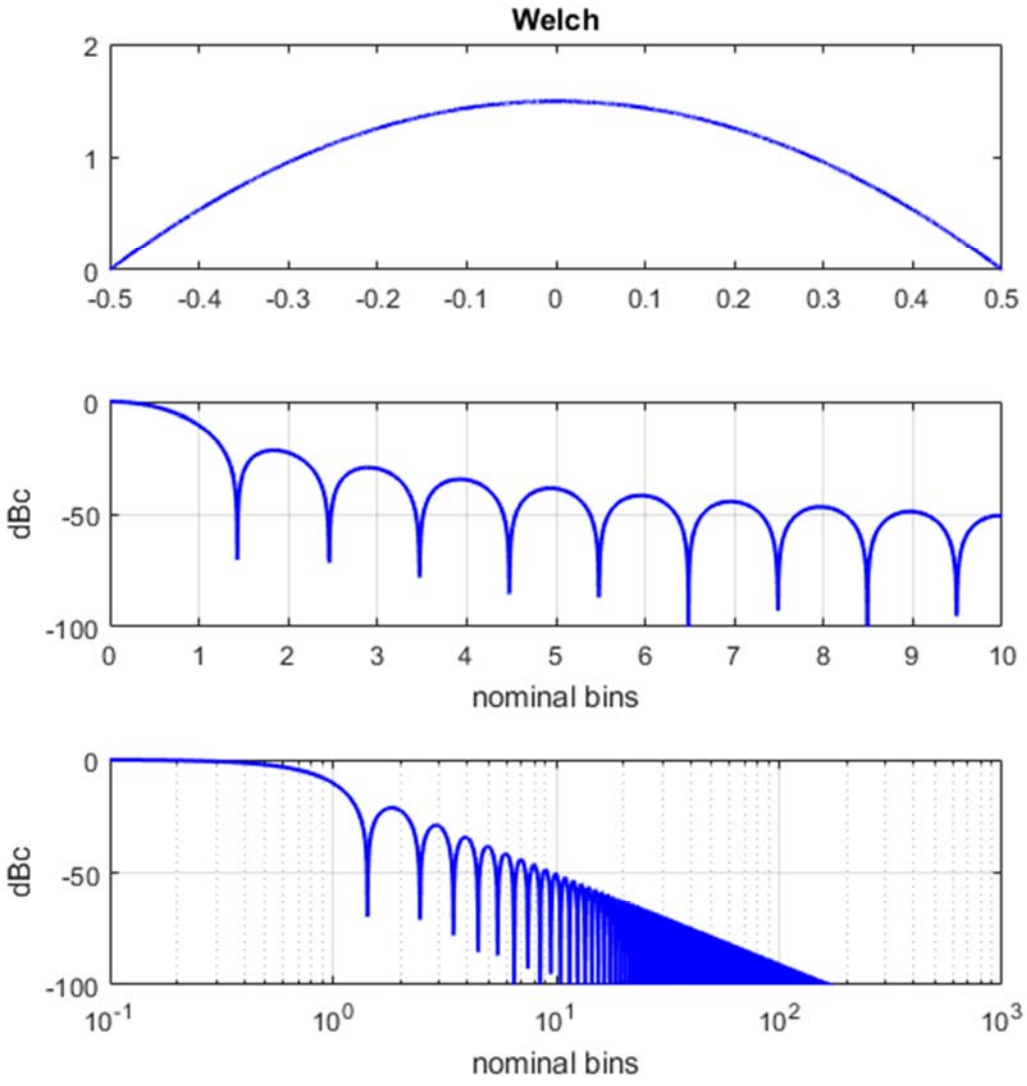


WINDOW SPECTRUM CHARACTERISTICS

half-power bandwidth = 1.1554 (normalized to 1/T)
-3 dB bandwidth = 1.1535 (normalized to 1/T)
-18 dB bandwidth = 2.4331 (normalized to 1/T)
noise bandwidth = 1.2001 (normalized to 1/T)
SNR loss = 0.79208 dB
first null = 1.4297 (normalized to 1/T)
PSL = -21.2929 dBc
ISL = -21.0298 dBc from first null outward

**Figure 15.**

## 4.6 Connes

This window taper function is a member of a family of Polynomial window taper functions. Specifically, it is the square of an inverted parabola with form scaled to provide unit DC response as

$$w(t) = A\frac{\left(\alpha^2 - 4t^2\right)^2}{\alpha^4}\,\mathrm{rect}(t), \tag{109}$$

with parameter

$$\alpha > 0\text{, but more typically } \alpha \geq 1\text{, and often just } \alpha = 1. \tag{110}$$

and with scale factor

$$A = \frac{15\alpha^4}{3 - 10\alpha^2 + 15\alpha^4}, \tag{111}$$

The Fourier Transform of the continuous time window taper function is calculated as

$$W(f) = \frac{A}{\alpha^4(\pi f)^5}\left[\begin{array}{c}\left(24 + 4\left(\alpha^2 - 3\right)(\pi f)^2 + \left(\alpha^2 - 1\right)^2(\pi f)^4\right)\sin(\pi f) \\ -4(\pi f)\left(6 + \left(\alpha^2 - 1\right)(\pi f)^2\right)\cos(\pi f)\end{array}\right]. \tag{112}$$

Plots and characteristics for a sample family member are given in Figure 16.

Several sources describe the Connes window, including Anterrieu, et al.[6]

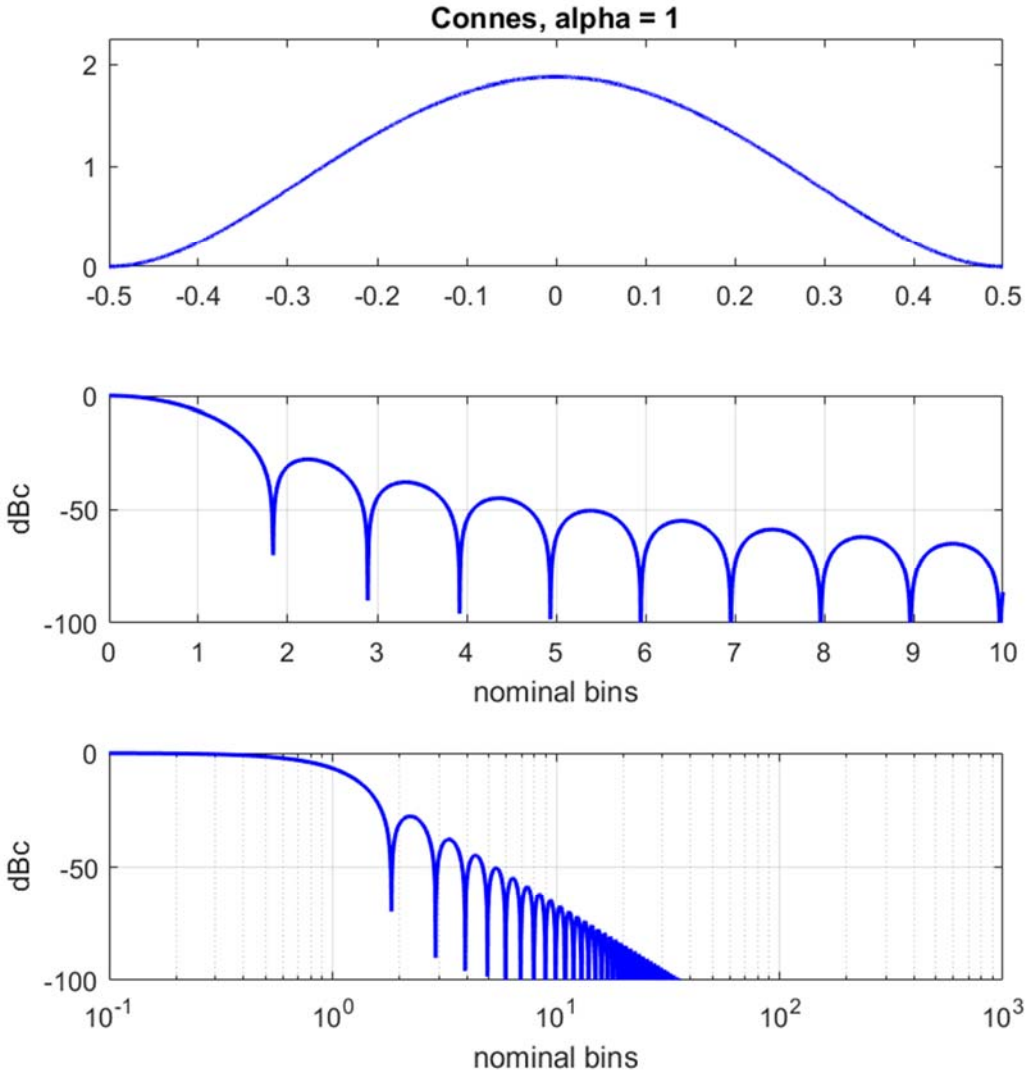


WINDOW SPECTRUM CHARACTERISTICS

half-power bandwidth = 1.3748 (normalized to 1/T)
-3 dB bandwidth = 1.3726 (normalized to 1/T)
-18 dB bandwidth = 2.9925 (normalized to 1/T)
noise bandwidth = 1.4287 (normalized to 1/T)
SNR loss = 1.549 dB
first null = 1.8359 (normalized to 1/T)
PSL = -27.7222 dBc
ISL = -28.6901 dBc from first null outward

**Figure 16.**

## 4.7 Parzen Algebraic Family

Parzen[15] also proposed a generalized window characteristic, that he called an Algebraic Family of windows, with form that we scale to provide unit DC response as

$$w(t) = A\left(1 - \gamma |2t|^{u}\right) \mathrm{rect}(t), \tag{113}$$

where parameters are constrained to

$$\begin{aligned} &0 < \gamma \le 1, \text{ and} \\ &u > 0, \end{aligned} \tag{114}$$

and with scale factor

$$A = \left(1 - \frac{\gamma}{1+u}\right)^{-1}. \tag{115}$$

The Welch window taper function of the previous section is simply the case where $\gamma = 1$ and $u = 2$.

The Fourier Transform of the continuous time window taper function is not readily calculated in closed-form. It may be numerically calculated for specific parameters, i.e. using a DFT on discrete-time samples of the window function.

Figure 17 illustrates the arbitrary case for $\gamma = 0.95$ and $u = 1.35$.

Parzen[1] additionally presents a Cosine Family, Exponential Family, and Geometric Family of window functions. These will be discussed later.

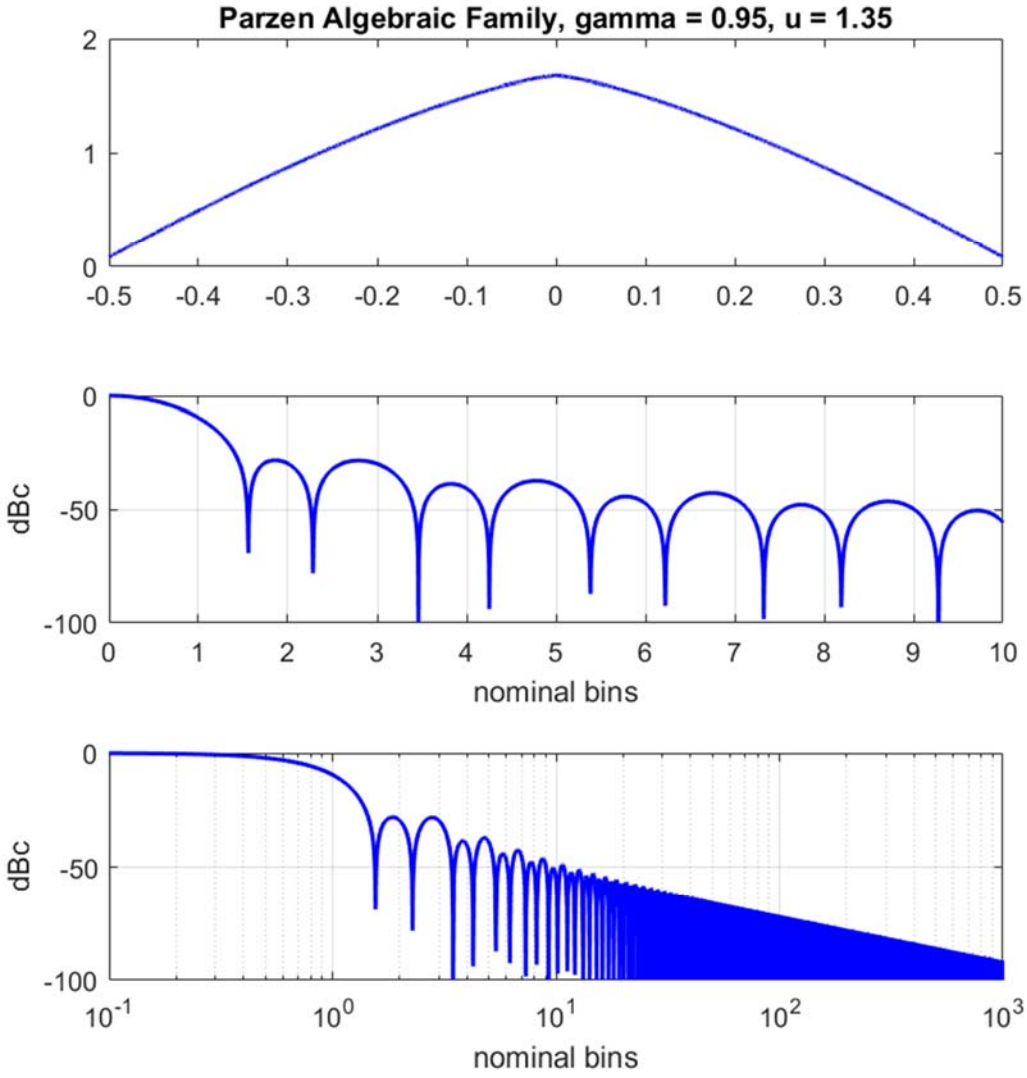


WINDOW SPECTRUM CHARACTERISTICS

half-power bandwidth = 1.181 (normalized to 1/T)
-3 dB bandwidth = 1.1791 (normalized to 1/T)
-18 dB bandwidth = 2.5521 (normalized to 1/T)
noise bandwidth = 1.2269 (normalized to 1/T)
SNR loss = 0.88799 dB
first null = 1.5586 (normalized to 1/T)
PSL = -28.1244 dBc
ISL = -25.5919 dBc from first null outward

**Figure 17.**

## 4.8 Singla-Singh Polynomial

Any number of polynomials might be used to generate all manner of window taper functions. We present here but one example, from Singla and Singh,[16] with form scaled for unit DC gain as

$$w(t) = 2\left(1 - 4t^2\left(3 - 4|t|\right)\right)\text{rect}(t). \tag{116}$$

The Fourier Transform of the continuous time window taper function is calculated as

$$W(f) = \frac{12}{\pi^4 f^4}\left(2 - 2\cos(\pi f) - \pi f \sin(\pi f)\right). \tag{117}$$

Plots and characteristics are given in Figure 18.

Singla and Singh present several others.

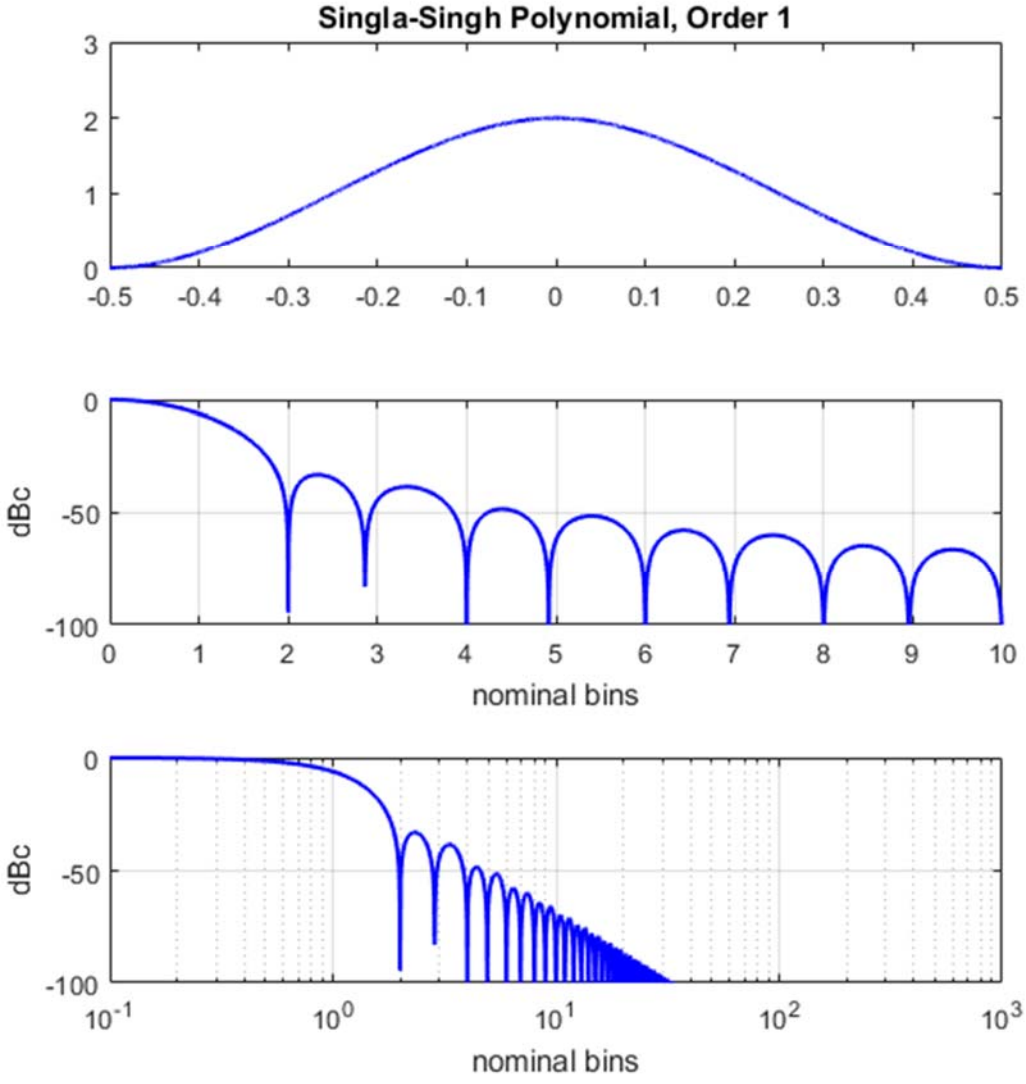


WINDOW SPECTRUM CHARACTERISTICS

half-power bandwidth = 1.4265 (normalized to 1/T)
-3 dB bandwidth = 1.4242 (normalized to 1/T)
-18 dB bandwidth = 3.1551 (normalized to 1/T)
noise bandwidth = 1.4858 (normalized to 1/T)
SNR loss = 1.7196 dB
first null = 2 (normalized to 1/T)
PSL = -33.0607 dBc
ISL = -33.9165 dBc from first null outward

**Figure 18.**

## 4.9 Sinc Lobe (a.k.a. Riemann, Daniell)

This window taper function is defined as the central lobe of the sinc function. As such, scaled for unit DC gain, we identify

$$w(t) = A\,\mathrm{sinc}(2t)\,\mathrm{rect}(t), \tag{118}$$

where we numerically calculate

$$A \approx 1.69638. \tag{119}$$

The Fourier Transform of the continuous time window taper function is not readily calculated in closed-form. Consequently, we simply identify it as

$$W(f) = A\int_{-1/2}^{1/2} \mathrm{sinc}(2t)\,e^{-j2\pi ft}\,dt, \tag{120}$$

but note that this can be written as the convolution

$$W(f) = \frac{A}{2}\,\mathrm{rect}\left(\frac{f}{2}\right) * \mathrm{sinc}(f). \tag{121}$$

Plots and characteristics are given in Figure 19.

Harris[4] calls this a Riemann Window, referencing Bary.[17]

Parzen[13] associates this window with Daniell.

Some references also call this a Lanczos window, although others use this name as a family of windows of which the Sinc Lobe is merely a specific member. We will proceed in this report with the latter definition.

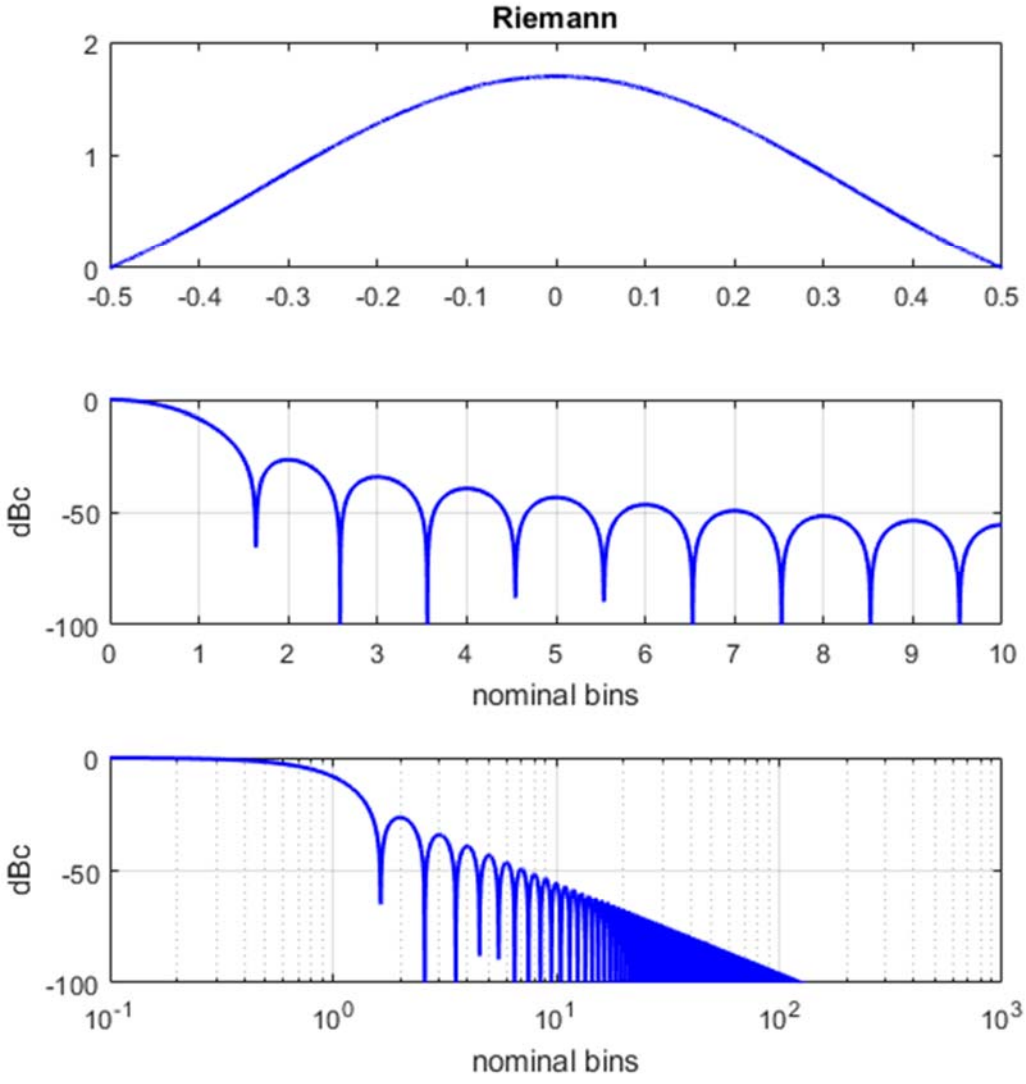


WINDOW SPECTRUM CHARACTERISTICS

half-power bandwidth = 1.2516 (normalized to 1/T)
-3 dB bandwidth = 1.2495 (normalized to 1/T)
-18 dB bandwidth = 2.7017 (normalized to 1/T)
noise bandwidth = 1.2991 (normalized to 1/T)
SNR loss = 1.1365 dB
first null = 1.6367 (normalized to 1/T)
PSL = -26.4051 dBc
ISL = -26.7918 dBc from first null outward

**Figure 19.**

## 4.10 Fejér

This window taper function is defined by Achieser[18] as the central lobe of the sinc function squared. As such, scaled for unit DC gain, we identify

$$w(t) = A\,\mathrm{sinc}^2(2t)\,\mathrm{rect}(t), \tag{122}$$

where we numerically calculate

$$A \approx 2.21527. \tag{123}$$

The Fourier Transform of the continuous time window taper function is not readily calculated in closed-form. Consequently, we simply identify it as

$$W(f) = A\int_{-1/2}^{1/2} \mathrm{sinc}^2(2t)\,e^{-j2\pi ft}dt, \tag{124}$$

but note that this can be written as the convolution

$$W(f) = \frac{A}{2}\Lambda\left(\frac{f}{2}\right) * \mathrm{sinc}(f). \tag{125}$$

Plots and characteristics are given in Figure 20.

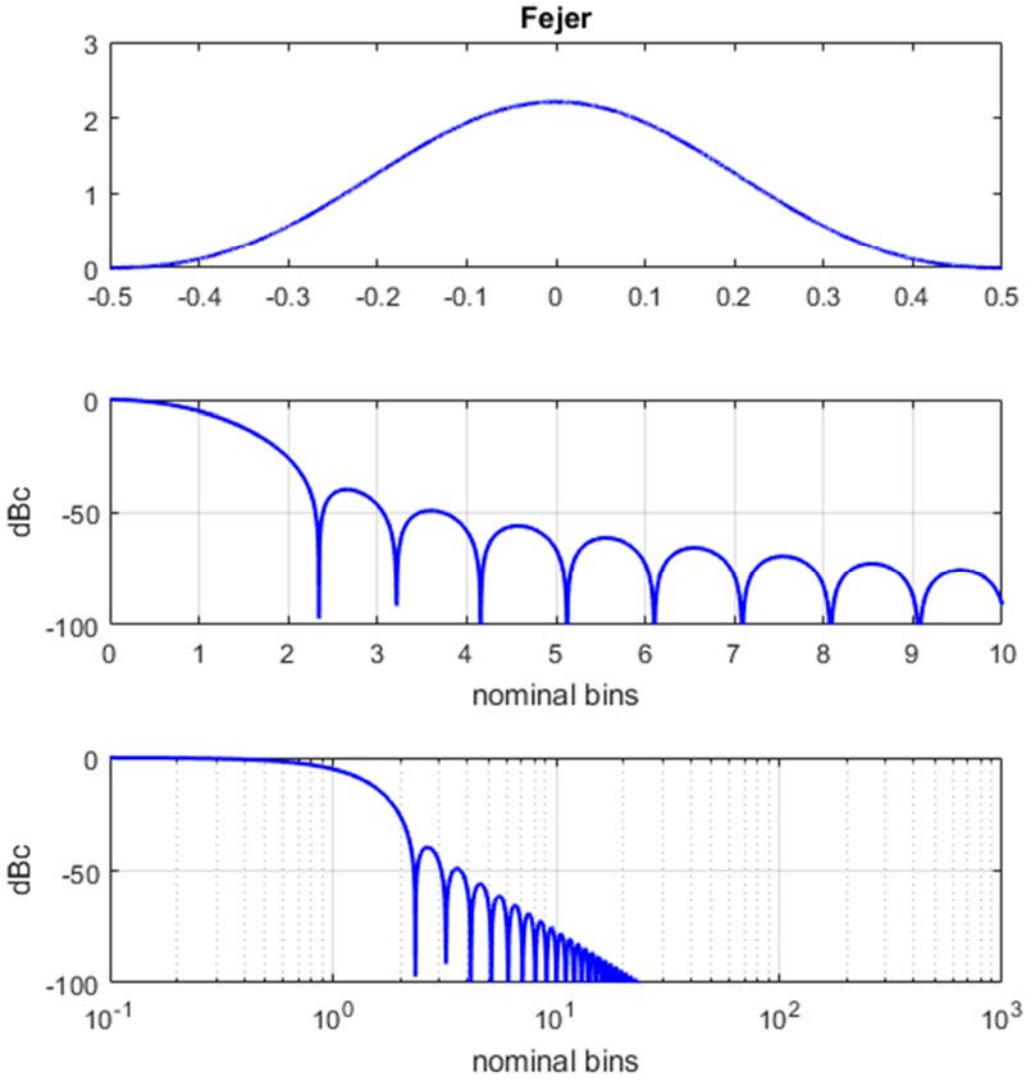


WINDOW SPECTRUM CHARACTERISTICS

half-power bandwidth = 1.56 (normalized to 1/T)
-3 dB bandwidth = 1.5574 (normalized to 1/T)
-18 dB bandwidth = 3.5195 (normalized to 1/T)
noise bandwidth = 1.6311 (normalized to 1/T)
SNR loss = 2.1248 dB
first null = 2.3438 (normalized to 1/T)
PSL = -39.6017 dBc
ISL = -41.8492 dBc from first null outward

**Figure 20.**

## 4.11 de la Vallée Poussin (a.k.a. Jackson)

This window taper function is defined by Achieser[18] as the central lobe of the sinc function to the fourth power. As such, scaled for unit DC gain, we identify

$$w(t) = A\,\mathrm{sinc}^4(2t)\,\mathrm{rect}(t), \tag{126}$$

where we numerically calculate

$$A \approx 3.00886. \tag{127}$$

The Fourier Transform of the continuous time window taper function is not readily calculated in closed-form. Consequently, we simply identify it as

$$W(f) = A\int_{-1/2}^{1/2} \mathrm{sinc}^4(2t)\,e^{-j2\pi ft}dt\,. \tag{128}$$

We note that this may be written as a convolution of two triangle functions and a sinc function.

Plots and characteristics are given in Figure 21.

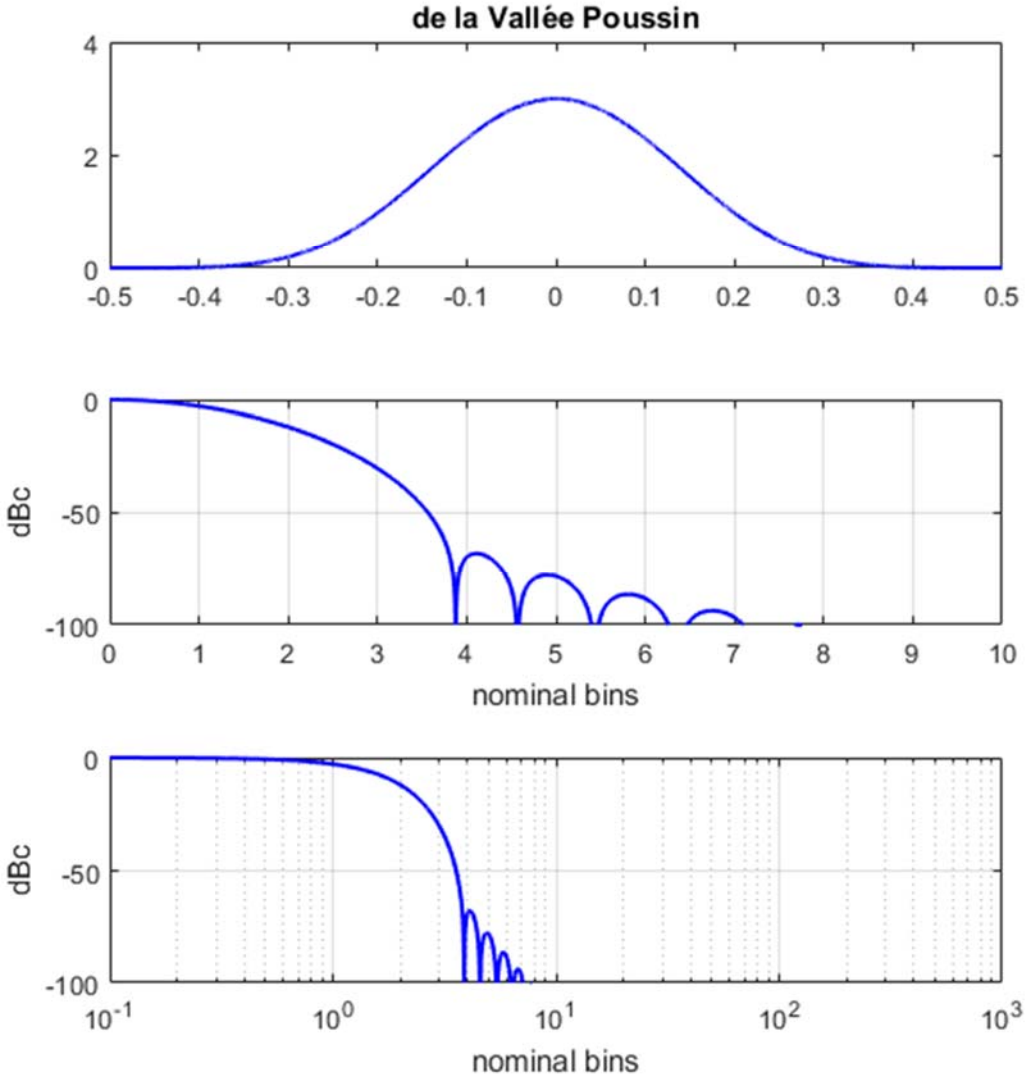


WINDOW SPECTRUM CHARACTERISTICS

half-power bandwidth = 2.0588 (normalized to 1/T)
-3 dB bandwidth = 2.0554 (normalized to 1/T)
-18 dB bandwidth = 4.8207 (normalized to 1/T)
noise bandwidth = 2.17 (normalized to 1/T)
SNR loss = 3.3646 dB
first null = 3.875 (normalized to 1/T)
PSL = -67.9755 dBc
ISL = -72.5827 dBc from first null outward

**Figure 21.**

## 4.12 Lanczos

Proakis and Manolakis[19] define this window as a family of windows that are a Sinc Lobe to some positive power. Accordingly, we identify the Lanczos window, scaled for unit DC gain, as

$$w(t) = A\,\mathrm{sinc}^{L}(2t)\,\mathrm{rect}(t), \tag{129}$$

where we identify the parameter that specifies the power as

$$L > 0\,. \tag{130}$$

We numerically calculate the gain parameter as

$$A = \left( \int_{-1/2}^{1/2} \mathrm{sinc}^{L}(2t)\,dt \right)^{-1}. \tag{131}$$

The Fourier Transform of the continuous time window taper function is not readily calculated in closed-form. Consequently, we simply identify it as

$$W(f) = A \int_{-1/2}^{1/2} \mathrm{sinc}^{L}(2t)\,e^{-j2\pi ft}dt\,. \tag{132}$$

We note that especially if $L$ is an integer value, this may be written as a convolution of multiple rect functions, perhaps triangle functions, and a sinc function.

We note that the Lanczos family of window taper functions includes the following members previously discussed

- Sinc Lobe, for $L = 1$,
- Fejér, for $L = 2$, and
- de la Vallée Poussin, for $L = 4$.

Plots and characteristics for $L = 3$ are given in Figure 22.

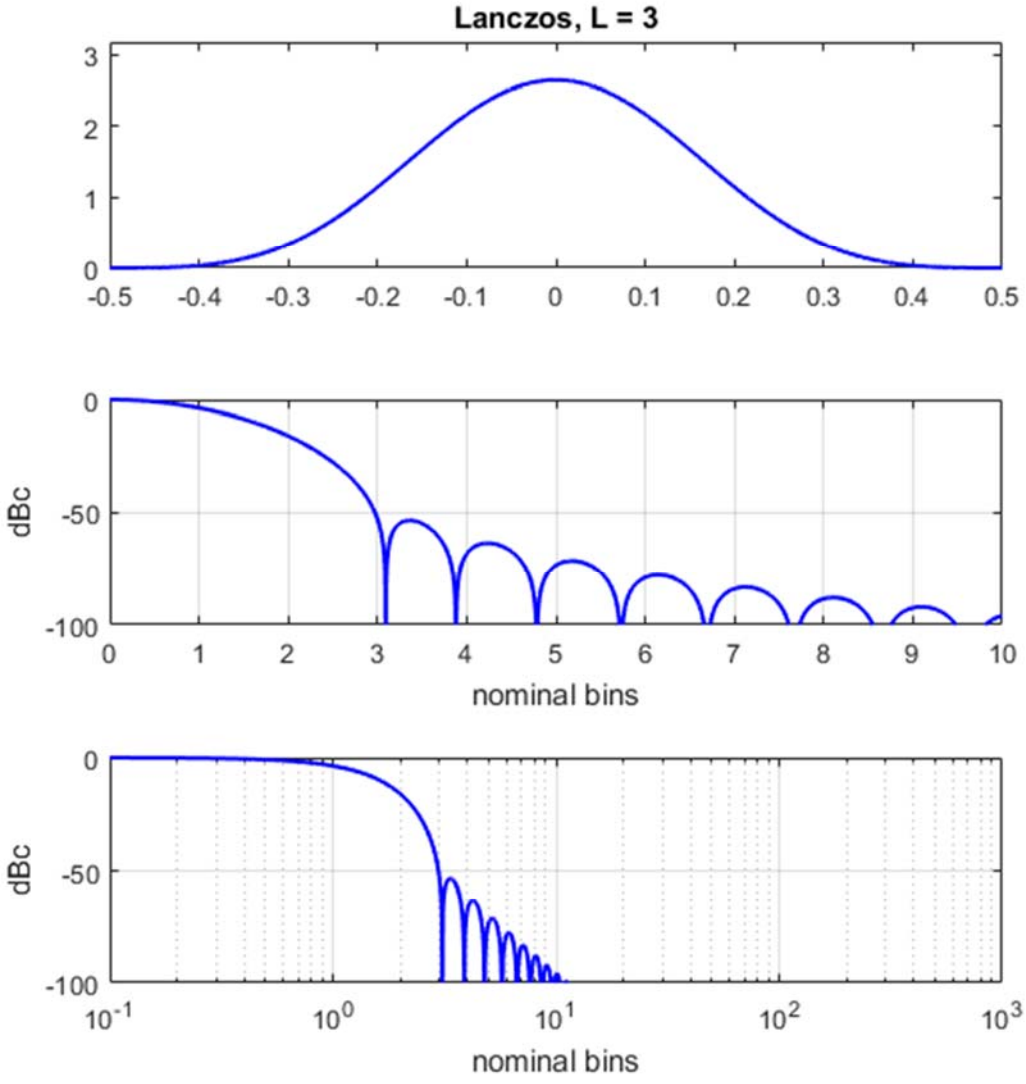


WINDOW SPECTRUM CHARACTERISTICS

half-power bandwidth = 1.8252 (normalized to 1/T)
-3 dB bandwidth = 1.8221 (normalized to 1/T)
-18 dB bandwidth = 4.2162 (normalized to 1/T)
noise bandwidth = 1.918 (normalized to 1/T)
SNR loss = 2.8286 dB
first null = 3.0938 (normalized to 1/T)
PSL = -53.3396 dBc
ISL = -56.8992 dBc from first null outward

**Figure 22.**

## 4.13 Hamming

The Hamming window is defined as a particular member of a family of "raised cosine" functions of the form scaled for unit DC gain with

$$w(t) = \left(1 + \frac{(1-\alpha)}{\alpha}\cos(2\pi t)\right)\mathrm{rect}(t). \tag{133}$$

In particular, for the Hamming window, the parameter α is chosen to minimize the PSL, which causes us to select

$$\alpha = \frac{25}{46}, \tag{134}$$

although more often this is rounded to

$$\alpha = 0.54. \tag{135}$$

The Fourier Transform of the continuous time window taper function is calculated as

$$W(f) = \left[\mathrm{sinc}(f) + \frac{(1-\alpha)}{2\alpha}\mathrm{sinc}(f-1) + \frac{(1-\alpha)}{2\alpha}\mathrm{sinc}(f+1)\right]. \tag{136}$$

Plots and characteristics are given in Figure 23. Note that sidelobes fall off at a rate of –6 dB per octave due to the residual discontinuity at the window ends.

The Hamming window is named after American mathematician Richard Wesley Hamming.

The earliest discussion of the benefits of spectral smoothing with what is later named the Hamming window is in an unpublished memorandum by Tukey and Hamming.[20]

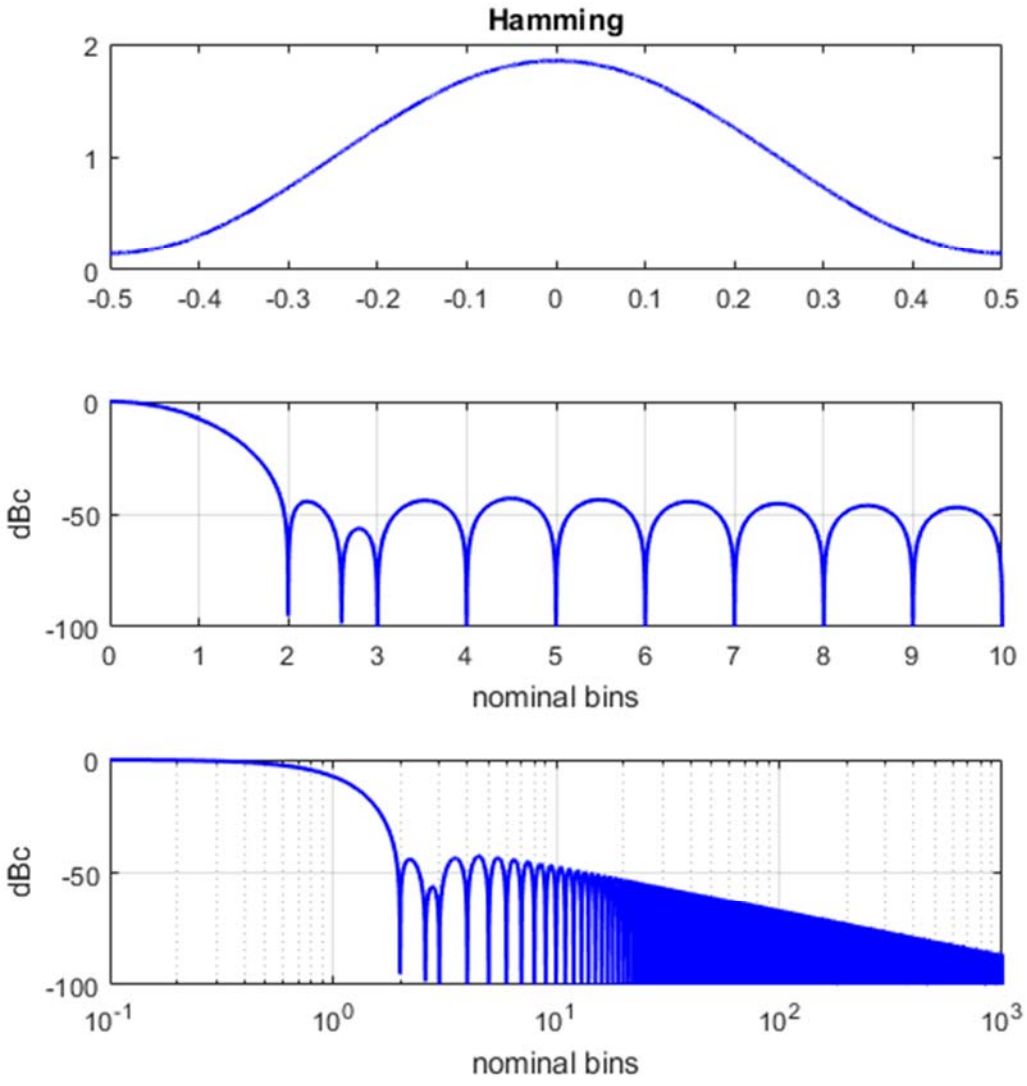


WINDOW SPECTRUM CHARACTERISTICS

half-power bandwidth = 1.303 (normalized to 1/T)
-3 dB bandwidth = 1.3009 (normalized to 1/T)
-18 dB bandwidth = 2.9418 (normalized to 1/T)
noise bandwidth = 1.3629 (normalized to 1/T)
SNR loss = 1.3446 dB
first null = 2 (normalized to 1/T)
PSL = -42.6751 dBc
ISL = -34.3605 dBc from first null outward

**Figure 23.**

## 4.14 Hann (a.k.a. Hanning)

The Hann window is defined as a particular member of a family of "raised cosine" functions of the form scaled for unit DC gain with

$$w(t) = \left(1 + \frac{(1-\alpha)}{\alpha}\cos(2\pi t)\right)\mathrm{rect}(t). \tag{137}$$

In particular, for the Hann window

$$\alpha = \frac{1}{2}, \tag{138}$$

chosen to maximize the asymptotic sidelobe taper rate. The Hann window may also then be written as

$$w(t) = \left(1 + \cos(2\pi t)\right)\mathrm{rect}(t) = 2\cos^2(\pi t)\,\mathrm{rect}(t). \tag{139}$$

As such, it is also a member of the "Power-of-cosine" ($\cos^m$) window family.

As with the Hamming window, the Fourier Transform of the continuous time window taper function is calculated as

$$W(f) = \left[\mathrm{sinc}(f) + \frac{(1-\alpha)}{2\alpha}\mathrm{sinc}(f-1) + \frac{(1-\alpha)}{2\alpha}\mathrm{sinc}(f+1)\right]. \tag{140}$$

Plots and characteristics are given in Figure 24. Note how the sidelobes fall off at a fairly steep −18 dB per octave.

The Hann window is named after Austrian meteorologist Julius Ferdinand von Hann in an early reference by Blackman and Tukey.[8]

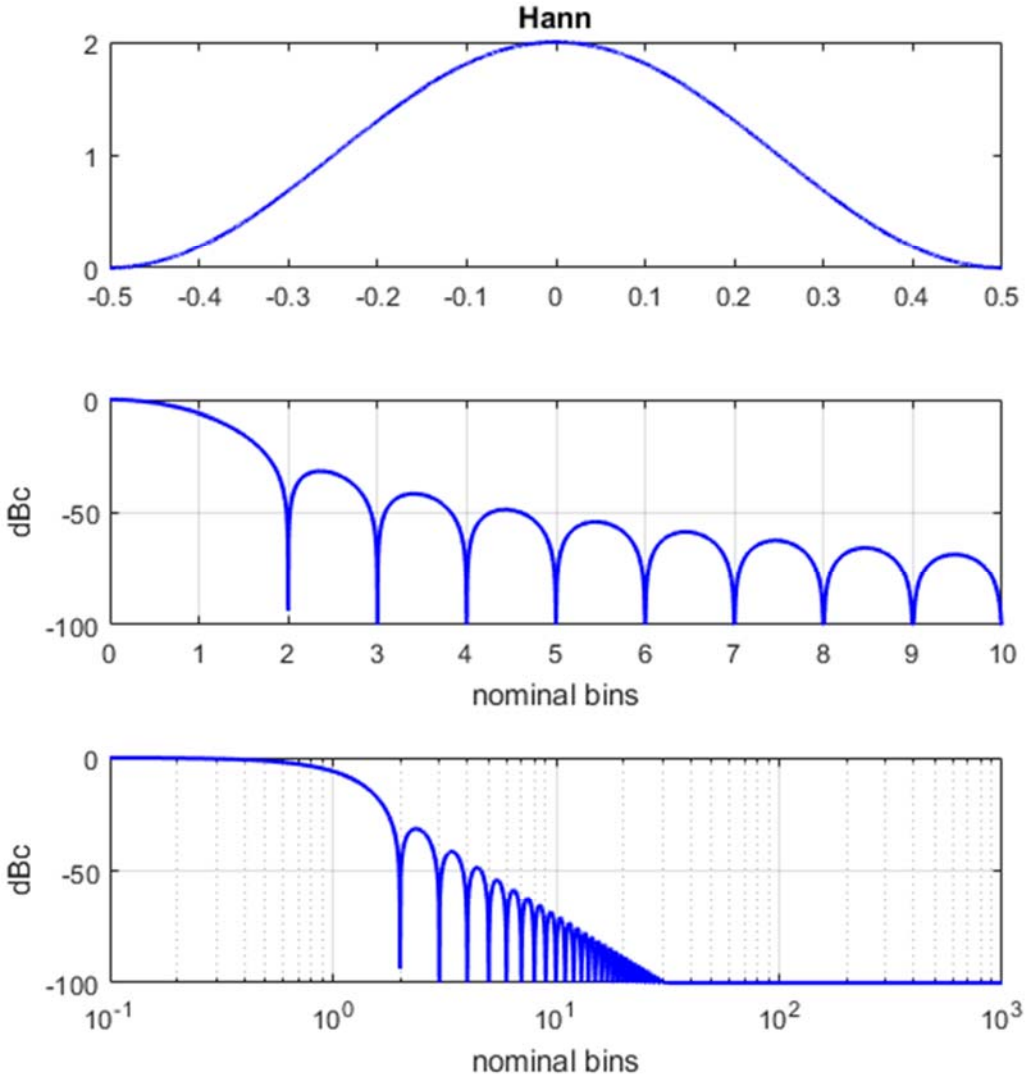


WINDOW SPECTRUM CHARACTERISTICS

half-power bandwidth = 1.4405 (normalized to 1/T)
-3 dB bandwidth = 1.4381 (normalized to 1/T)
-18 dB bandwidth = 3.1794 (normalized to 1/T)
noise bandwidth = 1.4999 (normalized to 1/T)
SNR loss = 1.7606 dB
first null = 2 (normalized to 1/T)
PSL = -31.4674 dBc
ISL = -32.8867 dBc from first null outward

**Figure 24.**

## 4.15 Generalized Raised Cosine

The Generalized Raised Cosine window is defined as a family of "raised cosine" functions of the form scaled for unit DC gain with

$$w(t) = \left(1 + \frac{(1-\alpha)}{\alpha}\cos(2\pi t)\right)\mathrm{rect}(t), \tag{141}$$

where we might choose the parameter $\alpha$ in the range

$$1/2 \le \alpha \le 1. \tag{142}$$

Specific values of $\alpha$ yield Hamming, Hann, or even Rectangular window taper functions. However, other values of $\alpha$ might be used. Various $\alpha$ generally trade between PSL and the sidelobe taper rate.

The Fourier Transform of the continuous time window taper function is calculated as

$$W(f) = \left[\mathrm{sinc}(f) + \frac{(1-\alpha)}{2\alpha}\mathrm{sinc}(f-1) + \frac{(1-\alpha)}{2\alpha}\mathrm{sinc}(f+1)\right]. \tag{143}$$

Plots and characteristics are given in Figure 25 for $\alpha = 0.6$.

This window taper function is also sometimes called a "Generalized Hamming" window, although we will attribute this name to a different formulation.

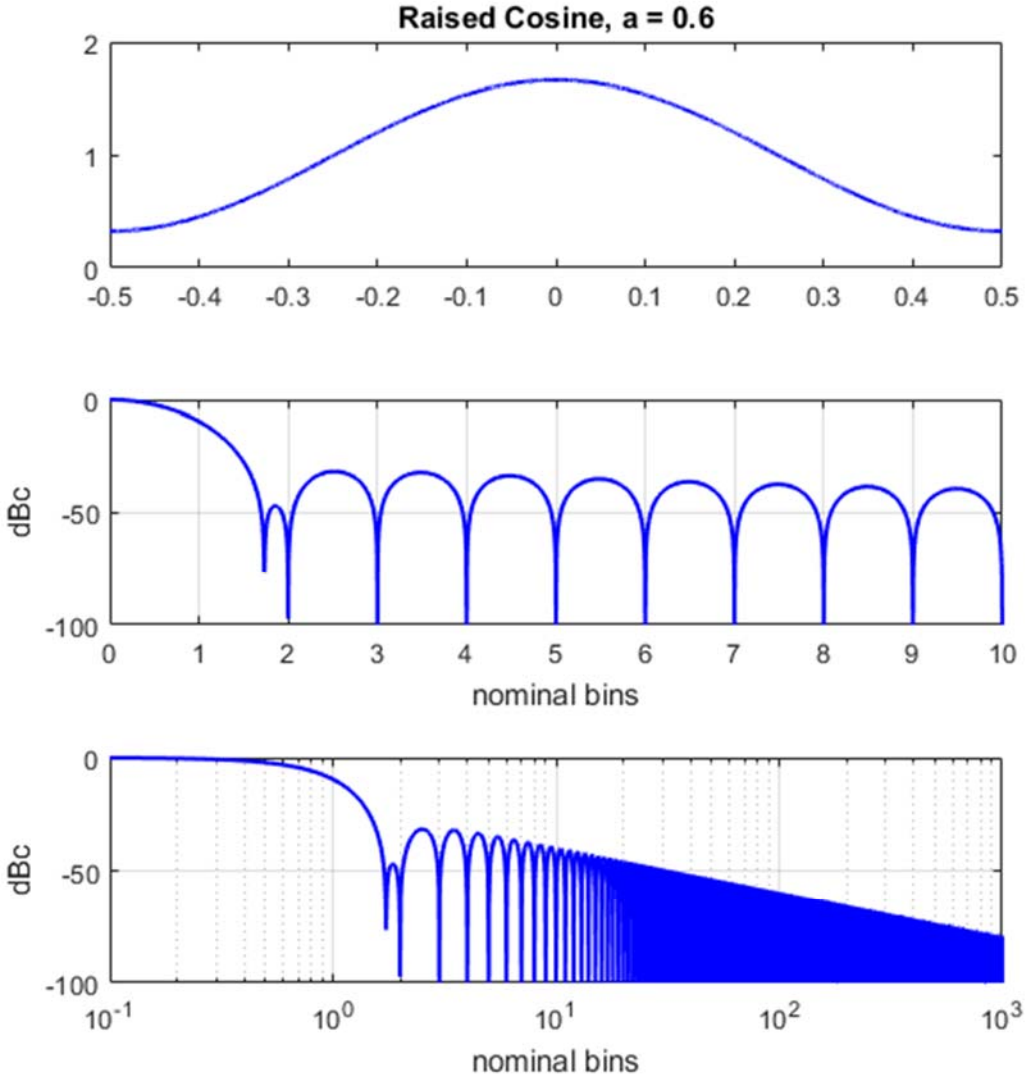


WINDOW SPECTRUM CHARACTERISTICS

half-power bandwidth = 1.1695 (normalized to 1/T)
-3 dB bandwidth = 1.1676 (normalized to 1/T)
-18 dB bandwidth = 2.5981 (normalized to 1/T)
noise bandwidth = 1.2223 (normalized to 1/T)
SNR loss = 0.87161 dB
first null = 1.7305 (normalized to 1/T)
PSL = -31.5966 dBc
ISL = -24.9946 dBc from first null outward

**Figure 25.**

## 4.16 Generalized Hamming (a.k.a. Webster-Hamming)

The concept of a "generalized Hamming" window taper function was proposed by Webster,[21] who asserted a form which we scale for unit DC gain as

$$w(t) = A\left(\alpha \cos^{v}(\pi t) + (1-\alpha)\cos^{v+2}(\pi t)\right)\mathrm{rect}(t), \tag{144}$$

where we select the parameter $\alpha$ as

$$\alpha = \frac{2+3v+v^2}{23+9v+v^2}, \tag{145}$$

and the power to which the cosines are raised is defined by parameter

$$v > -1/2, \tag{146}$$

with gain parameter calculated as

$$A = \frac{2\sqrt{\pi}\,\Gamma\left(\frac{4+v}{2}\right)}{(1+\alpha+v)\Gamma\left(\frac{1+v}{2}\right)}. \tag{147}$$

The specific value $v = 0$ yields the traditional Hamming window taper function.

The Fourier Transform of the continuous time window taper function is not readily calculated in closed-form. It may be numerically calculated for specific parameters, i.e. using a DFT on discrete-time samples of the window function.

Plots and characteristics are given in Figure 26 for $v = 1.0$.

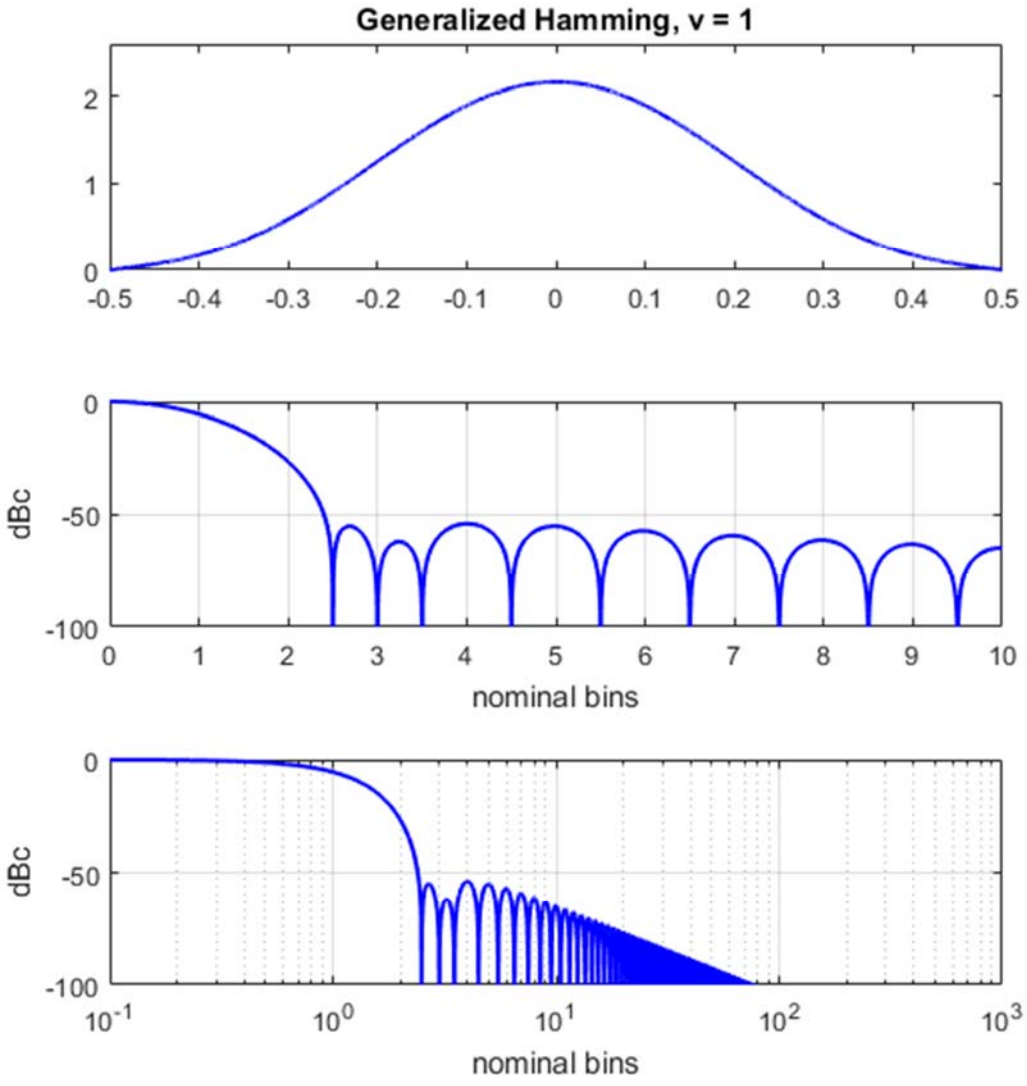


WINDOW SPECTRUM CHARACTERISTICS

half-power bandwidth = 1.5001 (normalized to 1/T)
-3 dB bandwidth = 1.4976 (normalized to 1/T)
-18 dB bandwidth = 3.4378 (normalized to 1/T)
noise bandwidth = 1.5735 (normalized to 1/T)
SNR loss = 1.9688 dB
first null = 2.5 (normalized to 1/T)
PSL = -53.891 dBc
ISL = -50.2509 dBc from first null outward

**Figure 26.**

## 4.17 Power-of-Cosine (a.k.a. Cos$^m$)

The generalized Power-of-Cosine window is defined as a family of functions of the form scaled for unit DC gain as

$$w(t) = \left( \frac{\sqrt{\pi}\,\Gamma\left(1+\frac{m}{2}\right)}{\Gamma\left(\frac{1}{2}+\frac{m}{2}\right)} \right) \cos^m(\pi t)\,\mathrm{rect}(t), \tag{148}$$

where

$$\begin{aligned} &m = \text{integer values, } m \geq 0 \text{ , and} \\ &\Gamma(z) = \text{ gamma function.} \end{aligned} \tag{149}$$

The case for $m = 0$ yields the Rectangle window.

The case for $m = 1$ is sometimes called a "Cosine Lobe" window, and is plotted in Figure 27.

The case for $m = 2$ yields the Hann window.

The Fourier Transform of the continuous time window taper function for arbitrary *m* is not readily calculated in closed-form. It may be numerically calculated for specific parameters, i.e. using a DFT on discrete-time samples of the window function.

Plots and characteristics are given in Figure 28 for $m = 3$.

Plots and characteristics are given in Figure 29 for $m = 4$.

As *m* increases, sidelobes decrease, sidelobe taper gets steeper, but mainlobe width increases.

Although *m* is commonly specified to be an integer, we observe that non-integer values of *m* are also feasible, and might offer utility, too.

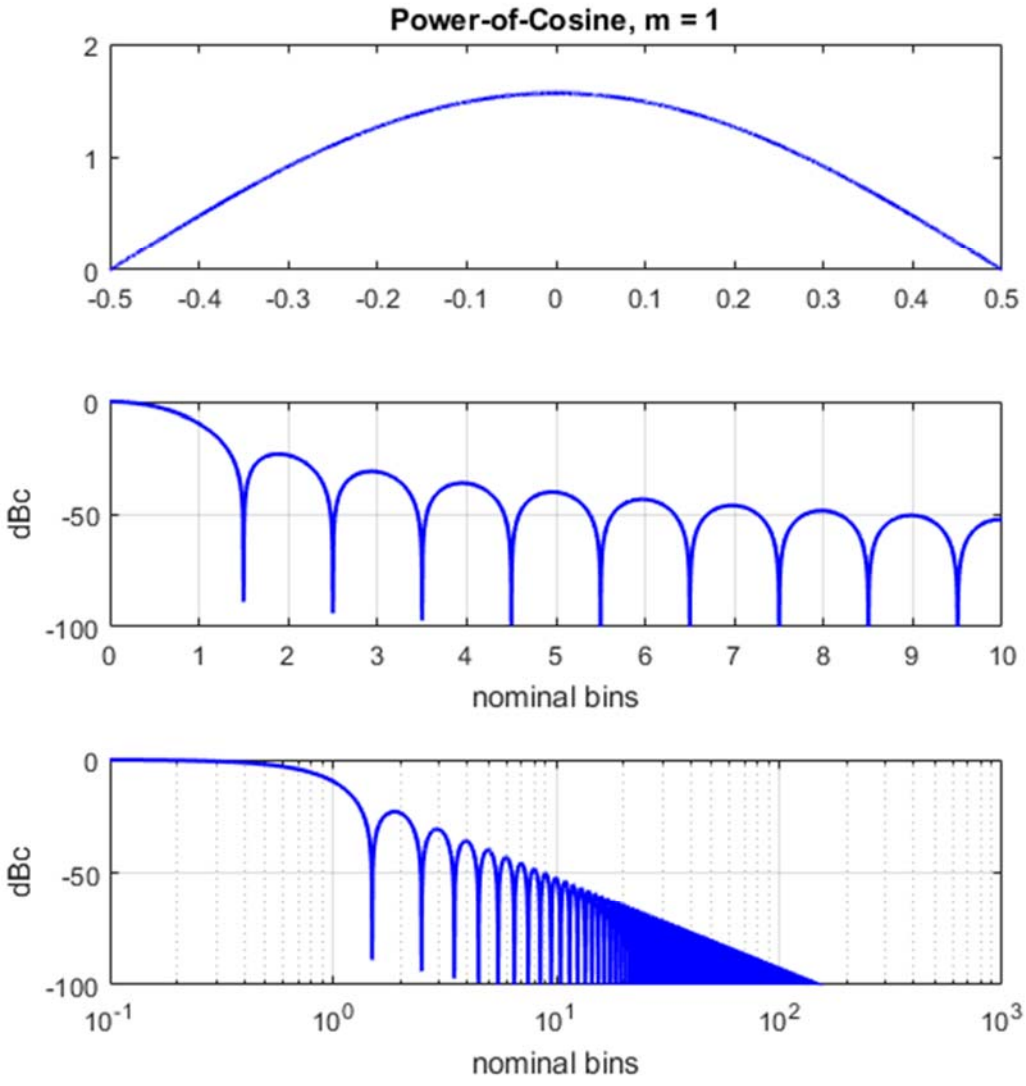


WINDOW SPECTRUM CHARACTERISTICS

half-power bandwidth = 1.189 (normalized to 1/T)
-3 dB bandwidth = 1.1871 (normalized to 1/T)
-18 dB bandwidth = 2.5263 (normalized to 1/T)
noise bandwidth = 1.2338 (normalized to 1/T)
SNR loss = 0.91236 dB
first null = 1.5 (normalized to 1/T)
PSL = -22.9988 dBc
ISL = -22.9634 dBc from first null outward

**Figure 27.**

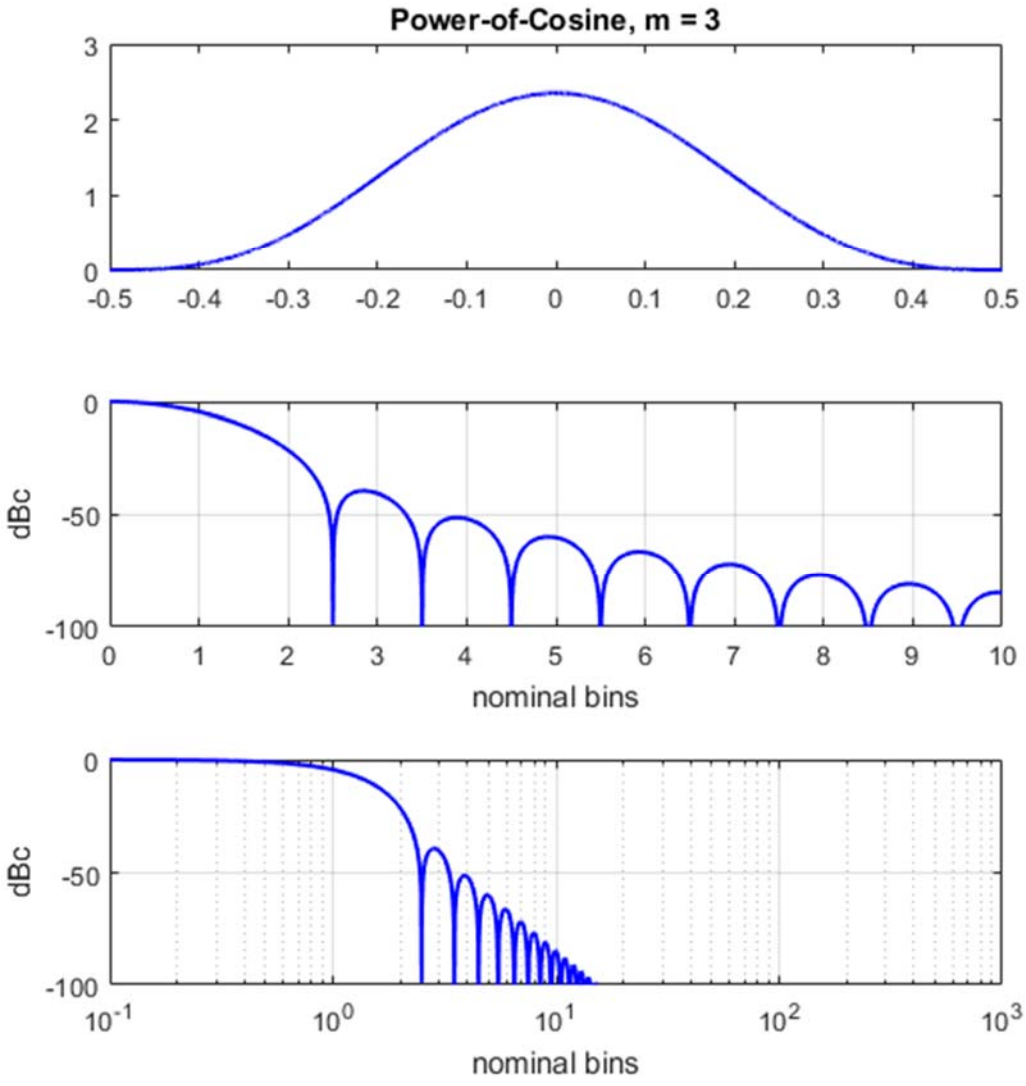


WINDOW SPECTRUM CHARACTERISTICS

half-power bandwidth = 1.6586 (normalized to 1/T)
-3 dB bandwidth = 1.6558 (normalized to 1/T)
-18 dB bandwidth = 3.7494 (normalized to 1/T)
noise bandwidth = 1.735 (normalized to 1/T)
SNR loss = 2.393 dB
first null = 2.5 (normalized to 1/T)
PSL = -39.2955 dBc
ISL = -41.6496 dBc from first null outward

**Figure 28.**

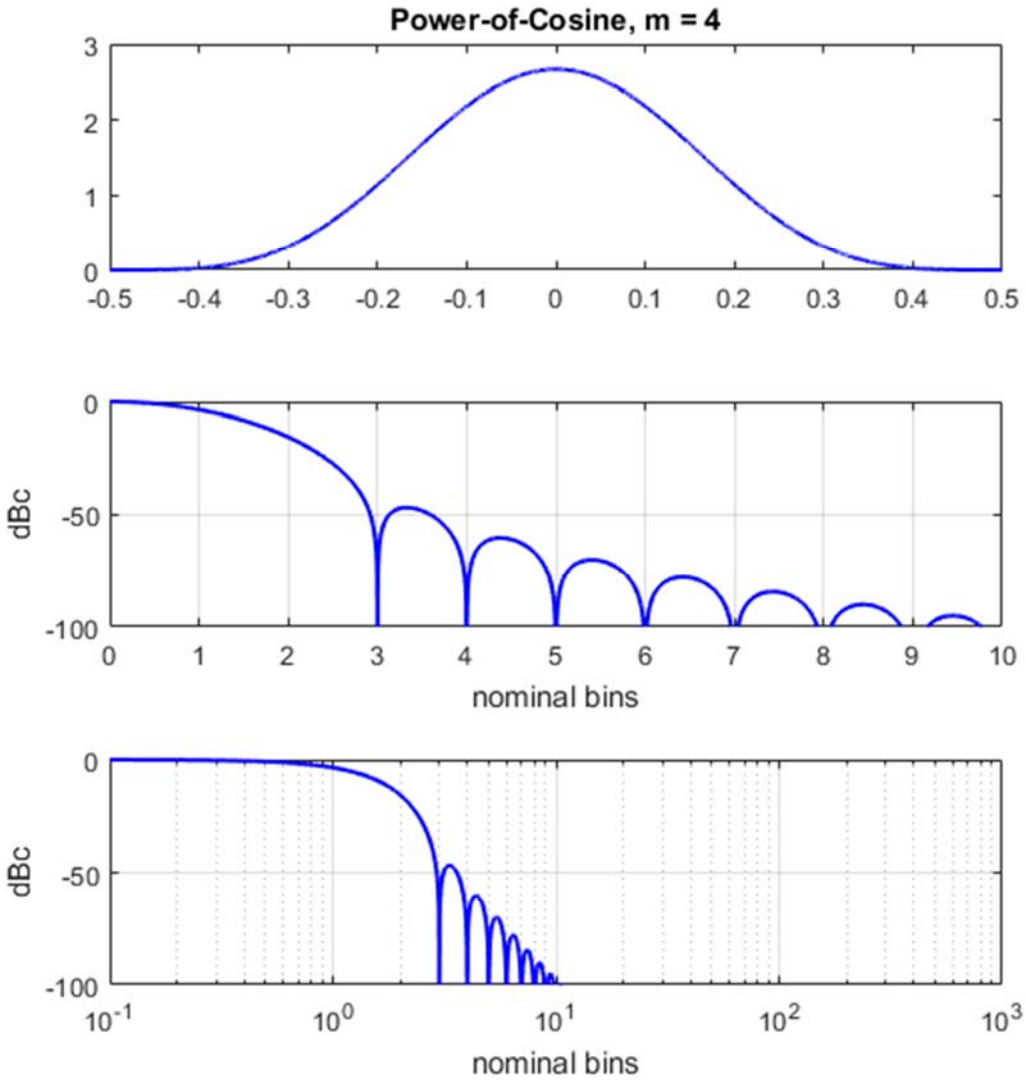


WINDOW SPECTRUM CHARACTERISTICS

half-power bandwidth = 1.8528 (normalized to 1/T)
-3 dB bandwidth = 1.8497 (normalized to 1/T)
-18 dB bandwidth = 4.2543 (normalized to 1/T)
noise bandwidth = 1.9446 (normalized to 1/T)
SNR loss = 2.8882 dB
first null = 3 (normalized to 1/T)
PSL = -46.7412 dBc
ISL = -49.7843 dBc from first null outward

**Figure 29.**

## 4.18 Raised Power-of-Cosine (a.k.a. General Cosine-Power)

The power-of-cosine window function of the previous section might be added to a rect function to yield a "raised power-of-cosine" window.[22] This window has the form scaled for unit DC gain as

$$w(t) = A\Big(\alpha + (1-\alpha)\cos^m(\pi t)\Big)\,\mathrm{rect}(t), \tag{150}$$

where

$$\begin{aligned} &\alpha = \text{ fractional ratio of pedestal for window, } 0 \le \alpha \le 1, \\ &m = \text{integer values, } m \ge 0, \end{aligned} \tag{151}$$

and the unit gain scale factor is

$$A = \left( \alpha + \frac{(1-\alpha)\Gamma\left(\frac{1+m}{2}\right)}{\sqrt{\pi}\,\Gamma\left(1+\frac{m}{2}\right)} \right)^{-1} . \tag{152}$$

The case for $\alpha = 0$ yields the power-of-cosine window of the previous section, and the case for $\alpha = 1$ yields the rectangle window.

The Fourier Transform of the continuous time window taper function for arbitrary *m* is not readily calculated in closed-form. It may be numerically calculated for specific parameters, i.e. using a DFT on discrete-time samples of the window function.

Plots and characteristics are given in Figure 30, Figure 31, and Figure 32 for various parameter combinations.

Although *m* is commonly specified to be an integer, we observe that non-integer values of *m* are also feasible, and might offer utility, too.

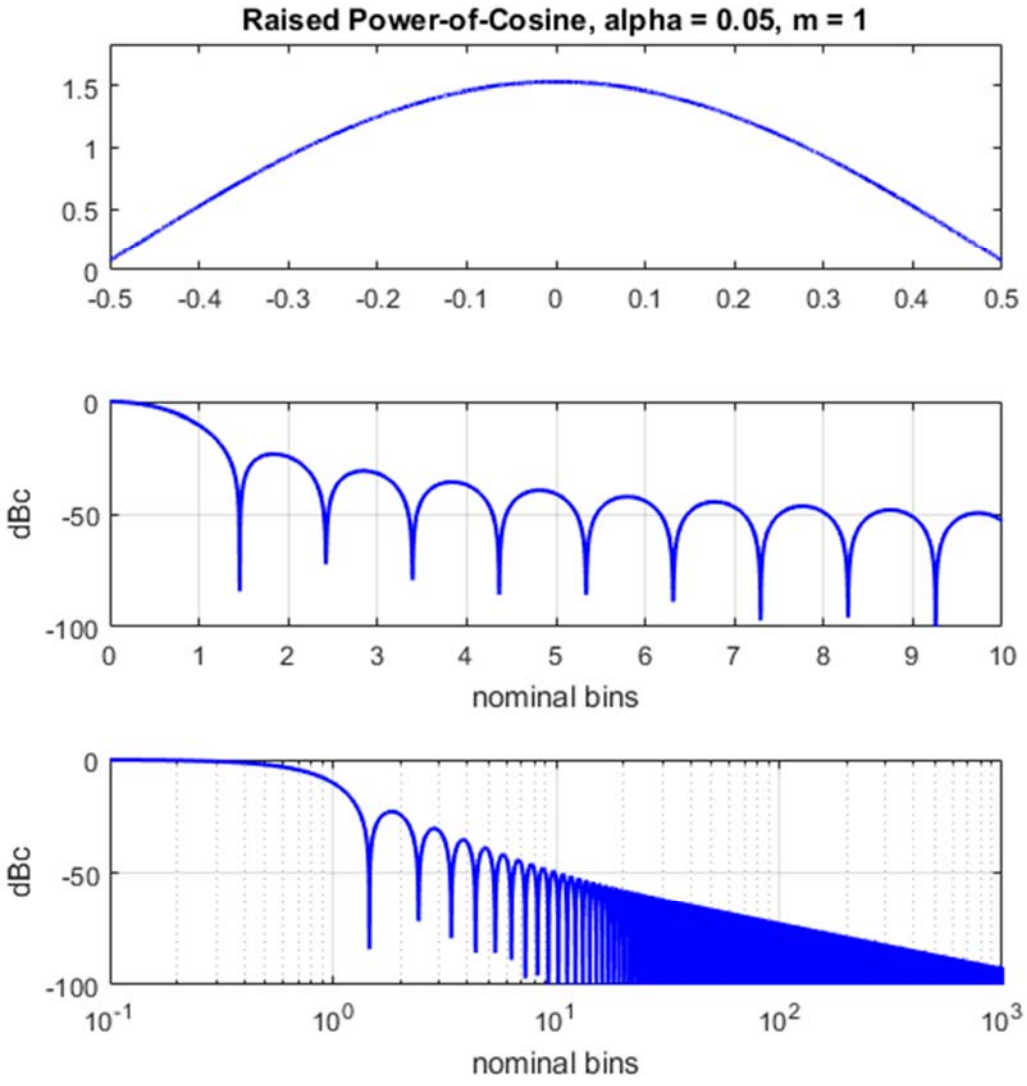


WINDOW SPECTRUM CHARACTERISTICS

half-power bandwidth = 1.1558 (normalized to 1/T)
-3 dB bandwidth = 1.1539 (normalized to 1/T)
-18 dB bandwidth = 2.4547 (normalized to 1/T)
noise bandwidth = 1.1994 (normalized to 1/T)
SNR loss = 0.79 dB
first null = 1.457 (normalized to 1/T)
PSL = -22.9868 dBc
ISL = -22.8295 dBc from first null outward

**Figure 30.**

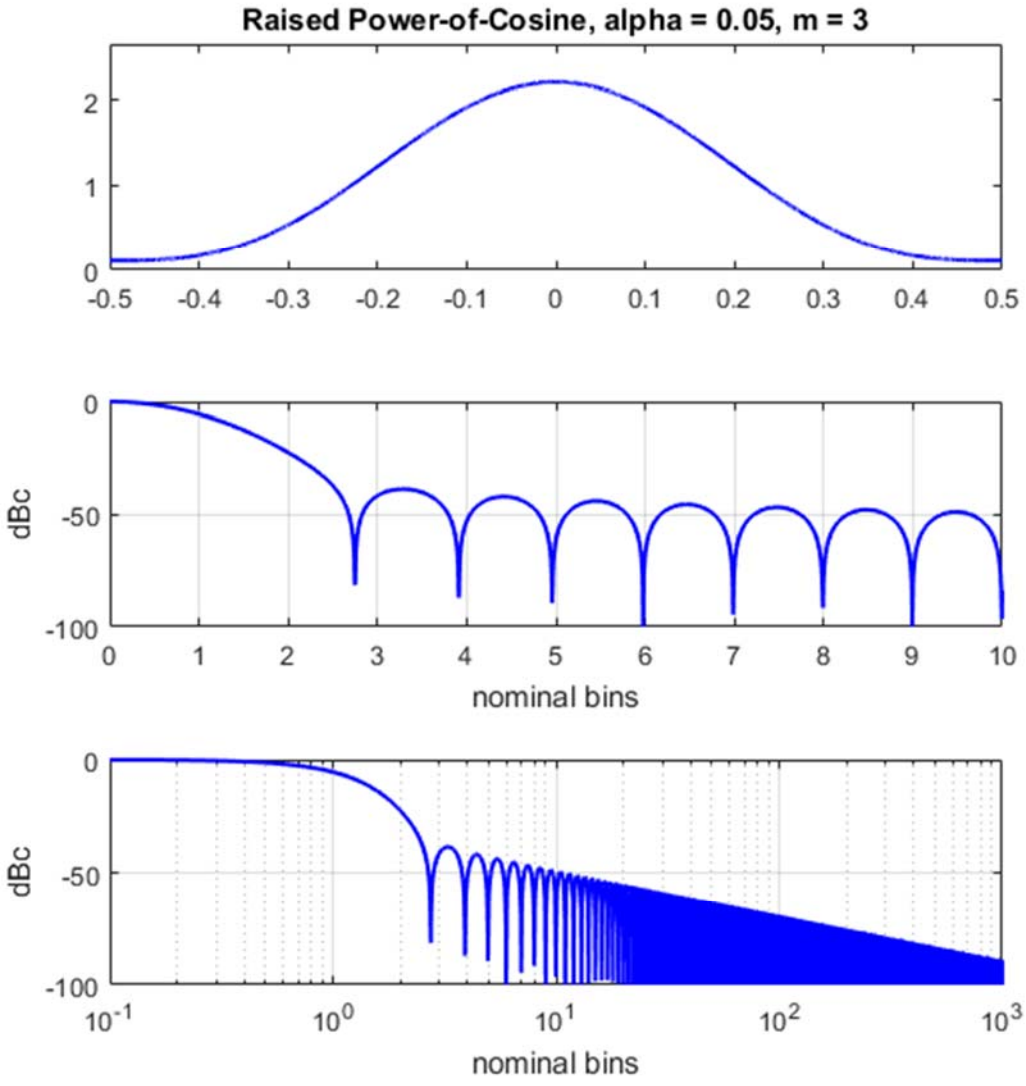


WINDOW SPECTRUM CHARACTERISTICS

half-power bandwidth = 1.491 (normalized to 1/T)
-3 dB bandwidth = 1.4885 (normalized to 1/T)
-18 dB bandwidth = 3.596 (normalized to 1/T)
noise bandwidth = 1.5818 (normalized to 1/T)
SNR loss = 1.991 dB
first null = 2.75 (normalized to 1/T)
PSL = -38.5457 dBc
ISL = -35.1559 dBc from first null outward

**Figure 31.**

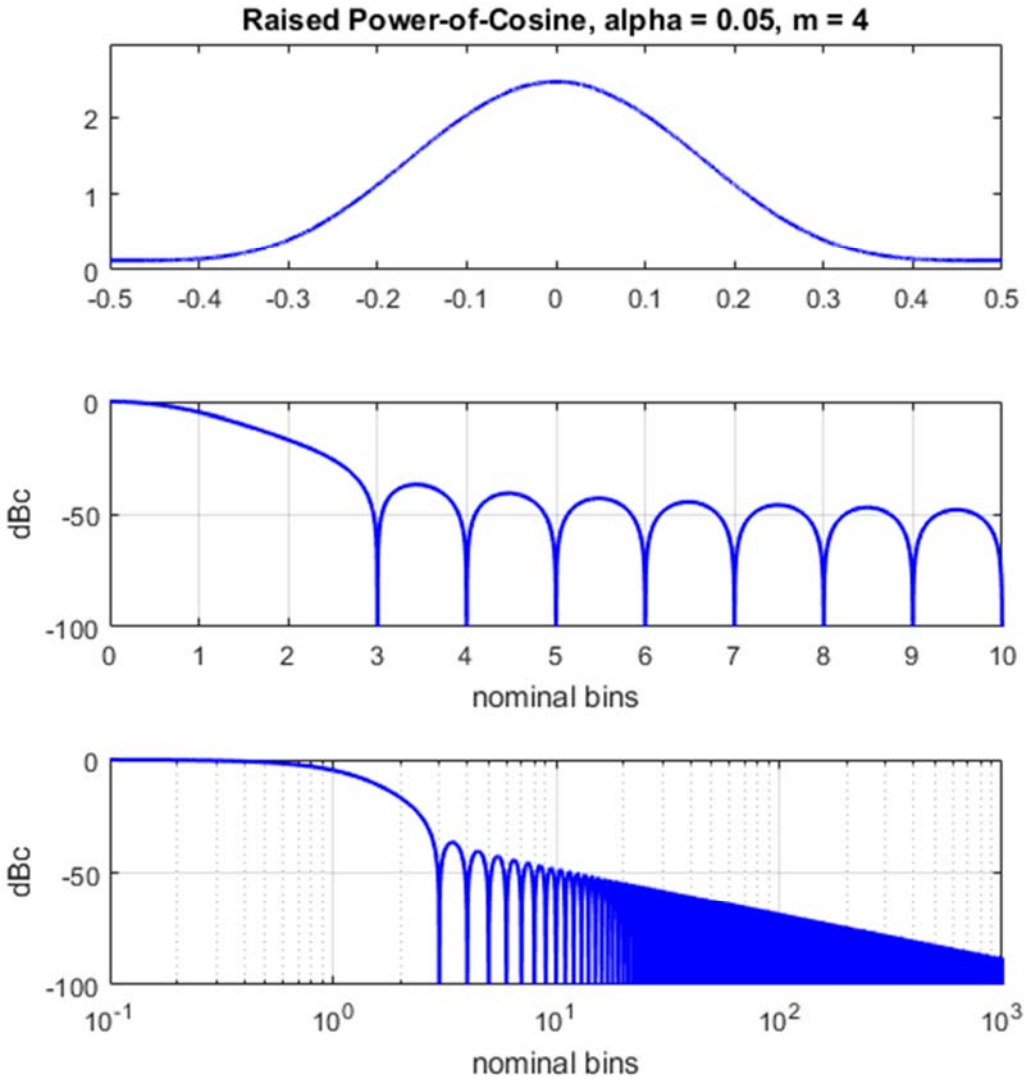


WINDOW SPECTRUM CHARACTERISTICS

half-power bandwidth = 1.5996 (normalized to 1/T)
-3 dB bandwidth = 1.5968 (normalized to 1/T)
-18 dB bandwidth = 4.176 (normalized to 1/T)
noise bandwidth = 1.7264 (normalized to 1/T)
SNR loss = 2.371 dB
first null = 3 (normalized to 1/T)
PSL = -36.5078 dBc
ISL = -34.3848 dBc from first null outward

**Figure 32.**

## 4.19 Parzen Cosine Family

Parzen[1] suggested a family of window taper functions of the form, which we have transmogrified and scaled for unit DC gain as

$$w(t) = A\left(1 + \cos\left(\pi \gamma |2t|^m\right)\right)\text{rect}(t), \tag{153}$$

where

$$\begin{aligned} &0 < \gamma \le 1 \text{ , and} \\ &m \ge 0 \text{ , not necessarily an integer,} \end{aligned} \tag{154}$$

with the unit DC gain scale factor calculated to be

$$A = \left( \int_{-1/2}^{1/2} \left(1 + \cos\left(\pi \gamma |2t|^m\right)\right) dt \right)^{-1} . \tag{155}$$

The Fourier Transform of the continuous time window taper function for arbitrary $m$ is not readily calculated in closed-form. It may be numerically calculated for specific parameters, i.e. using a DFT on discrete-time samples of the window function.

Example plots and characteristics are given in Figure 33 for a sample parameter combination.

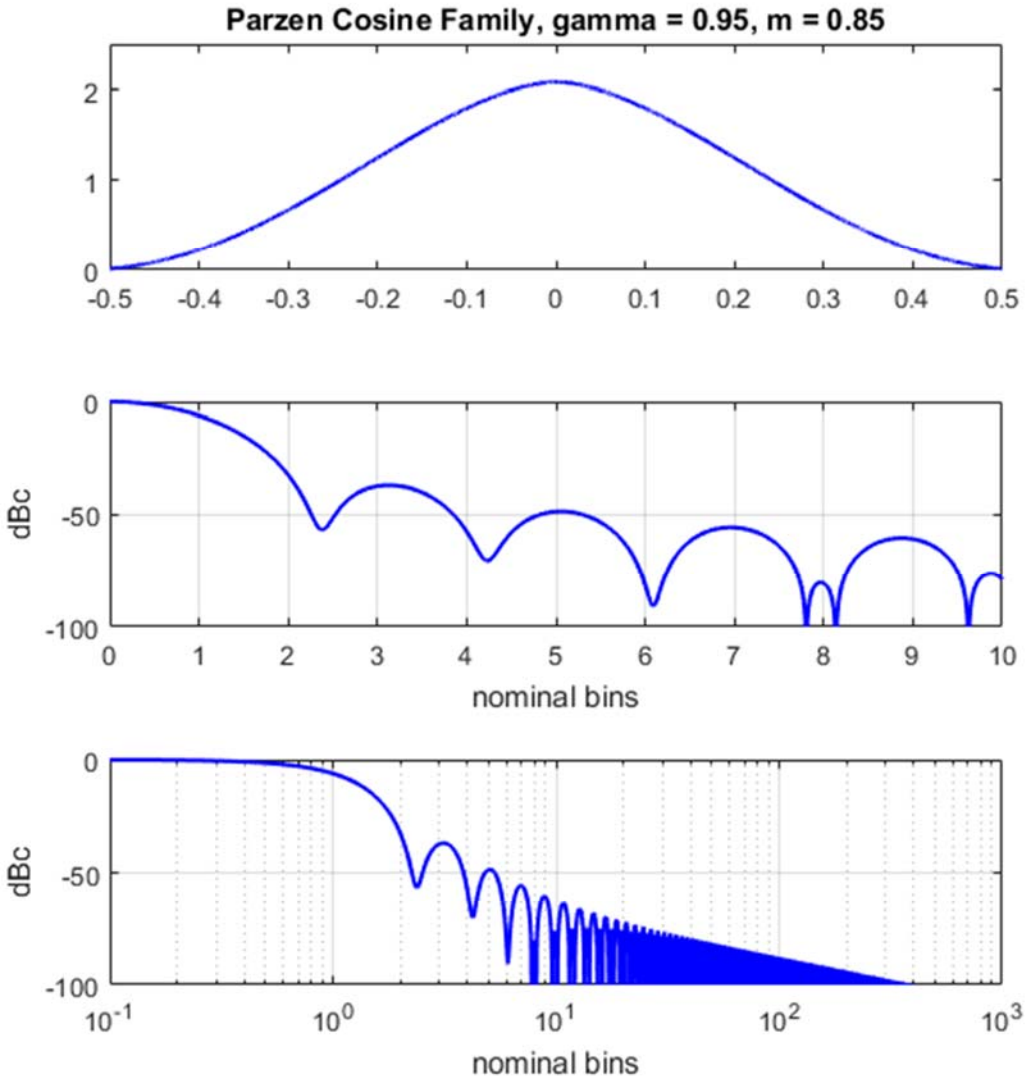


WINDOW SPECTRUM CHARACTERISTICS

half-power bandwidth = 1.4247 (normalized to 1/T)
-3 dB bandwidth = 1.4224 (normalized to 1/T)
-18 dB bandwidth = 3.2313 (normalized to 1/T)
noise bandwidth = 1.4914 (normalized to 1/T)
SNR loss = 1.736 dB
first null = 2.3789 (normalized to 1/T)
PSL = -36.8048 dBc
ISL = -36.6085 dBc from first null outward

**Figure 33.**

## 4.20 Bohman (a.k.a. Papoulis)

A Cosine Lobe window convolved with itself is known as the Bohman window.[23]

Its form scaled for unit DC gain is

$$w(t) = \left( \frac{\pi^2}{4}(1 - 2|t|)\cos(2\pi|t|) + \frac{\pi}{4}\sin(2\pi|t|) \right) \text{rect}(t), \tag{156}$$

The Fourier Transform of the continuous time window taper function is calculated as

$$W(f) = \frac{\cos^2\left(\frac{\pi}{2} f\right)}{\left(f^2 - 1\right)^2}. \tag{157}$$

Papoulis showed that this window is optimum in minimizing bias in spectral estimation.[24]

Plots and characteristics for this window are given in Figure 34.

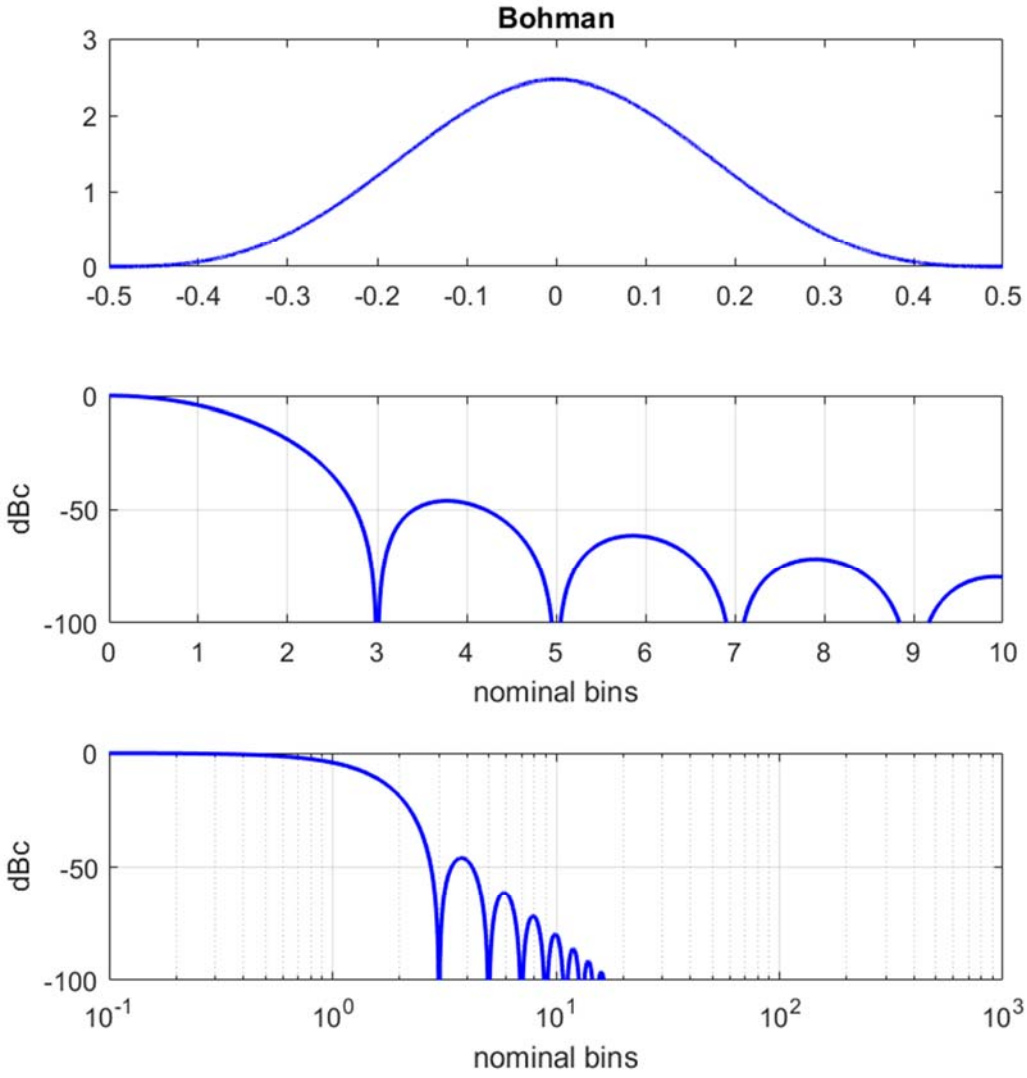


WINDOW SPECTRUM CHARACTERISTICS

half-power bandwidth = 1.7021 (normalized to 1/T)
-3 dB bandwidth = 1.6992 (normalized to 1/T)
-18 dB bandwidth = 3.9043 (normalized to 1/T)
noise bandwidth = 1.7858 (normalized to 1/T)
SNR loss = 2.5184 dB
first null = 3 (normalized to 1/T)
PSL = -45.9975 dBc
ISL = -46.7278 dBc from first null outward

**Figure 34.**

## 4.21 Trapezoid

The Trapezoid window is something between a Rectangle window and a Triangle window. It has a flat center section, and linear tapers towards the edges. It is a parametric window, with the form scaled for unit DC gain as

$$w(t) = \begin{cases} \dfrac{2}{1+2\alpha} & |t| \le \alpha \\ \dfrac{2(1-2|t|)}{1-(2\alpha)^2} & \alpha < |t| \le 1/2 \\ 0 & |t| > 1/2 \end{cases}, \tag{158}$$

where the taper parameter is the offset from aperture center specified as

$$0 \le \alpha \le 1/2 . \tag{159}$$

The window can also be constructed as the difference between two triangle functions.

The Fourier Transform of the continuous time window taper function is calculated as

$$W(f) = \frac{2(\cos(2\pi\alpha f) - \cos(\pi f))}{(1-4\alpha^2)\pi^2 f^2} . \tag{160}$$

Plots and characteristics are given in Figure 35 for $\alpha = 0.1$.

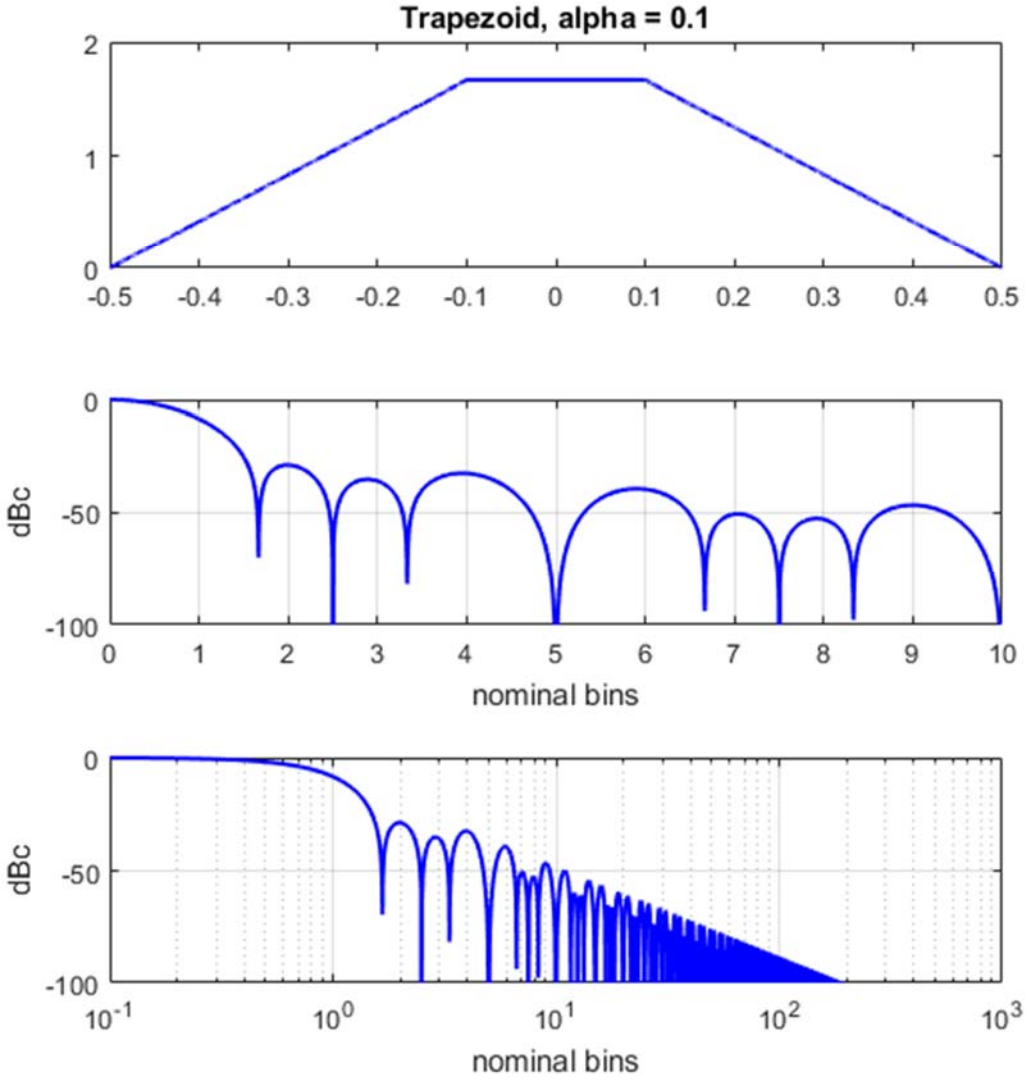


WINDOW SPECTRUM CHARACTERISTICS

half-power bandwidth = 1.2474 (normalized to 1/T)
-3 dB bandwidth = 1.2453 (normalized to 1/T)
-18 dB bandwidth = 2.7116 (normalized to 1/T)
noise bandwidth = 1.2964 (normalized to 1/T)
SNR loss = 1.127 dB
first null = 1.668 (normalized to 1/T)
PSL = -28.7573 dBc
ISL = -27.3536 dBc from first null outward

**Figure 35.**

## 4.22 Tukey (a.k.a. Tapered-Cosine, Cosine-Tapered)

The Tukey window is something between a Rectangle window and a Hann window.[25] It has a flat center section, and cosine tapers towards the edges. It is a parametric window, with the form scaled for unit DC gain as

$$w(t) = \begin{cases} \dfrac{2}{(\alpha - 1/2)} & |t| \le \alpha \\ \dfrac{1 + \cos\left( \dfrac{\pi(t-\alpha)}{(1/2-\alpha)} \right)}{(\alpha - 1/2)} & \alpha < |t| \le 1/2 \\ 0 & |t| > 1/2 \end{cases}, \tag{161}$$

where the parameter

$$0 \le \alpha \le 1/2 . \tag{162}$$

Often the parameter $\alpha$ is specified by another parameter $r$, such that

$$\alpha = 1/2 - r/2 , \tag{163}$$

where

$$0 \le r \le 1 . \tag{164}$$

Note that $r = 0$ is equivalent to a Rectangle window, and $r = 1$ is equivalent to a Hann window.

The Fourier Transform of the continuous time window taper function is not readily calculated in closed-form for arbitrary $r$. It may be numerically calculated for specific parameters, i.e. using a DFT on discrete-time samples of the window function.

Plots and characteristics are given in Figure 36 for $r = 0.75$.

The Tukey window is named after American mathematician John Wilder Tukey.

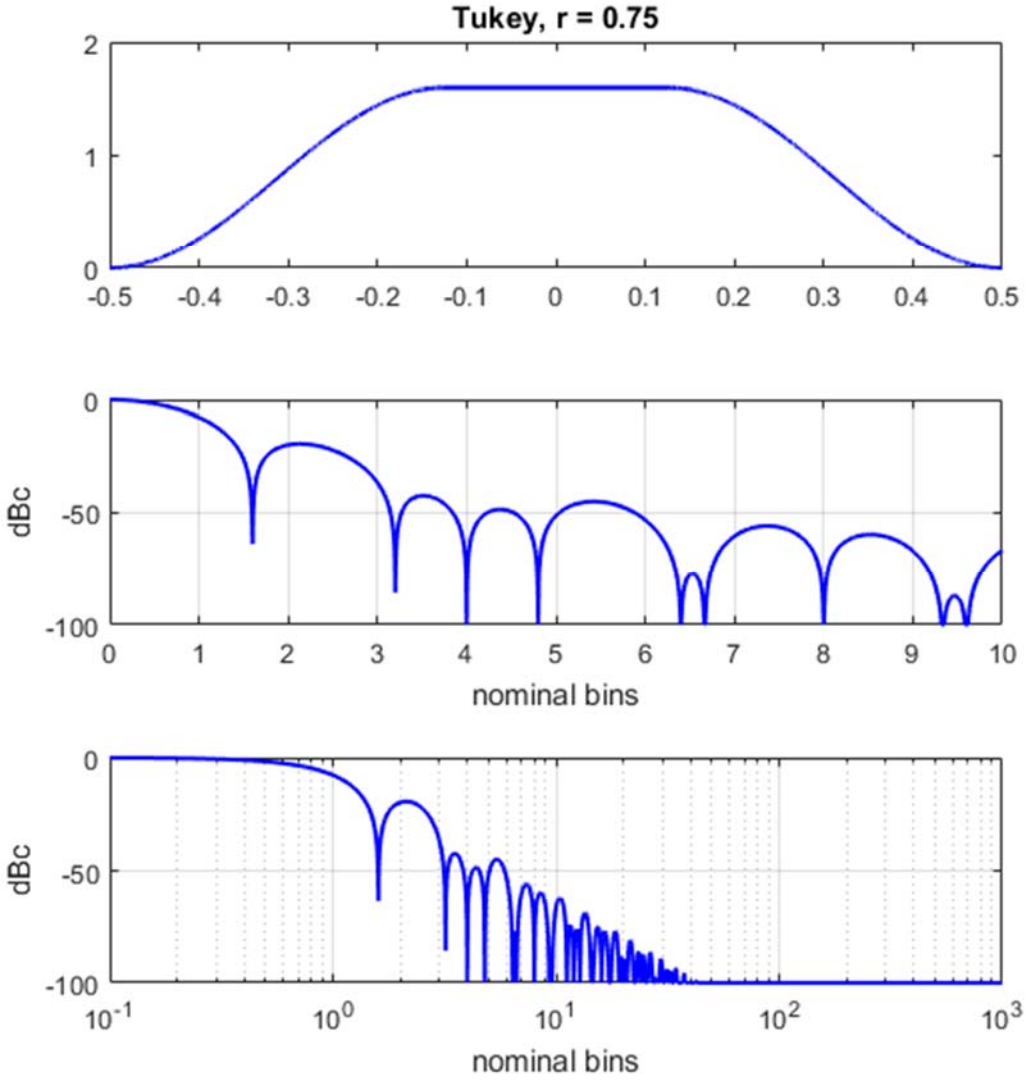


WINDOW SPECTRUM CHARACTERISTICS

half-power bandwidth = 1.3048 (normalized to 1/T)
-3 dB bandwidth = 1.3027 (normalized to 1/T)
-18 dB bandwidth = 2.7394 (normalized to 1/T)
noise bandwidth = 1.3601 (normalized to 1/T)
SNR loss = 1.3357 dB
first null = 1.6016 (normalized to 1/T)
PSL = -19.3943 dBc
ISL = -19.2425 dBc from first null outward

**Figure 36.**

## 4.23 Bartlett-Hann

The Bartlett-Hann window taper function is a combination of Bartlett and Hann window taper functions. Specifically, it is calculated with the form scaled for unit DC gain as

$$w(t) = 2\left(a_0 - a_1|t| + a_2\cos(2\pi t)\right)\text{rect}(t), \tag{165}$$

with coefficients

$$\begin{aligned} a_0 &= 0.62, \\ a_1 &= 0.48, \text{ and} \\ a_2 &= 0.38. \end{aligned} \tag{166}$$

The Fourier Transform of the continuous time window taper function is calculated as

$$W(f) = \left[\begin{array}{l} (2a_0 - a_1)\,\text{sinc}(f) \\ +a_2\,\text{sinc}(f-1) + a_2\,\text{sinc}(f+1) \\ +\dfrac{a_1}{2}\,\text{sinc}^2\left(\dfrac{f}{2}\right) \end{array}\right]. \tag{167}$$

Plots and characteristics are given in Figure 37.

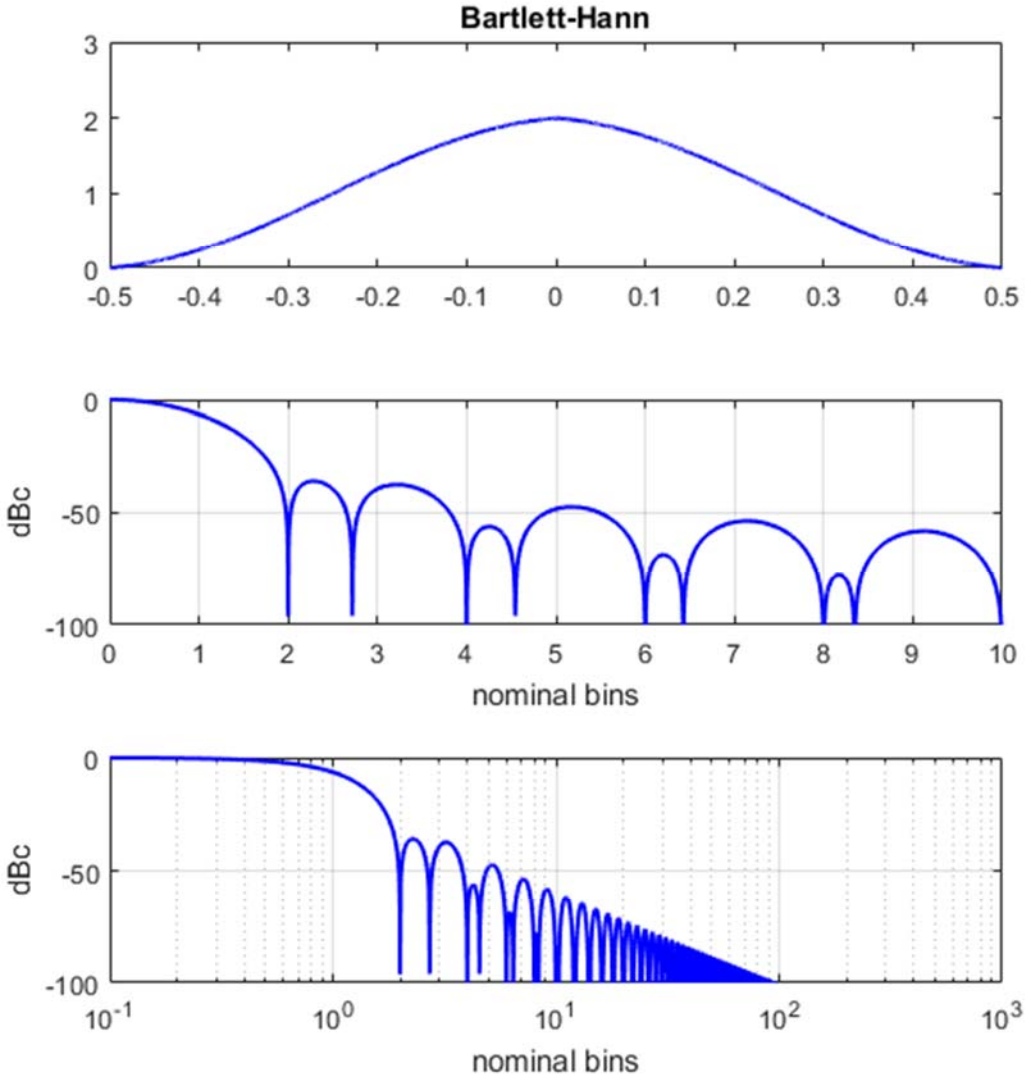


WINDOW SPECTRUM CHARACTERISTICS

half-power bandwidth = 1.3965 (normalized to 1/T)
-3 dB bandwidth = 1.3942 (normalized to 1/T)
-18 dB bandwidth = 3.105 (normalized to 1/T)
noise bandwidth = 1.4559 (normalized to 1/T)
SNR loss = 1.6314 dB
first null = 2 (normalized to 1/T)
PSL = -35.8727 dBc
ISL = -35.2536 dBc from first null outward

**Figure 37.**

## 4.24 Blackman

We recall that Generalized Raised Cosine windows of section 4.15 dealt with the sum of a constant and a single cosine term. The Blackman window now adds an additional cosine term. This additional cosine term is an additional degree of freedom with which to optimize window taper function spectral characteristics. What we today call the conventional Blackman window, Blackman himself called his "not very serious proposal" window function.[8]

The conventional Blackman window, scaled for unit DC gain, is defined as

$$w(t) = \left(1 + \frac{\alpha_1}{\alpha_0}\cos(2\pi t) + \frac{\alpha_2}{\alpha_0}\cos(4\pi t)\right)\mathrm{rect}(t), \tag{168}$$

where

$$\begin{aligned} \alpha_0 &= 0.42, \\ \alpha_1 &= 0.5, \text{ and} \\ \alpha_2 &= 0.08. \end{aligned} \tag{169}$$

Note that the ends of the conventional Blackman window taper function go to zero, that is

$$w(0.5) = w(-0.5) = 0\,. \tag{170}$$

The Fourier Transform of the continuous time window taper function is calculated as

$$W(f) = \left[\begin{array}{l} \mathrm{sinc}(f) \\ +\frac{\alpha_1}{2\alpha_0}\mathrm{sinc}(f-1) + \frac{\alpha_1}{2\alpha_0}\mathrm{sinc}(f+1) \\ +\frac{\alpha_2}{2\alpha_0}\mathrm{sinc}(f-2) + \frac{\alpha_2}{2\alpha_0}\mathrm{sinc}(f+2) \end{array}\right]. \tag{171}$$

Plots and characteristics are given in Figure 38. Note that the sidelobes taper at −18 dB per octave.

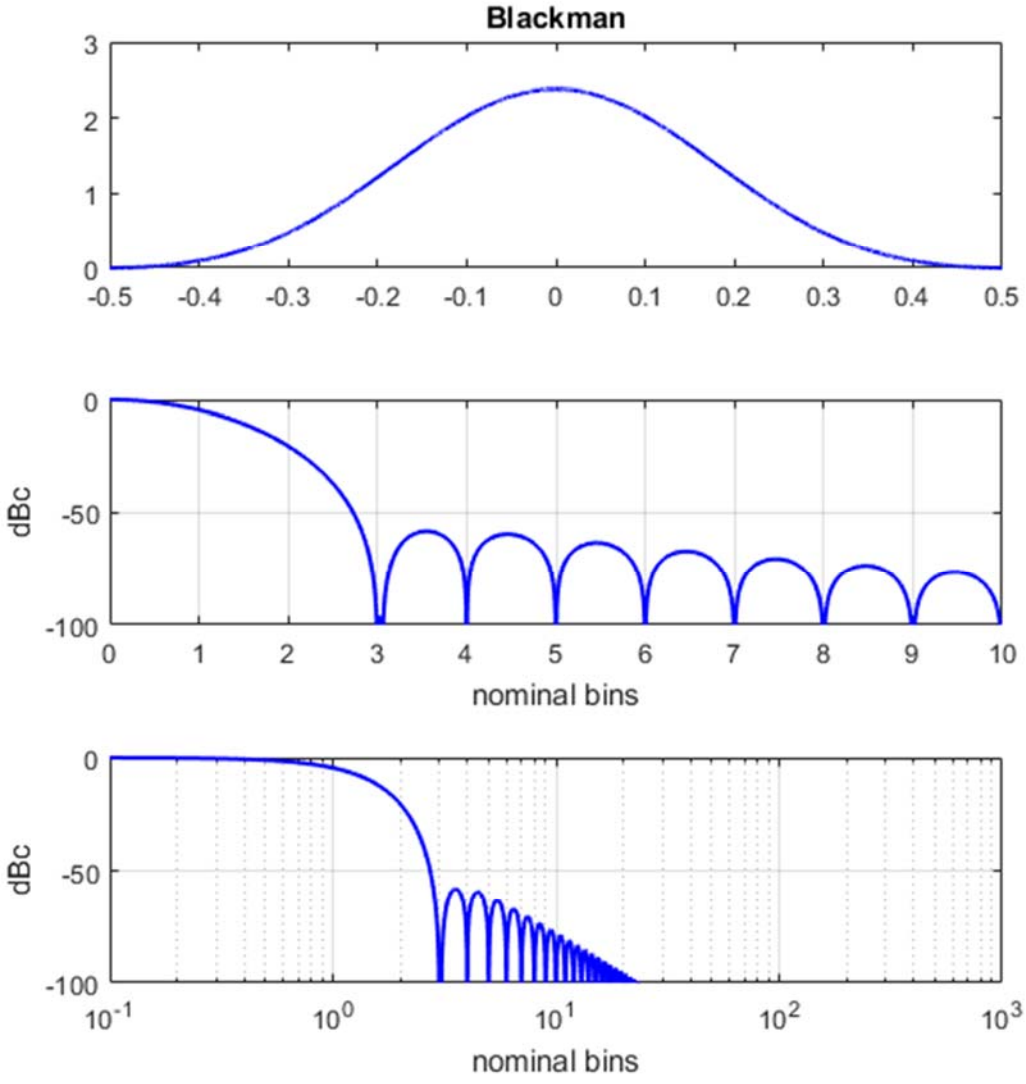


WINDOW SPECTRUM CHARACTERISTICS

half-power bandwidth = 1.6438 (normalized to 1/T)
-3 dB bandwidth = 1.641 (normalized to 1/T)
-18 dB bandwidth = 3.7931 (normalized to 1/T)
noise bandwidth = 1.7269 (normalized to 1/T)
SNR loss = 2.3726 dB
first null = 3 (normalized to 1/T)
PSL = -58.1088 dBc
ISL = -57.1626 dBc from first null outward

**Figure 38.**

## 4.25 Exact Blackman

By adjusting the coefficients of the Blackman slightly, the PSL may be reduced even more, but at the expense of a slower sidelobe taper. Blackman referred to his "not very serious proposal" window as an approximation to what we today call the Exact Blackman window.[8]

The Exact Blackman window, scaled for unit DC gain, is still defined as

$$w(t) = \left(1 + \frac{\alpha_1}{\alpha_0}\cos(2\pi t) + \frac{\alpha_2}{\alpha_0}\cos(4\pi t)\right)\text{rect}(t), \tag{172}$$

but now where the coefficients are stipulated as

$$\begin{aligned} \alpha_0 &= 7938/18608, \\ \alpha_1 &= 9240/18608, \text{ and} \\ \alpha_2 &= 1430/18608. \end{aligned} \tag{173}$$

Note that the ends of the Exact Blackman window taper function do not go absolutely to zero, that is

$$w(0.5) = w(-0.5) \neq 0. \tag{174}$$

The Fourier Transform of the continuous time window taper function is still calculated as

$$W(f) = \left[\begin{array}{l} \text{sinc}(f) \\ +\frac{\alpha_1}{2\alpha_0}\text{sinc}(f-1) + \frac{\alpha_1}{2\alpha_0}\text{sinc}(f+1) \\ +\frac{\alpha_2}{2\alpha_0}\text{sinc}(f-2) + \frac{\alpha_2}{2\alpha_0}\text{sinc}(f+2) \end{array}\right]. \tag{175}$$

Plots and characteristics are given in Figure 39 for $\alpha = 0.6$. Note that with respect to the conventional Blackman window taper function, PSL is reduced but at the expense of a slower sidelobe taper.

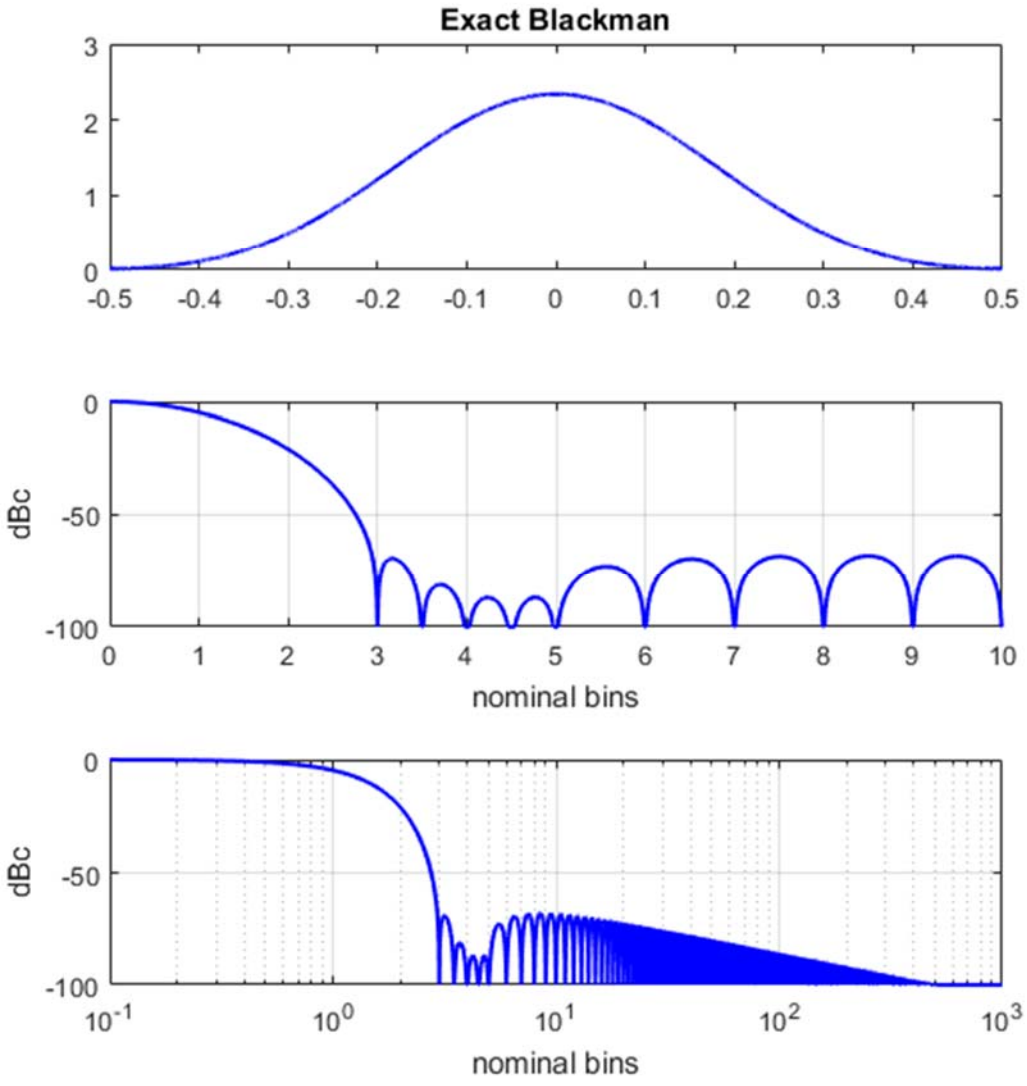


WINDOW SPECTRUM CHARACTERISTICS

half-power bandwidth = 1.6088 (normalized to 1/T)
-3 dB bandwidth = 1.6061 (normalized to 1/T)
-18 dB bandwidth = 3.7488 (normalized to 1/T)
noise bandwidth = 1.6938 (normalized to 1/T)
SNR loss = 2.2886 dB
first null = 3 (normalized to 1/T)
PSL = -68.2361 dBc
ISL = -57.7344 dBc from first null outward

**Figure 39.**

## 4.26 Blackman-Harris Family

The Blackman-Harris family of window taper functions are defined by a sum of cosine terms, namely

$$w(t) = A\left(\sum_{l=0}^{L-1} \alpha_l \cos(2\pi l\, t)\right)\mathrm{rect}(t), \tag{176}$$

where

$l$ = coefficient index, $0 \le l \le L-1$,
$L$ = "order" of the window function, and
$\alpha_l$ = coefficient, and
$A$ = scale factor that might be used to force a unity DC gain. (177)

This family of window functions is discussed extensively by Blackman, et al.[7,8,9,10] Harris used gradient search techniques to find specific coefficients to optimize the window functions in various respects. These specific windows are then called Blackman-Harris windows.[4]

The Raised-Cosine family of window taper functions are in fact a subset of the Blackman-Harris family where the number of terms, or order, is $L = 2$. The conventional Blackman, and Exact Blackman window taper functions of the previous sections are also members of this family with $L = 3$. Most other practical window taper functions from this family use $L = 3$ or $L = 4$.

Classically, $A = 1$ and $\alpha_0 \neq 1$ for conventional Blackman-Harris family windows, causing a peak value of unity for the window function itself. However, we will stipulate to unity DC gain, which requires scaling the classical window function by

$$A = 1/\alpha_0\,. \tag{178}$$

Blackman-Harris window taper functions scaled to unity DC gain are sometimes called "Rife–Vincent" window taper functions.[26,27]

The Fourier Transform of a continuous time window taper function from this family, scaled to unity DC gain, is calculated as

$$W(f) = \mathrm{sinc}(f) + \frac{1}{2\alpha_0}\sum_{l=1}^{L-1}\left(\alpha_l\,\mathrm{sinc}(f-l) + \alpha_l\,\mathrm{sinc}(f+l)\right). \tag{179}$$

We offer the comment that very low sidelobe levels can be achieved by these window taper functions, but also that very small changes in coefficients can have significant impact on the ultra-low sidelobe level.

Specific names for particular coefficient sets are not consistent in the literature, or in available software tools.

Table 1 gives coefficients for some of the more popular Blackman-Harris window taper functions. Plots for these are given in Figure 40 through Figure 50. We note that our performance numbers differ slightly from those of Harris.

## 4.27 Nuttall (a.k.a. Nutall) Family

Nuttall[28] window taper functions are members of the Blackman-Harris family of window functions, where the coefficients are chosen to achieve some very specific characteristics.

Nuttall developed different sets of coefficients to satisfy a number of different optimization criteria, for both $L = 3$ and $L = 4$ . This resulted in a number of different specific window taper functions.

Specific names for particular coefficient sets are not consistent in the literature, or in available software tools.

Table 1 gives coefficients for some of the more popular Nuttall window taper functions. Plots for these are given in Figure 40 through Figure 50.

## 4.28 Mottaghi-Kashtiban-Shayesteh

Other coefficient sets for the Blackman-Harris family have also been favored by some authors for specific purposes. One such set of coefficients was proposed by Mottaghi-Kashtiban and Shayesteh,[29] for the purpose of improving on the Hamming window.

Note that this window adjusts its coefficients based on discrete-time window length.

This particular window taper function is also included in Table 1. Plots for this window are given in Figure 51 and Figure 52.

**Table 1.**

| $\alpha_0$ | $\alpha_1$ | $\alpha_2$ | $\alpha_3$ | ***Window Taper Function*** |
|---|---|---|---|---|
| 0.44959 | 0.49364 | 0.05677 | | −61 dB Three-Term Blackman-Harris[4] |
| 0.42323 | 0.49755 | 0.07922 | | −67 dB Three-Term Blackman-Harris[4] |
| 0.4243801 | 0.4973406 | 0.0782793 | | Three-Term Nuttall,<br>Minimum Sidelobe[28]<br>(a.k.a. Three-Term Blackman-Harris) |
| 0.40897 | 0.5 | 0.09103 | | Three-Term Nuttall,<br>Continuous First Derivative[28] |
| 0.375 | 0.5 | 0.125 | | Three-Term Nuttall,<br>Continuous Third Derivative[28] |
| 0.40217 | 0.49703 | 0.09892 | 0.00188 | −74 dB Four-Term Blackman-Harris[28,†] |
| 0.35875 | 0.48829 | 0.14128 | 0.01168 | −92 dB Four-Term Blackman-Harris[4] |
| 0.3635819 | 0.4891775 | 0.1365995 | 0.0106411 | Four-Term Nuttall,<br>Minimum Sidelobe[28]<br>(a.k.a. Blackman-Nuttall ) |
| 0.355768 | 0.487396 | 0.144232 | 0.012604 | Four-Term Nuttall,<br>Continuous First Derivative[28] |
| 0.338946 | 0.481973 | 0.161054 | 0.018027 | Four-Term Nuttall,<br>Continuous Third Derivative[28] |
| 10/32 | 15/32 | 6/32 | 1/32 | Four-Term Nuttall,<br>Continuous Fifth Derivative[28] |
| 0.5363 - 0.14/($N$-1) | 0.996 – $\alpha_0$ | 0 | 0.004 | Mottaghi-Kashtiban-Shayesteh[29] |

† Harris[4] contains a slight error in his listed coefficients.

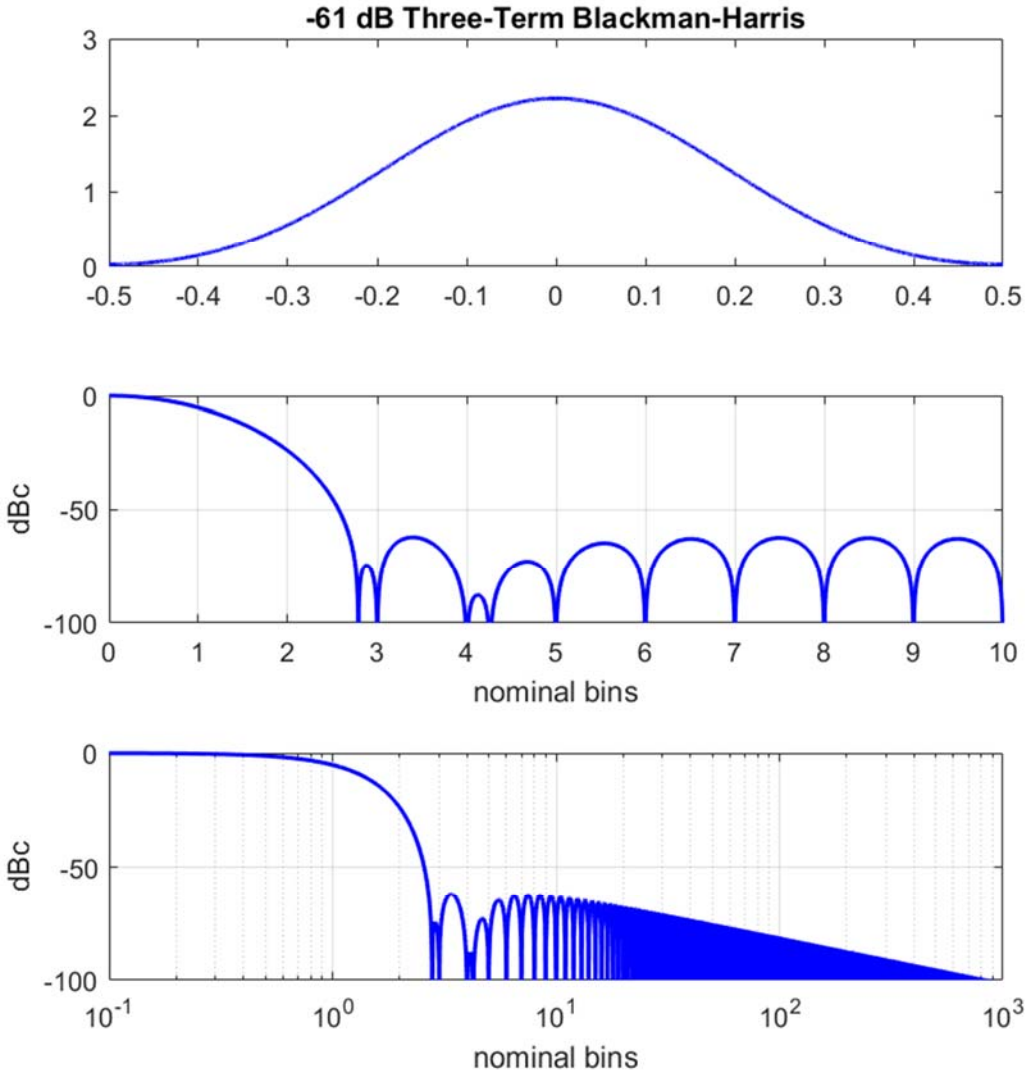


WINDOW SPECTRUM CHARACTERISTICS

half-power bandwidth = 1.5322 (normalized to 1/T)
-3 dB bandwidth = 1.5296 (normalized to 1/T)
-18 dB bandwidth = 3.5475 (normalized to 1/T)
noise bandwidth = 1.6108 (normalized to 1/T)
SNR loss = 2.0705 dB
first null = 2.7891 (normalized to 1/T)
PSL = -62.0526 dBc
ISL = -51.9816 dBc from first null outward

**Figure 40.**

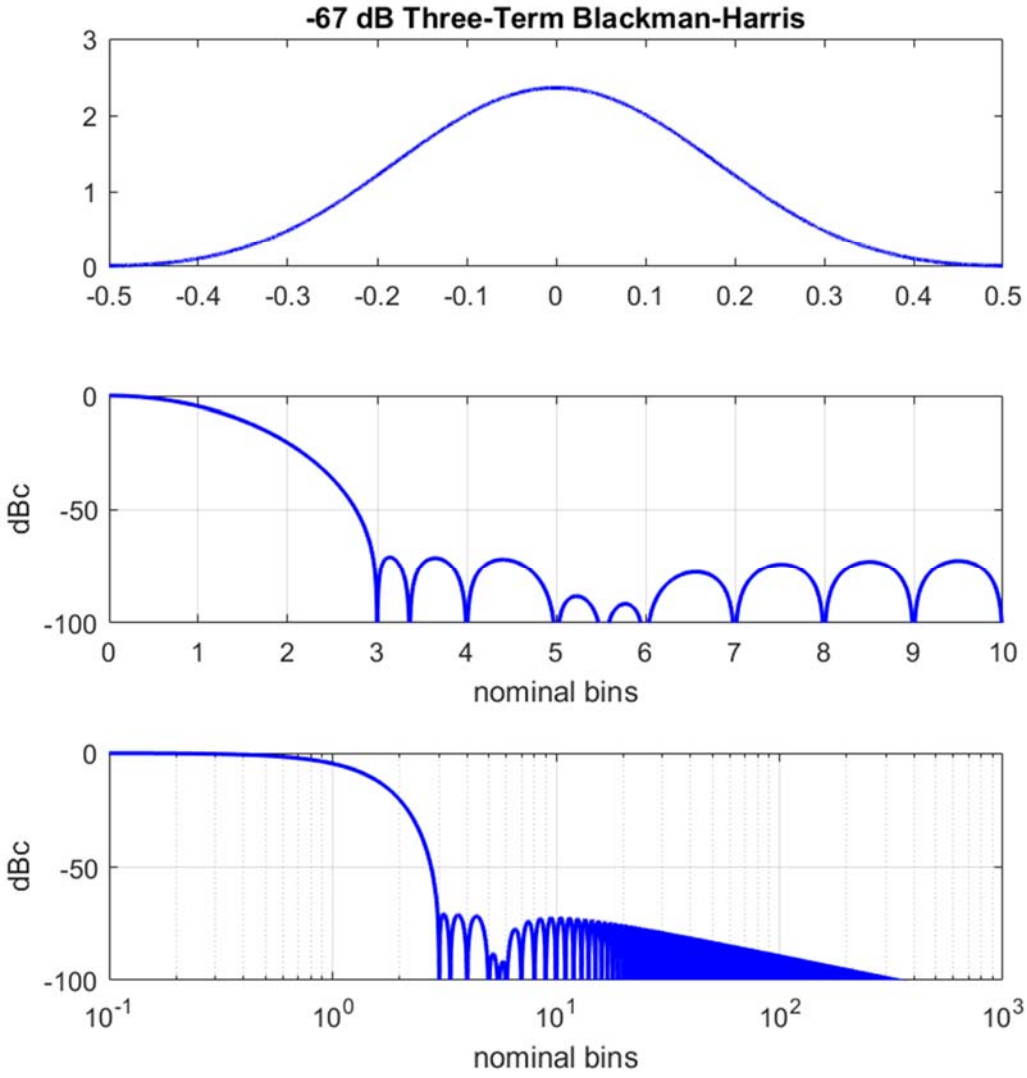


WINDOW SPECTRUM CHARACTERISTICS

half-power bandwidth = 1.6236 (normalized to 1/T)
-3 dB bandwidth = 1.6209 (normalized to 1/T)
-18 dB bandwidth = 3.7761 (normalized to 1/T)
noise bandwidth = 1.7086 (normalized to 1/T)
SNR loss = 2.3265 dB
first null = 3 (normalized to 1/T)
PSL = -70.8075 dBc
ISL = -60.9597 dBc from first null outward

**Figure 41.**

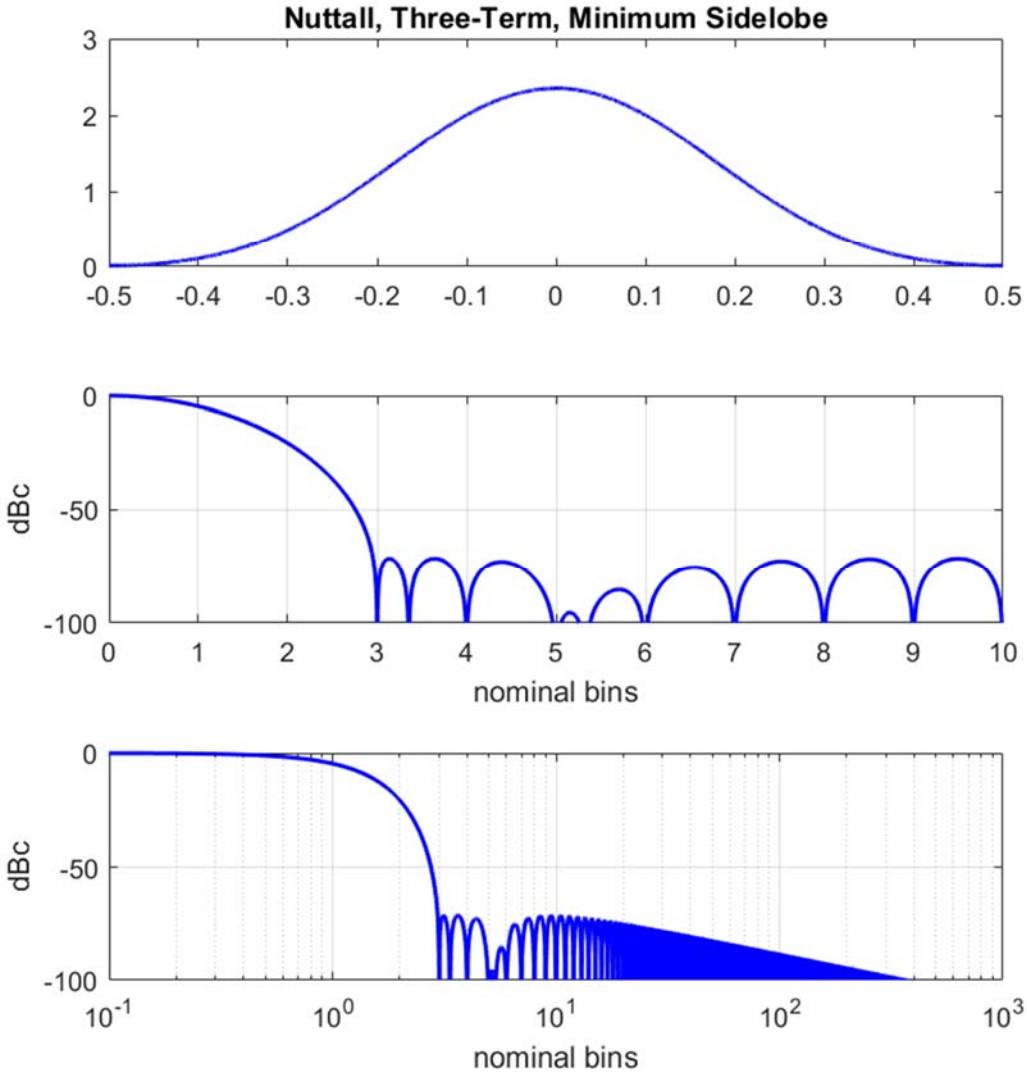


WINDOW SPECTRUM CHARACTERISTICS

half-power bandwidth = 1.6189 (normalized to 1/T)
-3 dB bandwidth = 1.6162 (normalized to 1/T)
-18 dB bandwidth = 3.766 (normalized to 1/T)
noise bandwidth = 1.7038 (normalized to 1/T)
SNR loss = 2.3142 dB
first null = 3 (normalized to 1/T)
PSL = -71.4601 dBc
ISL = -60.2546 dBc from first null outward

**Figure 42.**

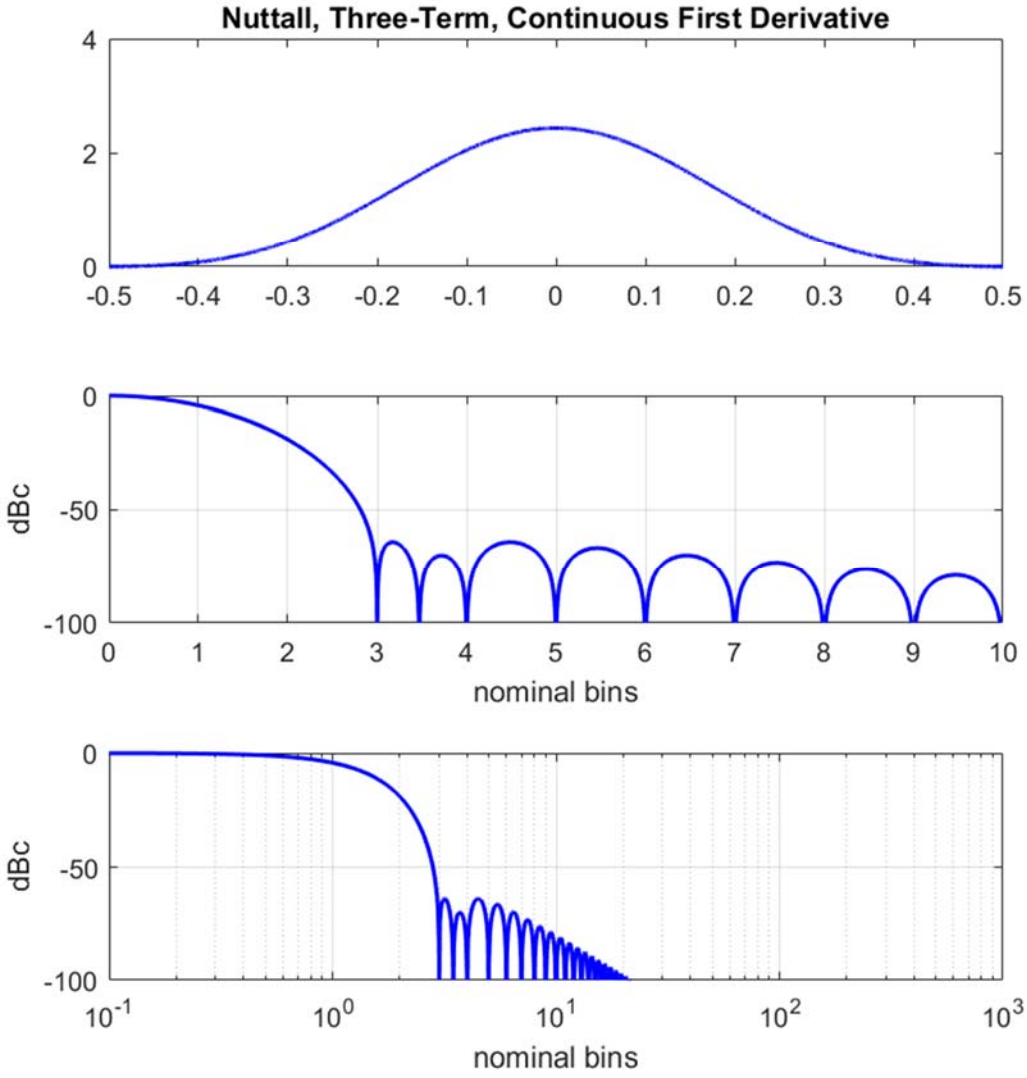


WINDOW SPECTRUM CHARACTERISTICS

half-power bandwidth = 1.6857 (normalized to 1/T)
-3 dB bandwidth = 1.6829 (normalized to 1/T)
-18 dB bandwidth = 3.9026 (normalized to 1/T)
noise bandwidth = 1.7722 (normalized to 1/T)
SNR loss = 2.4852 dB
first null = 3 (normalized to 1/T)
PSL = -64.1868 dBc
ISL = -62.4303 dBc from first null outward

**Figure 43.**

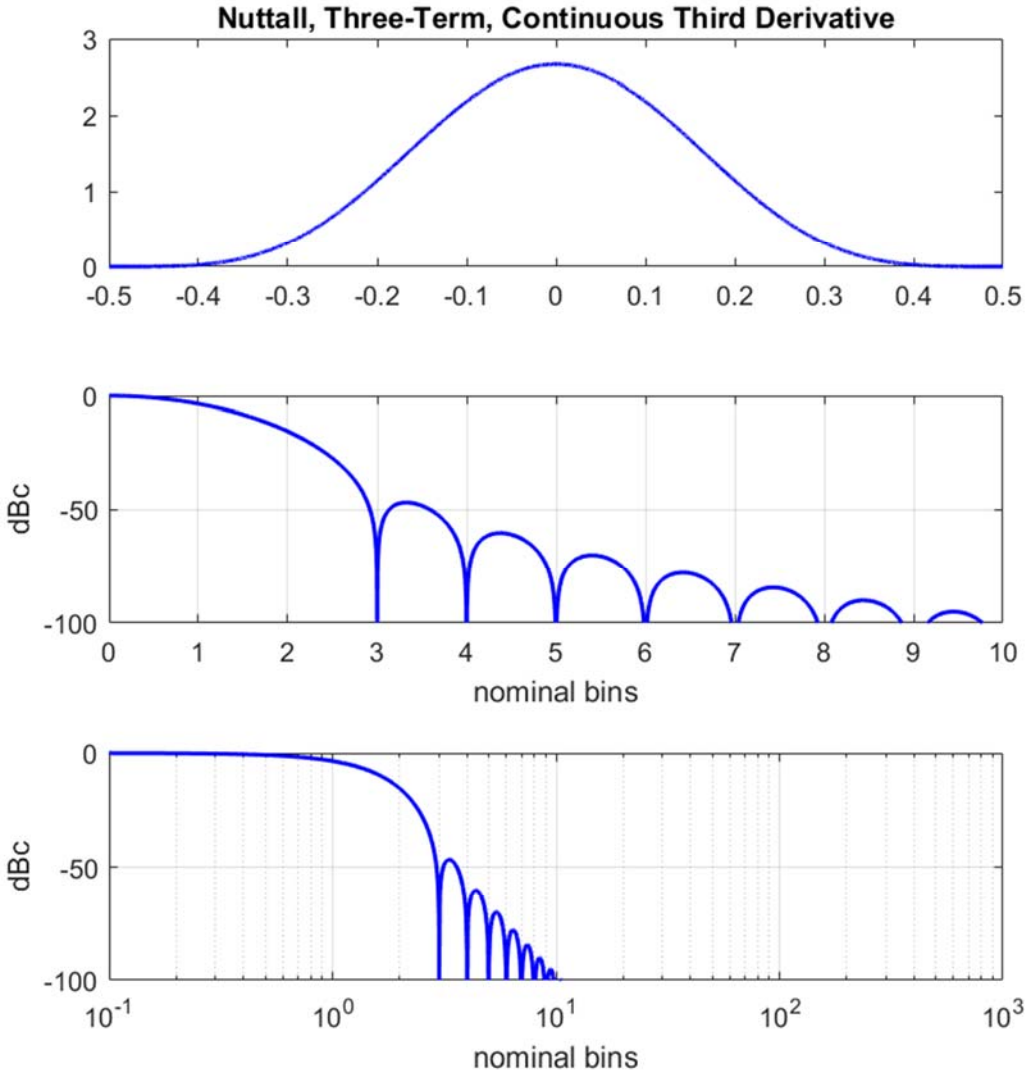


WINDOW SPECTRUM CHARACTERISTICS

half-power bandwidth = 1.8528 (normalized to 1/T)
-3 dB bandwidth = 1.8497 (normalized to 1/T)
-18 dB bandwidth = 4.2543 (normalized to 1/T)
noise bandwidth = 1.9446 (normalized to 1/T)
SNR loss = 2.8882 dB
first null = 3 (normalized to 1/T)
PSL = -46.7412 dBc
ISL = -49.7843 dBc from first null outward

**Figure 44.**

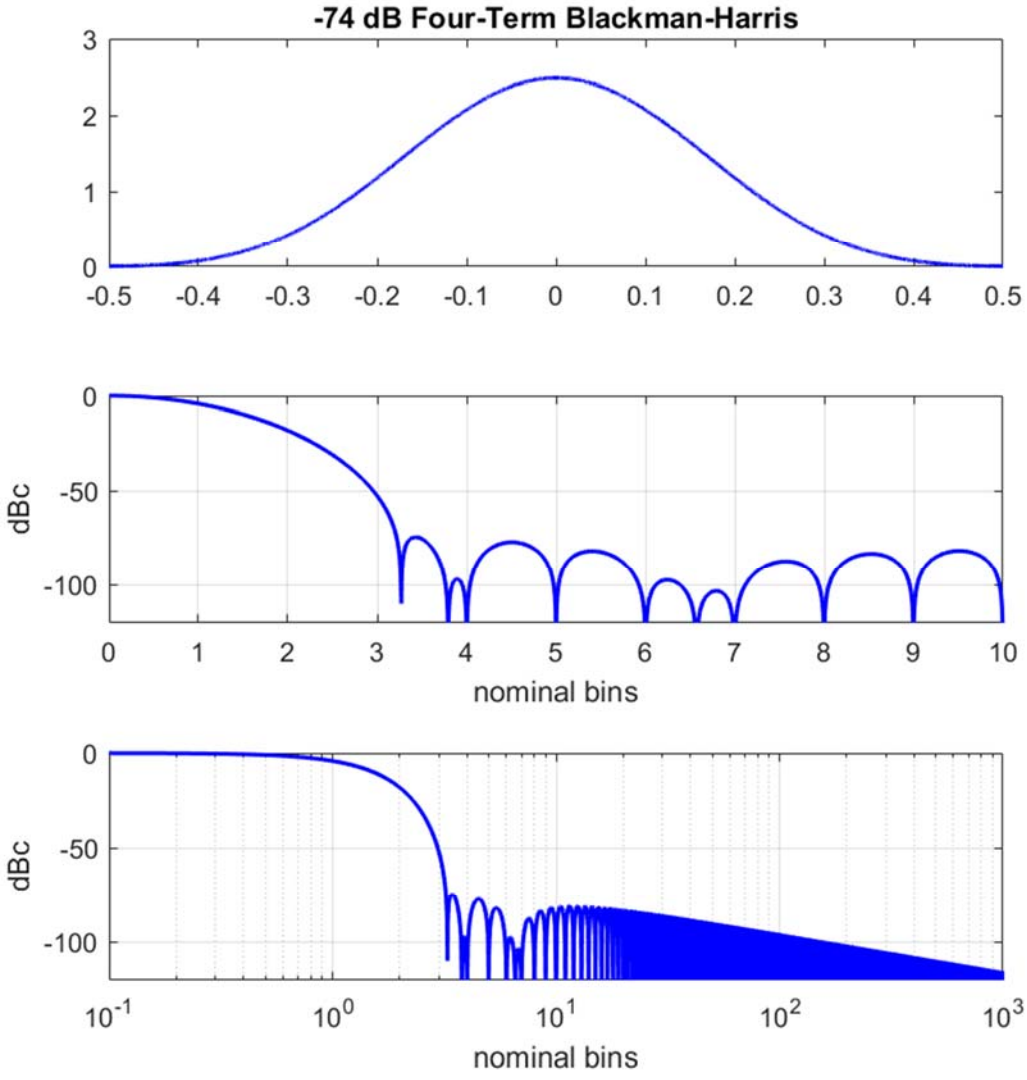


WINDOW SPECTRUM CHARACTERISTICS

half-power bandwidth = 1.7028 (normalized to 1/T)
-3 dB bandwidth = 1.7 (normalized to 1/T)
-18 dB bandwidth = 3.9804 (normalized to 1/T)
noise bandwidth = 1.7941 (normalized to 1/T)
SNR loss = 2.5384 dB
first null = 3.2695 (normalized to 1/T)
PSL = -74.3918 dBc
ISL = -68.2994 dBc from first null outward

**Figure 45.**

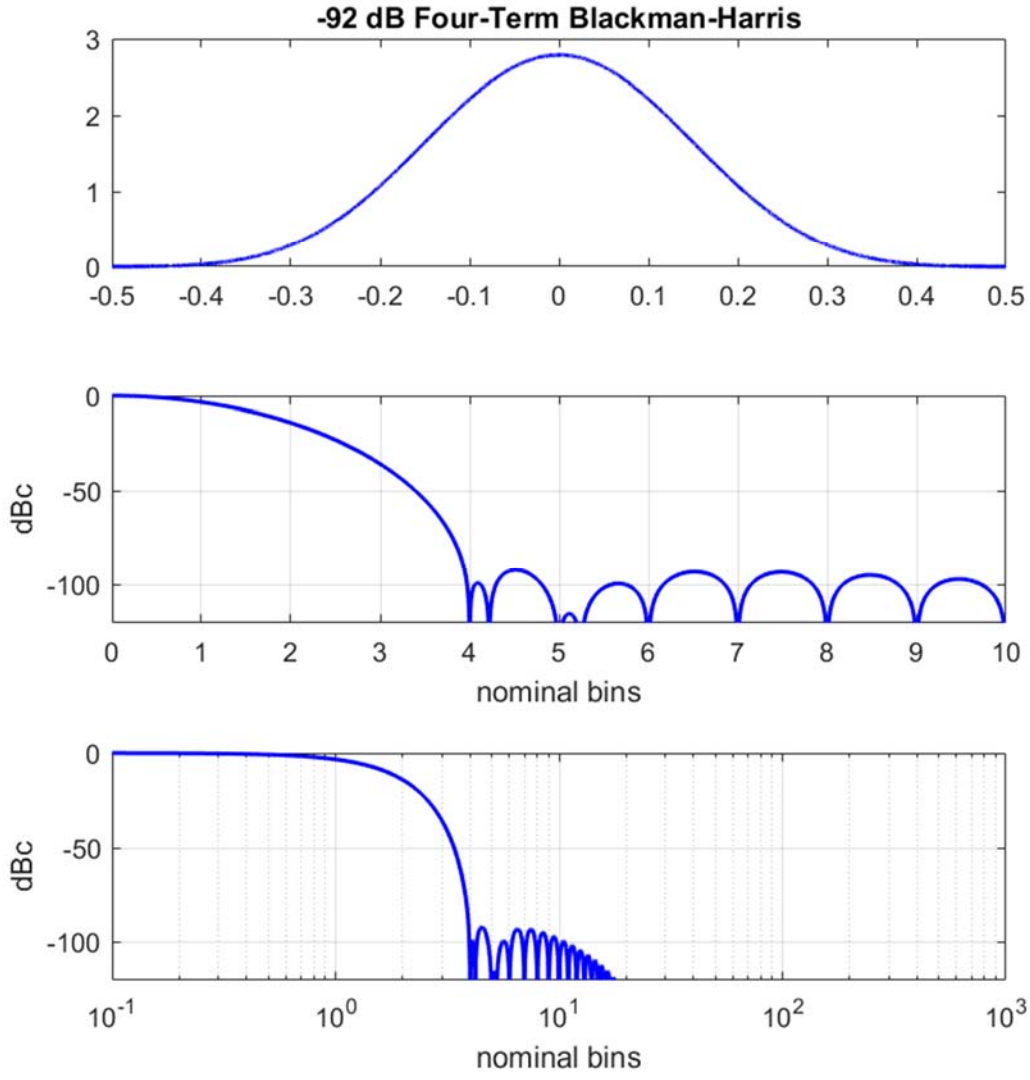


WINDOW SPECTRUM CHARACTERISTICS

half-power bandwidth = 1.8996 (normalized to 1/T)
-3 dB bandwidth = 1.8964 (normalized to 1/T)
-18 dB bandwidth = 4.4718 (normalized to 1/T)
noise bandwidth = 2.0045 (normalized to 1/T)
SNR loss = 3.02 dB
first null = 4 (normalized to 1/T)
PSL = -92.0099 dBc
ISL = -89.1922 dBc from first null outward

**Figure 46.**

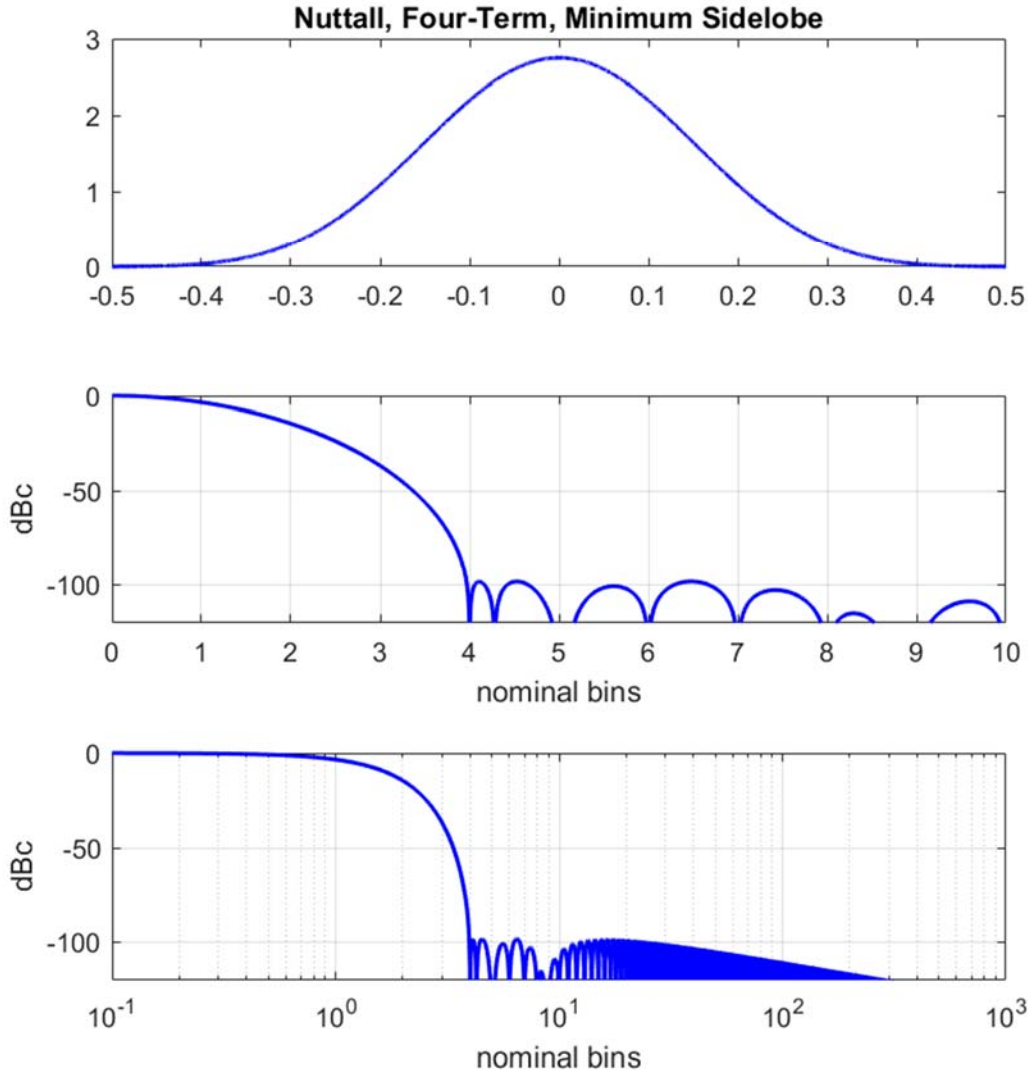


WINDOW SPECTRUM CHARACTERISTICS

half-power bandwidth = 1.872 (normalized to 1/T)
-3 dB bandwidth = 1.8689 (normalized to 1/T)
-18 dB bandwidth = 4.4151 (normalized to 1/T)
noise bandwidth = 1.9762 (normalized to 1/T)
SNR loss = 2.9584 dB
first null = 4 (normalized to 1/T)
PSL = -98.1697 dBc
ISL = -85.2311 dBc from first null outward

**Figure 47.**

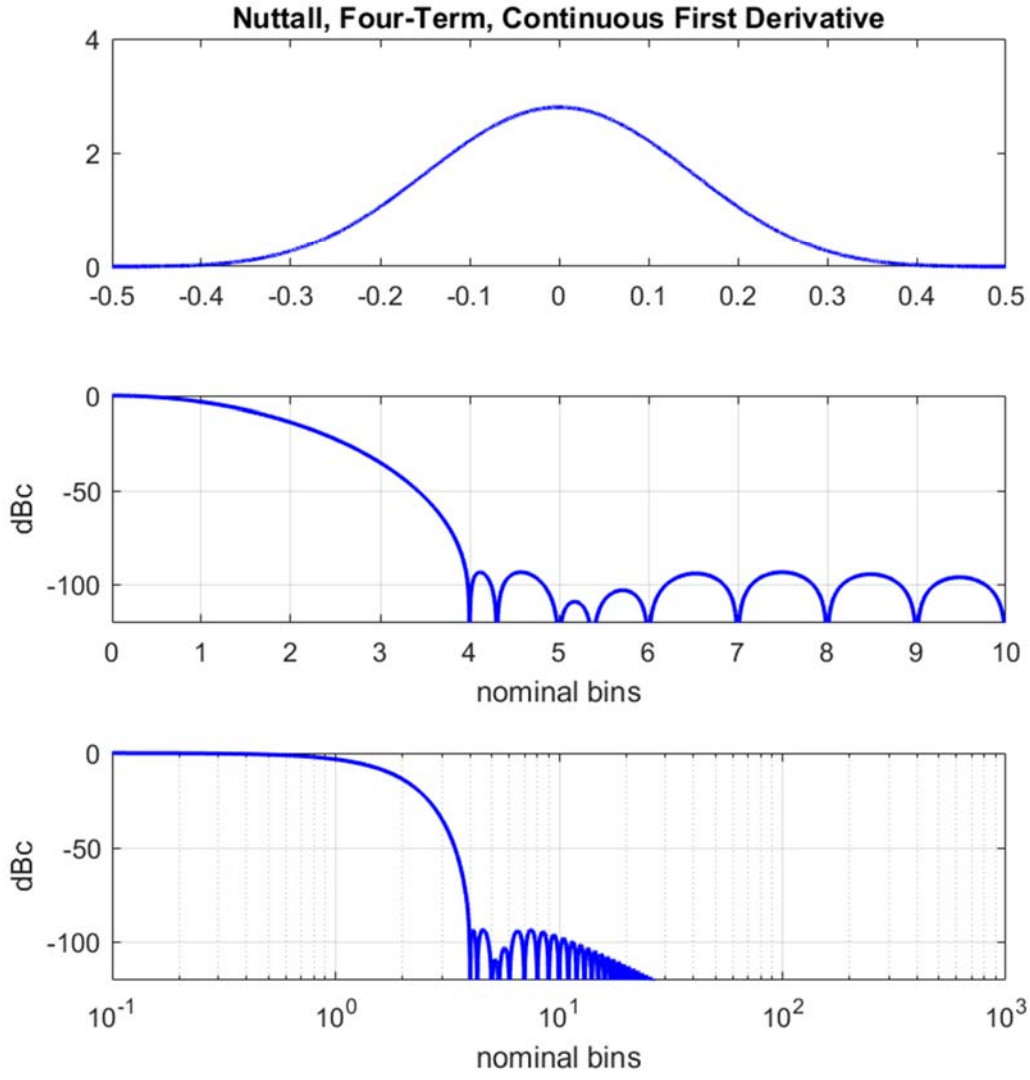


WINDOW SPECTRUM CHARACTERISTICS

half-power bandwidth = 1.9156 (normalized to 1/T)
-3 dB bandwidth = 1.9123 (normalized to 1/T)
-18 dB bandwidth = 4.5093 (normalized to 1/T)
noise bandwidth = 2.0214 (normalized to 1/T)
SNR loss = 3.0564 dB
first null = 4 (normalized to 1/T)
PSL = -93.3243 dBc
ISL = -89.1169 dBc from first null outward

**Figure 48.**

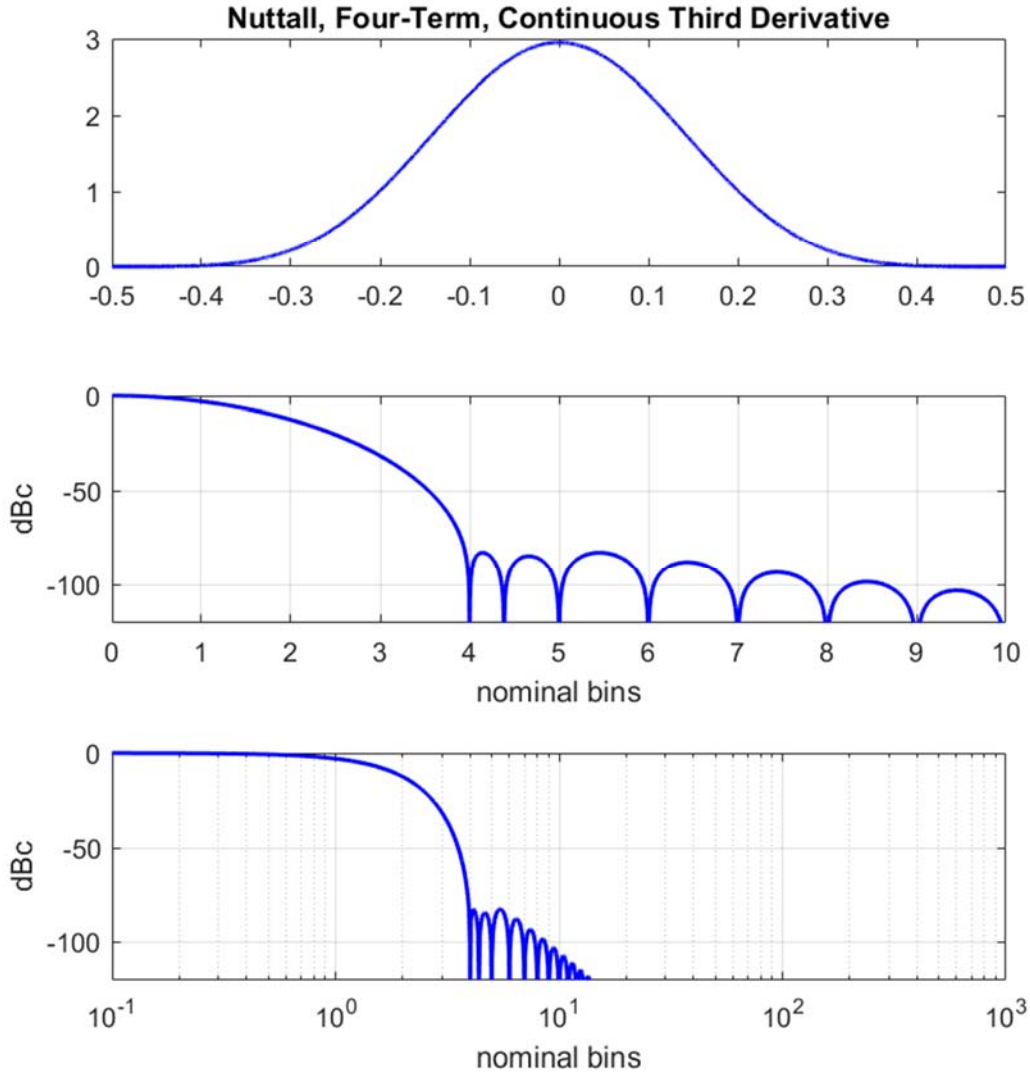


WINDOW SPECTRUM CHARACTERISTICS

half-power bandwidth = 2.0159 (normalized to 1/T)
-3 dB bandwidth = 2.0125 (normalized to 1/T)
-18 dB bandwidth = 4.7279 (normalized to 1/T)
noise bandwidth = 2.1254 (normalized to 1/T)
SNR loss = 3.2745 dB
first null = 4 (normalized to 1/T)
PSL = -82.6025 dBc
ISL = -82.4577 dBc from first null outward

**Figure 49.**

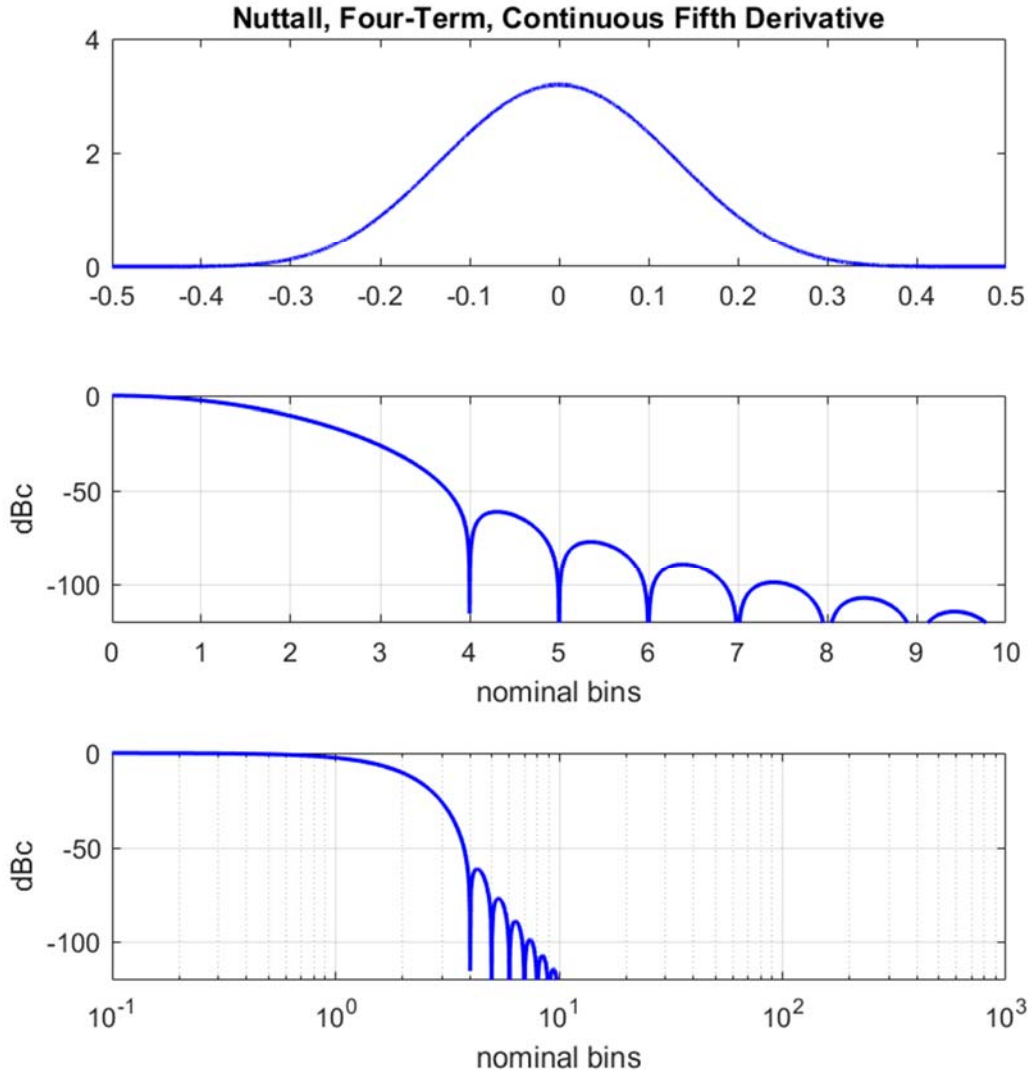


WINDOW SPECTRUM CHARACTERISTICS

half-power bandwidth = 2.1922 (normalized to 1/T)
-3 dB bandwidth = 2.1886 (normalized to 1/T)
-18 dB bandwidth = 5.1276 (normalized to 1/T)
noise bandwidth = 2.3101 (normalized to 1/T)
SNR loss = 3.6364 dB
first null = 4 (normalized to 1/T)
PSL = -60.9486 dBc
ISL = -64.9927 dBc from first null outward

**Figure 50.**

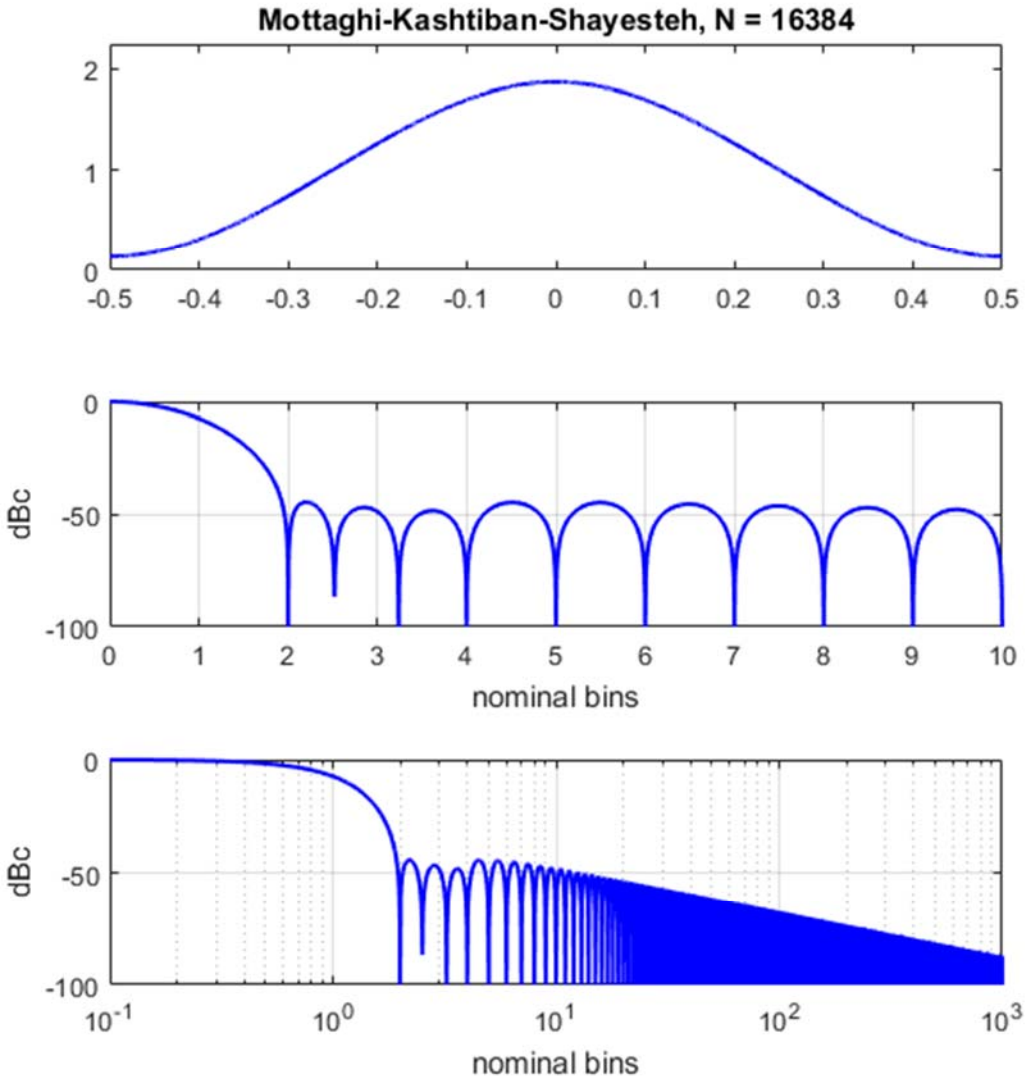


WINDOW SPECTRUM CHARACTERISTICS

half-power bandwidth = 1.3078 (normalized to 1/T)
-3 dB bandwidth = 1.3056 (normalized to 1/T)
-18 dB bandwidth = 2.9488 (normalized to 1/T)
noise bandwidth = 1.3675 (normalized to 1/T)
SNR loss = 1.359 dB
first null = 2 (normalized to 1/T)
PSL = -44.2999 dBc
ISL = -35.4579 dBc from first null outward

**Figure 51.**

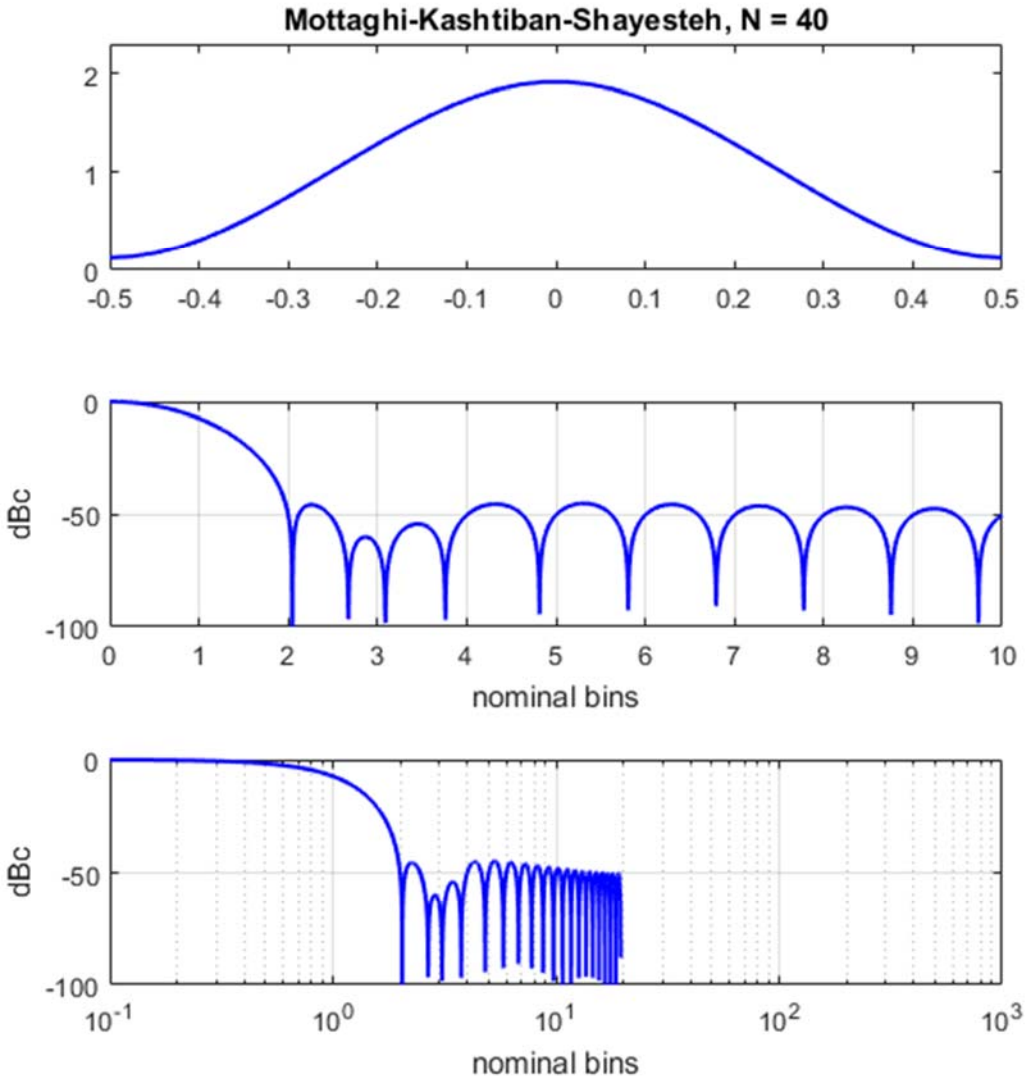


WINDOW SPECTRUM CHARACTERISTICS

half-power bandwidth = 1.3086 (normalized to 1/T)
-3 dB bandwidth = 1.3064 (normalized to 1/T)
-18 dB bandwidth = 2.9689 (normalized to 1/T)
noise bandwidth = 1.4051 (normalized to 1/T)
SNR loss = 1.477 dB
first null = 2.0469 (normalized to 1/T)
PSL = -44.8693 dBc
ISL = -36.664 dBc from first null outward

**Figure 52. (calculated with 40 samples)**

## 4.29 Exponential (a.k.a. Poisson)

The Exponential window taper function is a truncated two-sided decaying exponential function which in its form scaled for unit DC gain is

$$w(t) = Ae^{-2\alpha|t|}\,\mathrm{rect}(t), \tag{180}$$

where decay parameter

$$\alpha > 0, \tag{181}$$

and the desired scale factor is

$$A = \left( \int_{-1/2}^{1/2} e^{-2\alpha|t|} dt \right)^{-1} = \frac{\alpha}{\left(1 - e^{-\alpha}\right)}. \tag{182}$$

The Fourier Transform of the continuous time window taper function is calculated to be

$$W(f) = \frac{\alpha\left(\alpha\cos(\pi f) - \pi f \sin(\pi f) - \alpha e^{\alpha}\right)}{\left(\alpha^2 + \pi^2 f^2\right)\left(1 - e^{\alpha}\right)}. \tag{183}$$

Plots and characteristics for this window for several values of $\alpha$ are given in Figure 53, Figure 54, and Figure 55.

Harris[4] calls this a Poisson window and references Bary[17] for this window.

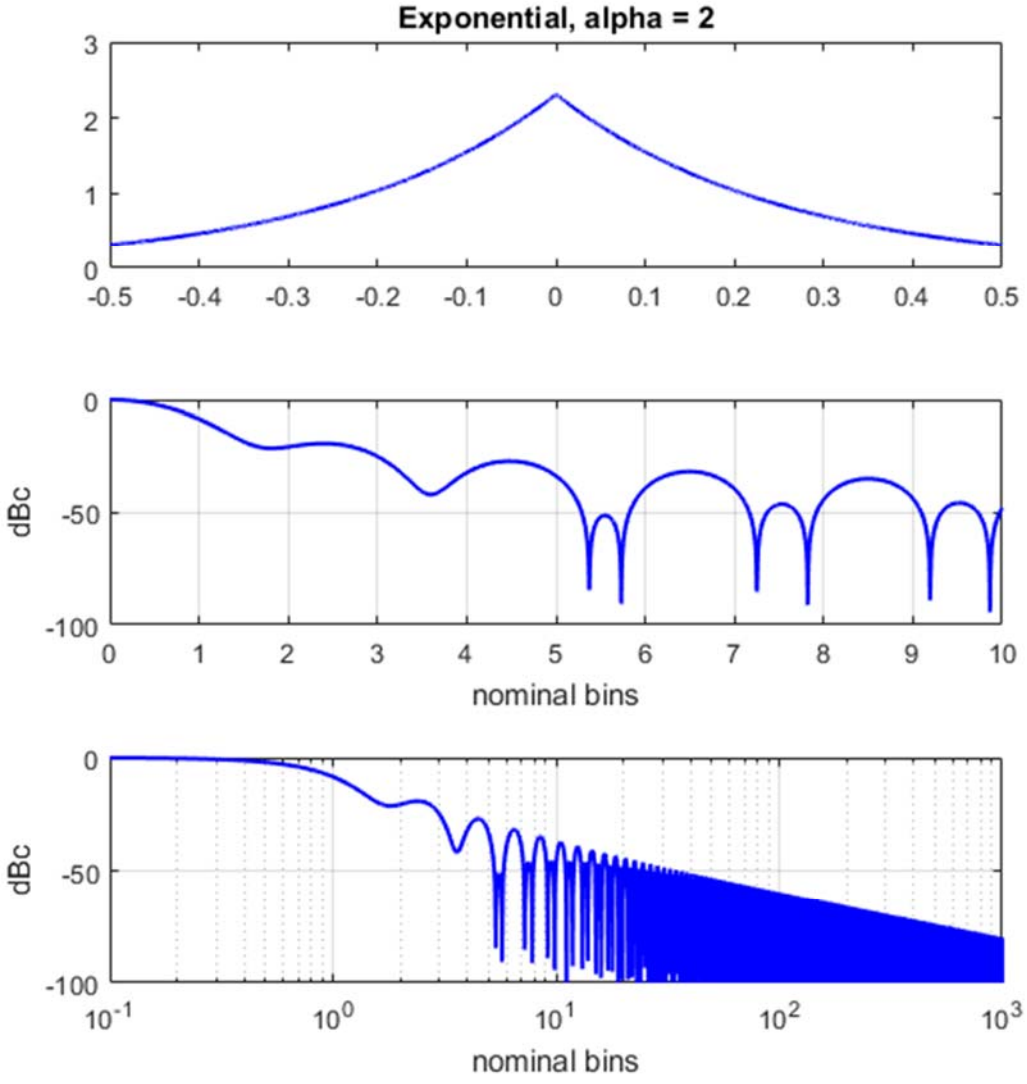


WINDOW SPECTRUM CHARACTERISTICS

half-power bandwidth = 1.2129 (normalized to 1/T)
-3 dB bandwidth = 1.2108 (normalized to 1/T)
-18 dB bandwidth = 2.9566 (normalized to 1/T)
noise bandwidth = 1.3131 (normalized to 1/T)
SNR loss = 1.1829 dB
first null = 1.8164 (normalized to 1/T)
PSL = -19.1924 dBc
ISL = -16.6911 dBc from first null outward

**Figure 53.**

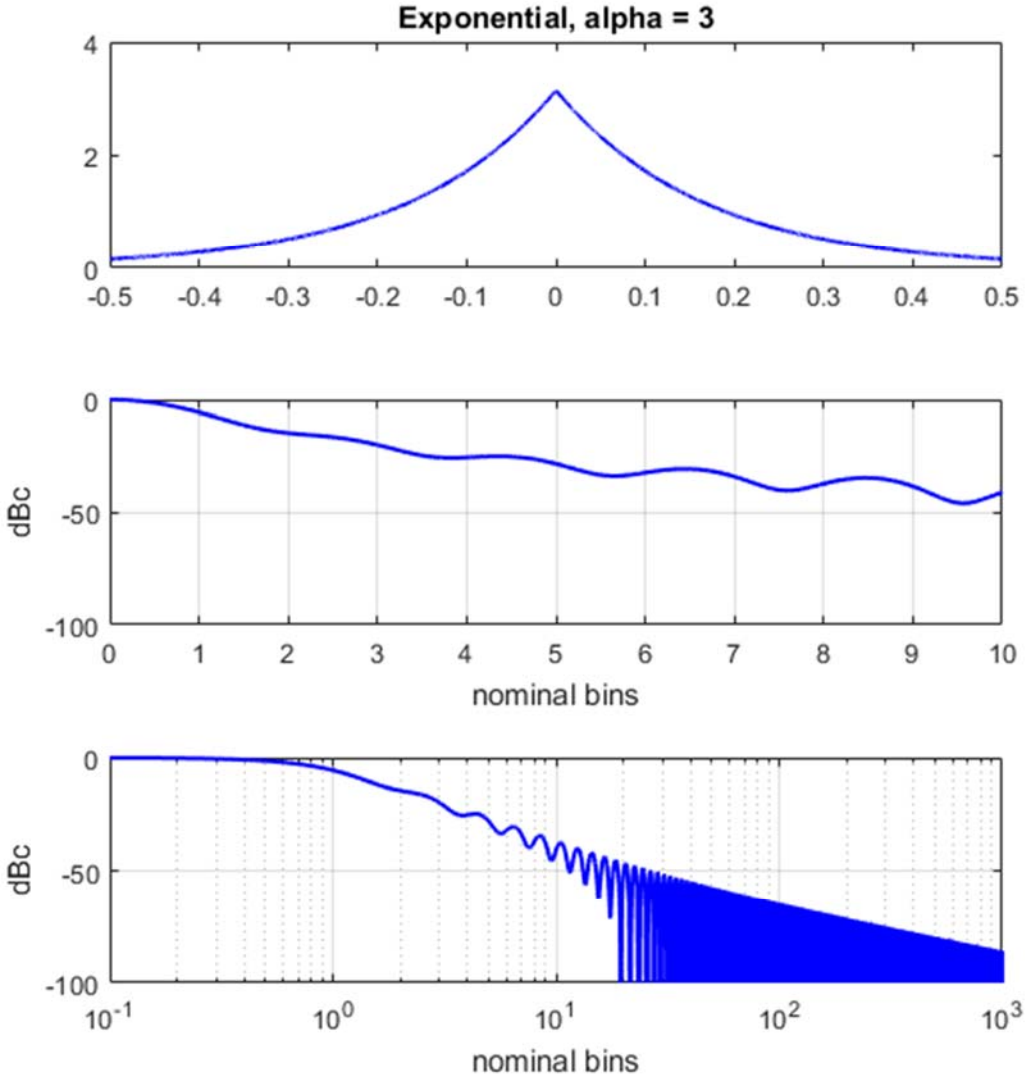


WINDOW SPECTRUM CHARACTERISTICS

half-power bandwidth = 1.4539 (normalized to 1/T)
-3 dB bandwidth = 1.4513 (normalized to 1/T)
-18 dB bandwidth = 5.5544 (normalized to 1/T)
noise bandwidth = 1.6573 (normalized to 1/T)
SNR loss = 2.1939 dB
first null = 3.8203 (normalized to 1/T)
PSL = -24.8715 dBc
ISL = -21.6408 dBc from first null outward

**Figure 54.**

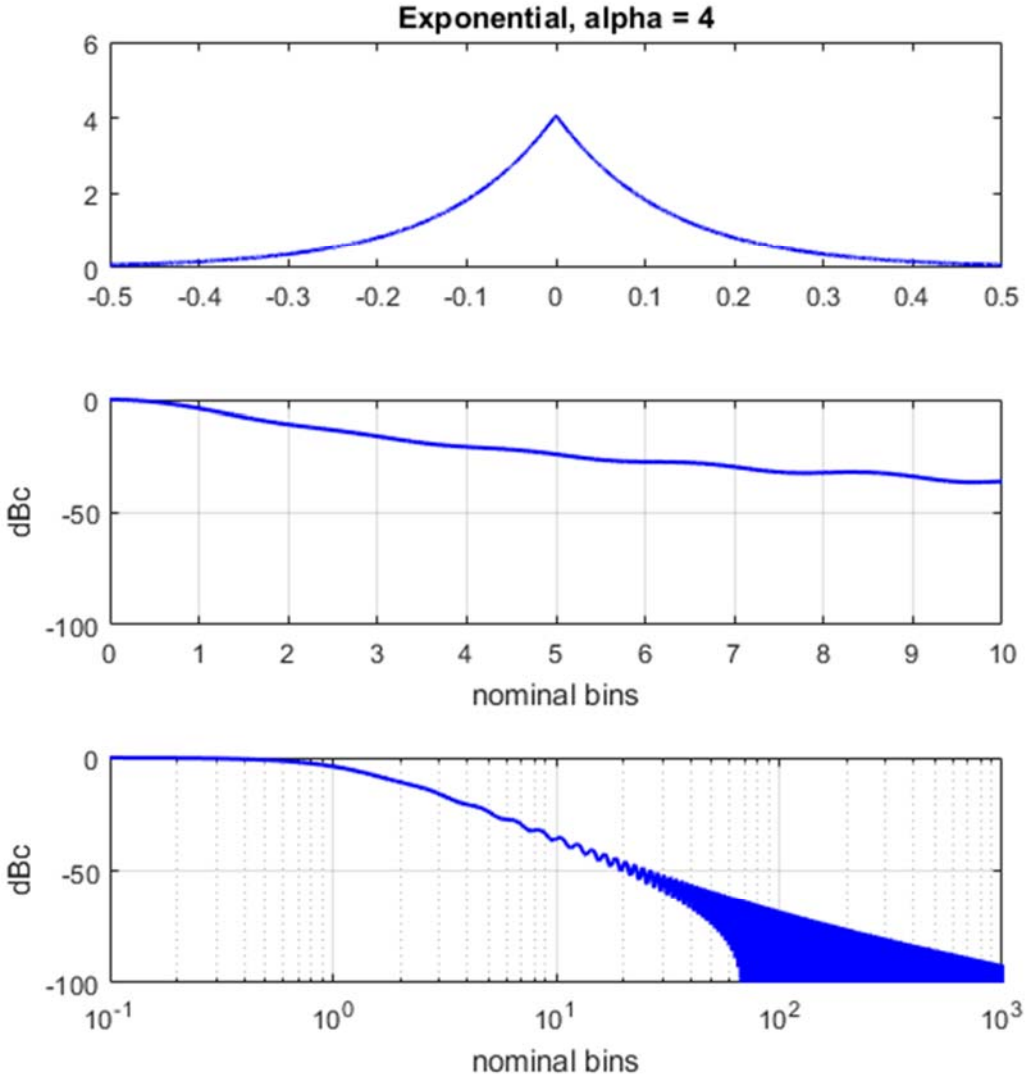


WINDOW SPECTRUM CHARACTERISTICS

half-power bandwidth = 1.7494 (normalized to 1/T)
-3 dB bandwidth = 1.7462 (normalized to 1/T)
-18 dB bandwidth = 6.6577 (normalized to 1/T)
noise bandwidth = 2.0747 (normalized to 1/T)
SNR loss = 3.1696 dB
first null = 7.7852 (normalized to 1/T)
PSL = -31.8897 dBc
ISL = -27.299 dBc from first null outward

**Figure 55.**

## 4.30 Hanning-Poisson

This window is a product of an Exponential (Poisson) window and a Hann (Hanning) window. Scaled for unit DC gain, this becomes

$$w(t) = Ae^{-2\alpha|t|}\left(1+\cos(2\pi t)\right)\mathrm{rect}(t), \tag{184}$$

where decay parameter

$$\alpha > 0, \tag{185}$$

and the desired scale factor is

$$A = \left( \int_{-1/2}^{1/2} e^{-2\alpha|t|}\left(1+\cos(2\pi t)\right)dt \right)^{-1} = \frac{\alpha\left(\alpha^2+\pi^2\right)}{\left(2\alpha^2+\pi^2-\pi^2 e^{-\alpha}\right)}. \tag{186}$$

The Fourier Transform of the continuous time window taper function is calculated to be

$$W(f) = \frac{A\left(\begin{array}{l}\alpha\left(2\alpha^4+\alpha^2\left(3+4f^2\right)\pi^2+\left(1-f^2+2f^4\right)\pi^4\right)\\ -e^{-\alpha}\pi^2\left(\begin{array}{l}\alpha\left(\alpha^2+\left(1-3f^2\right)\pi^2\right)\cos(\pi f)\\ +\pi f\left(-3\alpha^2+\left(-1+f^2\right)\pi^2\right)\sin(\pi f)\end{array}\right)\end{array}\right)}{\left(\begin{array}{l}\alpha^6+\alpha^4\left(2+3f^2\right)\pi^2\\ +\alpha^2\left(1+3f^4\right)\pi^4+f^2\left(-1+f^2\right)^2\pi^6\end{array}\right)}. \tag{187}$$

Plots and characteristics for this window for several values of $\alpha$ are given in Figure 56, Figure 57, and Figure 58. Note that as $\alpha$ increases, distinct sidelobes disappear into the asymptote. Consequently, the first null and parameters that depend on the first null become indistinct.

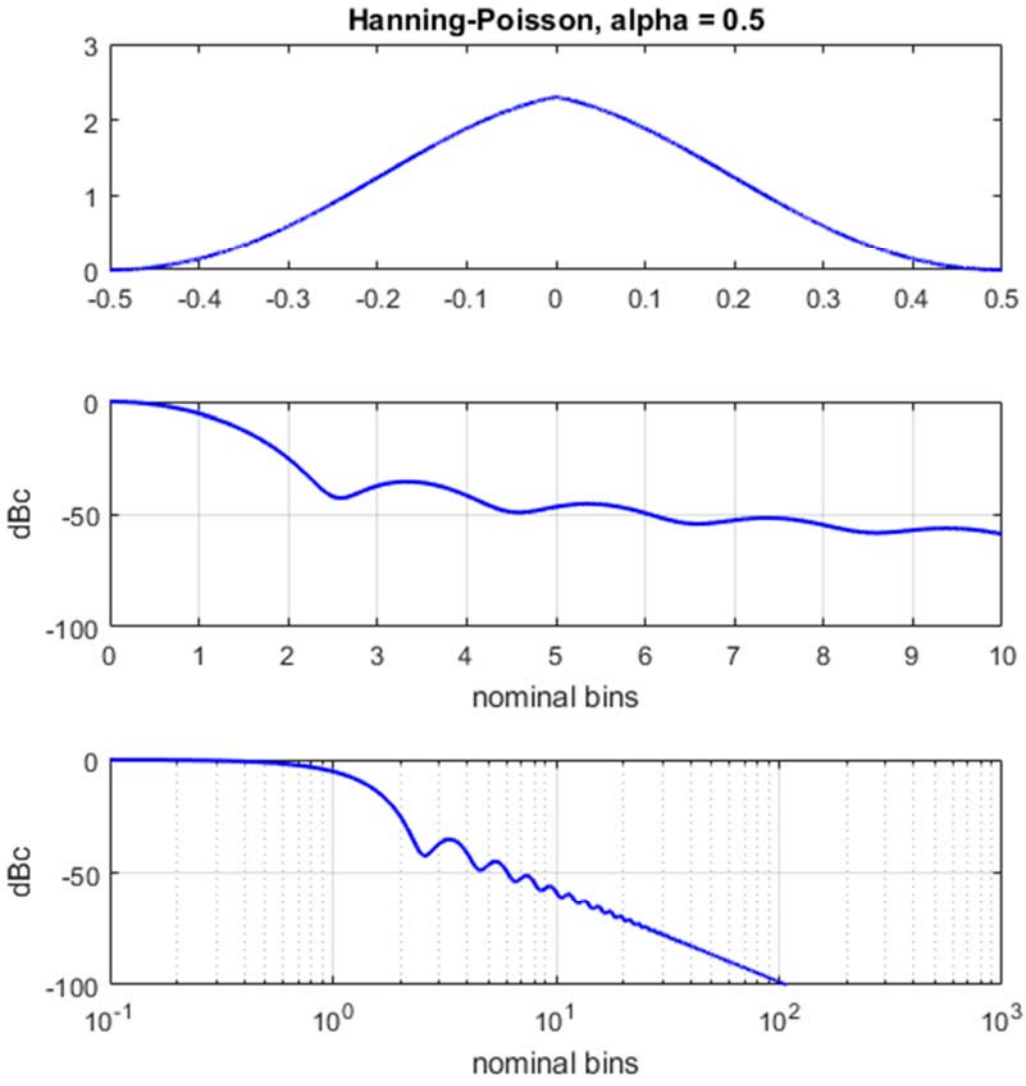


WINDOW SPECTRUM CHARACTERISTICS

half-power bandwidth = 1.5344 (normalized to 1/T)
-3 dB bandwidth = 1.5318 (normalized to 1/T)
-18 dB bandwidth = 3.507 (normalized to 1/T)
noise bandwidth = 1.6091 (normalized to 1/T)
SNR loss = 2.0658 dB
first null = 2.5859 (normalized to 1/T)
PSL = -35.2444 dBc
ISL = -33.8138 dBc from first null outward

**Figure 56.**

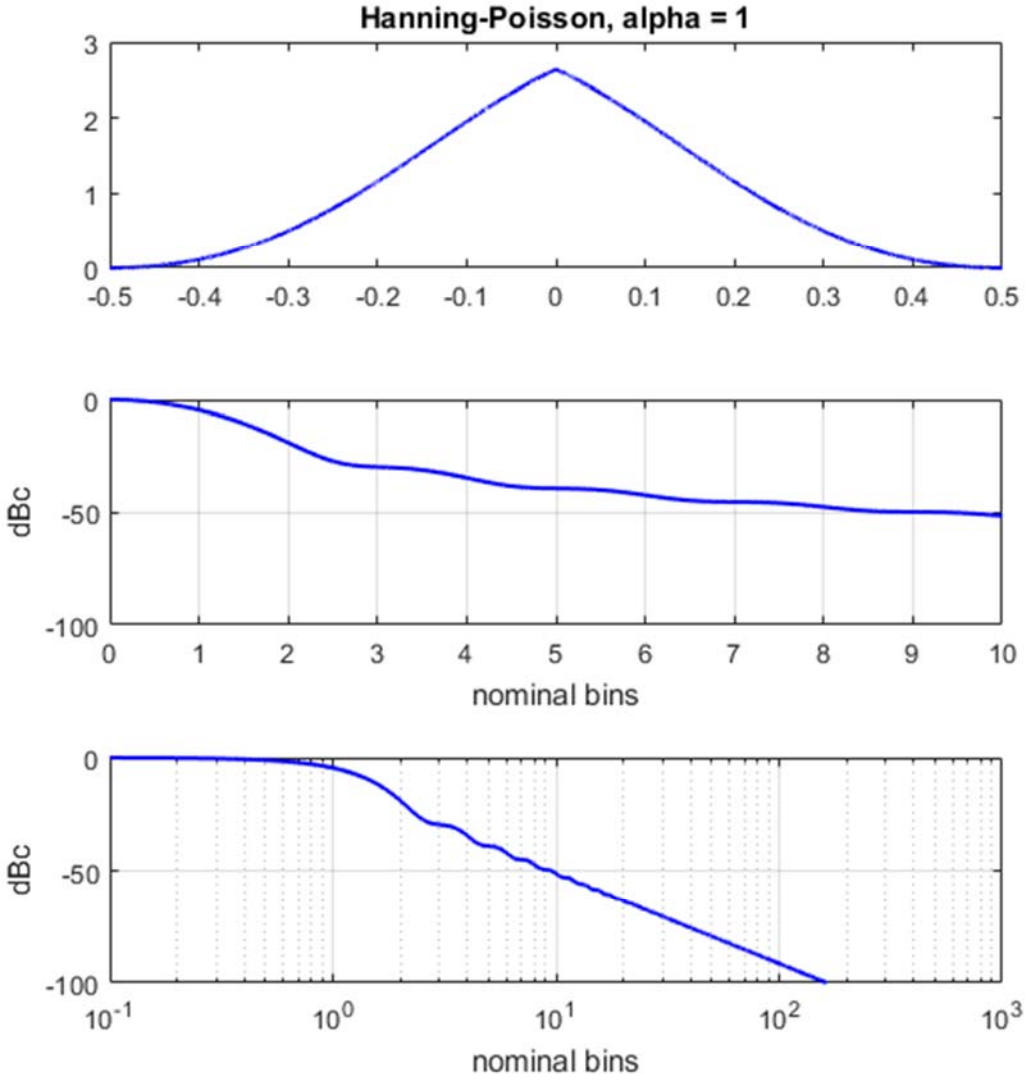


WINDOW SPECTRUM CHARACTERISTICS

half-power bandwidth = 1.6359 (normalized to 1/T)
-3 dB bandwidth = 1.6332 (normalized to 1/T)
-18 dB bandwidth = 3.9032 (normalized to 1/T)
noise bandwidth = 1.7333 (normalized to 1/T)
SNR loss = 2.3886 dB
first null = NaN (normalized to 1/T)
PSL = NaN dBc
ISL = NaN dBc from first null outward

**Figure 57.**

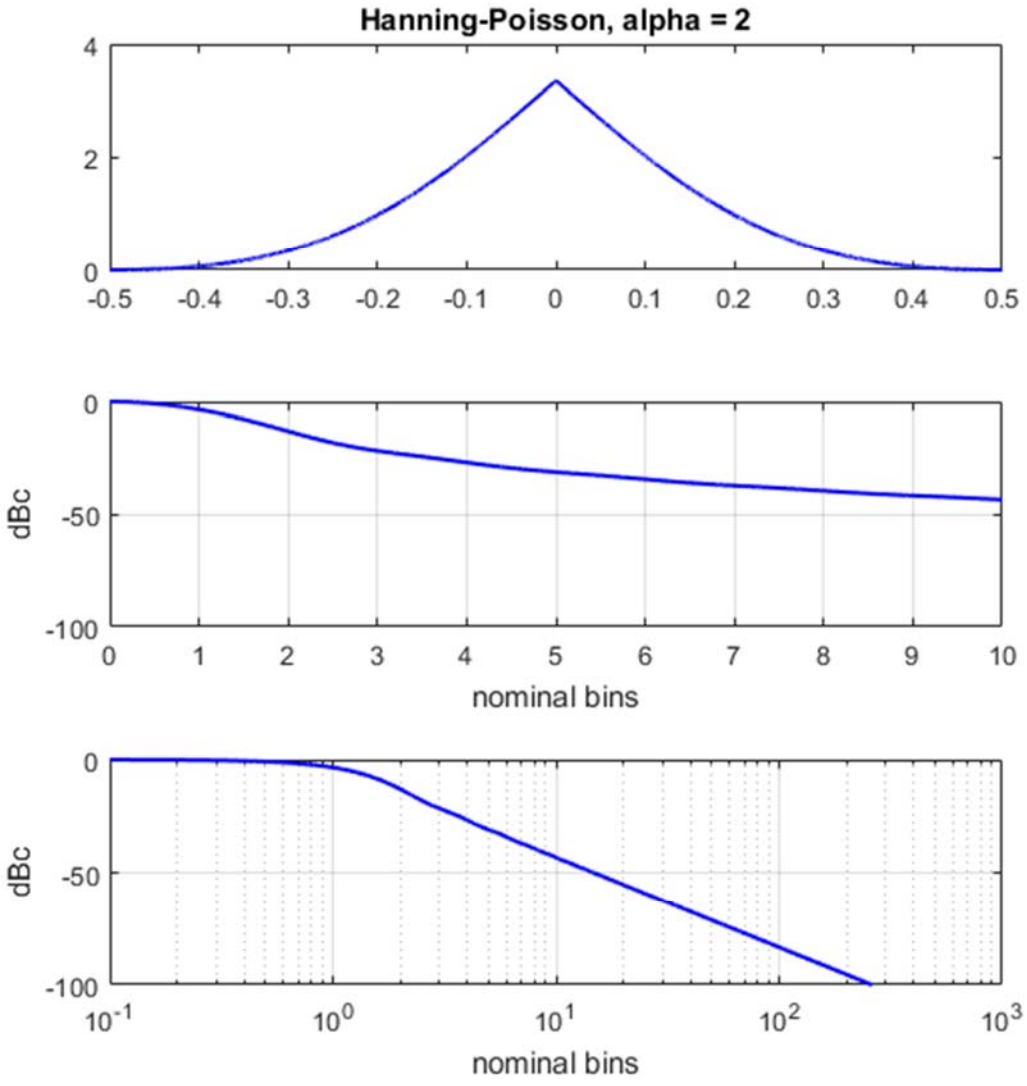


WINDOW SPECTRUM CHARACTERISTICS

half-power bandwidth = 1.8619 (normalized to 1/T)
-3 dB bandwidth = 1.8587 (normalized to 1/T)
-18 dB bandwidth = 4.9903 (normalized to 1/T)
noise bandwidth = 2.0221 (normalized to 1/T)
SNR loss = 3.0581 dB
first null = NaN (normalized to 1/T)
PSL = NaN dBc
ISL = NaN dBc from first null outward

**Figure 58.**

## 4.31 Gaussian (a.k.a. Weierstrass)

The Gaussian window taper function is a truncated Gaussian function, which in its form scaled for unit DC gain is

$$w(t) = Ae^{-2\alpha^2 t^2}\ \mathrm{rect}(t), \tag{188}$$

where truncation parameter

$$\alpha \ = \text{number of standard deviations at which truncation occurs,} \tag{189}$$

and the desired scale factor is

$$A = \left( \int_{-1/2}^{1/2} e^{-2\alpha^2 t^2} dt \right)^{-1} = \frac{\alpha\sqrt{2/\pi}}{\mathrm{erf}\left(\alpha/\sqrt{2}\right)}\ , \tag{190}$$

where we identify the error function as

$$\mathrm{erf}(z) = \frac{2}{\sqrt{\pi}} \int_0^z e^{-x^2} dx \ \ = \text{Gaussian error function.} \tag{191}$$

The Fourier Transform of the continuous time window taper function is calculated to be the convolution

$$W(f) = A\frac{\sqrt{\pi/2}}{\alpha} e^{\frac{-\pi^2 f^2}{2\alpha^2}} * \mathrm{sinc}(f)\,. \tag{192}$$

For reasonably large $\alpha$ and small *f*, this can be approximated as

$$W(f) \approx e^{\frac{-\pi^2 f^2}{2\alpha^2}}\ . \tag{193}$$

Plots and characteristics for this window for several values of $\alpha$ are given in Figure 59, Figure 60, and Figure 61.

Achieser[18] calls this form a Weierstrass kernel.

We observe that the exponential is a quadratic function in Eq. (188). A more generalized Gaussian window taper function might use some other power of $|t|$.

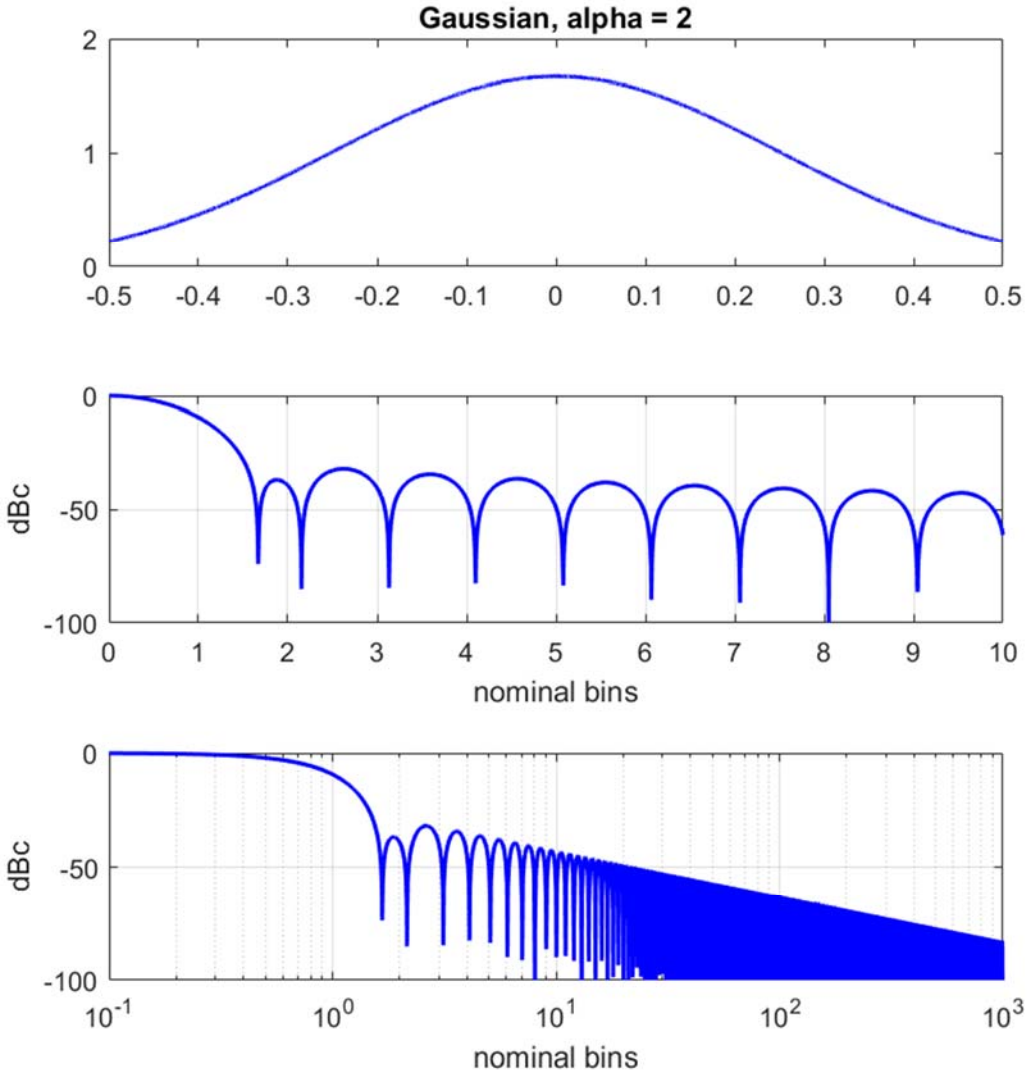


WINDOW SPECTRUM CHARACTERISTICS

half-power bandwidth = 1.1829 (normalized to 1/T)
-3 dB bandwidth = 1.1809 (normalized to 1/T)
-18 dB bandwidth = 2.6078 (normalized to 1/T)
noise bandwidth = 1.2328 (normalized to 1/T)
SNR loss = 0.90883 dB
first null = 1.668 (normalized to 1/T)
PSL = -31.8939 dBc
ISL = -27.2381 dBc from first null outward

**Figure 59.**

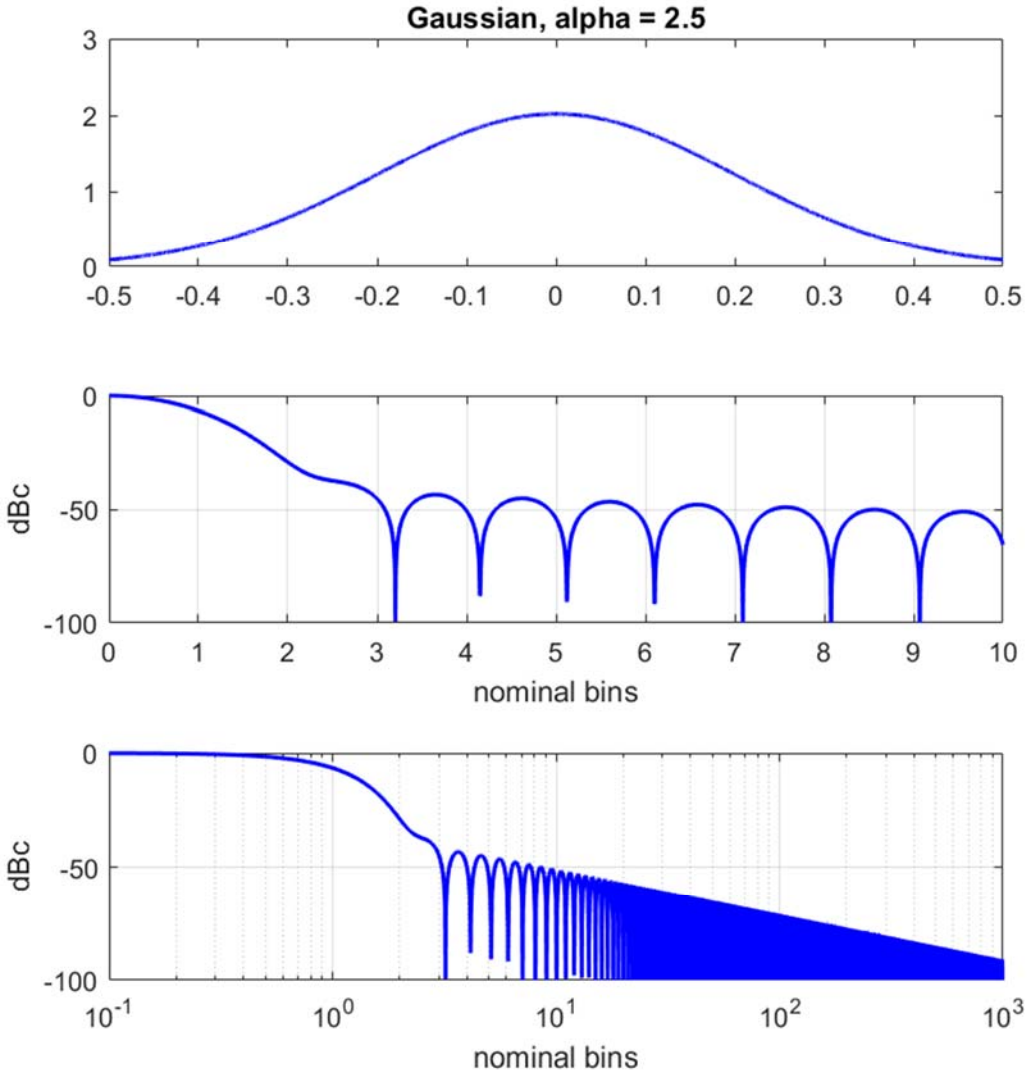


WINDOW SPECTRUM CHARACTERISTICS

half-power bandwidth = 1.3732 (normalized to 1/T)
-3 dB bandwidth = 1.3709 (normalized to 1/T)
-18 dB bandwidth = 3.1992 (normalized to 1/T)
noise bandwidth = 1.4457 (normalized to 1/T)
SNR loss = 1.6007 dB
first null = 3.2031 (normalized to 1/T)
PSL = -43.2552 dBc
ISL = -38.0489 dBc from first null outward

**Figure 60.**

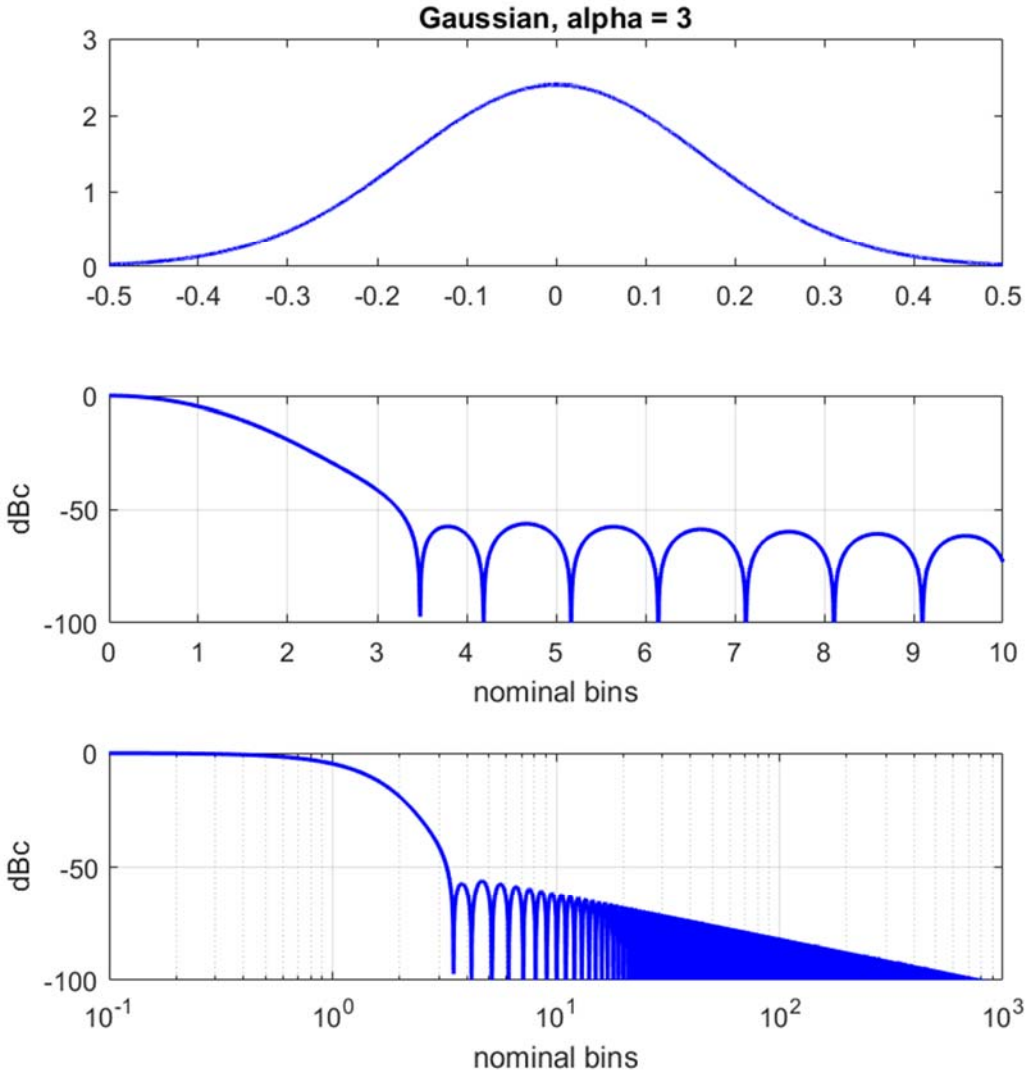


WINDOW SPECTRUM CHARACTERISTICS

half-power bandwidth = 1.6042 (normalized to 1/T)
-3 dB bandwidth = 1.6015 (normalized to 1/T)
-18 dB bandwidth = 3.8744 (normalized to 1/T)
noise bandwidth = 1.7018 (normalized to 1/T)
SNR loss = 2.3091 dB
first null = 3.4805 (normalized to 1/T)
PSL = -56.071 dBc
ISL = -50.0962 dBc from first null outward

**Figure 61.**

## 4.32 Parzen Exponential Family

Parzen[1] suggested a family of window taper functions of the form, which we have scaled for unit DC gain as

$$w(t) = A\, e^{-|2\alpha t|^r}\ \mathrm{rect}(t), \tag{194}$$

where parameters

$$\begin{aligned} &\alpha > 0\ , \text{ and} \\ &r > 0\ , \end{aligned} \tag{195}$$

and the desired scale factor for unit DC gain is

$$A = \left( \int_{-1/2}^{1/2} e^{-|2\alpha t|^r}\, dt \right)^{-1}\ . \tag{196}$$

The Fourier Transform of the continuous time window taper function is not readily calculated in closed-form. It may be numerically calculated for specific parameters, i.e. using a DFT on discrete-time samples of the window function.

Plots and characteristics for this window for an example parameter set are given in Figure 62.

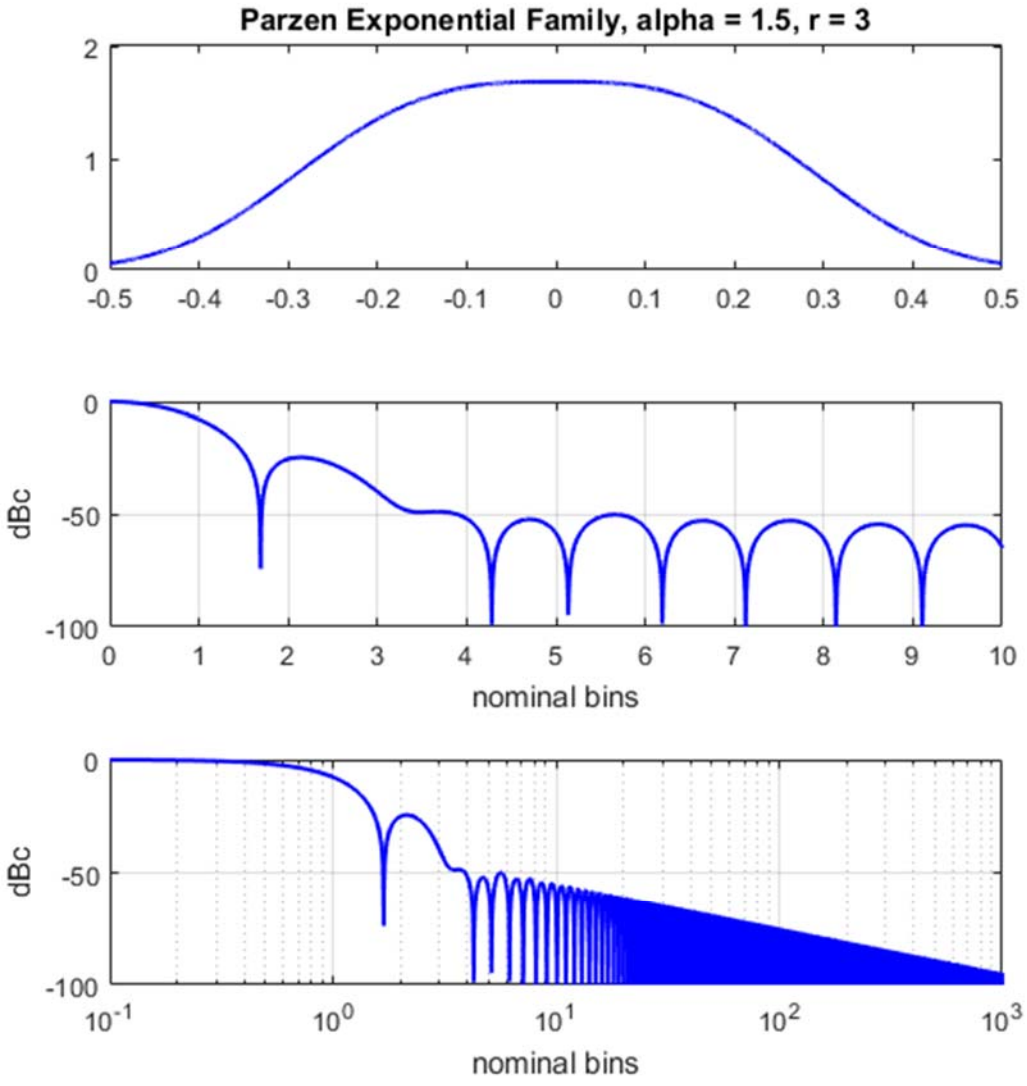


WINDOW SPECTRUM CHARACTERISTICS

half-power bandwidth = 1.2944 (normalized to 1/T)
-3 dB bandwidth = 1.2922 (normalized to 1/T)
-18 dB bandwidth = 2.7998 (normalized to 1/T)
noise bandwidth = 1.3463 (normalized to 1/T)
SNR loss = 1.291 dB
first null = 1.6914 (normalized to 1/T)
PSL = -24.4855 dBc
ISL = -24.6304 dBc from first null outward

**Figure 62.**

## 4.33 Dolph-Chebyshev (a.k.a. Chebyshev, Tchebyschev)

The Dolph-Chebyshev window seeks to achieve the most narrow mainlobe for a given PSL.[30] It is unique among the other windows presented heretofore in the report in several respects. Unlike more typical window taper functions, this window is defined by its frequency response. The frequency response of the continuous time window taper function is calculated to be

$$W(f) = \frac{\psi(f,N)\cos\left(\pi\sqrt{f^2 - A^2}\right)}{\cos\left(\pi\sqrt{-A^2}\right)}, \tag{197}$$

where

$$A = \frac{\operatorname{acosh}(\eta)}{\pi} = \frac{\ln\left(\eta + \sqrt{\eta^2 - 1}\right)}{\pi}, \tag{198}$$

$$\eta = 10^{-S/20}, \text{ and} \tag{199}$$

$S$ = sidelobe level with respect to mainlobe peak in dBc, with $S < 0$. (200)

The function $\psi$ specifies the sign of the expression, and equates to

$$\psi(f,N) = \begin{cases} +1 & for\ N\ odd, or\ f \geq 0 \\ -1 & else \end{cases}, \tag{201}$$

where $N$ = the expected discrete-time window function length. We note that for even $N$, this window taper function is not symmetric with $f$, thereby somewhat rare among window functions.

The actual window taper function itself is normally numerically calculated from the frequency response.[31] See Appendix A.

Plots and characteristics for this window for various sidelobe levels are given in Figure 63 through Figure 66.

This is not a particularly practical window function in that the continuous window has infinite noise bandwidth and infinite ISL, owing to the sidelobes never tapering towards zero. Note that this requires impulses at the ends of the window function itself, in fact violating the property in Eq. (31). While achievable for sampled window functions, noise bandwidth and ISL become highly dependent on the sample-length of the discrete time window. Nevertheless, it represents an ideal; a limit to what is achievable.

***Original Formulation***

The origin of this window function is via a development by Dolph that employed Chebyshev polynomials. Specifically, the discrete-frequency spectrum of the window taper function is developed directly to be

$$W_K(k) = N \frac{T_{N-1}\left( x_0 \cos\left( \pi \frac{f}{f_s} \right) \right)}{T_{N-1}(x_0)}, \quad \text{for } 0 \le k \le K-1, \tag{202}$$

where Chebyshev polynomials of the first kind are defined as those satisfying

$$T_n(x) = \cos\left( n \ \text{acos}(x) \right), \quad \text{for } x > -1 \ , \tag{203}$$

and for this development, the sidelobe-level parameter is

$$x_0 = \cosh\left( \frac{1}{N-1} \text{acosh}(\eta) \right), \tag{204}$$

where $\eta$ is defined as in Eq. (199).

Frequency in Eq. (202) takes on the discrete values

$$f = \frac{k}{K} f_s, \quad \text{for } 0 \le k \le K-1, \tag{205}$$

where for a unit-length aperture, we identify the sampling frequency as

$$f_s = N-1. \tag{206}$$

Recall that we expect $K \ge N$.

As *N* gets very large, with samples approaching the continuous case, we may employ Eq. (198), and note that

$$T_{N-1}\left( x_0 \cos\left( \pi \frac{f}{f_s} \right) \right) \xrightarrow[N\to\infty]{} +\cos\left( \pi \sqrt{f^2 - A^2} \right) \quad \textit{for } N \textit{ odd}, \textit{or } f \ge 0, \text{ and}$$

$$T_{N-1}\left( x_0 \cos\left( \pi \frac{f}{f_s} \right) \right) \xrightarrow[N\to\infty]{} -\cos\left( \pi \sqrt{f^2 - A^2} \right) \quad \textit{else}. \tag{207}$$

ultimately allowing the form given in Eq. (197).

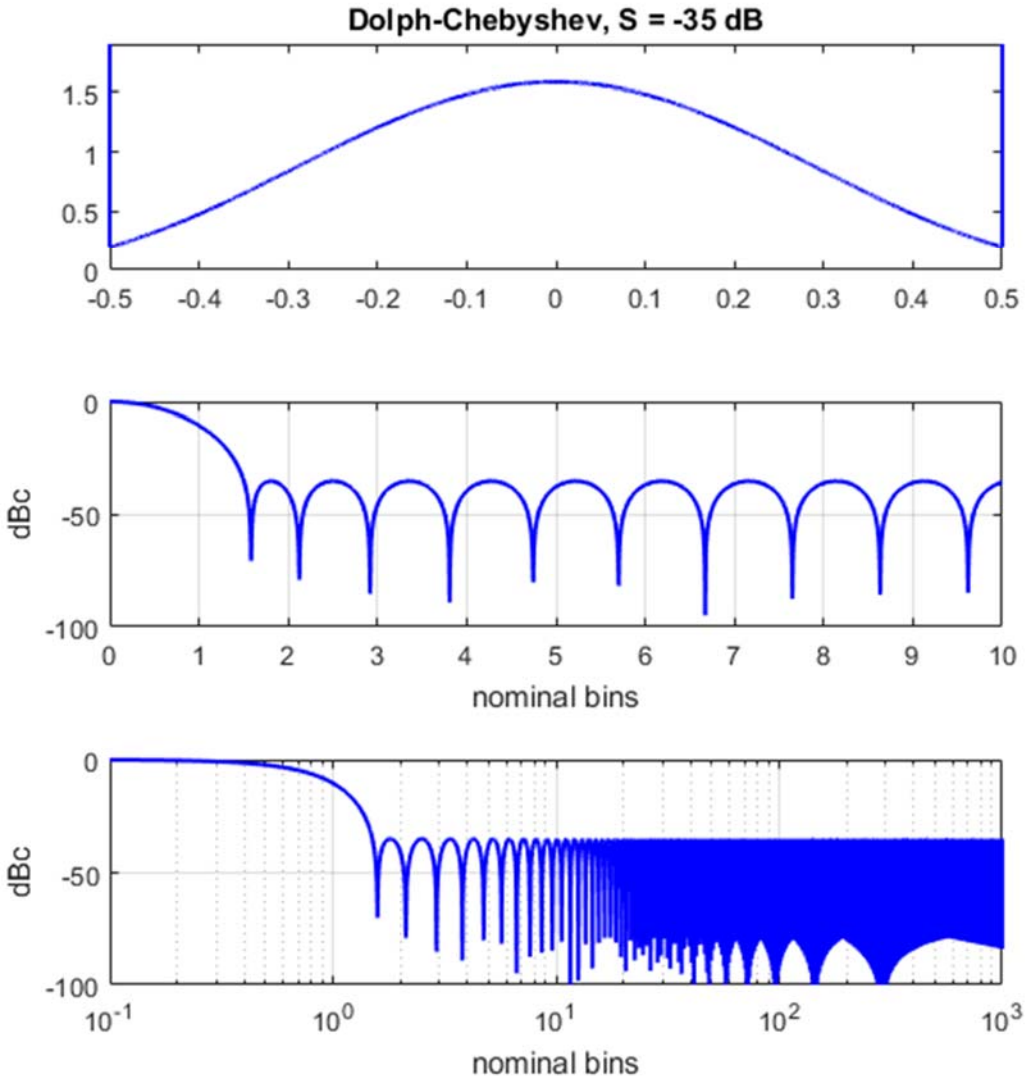


WINDOW SPECTRUM CHARACTERISTICS

half-power bandwidth = 1.1306 (normalized to 1/T)
-3 dB bandwidth = 1.1287 (normalized to 1/T)
-18 dB bandwidth = 2.4906 (normalized to 1/T)
noise bandwidth = Inf (normalized to 1/T)
SNR loss = Inf dB
first null = 1.5859 (normalized to 1/T)
PSL = -35 dBc
ISL = Inf dBc from first null outward

**Figure 63.**

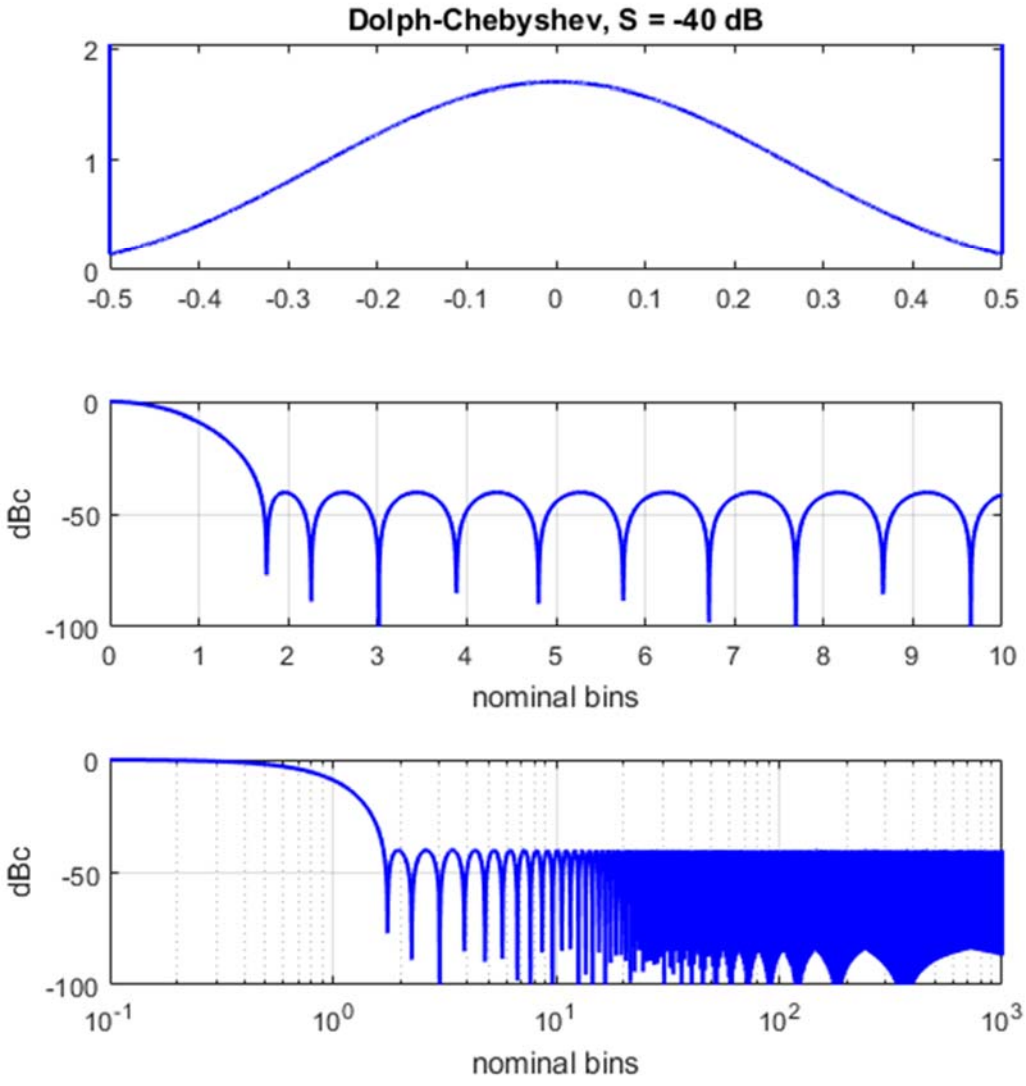


WINDOW SPECTRUM CHARACTERISTICS

half-power bandwidth = 1.1999 (normalized to 1/T)
-3 dB bandwidth = 1.1979 (normalized to 1/T)
-18 dB bandwidth = 2.6765 (normalized to 1/T)
noise bandwidth = Inf (normalized to 1/T)
SNR loss = Inf dB
first null = 1.7578 (normalized to 1/T)
PSL = -40 dBc
ISL = Inf dBc from first null outward

**Figure 64.**

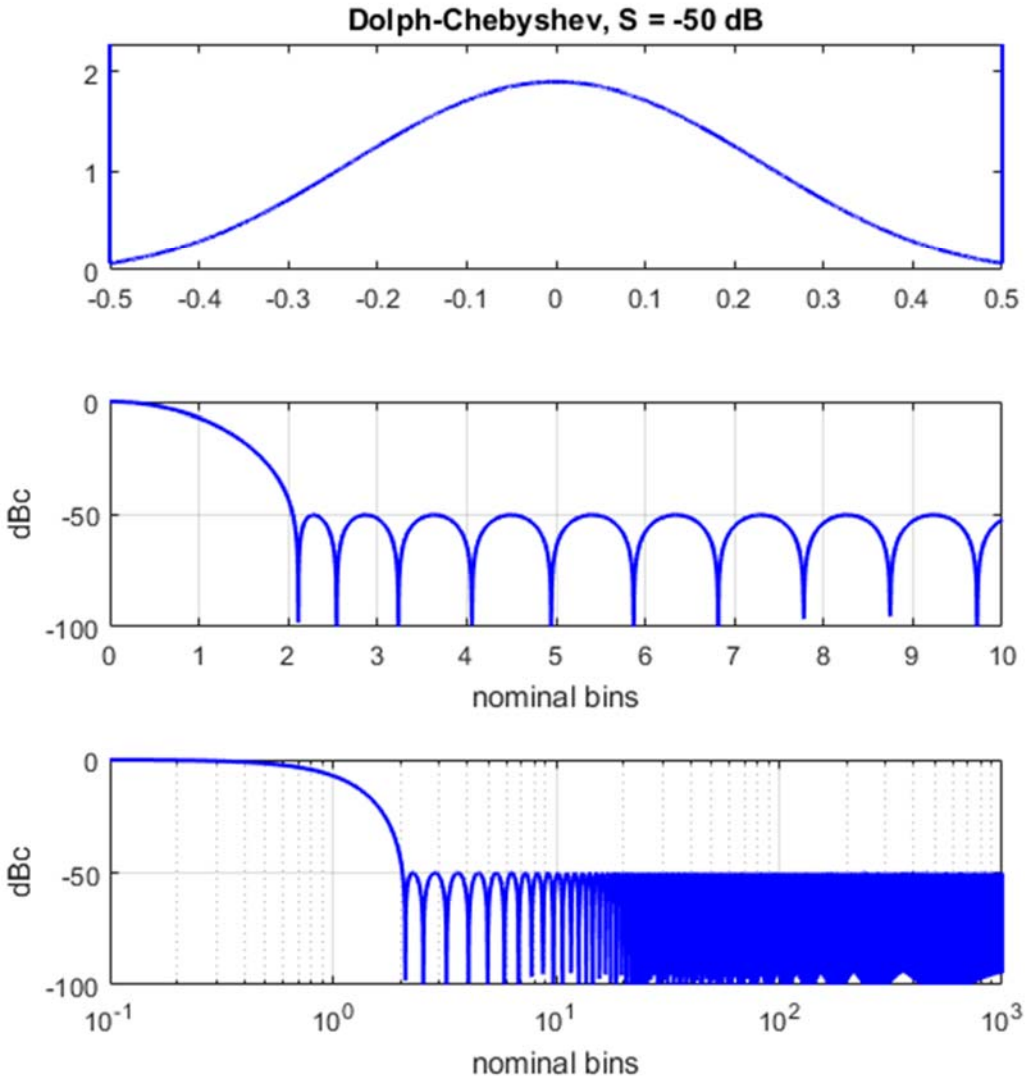


WINDOW SPECTRUM CHARACTERISTICS

half-power bandwidth = 1.3278 (normalized to 1/T)
-3 dB bandwidth = 1.3256 (normalized to 1/T)
-18 dB bandwidth = 3.0156 (normalized to 1/T)
noise bandwidth = Inf (normalized to 1/T)
SNR loss = Inf dB
first null = 2.1133 (normalized to 1/T)
PSL = -50 dBc
ISL = Inf dBc from first null outward

**Figure 65.**

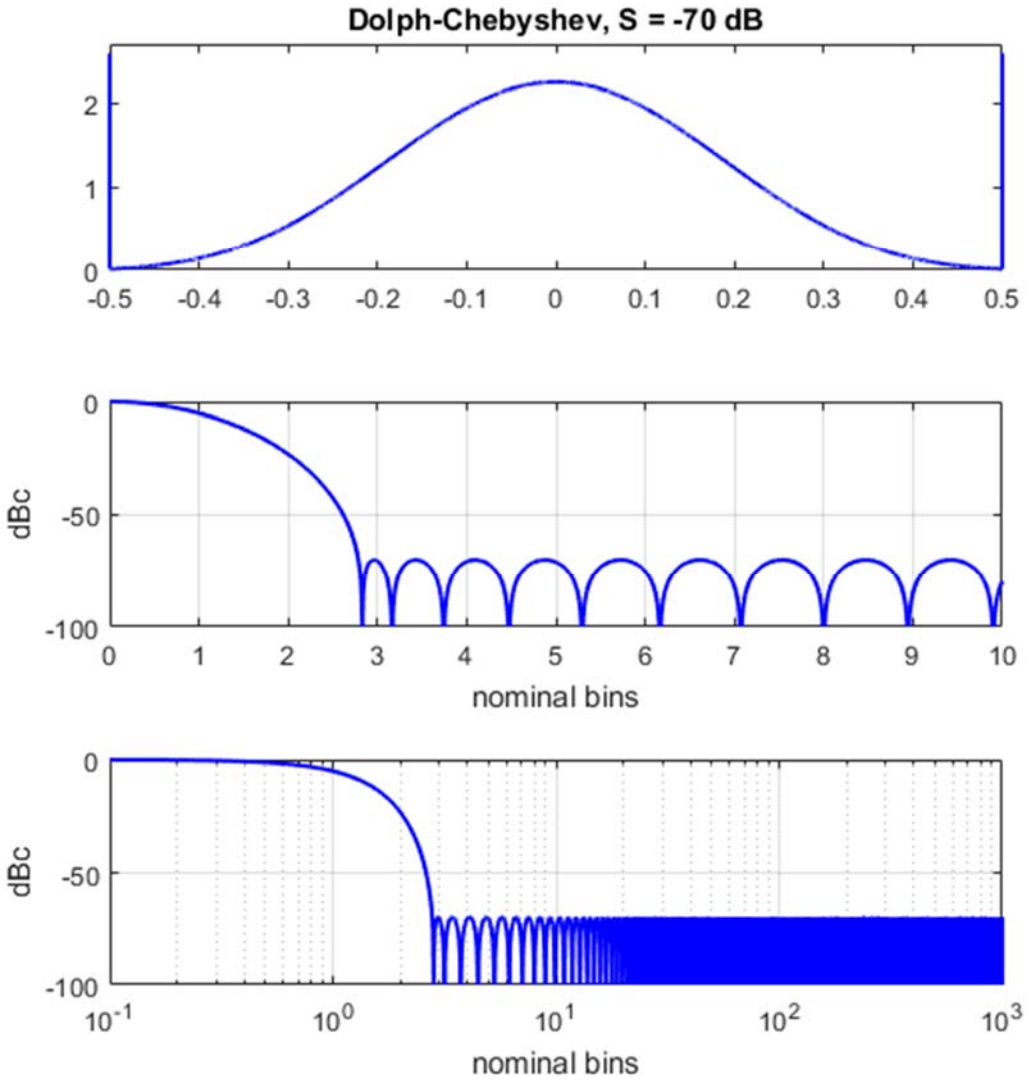


WINDOW SPECTRUM CHARACTERISTICS

half-power bandwidth = 1.5524 (normalized to 1/T)
-3 dB bandwidth = 1.5498 (normalized to 1/T)
-18 dB bandwidth = 3.6002 (normalized to 1/T)
noise bandwidth = Inf (normalized to 1/T)
SNR loss = Inf dB
first null = 2.832 (normalized to 1/T)
PSL = -70 dBc
ISL = Inf dBc from first null outward

**Figure 66.**

## 4.34 Taylor

The Taylor[32] window taper function approximates the Dolph-Chebyshev window's constant sidelobe level for a parameterized number of near-in sidelobes, but then allows a taper beyond. This makes it realizable, and in fact popular in some signal processing circles, especially radar signal processing.

The window function itself, scaled for unit DC gain, is calculated as[33]

$$w(t) = \left(1 + 2\sum_{m=1}^{(\bar{n}-1)} F_m \cos(2\pi m t)\right) \mathrm{rect}(t), \tag{208}$$

where the coefficients are calculated as

$$F_m = \frac{-\left(\frac{(-1)^m}{2}\right)\prod_{n=1}^{(\bar{n}-1)}\left(1 - \frac{\frac{m^2}{\sigma^2}}{A^2 + \left(n - \frac{1}{2}\right)^2}\right)}{\prod_{\substack{n=1 \\ n\neq m}}^{(\bar{n}-1)}\left(1 - \frac{m^2}{n^2}\right)}, \qquad \text{for } 1 \le m \le (\bar{n}-1), \tag{209}$$

with

$$\sigma^2 = \frac{(\bar{n})^2}{A^2 + \left(\bar{n} - \frac{1}{2}\right)^2}, \tag{210}$$

where

$$A = \frac{\mathrm{acosh}(\eta)}{\pi} = \frac{\ln\left(\eta + \sqrt{\eta^2 - 1}\right)}{\pi}, \tag{211}$$

and

$$\eta = 10^{-S/20}, \tag{212}$$

where

$S$ = sidelobe level with respect to mainlobe peak in dBc, with $S < 0$, and
$\bar{n}$ = the distance from the mainlobe for which sidelobes are constant. (213)

The Fourier Transform of the continuous time window taper function is calculated to be

$$W(f) = \mathrm{sinc}(f) + \sum_{m=1}^{(\bar{n}-1)} F_m \left( \mathrm{sinc}(f-m) + \mathrm{sinc}(f+m) \right). \tag{214}$$

We make the following observations.

- For $\bar{n} = 1$, the Taylor window reduces to a rectangle window.
- As $\bar{n} \to \infty$, the Taylor window approaches a Dolph-Chebyshev window.

Taylor suggests minimum values for $\bar{n}$ depending on sidelobe level *S*. Specifically, he suggests $\bar{n} \geq 3$ for $S = -25$ dBc, and $\bar{n} \geq 6$ for $S = -40$ dBc. For Discrete Time window taper functions, the following restrictions have been proposed to assure desired sidelobe characteristics are in fact achievable.[34]

$$\frac{|S|}{9} \leq \bar{n} \leq \frac{N}{5} \quad \text{for } -50 \leq S \leq -30 . \tag{215}$$

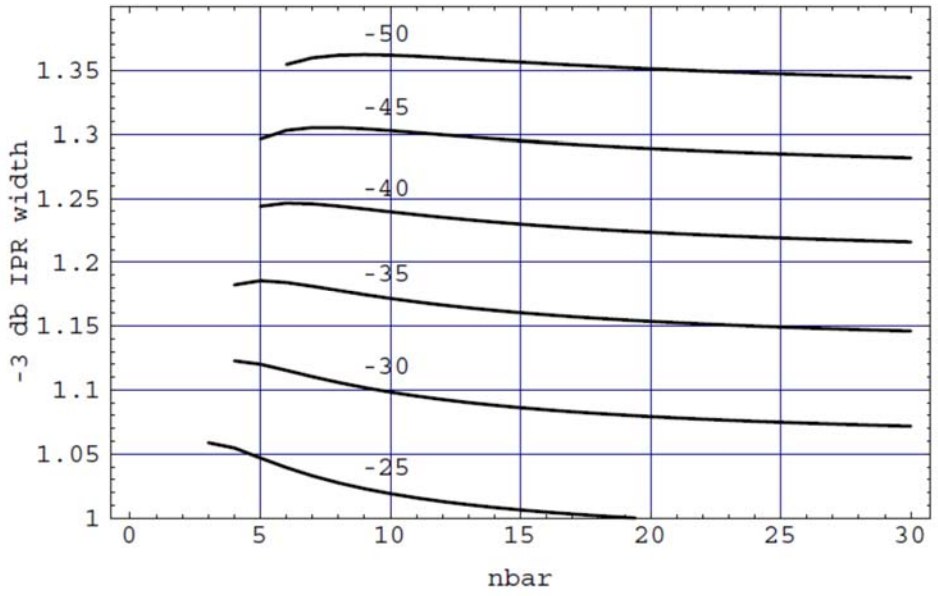


**Figure 67. Taylor window -3 dB mainlobe width for various combinations of $\bar{n}$ and S.[34]**

Plots and characteristics for this window for several parameter combinations are given in Figure 68 through Figure 71.

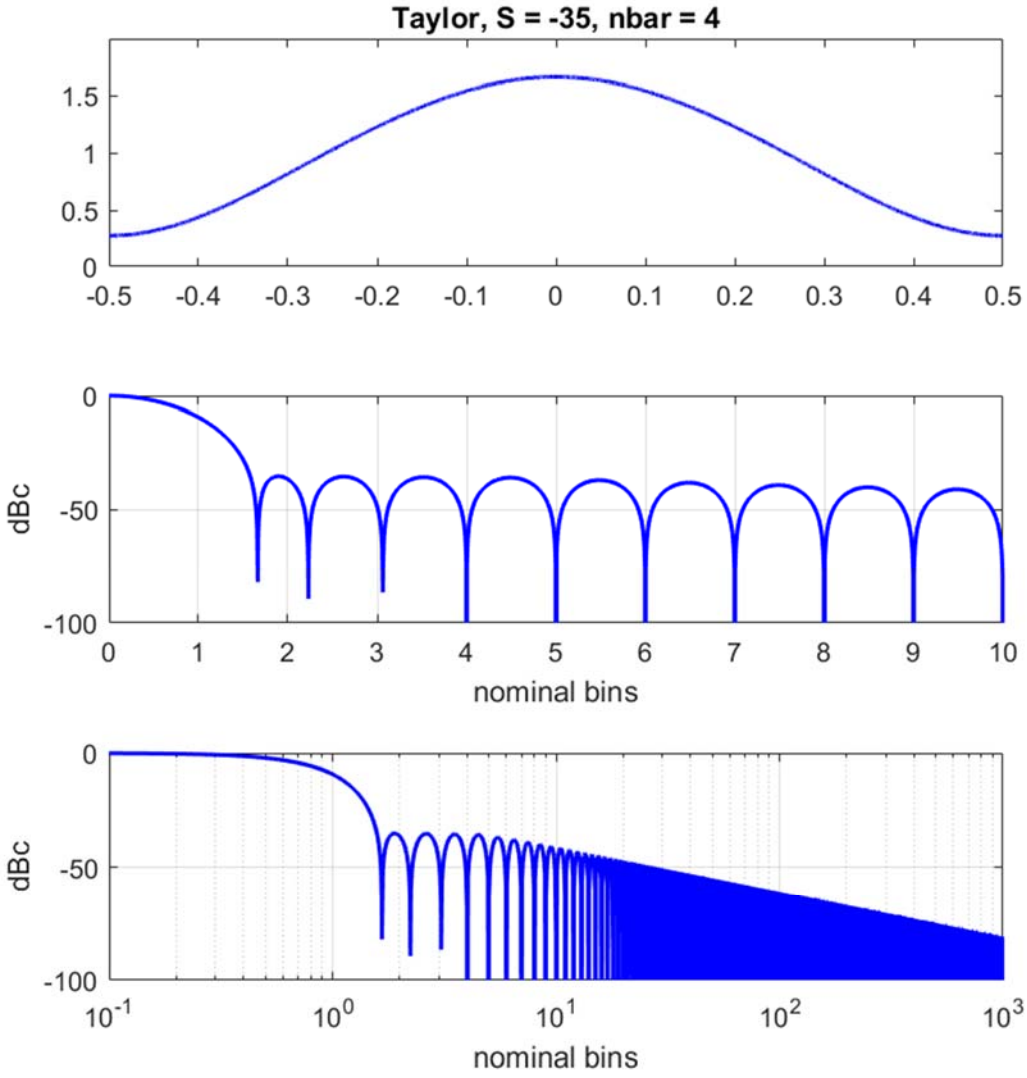


WINDOW SPECTRUM CHARACTERISTICS

half-power bandwidth = 1.1841 (normalized to 1/T)
-3 dB bandwidth = 1.1822 (normalized to 1/T)
-18 dB bandwidth = 2.6112 (normalized to 1/T)
noise bandwidth = 1.2343 (normalized to 1/T)
SNR loss = 0.91408 dB
first null = 1.6641 (normalized to 1/T)
PSL = -35.1672 dBc
ISL = -27.1388 dBc from first null outward

**Figure 68.**

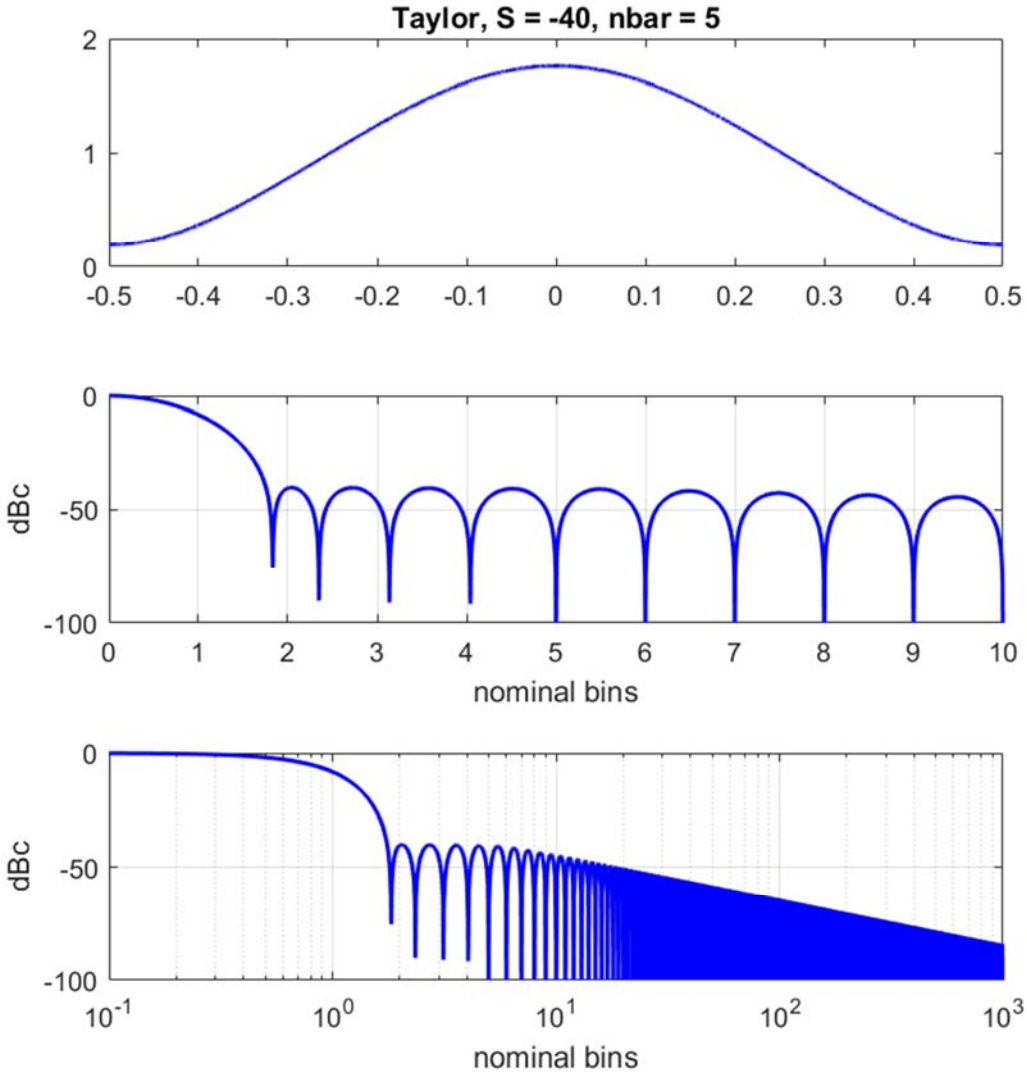


WINDOW SPECTRUM CHARACTERISTICS

half-power bandwidth = 1.246 (normalized to 1/T)
-3 dB bandwidth = 1.244 (normalized to 1/T)
-18 dB bandwidth = 2.7813 (normalized to 1/T)
noise bandwidth = 1.3006 (normalized to 1/T)
SNR loss = 1.1413 dB
first null = 1.832 (normalized to 1/T)
PSL = -40.1418 dBc
ISL = -31.37 dBc from first null outward

**Figure 69.**

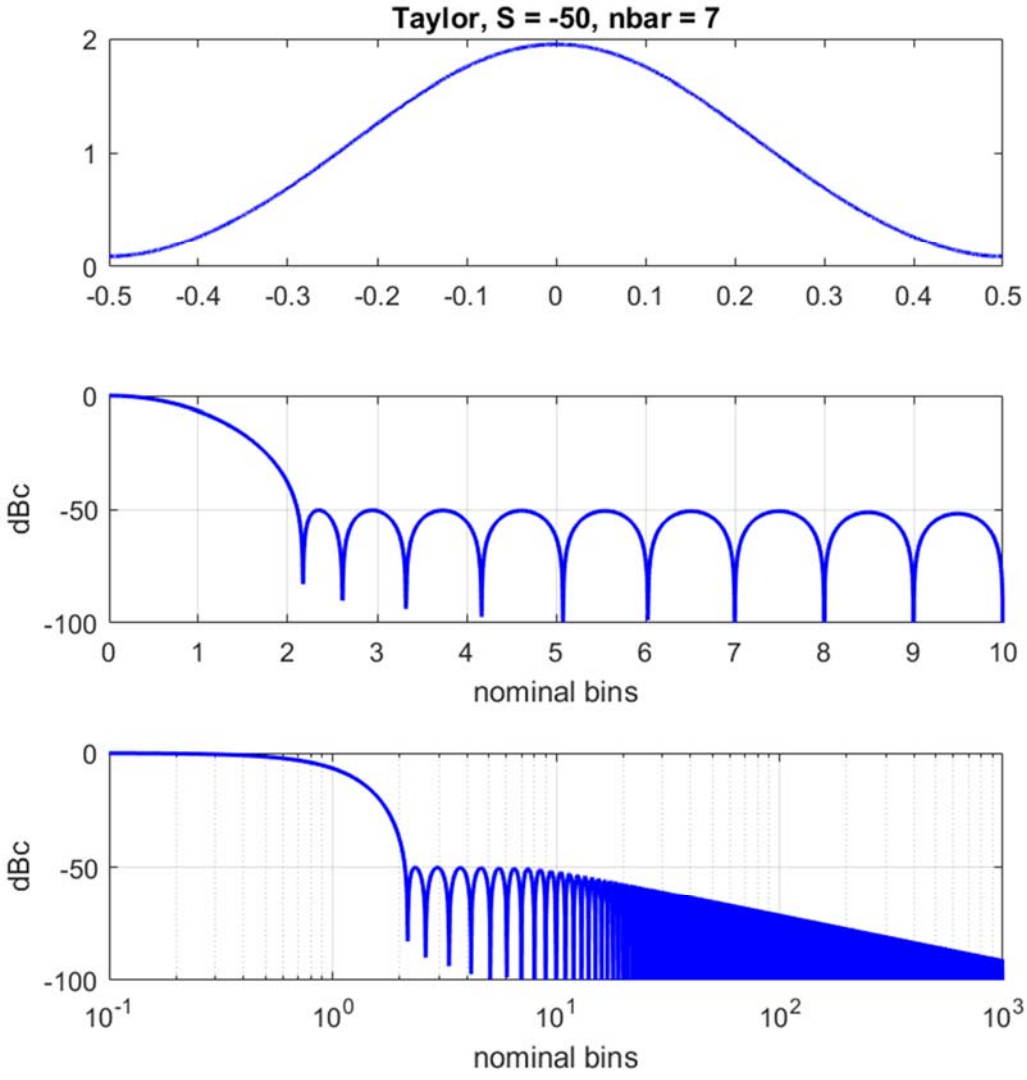


WINDOW SPECTRUM CHARACTERISTICS

half-power bandwidth = 1.3623 (normalized to 1/T)
-3 dB bandwidth = 1.36 (normalized to 1/T)
-18 dB bandwidth = 3.0947 (normalized to 1/T)
noise bandwidth = 1.4264 (normalized to 1/T)
SNR loss = 1.5423 dB
first null = 2.1719 (normalized to 1/T)
PSL = -50.0819 dBc
ISL = -39.9365 dBc from first null outward

**Figure 70.**

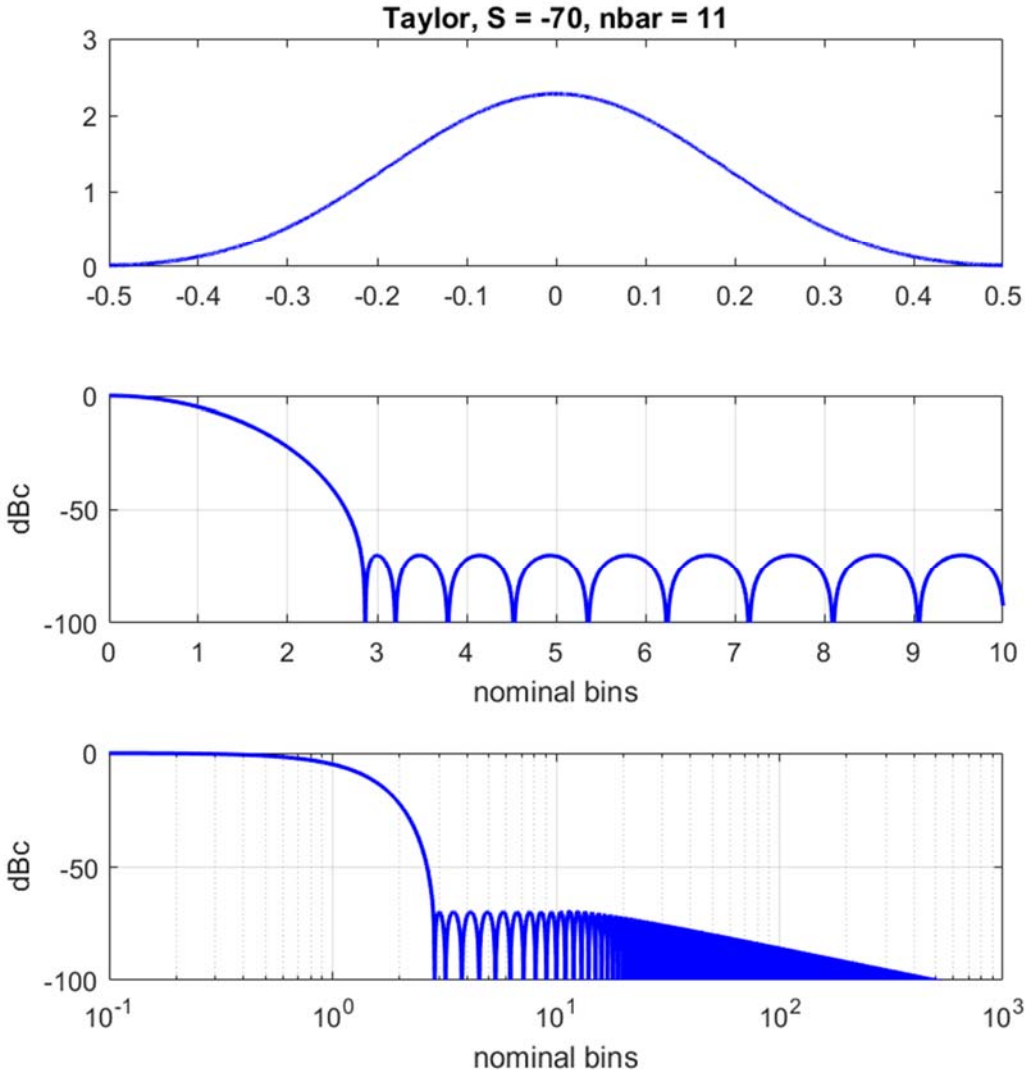


WINDOW SPECTRUM CHARACTERISTICS

half-power bandwidth = 1.5719 (normalized to 1/T)
-3 dB bandwidth = 1.5692 (normalized to 1/T)
-18 dB bandwidth = 3.6454 (normalized to 1/T)
noise bandwidth = 1.6532 (normalized to 1/T)
SNR loss = 2.1831 dB
first null = 2.8672 (normalized to 1/T)
PSL = -69.5168 dBc
ISL = -57.4146 dBc from first null outward

**Figure 71.**

## 4.35 Cauchy (a.k.a. Abel-Poisson)

The Cauchy window taper function scaled for unit DC gain, is calculated as

$$w(t) = A\left(\frac{1}{1+(2\alpha t)^2}\right)\mathrm{rect}(t), \tag{216}$$

where the decay parameter

$$\alpha > 0\ . \tag{217}$$

and the unit DC gain scale factor is

$$A = \frac{\alpha}{\mathrm{atan}(\alpha)}, \tag{218}$$

The Fourier Transform of the continuous time window taper function is calculated to be the convolution

$$W(f) = \frac{(\pi/2)e^{\frac{-\pi|f|}{a}}}{\mathrm{atan}(a)} * \mathrm{sinc}(f)\,. \tag{219}$$

This essentially describes a smoothed two-sided exponential for small *f*, and a smoothed sinc function for larger *f*.

Plots and characteristics for this window for several parameter combinations are given in Figure 72, Figure 73, and Figure 74.

While Harris[4] calls this a Cauchy window, Achieser[18] refers to this as a Abel-Poisson kernel.

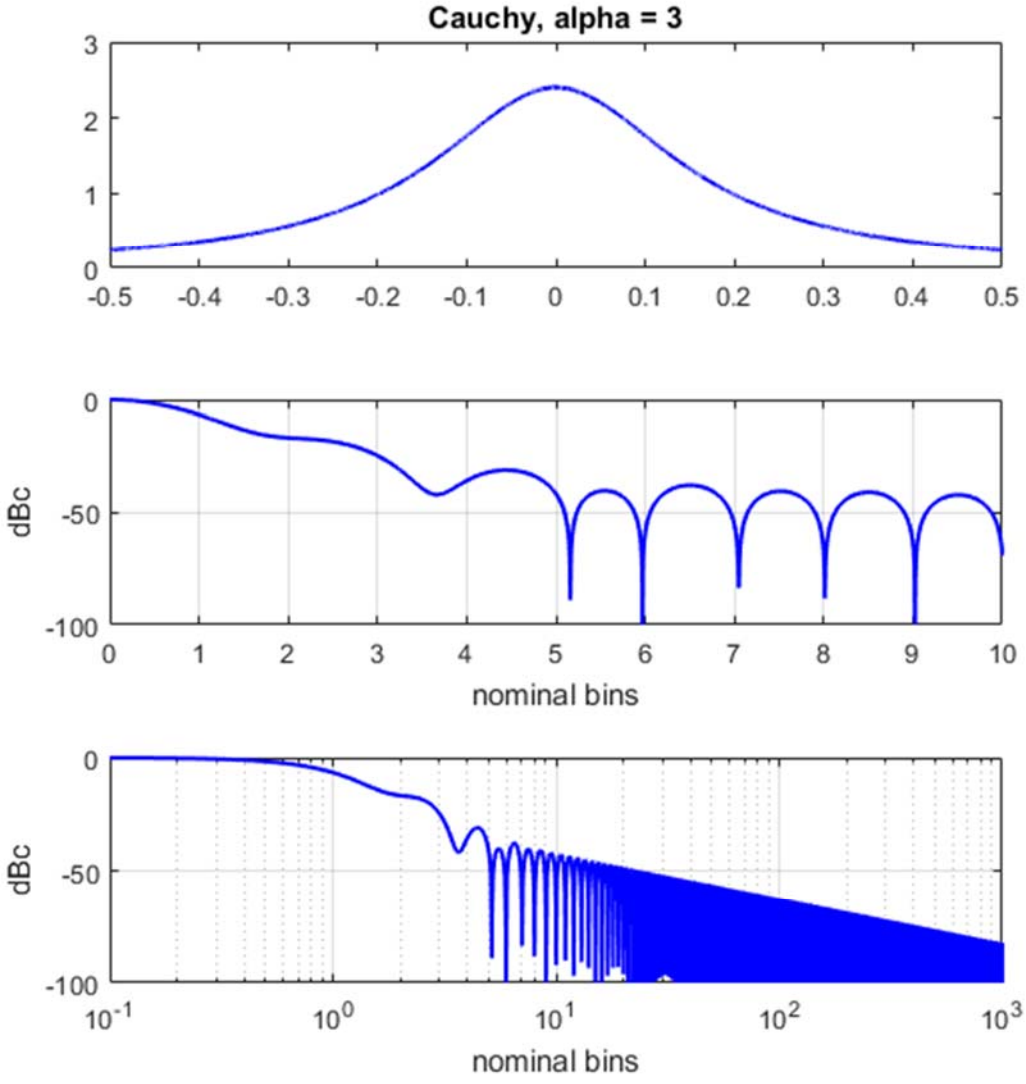


WINDOW SPECTRUM CHARACTERISTICS

half-power bandwidth = 1.3435 (normalized to 1/T)
-3 dB bandwidth = 1.3412 (normalized to 1/T)
-18 dB bandwidth = 4.8616 (normalized to 1/T)
noise bandwidth = 1.4894 (normalized to 1/T)
SNR loss = 1.7301 dB
first null = 3.6641 (normalized to 1/T)
PSL = -31.0057 dBc
ISL = -28.2638 dBc from first null outward

**Figure 72.**

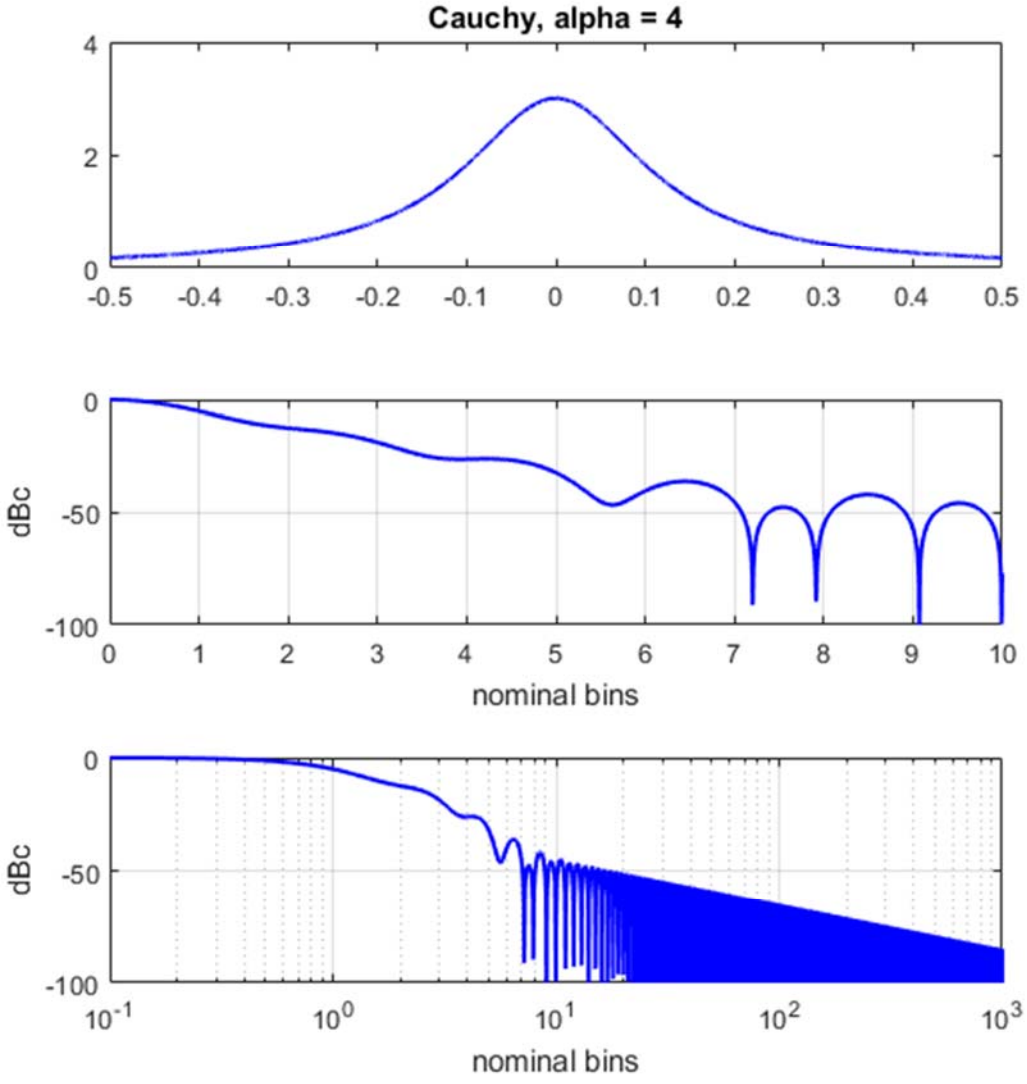


WINDOW SPECTRUM CHARACTERISTICS

half-power bandwidth = 1.5194 (normalized to 1/T)
-3 dB bandwidth = 1.5167 (normalized to 1/T)
-18 dB bandwidth = 5.863 (normalized to 1/T)
noise bandwidth = 1.7763 (normalized to 1/T)
SNR loss = 2.4951 dB
first null = 3.9219 (normalized to 1/T)
PSL = -26.0221 dBc
ISL = -25.2828 dBc from first null outward

**Figure 73.**

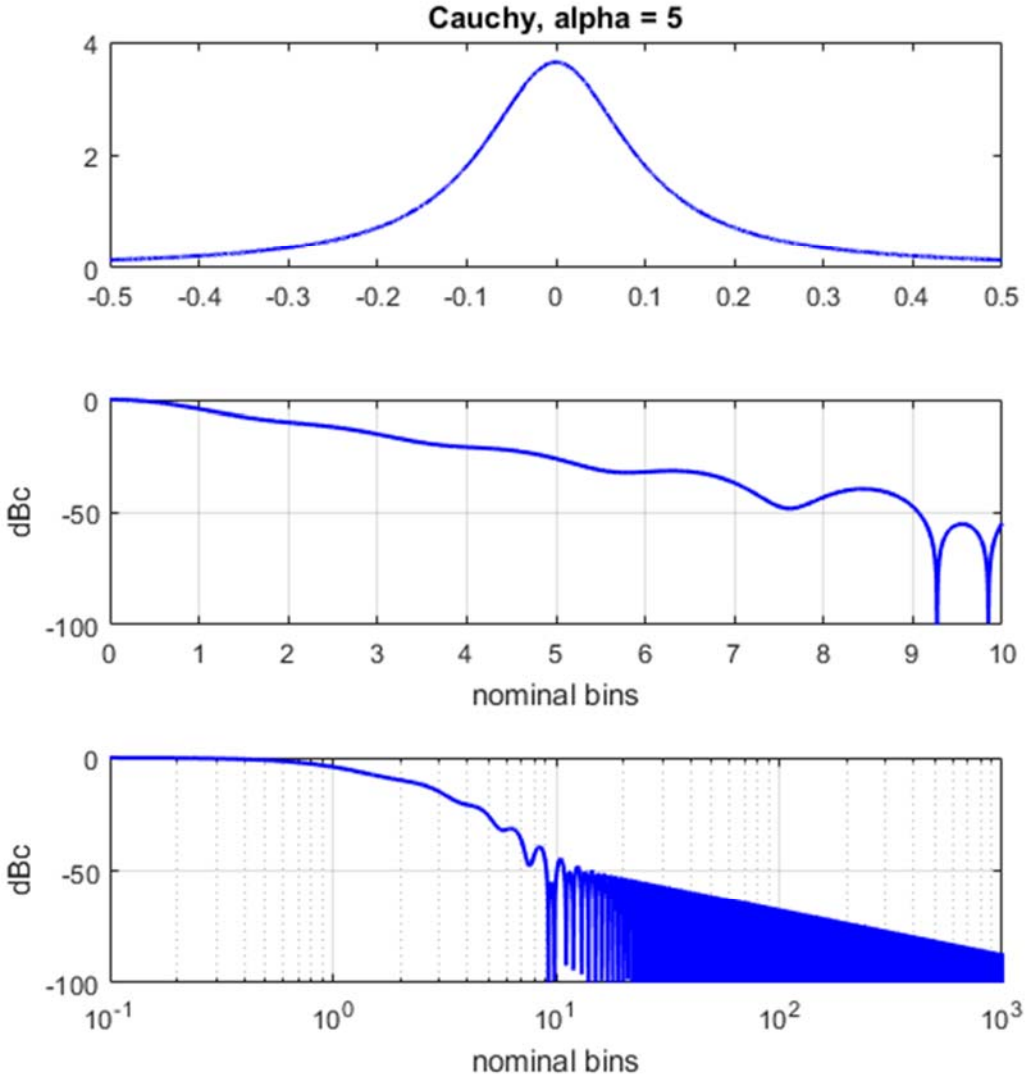


WINDOW SPECTRUM CHARACTERISTICS

half-power bandwidth = 1.691 (normalized to 1/T)
-3 dB bandwidth = 1.6879 (normalized to 1/T)
-18 dB bandwidth = 6.7595 (normalized to 1/T)
noise bandwidth = 2.0753 (normalized to 1/T)
SNR loss = 3.1708 dB
first null = 5.8008 (normalized to 1/T)
PSL = -31.342 dBc
ISL = -30.3567 dBc from first null outward

**Figure 74.**

## 4.36 Parzen Geometric Family

Parzen[1] suggested a family of window taper functions of the form, which we have scaled for unit DC gain as

$$w(t) = \frac{A}{1 + |2\alpha\ t|^r}\ \mathrm{rect}(t), \tag{220}$$

where parameters

$$\begin{aligned} &\alpha > 0\ , \text{ and} \\ &r > 0\ , \end{aligned} \tag{221}$$

and the desired scale factor for unit DC gain is

$$A = \left( \int_{-1/2}^{1/2} \left( \frac{1}{1 + |2\alpha\ t|^r} \right) dt \right)^{-1}\ . \tag{222}$$

The Fourier Transform of the continuous time window taper function is not readily calculated in closed-form. It may be numerically calculated for specific parameters, i.e. using a DFT on discrete-time samples of the window function.

Plots and characteristics for this window for an example parameter set are given in Figure 75.

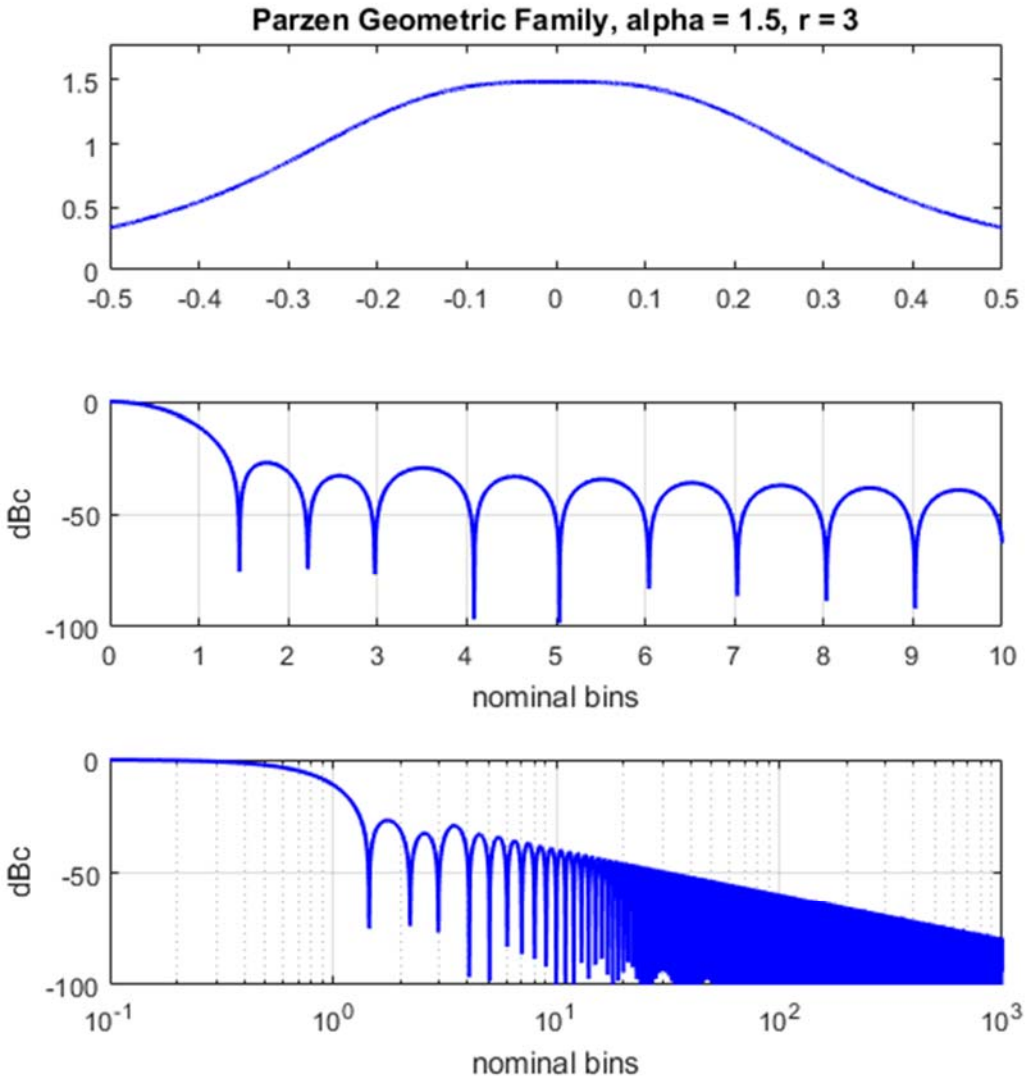


WINDOW SPECTRUM CHARACTERISTICS

half-power bandwidth = 1.1138 (normalized to 1/T)
-3 dB bandwidth = 1.112 (normalized to 1/T)
-18 dB bandwidth = 2.3978 (normalized to 1/T)
noise bandwidth = 1.1591 (normalized to 1/T)
SNR loss = 0.641 dB
first null = 1.4531 (normalized to 1/T)
PSL = -26.8388 dBc
ISL = -22.7794 dBc from first null outward

**Figure 75.**

## 4.37 Maximum Energy (a.k.a. Slepian) Tapers

Slepian and Pollak[35] investigated the question (rephrased in language consistent with this report) stated as "Given a finite aperture of data, how to we taper the data to maximize the energy in the mainlobe of the filter's transfer function, for some allowable mainlobe width?"

Their analysis uses prolate spheroidal wave functions, which are particularly suitable for investigating simultaneously aperture limited and effectively band-limited signals. The answer to the question posed above is in fact the prolate spheroidal wave function of order zero. The specific nature of this prolate spheroidal wave function becomes dependent on the allowable time-bandwidth product of the signal. In terms of window taper functions, this is the product of the aperture length and the window spectrum's allowable mainlobe width. Furthermore, maximizing energy in the window spectrum mainlobe means minimizing energy outside the mainlobe, that is, effectively minimizing the ISL.

In a follow-on to the Slepian and Pollak paper cited above, Landau and Pollak[36] apply this work directly to "Filter Theory," which is simply the window function we seek.

Actually calculating the specific prolate spheroidal wave function of order zero to provide the desired window function is something less-than-straightforward, in fact quite cumbersome, compared to other window taper functions in this report. Dickey, et al.,[37] describe a procedure for doing so in their Appendix B. We will forego repeating this procedure here in this report, and simply refer the interested reader to the report by Dickey, et al.

Instead, we will move to examine some approximations to the ideal Maximum Energy window taper function.

## 4.38 Kaiser-Bessel (a.k.a. Kaiser, $I_0$-sinh)

This window is an approximation to the ideal Maximum Energy taper described in the previous section. Instead of dealing with the difficulty of calculating the prolate spheroidal wave function, Kaiser[38] presents a window that uses an approximation based on calculating the zero-order modified Bessel function of the first kind. Kuo and Kaiser state "This family of window functions was 'discovered' by Kaiser in 1962 following a discussion with B. F. Logan of the Bell Telephone Laboratories."

The Kaiser-Bessel window taper function scaled for unit DC gain, is calculated as

$$w(t) = \frac{A}{I_0(\pi\alpha)} I_0\left(\pi\alpha\sqrt{1-(2t)^2}\right)\text{rect}(t), \tag{223}$$

where we identify the zero-order modified Bessel function of the first kind as

$$I_0(x) = 1 + \sum_{k=1}^{\infty}\left[\frac{1}{k!}\left(\frac{x}{2}\right)^k\right]^2, \tag{224}$$

and we trade spectral sidelobe level against mainlobe width by selecting the parameter

$$\alpha > 0, \tag{225}$$

with the unit DC gain scale factor calculated to be

$$A = \left[\frac{1}{I_0(\pi\alpha)}\int_{-1/2}^{1/2} I_0\left(\pi\alpha\sqrt{1-(2t)^2}\right)dt\right]^{-1} = \left[\frac{\sinh(\pi\alpha)}{I_0(\pi\alpha)\pi\alpha}\right]^{-1}. \tag{226}$$

The Fourier Transform of the continuous time window taper function is calculated to be

$$W(f) = \frac{A\sinh\left(\pi\sqrt{\alpha^2 - f^2}\right)}{I_0(\pi\alpha)\pi\sqrt{\alpha^2 - f^2}}. \tag{227}$$

Plots and characteristics for this window for several parameter combinations are given in Figure 76 through Figure 79.

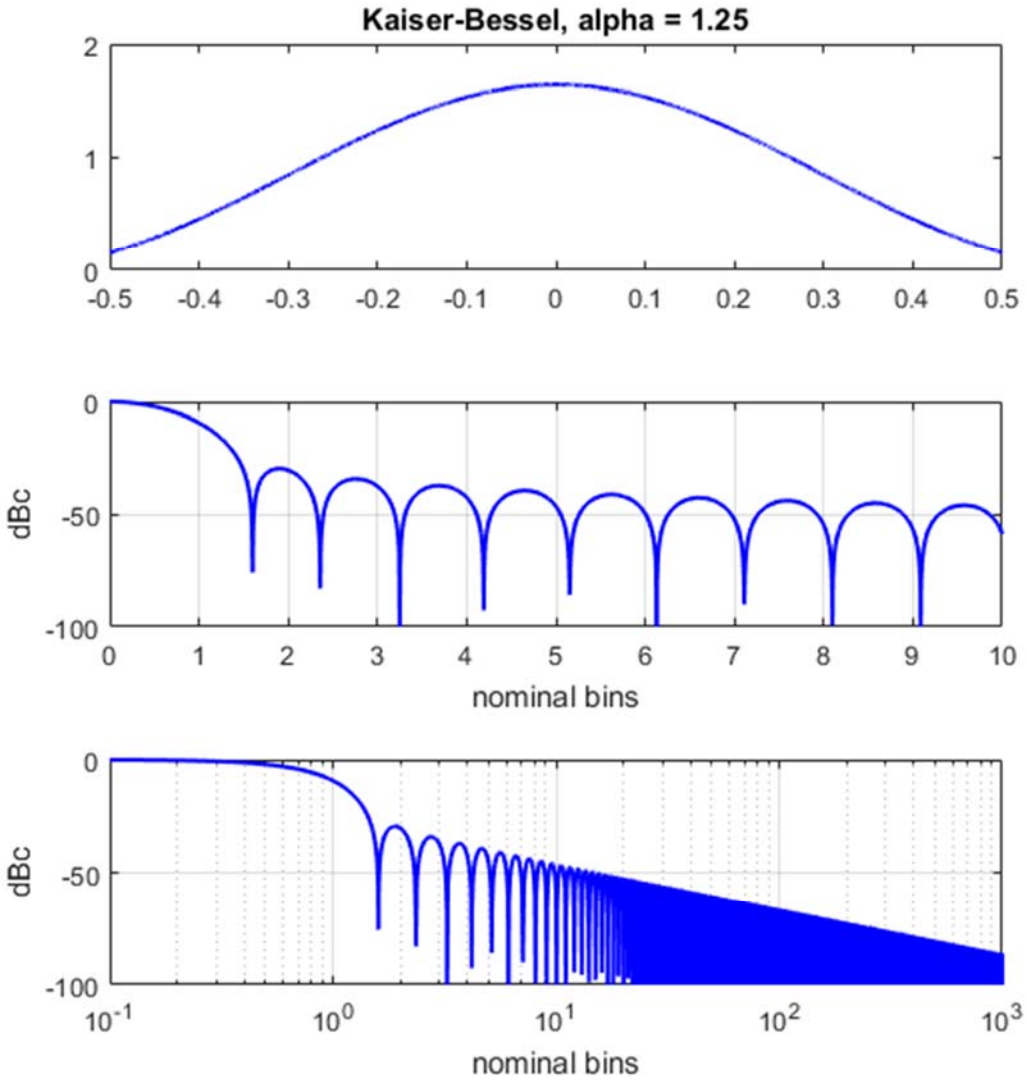


WINDOW SPECTRUM CHARACTERISTICS

half-power bandwidth = 1.1917 (normalized to 1/T)
-3 dB bandwidth = 1.1897 (normalized to 1/T)
-18 dB bandwidth = 2.5947 (normalized to 1/T)
noise bandwidth = 1.2385 (normalized to 1/T)
SNR loss = 0.92908 dB
first null = 1.6016 (normalized to 1/T)
PSL = -29.4682 dBc
ISL = -27.9494 dBc from first null outward

**Figure 76.**

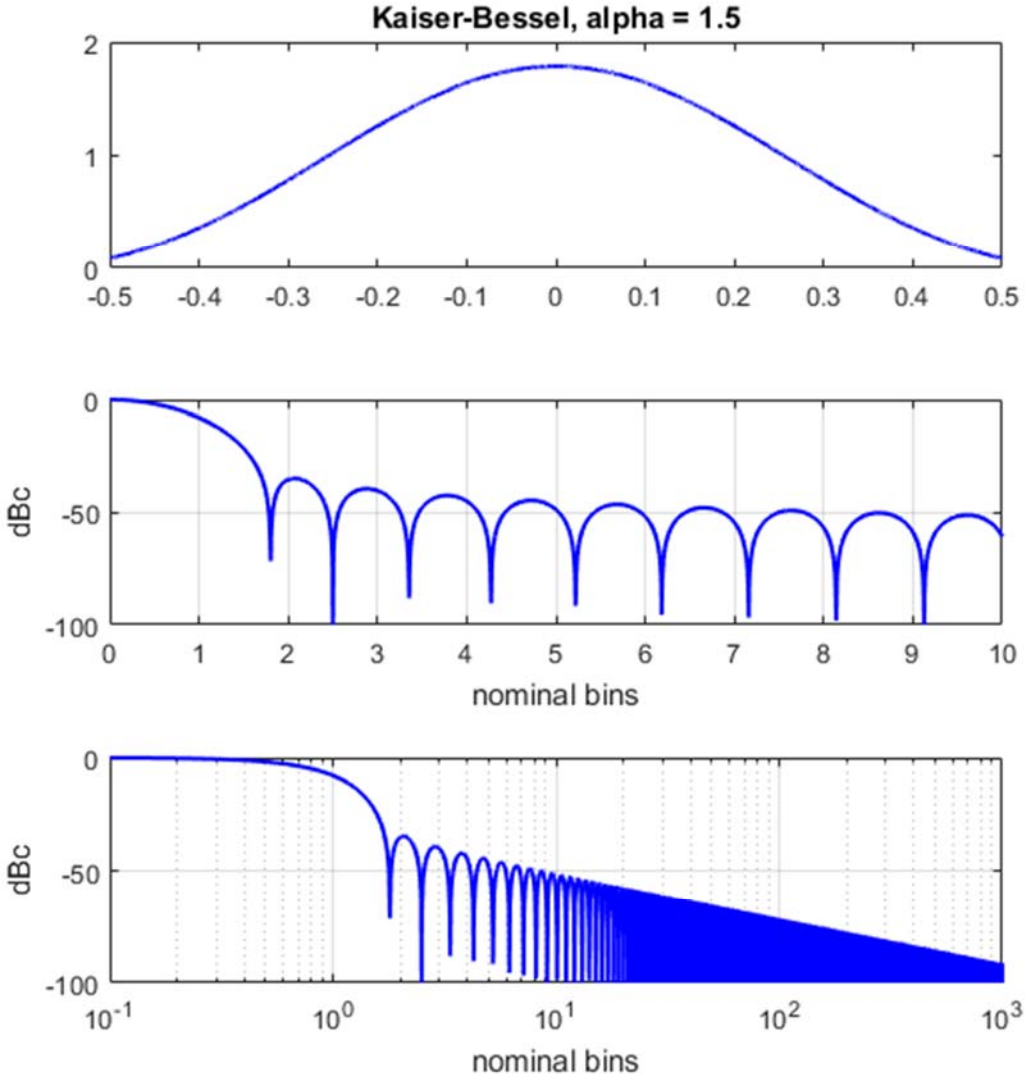


WINDOW SPECTRUM CHARACTERISTICS

half-power bandwidth = 1.2738 (normalized to 1/T)
-3 dB bandwidth = 1.2717 (normalized to 1/T)
-18 dB bandwidth = 2.8212 (normalized to 1/T)
noise bandwidth = 1.3271 (normalized to 1/T)
SNR loss = 1.2289 dB
first null = 1.8047 (normalized to 1/T)
PSL = -34.7092 dBc
ISL = -33.6996 dBc from first null outward

**Figure 77.**

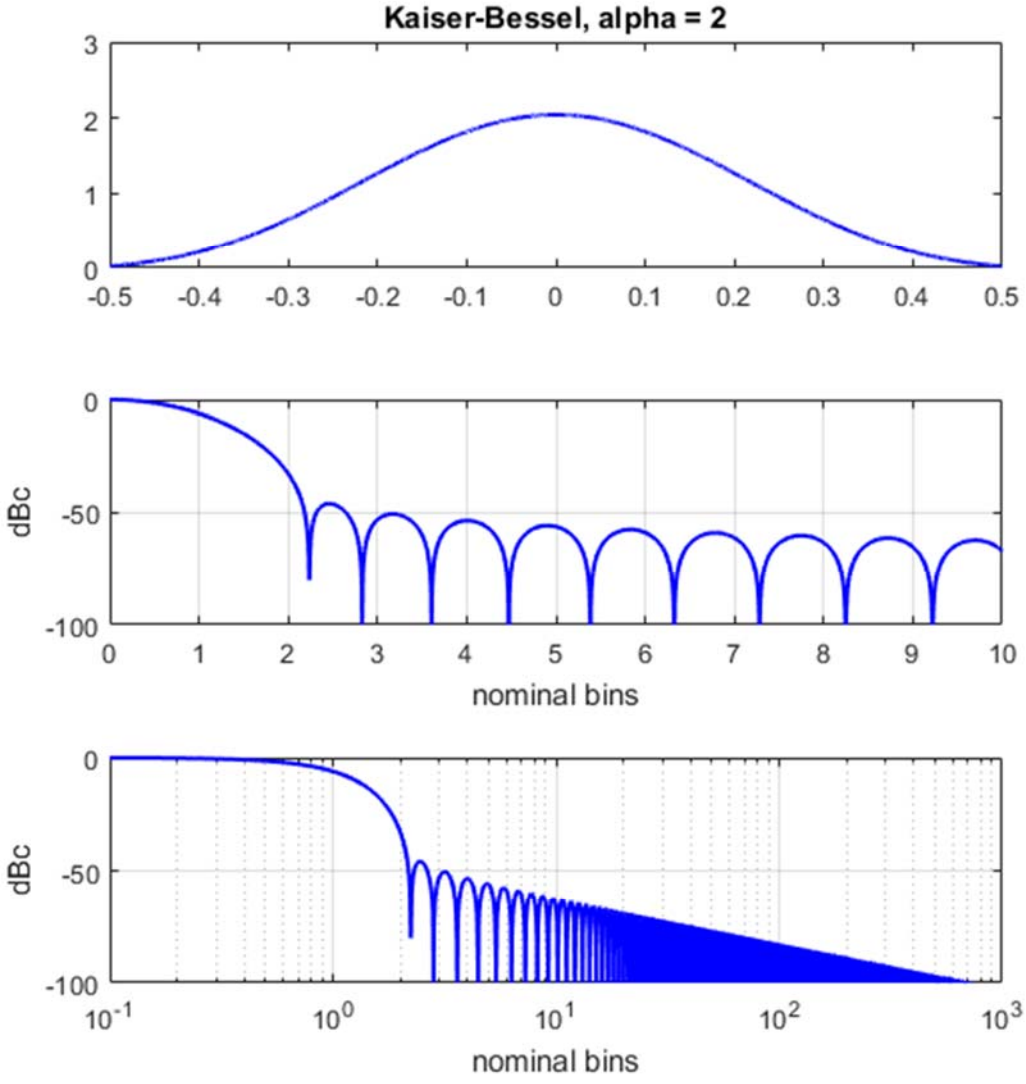


WINDOW SPECTRUM CHARACTERISTICS

half-power bandwidth = 1.4295 (normalized to 1/T)
-3 dB bandwidth = 1.4271 (normalized to 1/T)
-18 dB bandwidth = 3.2445 (normalized to 1/T)
noise bandwidth = 1.4964 (normalized to 1/T)
SNR loss = 1.7506 dB
first null = 2.2344 (normalized to 1/T)
PSL = -45.8531 dBc
ISL = -45.7783 dBc from first null outward

**Figure 78.**

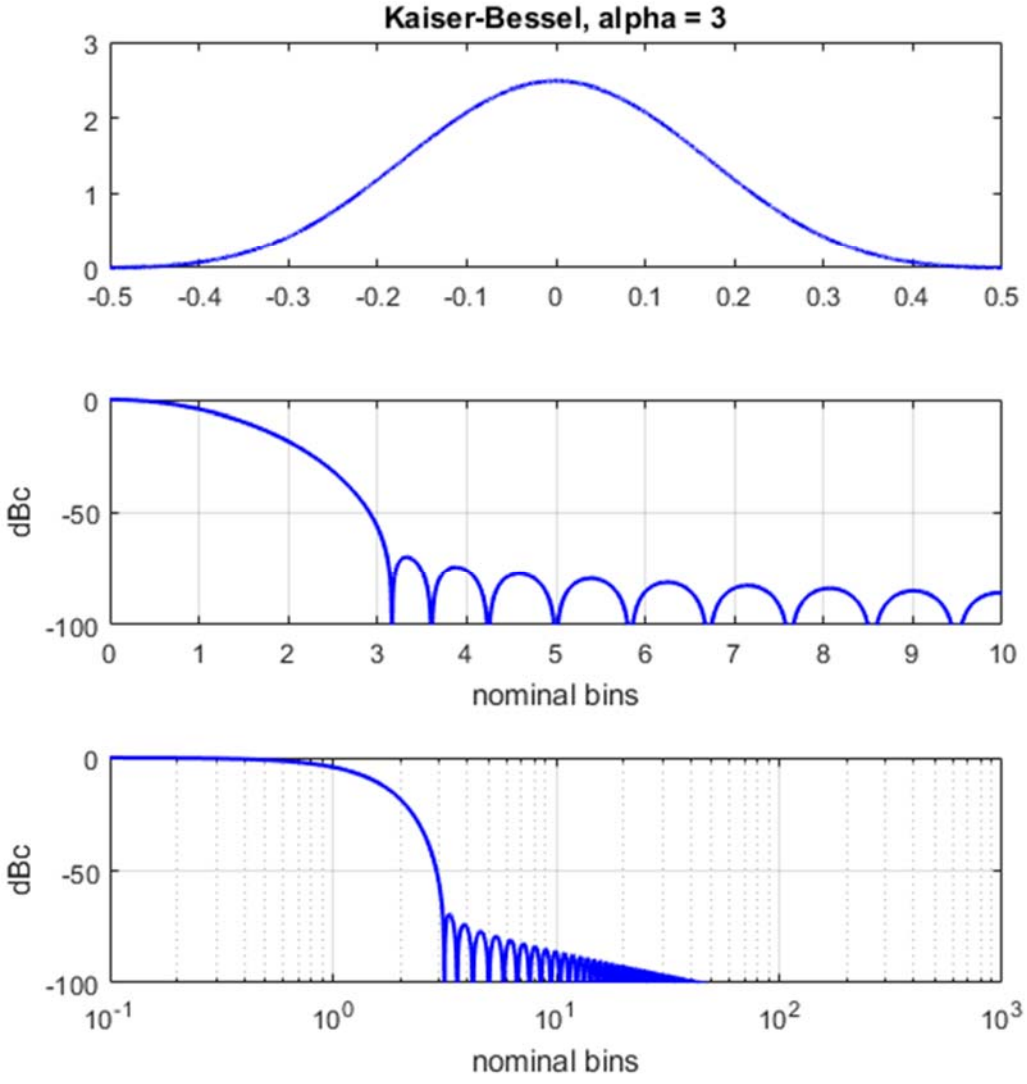


WINDOW SPECTRUM CHARACTERISTICS

half-power bandwidth = 1.7054 (normalized to 1/T)
-3 dB bandwidth = 1.7026 (normalized to 1/T)
-18 dB bandwidth = 3.9721 (normalized to 1/T)
noise bandwidth = 1.7953 (normalized to 1/T)
SNR loss = 2.5415 dB
first null = 3.1641 (normalized to 1/T)
PSL = -69.6168 dBc
ISL = -71.0757 dBc from first null outward

**Figure 79.**

## 4.39 Cosh Family (a.k.a. van der Maas)

This window family was presented by Avci and Nacaroglu,[39] who state "It is derived in the same way as the Kaiser window, but has no power series expansion in its time domain representation – as the Kaiser window does. The design equations are empirically established for the proposed window."

The Cosh window taper function family scaled for unit DC gain, is calculated as

$$w(t) = A\frac{\cosh\left(\pi\alpha\sqrt{1-(2t)^2}\right)}{\cosh(\pi\alpha)}\text{rect}(t), \tag{228}$$

where we trade spectral sidelobe level against mainlobe width by selecting the parameter

$$\alpha > 0, \tag{229}$$

with the unit DC gain scale factor calculated to be

$$A = \left[\int_{-1/2}^{1/2}\frac{\cosh\left(\pi\alpha\sqrt{1-(2t)^2}\right)}{\cosh(\pi\alpha)}dt\right]^{-1}. \tag{230}$$

The Fourier Transform of the continuous time window taper function is not readily calculated in closed-form. It may be numerically calculated for specific parameters, i.e. using a DFT on discrete-time samples of the window function.

Plots and characteristics for this window for several parameter combinations are given in Figure 80, Figure 81, and Figure 82.

Avci and Nacaroglu also propose a modification to this window taper function by raising Eq. (228) to a power.[40]

Migliacco, et al.,[41] call this a "Knab" window, although Knab[42] himself attributes this form to van der Maas. We will reserve the nomenclature of a "Knab window" to another formulation presented later.

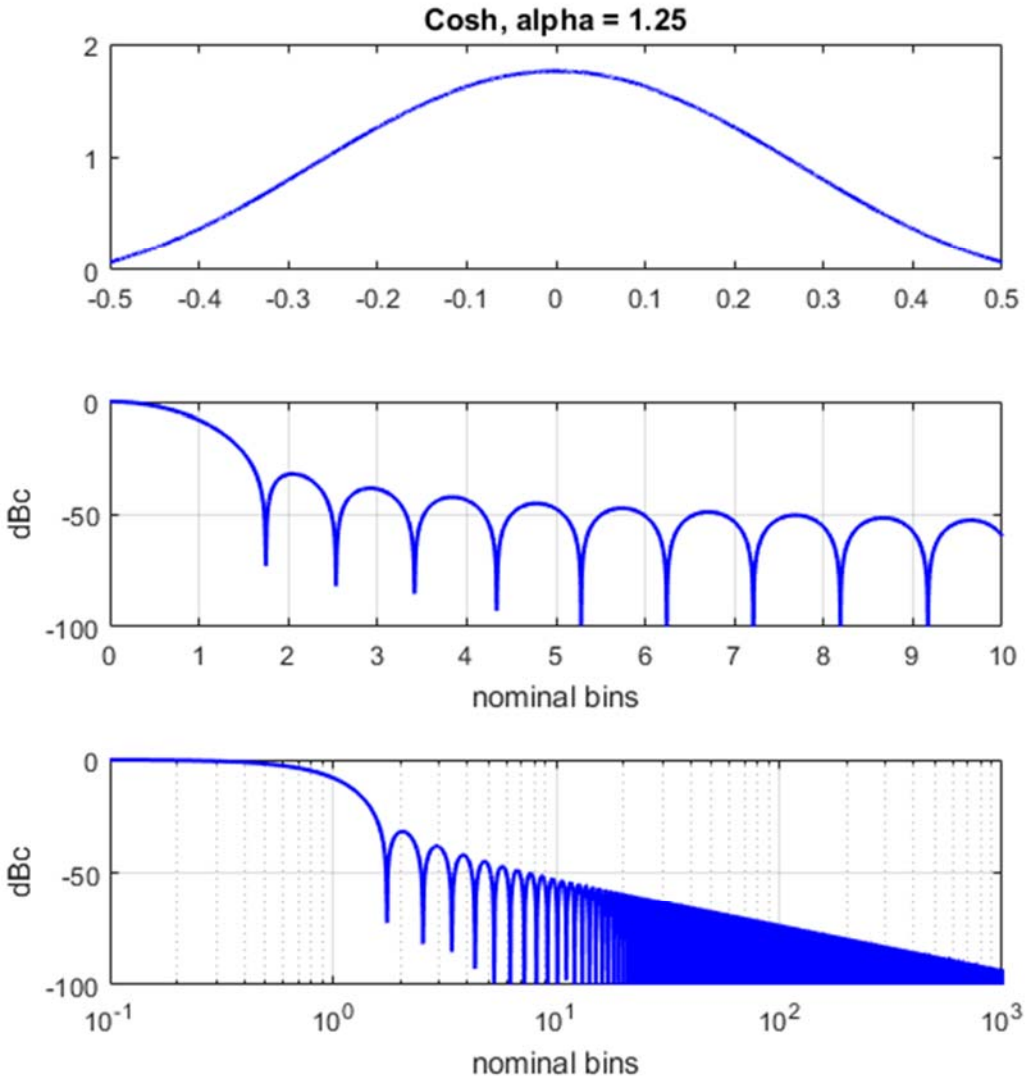


WINDOW SPECTRUM CHARACTERISTICS

half-power bandwidth = 1.2666 (normalized to 1/T)
-3 dB bandwidth = 1.2645 (normalized to 1/T)
-18 dB bandwidth = 2.7858 (normalized to 1/T)
noise bandwidth = 1.3179 (normalized to 1/T)
SNR loss = 1.1989 dB
first null = 1.75 (normalized to 1/T)
PSL = -31.7879 dBc
ISL = -31.9645 dBc from first null outward

**Figure 80.**

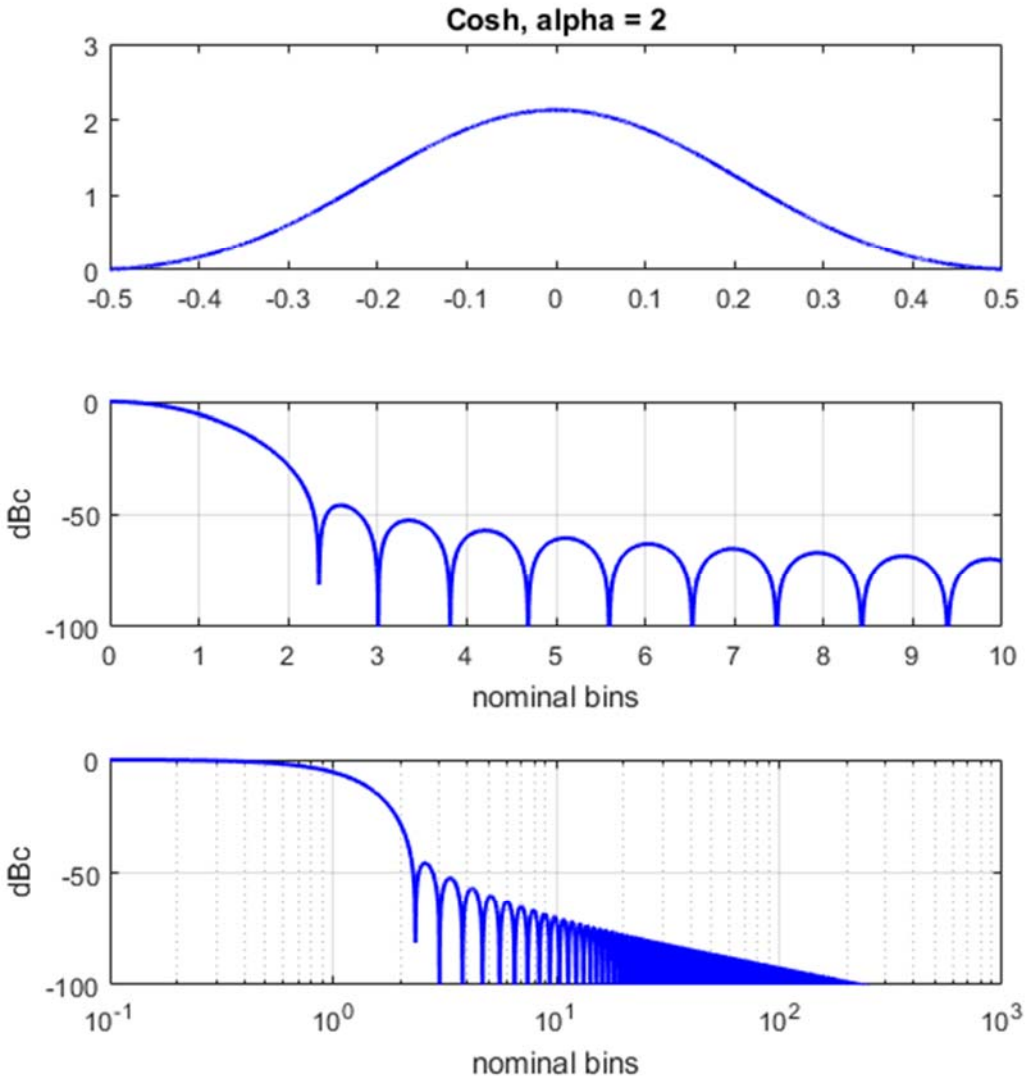


WINDOW SPECTRUM CHARACTERISTICS

half-power bandwidth = 1.4909 (normalized to 1/T)
-3 dB bandwidth = 1.4884 (normalized to 1/T)
-18 dB bandwidth = 3.3918 (normalized to 1/T)
noise bandwidth = 1.5615 (normalized to 1/T)
SNR loss = 1.9356 dB
first null = 2.3438 (normalized to 1/T)
PSL = -45.7279 dBc
ISL = -47.7103 dBc from first null outward

**Figure 81.**

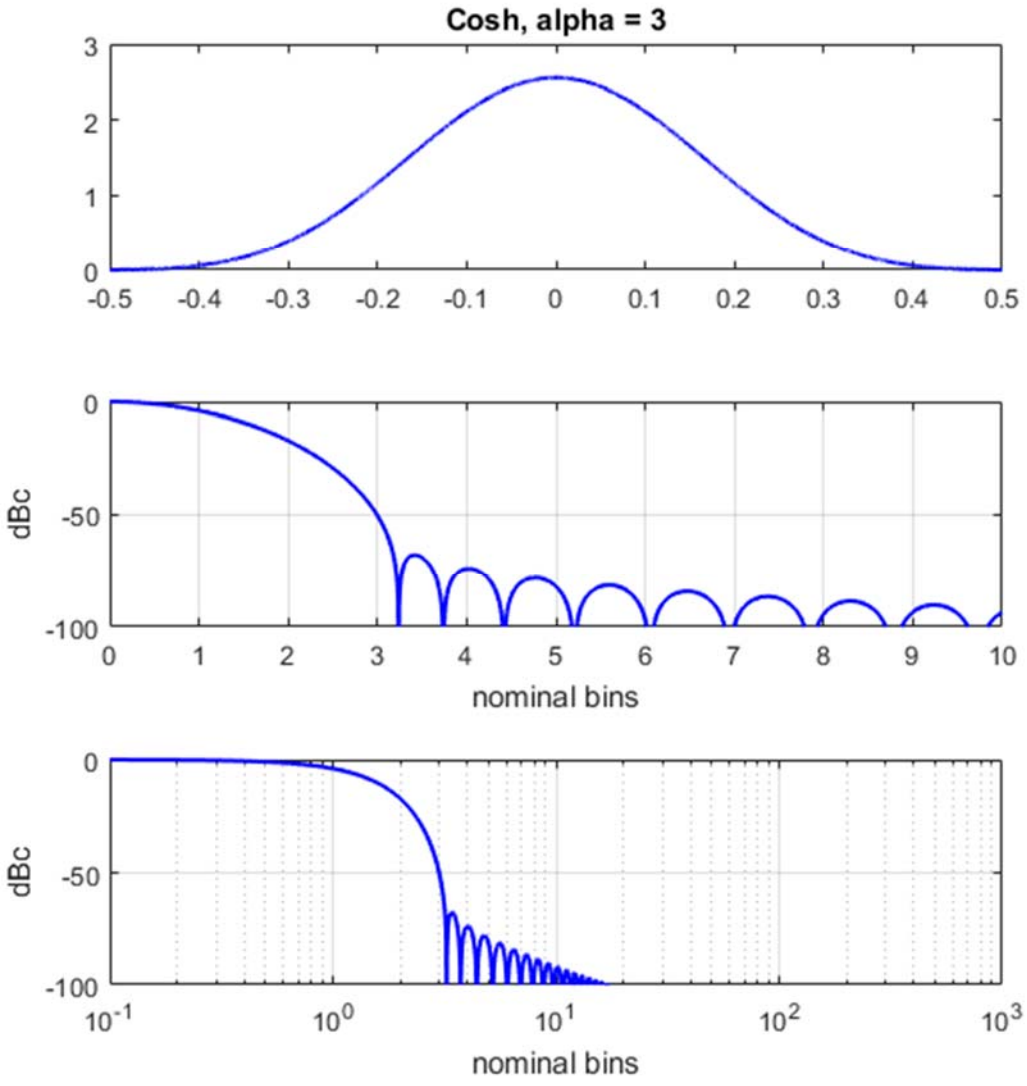


WINDOW SPECTRUM CHARACTERISTICS

half-power bandwidth = 1.7536 (normalized to 1/T)
-3 dB bandwidth = 1.7507 (normalized to 1/T)
-18 dB bandwidth = 4.0861 (normalized to 1/T)
noise bandwidth = 1.8463 (normalized to 1/T)
SNR loss = 2.663 dB
first null = 3.2383 (normalized to 1/T)
PSL = -67.828 dBc
ISL = -71.3135 dBc from first null outward

**Figure 82.**

## 4.40 Avci-Nacaroglu Exponential

This window family was presented by Avci and Nacaroglu,[43] who state, as with the Cosh family of window functions in the previous section, it is "derived in the same way of the derivation of Kaiser window, but it has the advantage of having no power series expansion in its time domain function."

This window taper function family scaled for unit DC gain, is calculated as

$$w(t) = Ae^{\pi\alpha\left(\sqrt{1-(2t)^2}-1\right)}, \tag{231}$$

where we trade spectral sidelobe level against mainlobe width by selecting the parameter

$$\alpha > 0\,, \tag{232}$$

with the unit DC gain scale factor calculated to be

$$A = \left[\int_{-1/2}^{1/2} e^{\pi\alpha\left(\sqrt{1-(2t)^2}-1\right)} dt\right]^{-1}. \tag{233}$$

The Fourier Transform of the continuous time window taper function is not readily calculated in closed-form. It may be numerically calculated for specific parameters, i.e. using a DFT on discrete-time samples of the window function.

Plots and characteristics for this window for several parameter combinations are given in Figure 83, Figure 84, and Figure 85.

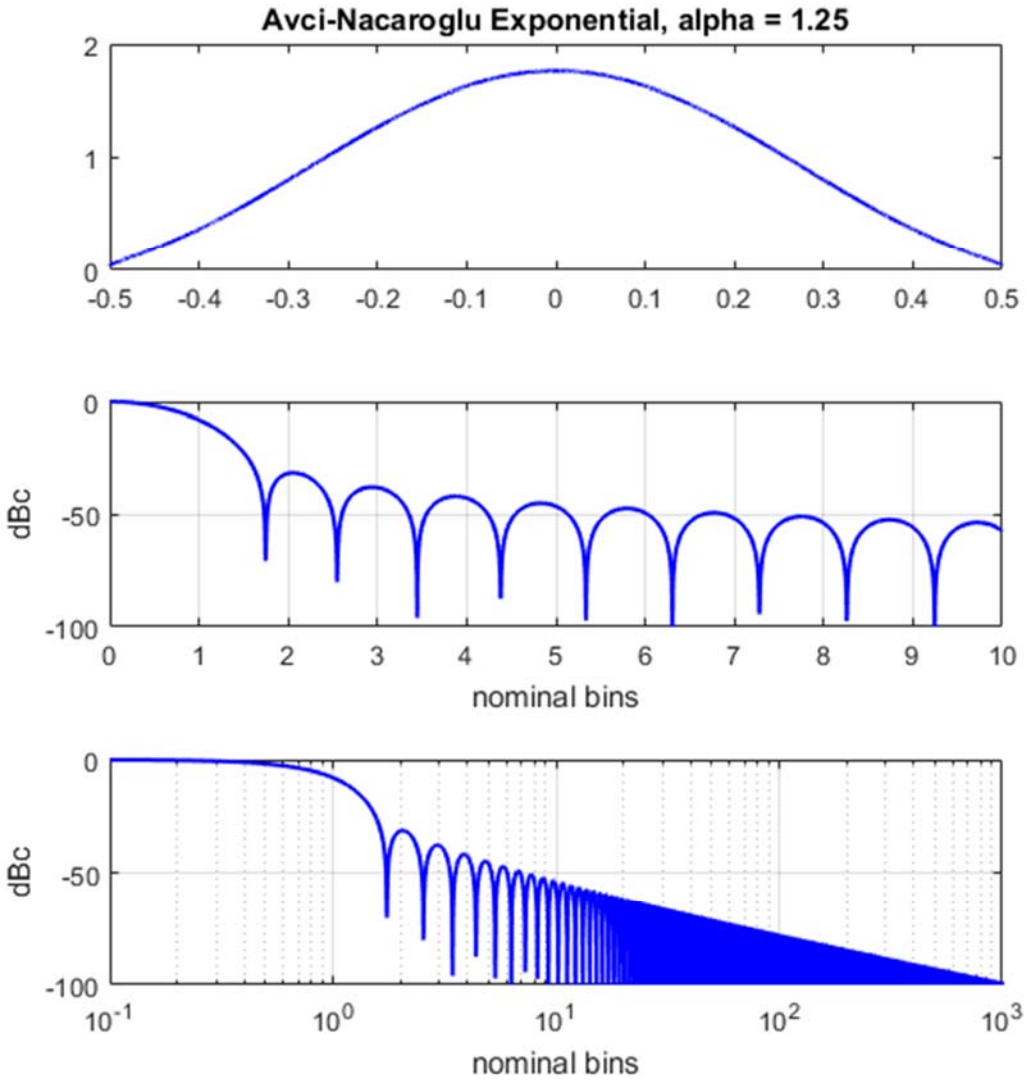


WINDOW SPECTRUM CHARACTERISTICS

half-power bandwidth = 1.2712 (normalized to 1/T)
-3 dB bandwidth = 1.2691 (normalized to 1/T)
-18 dB bandwidth = 2.7921 (normalized to 1/T)
noise bandwidth = 1.3224 (normalized to 1/T)
SNR loss = 1.2137 dB
first null = 1.7461 (normalized to 1/T)
PSL = -31.3468 dBc
ISL = -31.6616 dBc from first null outward

**Figure 83.**

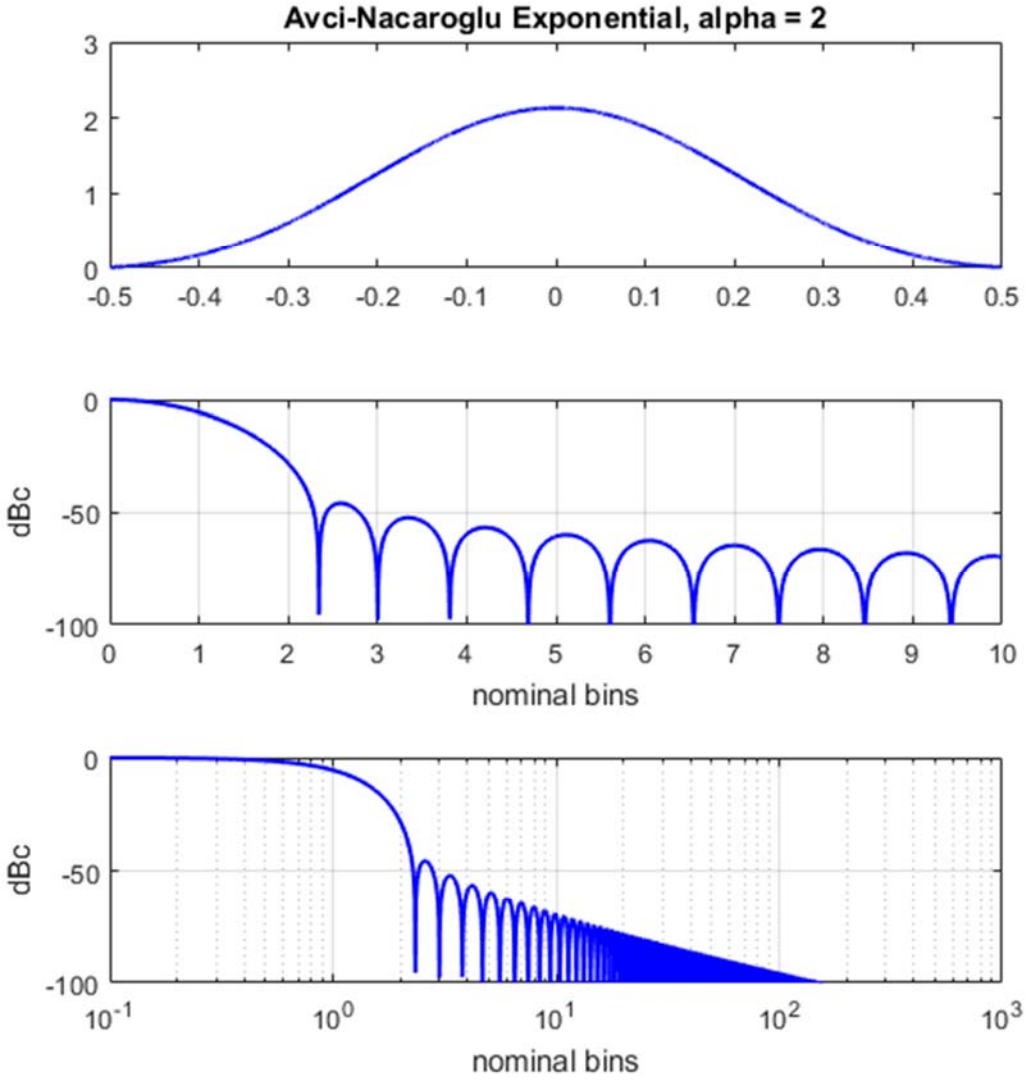


WINDOW SPECTRUM CHARACTERISTICS

half-power bandwidth = 1.4913 (normalized to 1/T)
-3 dB bandwidth = 1.4888 (normalized to 1/T)
-18 dB bandwidth = 3.3918 (normalized to 1/T)
noise bandwidth = 1.5619 (normalized to 1/T)
SNR loss = 1.9364 dB
first null = 2.3438 (normalized to 1/T)
PSL = -45.7 dBc
ISL = -47.599 dBc from first null outward

**Figure 84.**

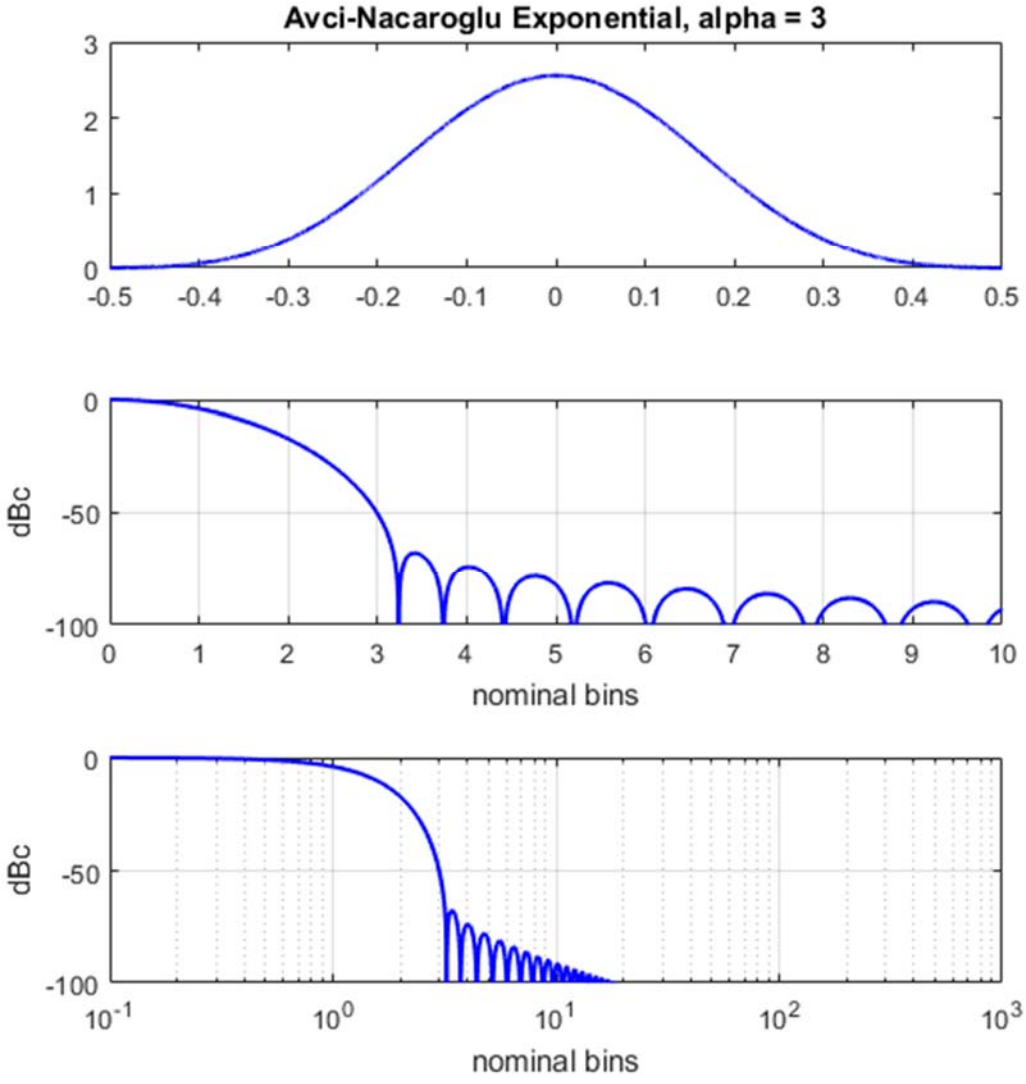


WINDOW SPECTRUM CHARACTERISTICS

half-power bandwidth = 1.7536 (normalized to 1/T)
-3 dB bandwidth = 1.7507 (normalized to 1/T)
-18 dB bandwidth = 4.0861 (normalized to 1/T)
noise bandwidth = 1.8463 (normalized to 1/T)
SNR loss = 2.663 dB
first null = 3.2383 (normalized to 1/T)
PSL = -67.8528 dBc
ISL = -71.33 dBc from first null outward

**Figure 85.**

## 4.41 Knab

Knab,[44] while investigating optimal interpolation kernels, proposed the following window taper function, scaled for unit DC gain as

$$w(t) = A\frac{\sinh\left(\pi\alpha\sqrt{1-(2t)^2}\right)}{\sinh(\pi\alpha)\sqrt{1-(2t)^2}}\text{rect}(t), \tag{234}$$

where we trade spectral sidelobe level against mainlobe width by selecting the parameter

$$\alpha > 0, \tag{235}$$

with the unit DC gain scale factor calculated to be

$$A = \left[\int_{-1/2}^{1/2}\left(\frac{\sinh\left(\pi\alpha\sqrt{1-(2t)^2}\right)}{\sinh(\pi\alpha)\sqrt{1-(2t)^2}}\right)dt\right]^{-1}. \tag{236}$$

The Fourier Transform of the continuous time window taper function is calculated to be the convolution

$$W(f) = \frac{A\pi}{2\sinh(\pi a)}\text{I}_0\left(\pi\sqrt{a^2-f^2}\right)\text{rect}\left(\frac{f}{2a}\right) * \text{sinc}(f). \tag{237}$$

The Fourier Transform of the continuous time window taper function is not readily calculated in closed-form. It may be numerically calculated for specific parameters, i.e. using a DFT on discrete-time samples of the window function.

Plots and characteristics for this window for several parameter combinations are given in Figure 86, Figure 87, and Figure 88.

We note that the name “Knab” window is sometime aliased to the Cosh family of window taper functions presented earlier.

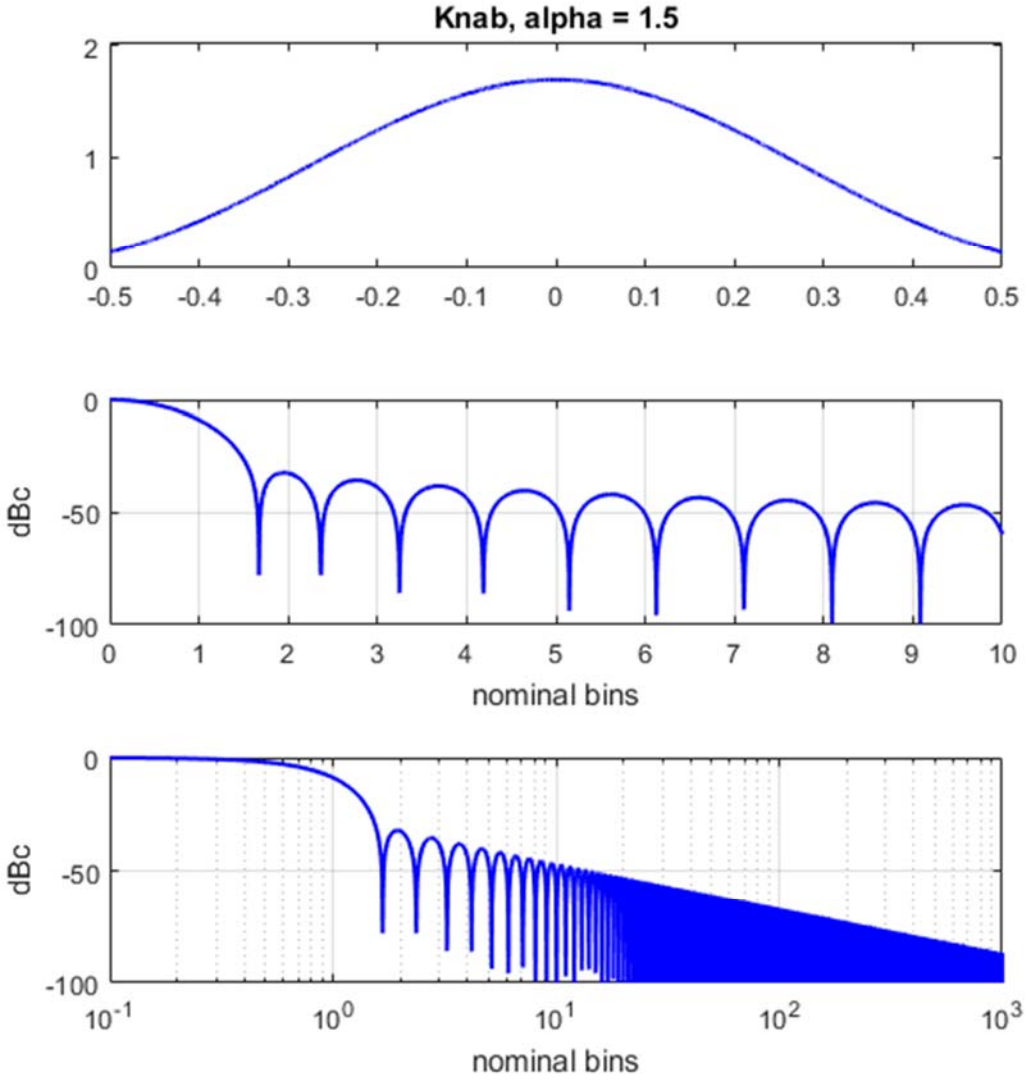


WINDOW SPECTRUM CHARACTERISTICS

half-power bandwidth = 1.2149 (normalized to 1/T)
-3 dB bandwidth = 1.2129 (normalized to 1/T)
-18 dB bandwidth = 2.6664 (normalized to 1/T)
noise bandwidth = 1.2641 (normalized to 1/T)
SNR loss = 1.018 dB
first null = 1.6719 (normalized to 1/T)
PSL = -32.1442 dBc
ISL = -29.8182 dBc from first null outward

**Figure 86.**

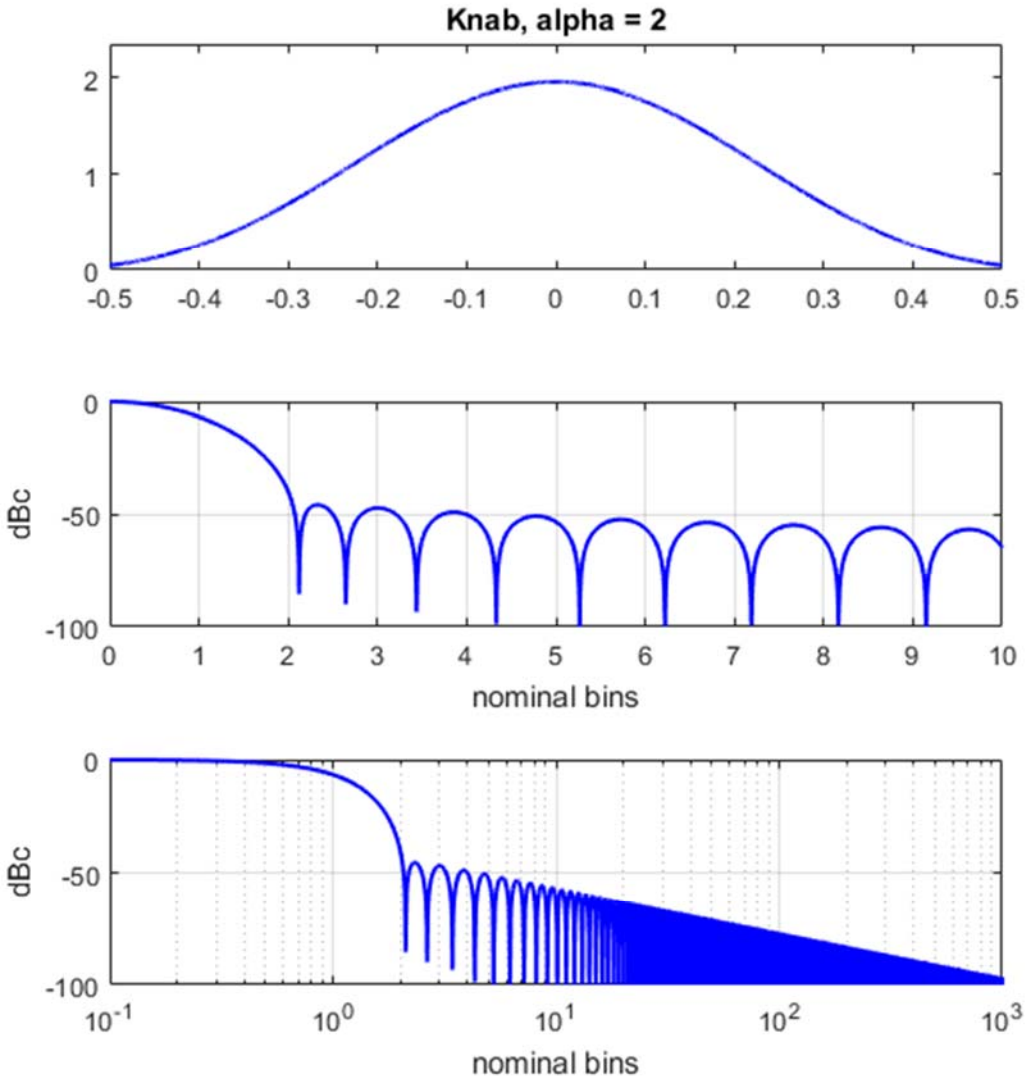


WINDOW SPECTRUM CHARACTERISTICS

half-power bandwidth = 1.3726 (normalized to 1/T)
-3 dB bandwidth = 1.3703 (normalized to 1/T)
-18 dB bandwidth = 3.1034 (normalized to 1/T)
noise bandwidth = 1.4358 (normalized to 1/T)
SNR loss = 1.571 dB
first null = 2.1211 (normalized to 1/T)
PSL = -45.4642 dBc
ISL = -41.9582 dBc from first null outward

**Figure 87.**

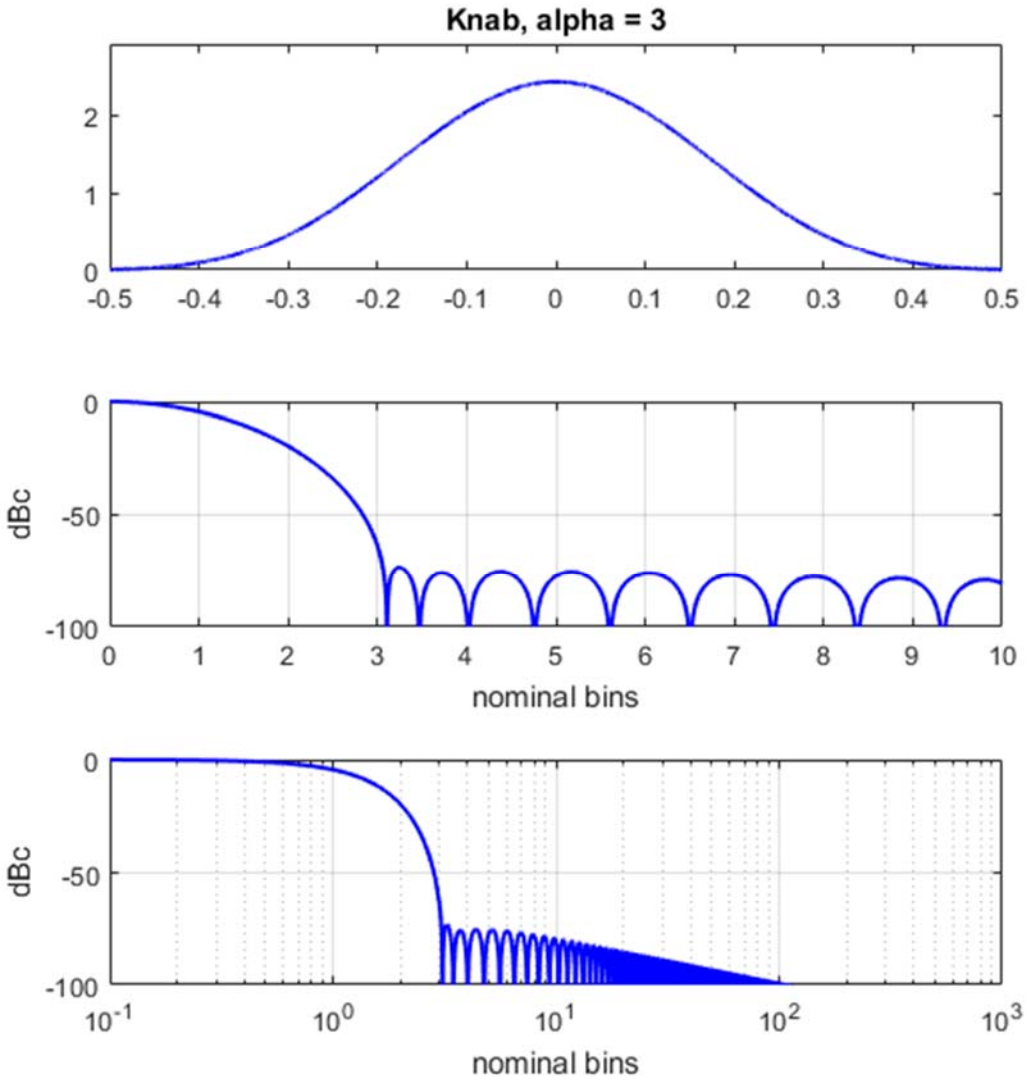


WINDOW SPECTRUM CHARACTERISTICS

half-power bandwidth = 1.6583 (normalized to 1/T)
-3 dB bandwidth = 1.6556 (normalized to 1/T)
-18 dB bandwidth = 3.8608 (normalized to 1/T)
noise bandwidth = 1.7457 (normalized to 1/T)
SNR loss = 2.42 dB
first null = 3.1055 (normalized to 1/T)
PSL = -73.3749 dBc
ISL = -67.8008 dBc from first null outward

**Figure 88.**

## 4.42 Barcilon-Temes

This window was developed by Barcilon and Temes[45] by using a "weighted" minimum-energy criterion for the sidelobes. It is in fact a compromise between the Kaiser-Bessel and the Dolph-Chebyshev windows. Like the Dolph-Chebyshev window, this window is normally specified by its frequency response. The frequency response of the continuous time window taper function is calculated to be

$$W(f) = \frac{2\left(\cos\left(C\sqrt{x^2-1}\right)\sinh(C) + \left(\sqrt{x^2-1}\right)\sin\left(C\sqrt{x^2-1}\right)\cosh(C)\right)}{x^2\left(C+\cosh(C)\sinh(C)\right)}, \qquad (238)$$

with the scaled frequency parameter

$$x = \frac{\pi}{C} f\ , \qquad (239)$$

where the parameter $C$ is effectively a time-bandwidth measure, which Harris equates to a different parameter $\alpha$ as

$$C = \operatorname{acosh}\left(10^{\alpha}\right). \qquad (240)$$

Note that Eq. (238) has a unit DC value.

The actual window taper function itself is normally numerically calculated from this frequency response with an Inverse-DFT.[4] See Appendix A.

Plots and characteristics for this window for various sidelobe levels are given in Figure 89, Figure 90, and Figure 91.

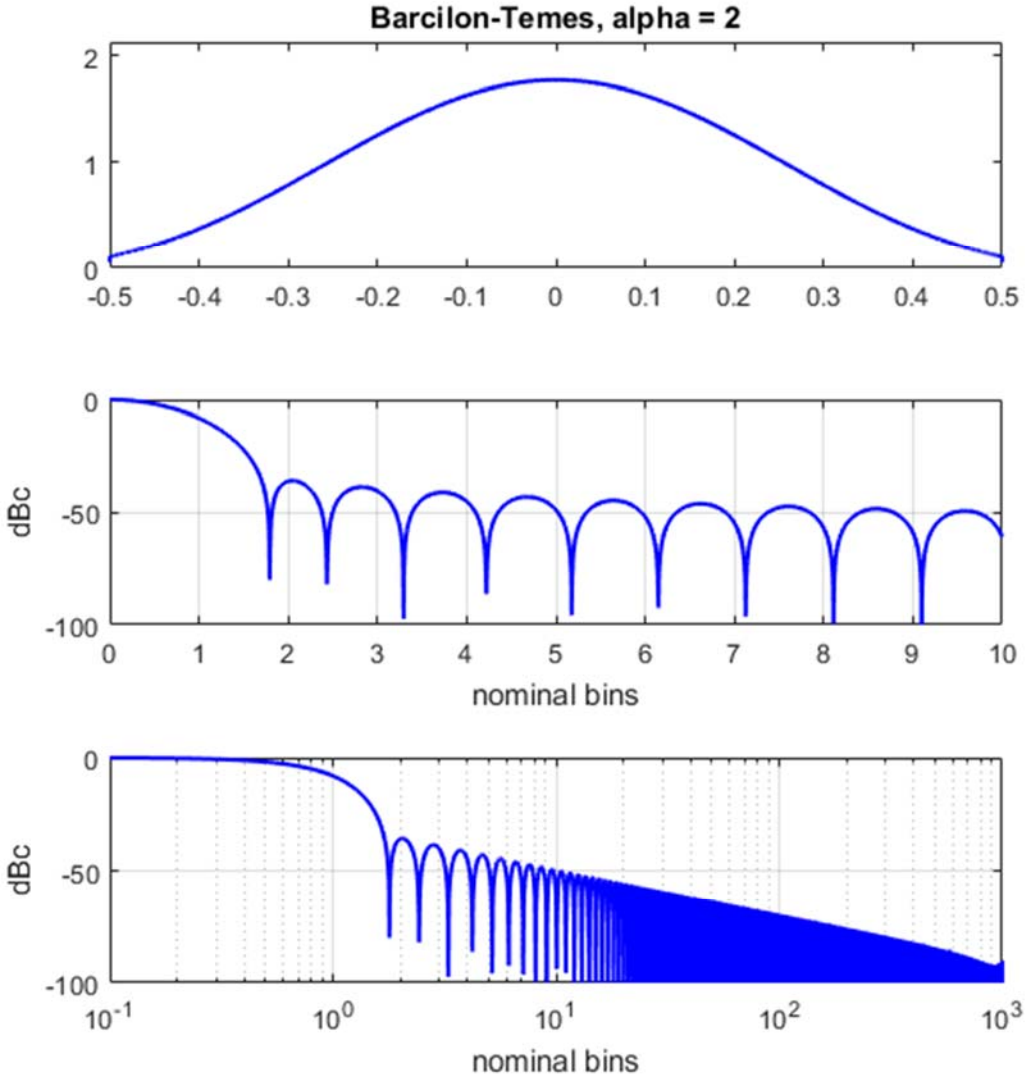


WINDOW SPECTRUM CHARACTERISTICS

half-power bandwidth = 1.2602 (normalized to 1/T)
-3 dB bandwidth = 1.2581 (normalized to 1/T)
-18 dB bandwidth = 2.7936 (normalized to 1/T)
noise bandwidth = 1.3138 (normalized to 1/T)
SNR loss = 1.1853 dB
first null = 1.793 (normalized to 1/T)
PSL = -35.7129 dBc
ISL = -33.1555 dBc from first null outward

**Figure 89.**

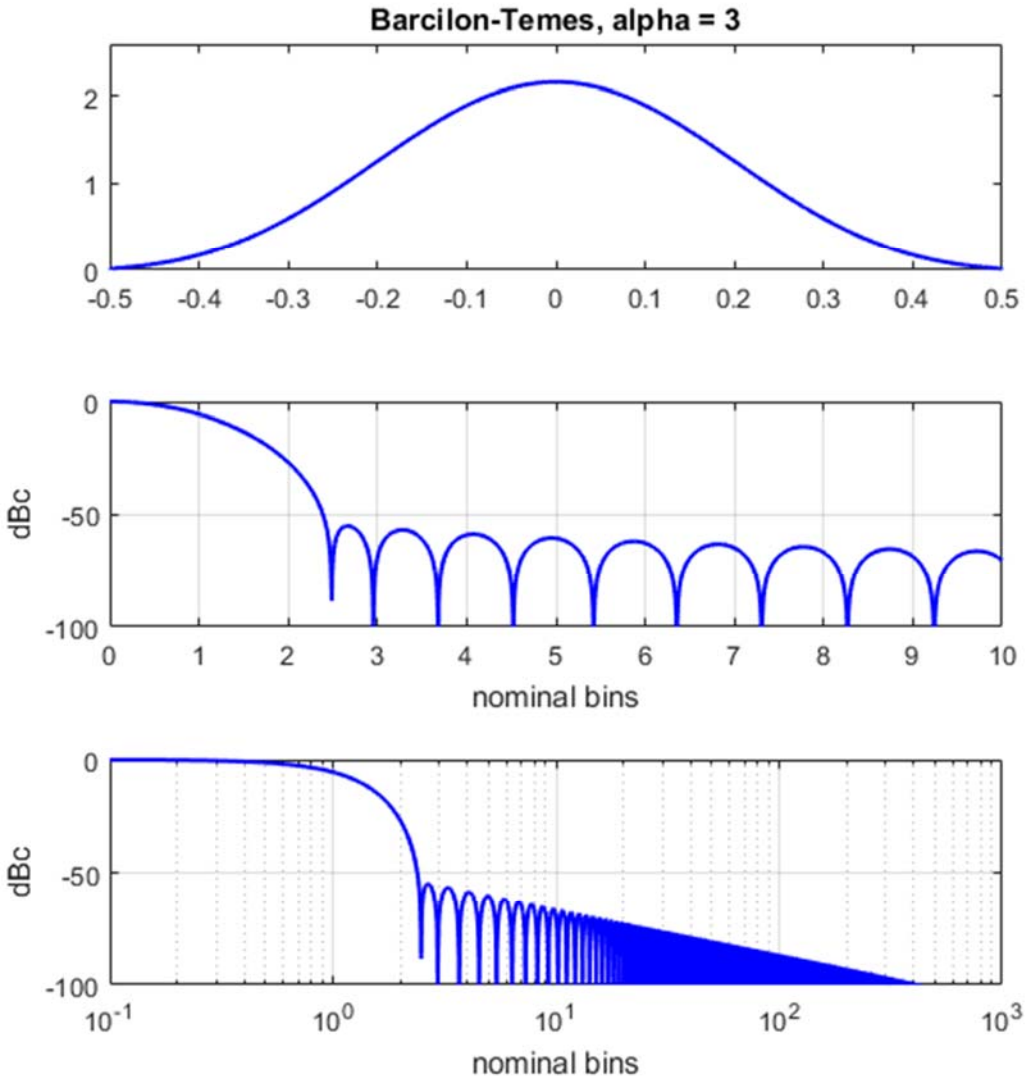


WINDOW SPECTRUM CHARACTERISTICS

half-power bandwidth = 1.4939 (normalized to 1/T)
-3 dB bandwidth = 1.4914 (normalized to 1/T)
-18 dB bandwidth = 3.4247 (normalized to 1/T)
noise bandwidth = 1.568 (normalized to 1/T)
SNR loss = 1.9533 dB
first null = 2.4883 (normalized to 1/T)
PSL = -54.8351 dBc
ISL = -52.2174 dBc from first null outward

**Figure 90.**

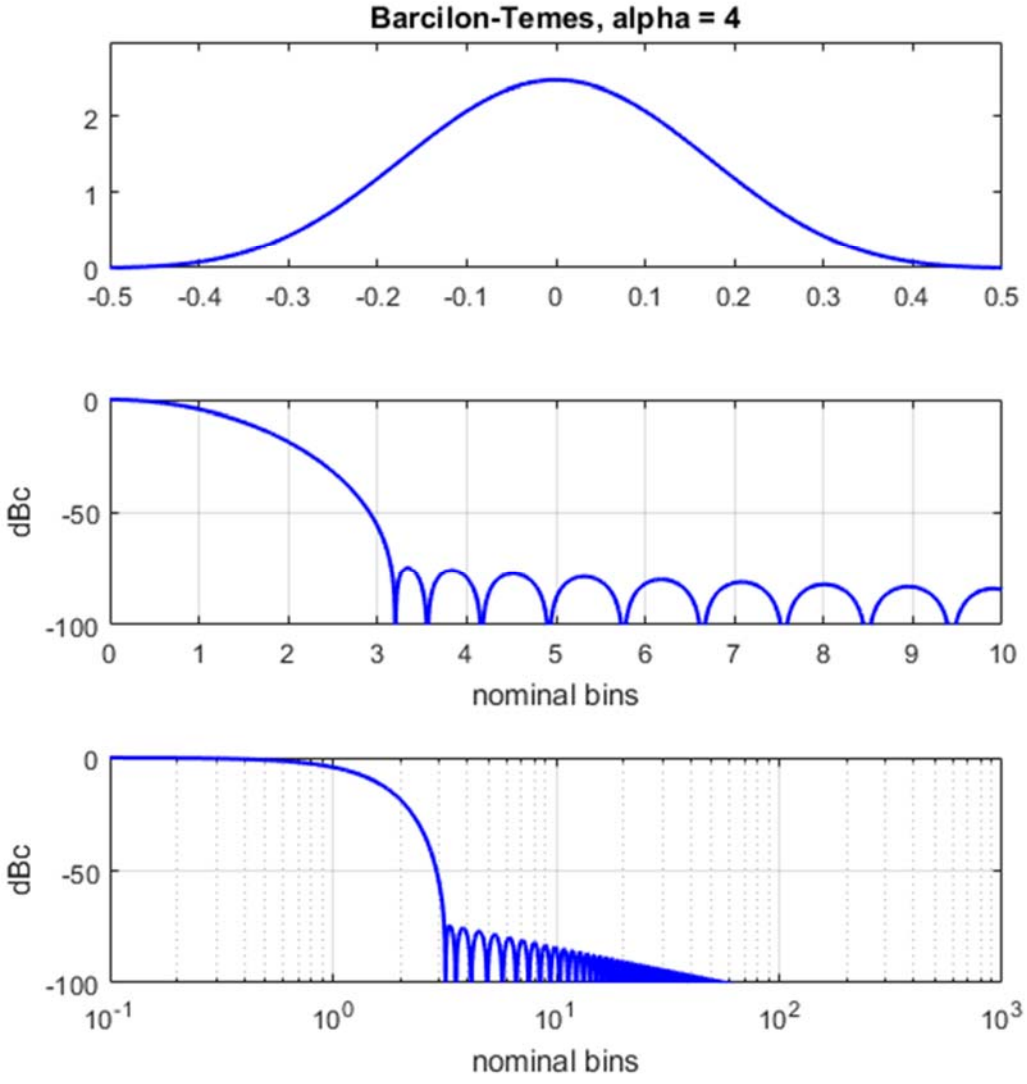


WINDOW SPECTRUM CHARACTERISTICS

half-power bandwidth = 1.6963 (normalized to 1/T)
-3 dB bandwidth = 1.6934 (normalized to 1/T)
-18 dB bandwidth = 3.9539 (normalized to 1/T)
noise bandwidth = 1.7869 (normalized to 1/T)
SNR loss = 2.521 dB
first null = 3.1992 (normalized to 1/T)
PSL = -74.4777 dBc
ISL = -71.5972 dBc from first null outward

**Figure 91.**

## 4.43 Ultraspherical (a.k.a. Unispherical)

Ultraspherical window taper functions were presented by Deczky,[46] and represent a class of window functions "based on the orthogonal polynomials known as the Gegenbauer or Ultraspherical Polynomials." They may be viewed as a generalization of the Dolph-Chebyshev window in that they contain two parameters; one parameter that controls PSL, and another parameter to specify the taper rate of the sidelobes. The Dolph-Chebyshev window is just a special case where the taper rate is zero, i.e. no sidelobe taper at all of the spectrum. Bergen and Antoniou[47] also offer an excellent discussion of this family of window functions.

Specifically, the discrete-frequency spectrum of the window taper function of length $N$ is developed directly to be

$$W_K(k) = N A C_{N-1}^{\alpha}\left( x_0 \cos\left( \pi \frac{f}{f_s} \right) \right), \quad \text{for } 0 \le k \le K-1, \tag{241}$$

where the Ultraspherical polynomial of degree $n$ is defined by the recurring relationships

$$C_0^{\alpha}(x) = 1,$$
$$C_1^{\alpha}(x) = 2x\alpha, \text{ and}$$
$$C_n^{\alpha}(x) = \frac{1}{n}\left( 2x(n+\alpha-1) C_{n-1}^{\alpha}(x) - (n+2\alpha-2) C_{n-2}^{\alpha}(x) \right). \tag{242}$$

The spectral sidelobe taper rate is controlled by

$$\alpha = \text{sidelobe taper rate parameter.} \tag{243}$$

As $\alpha$ increases, sidelobes roll-off increases. For low values of α, the roll-off rate is very roughly about $-20\alpha$ dB/decade.

For this development, we further refine the parameter

$$x_0 = \cosh\left( \frac{1}{N-1} \operatorname{acosh}\left( 10^{-\sigma/20} \right) \right), \tag{244}$$

where

$$\sigma = \text{sidelobe parameter.} \tag{245}$$

These parameters are not independent with respect to sidelobe taper and PSL. For example, the following table details PSL coefficients to calculate approximate $\sigma$ for various combinations of $\alpha$ and desired PSL in dBc.

**Table 2.**

| | $p_1$ | $p_0$ |
|---|---|---|
| $\alpha = 1$ | 1.1554 | 4.5627 |
| $\alpha = 2$ | 1.3279 | 12.7235 |
| $\alpha = 3$ | 1.5143 | 23.6411 |
| $\alpha = 4$ | 1.7134 | 36.9902 |

We calculate the approximate desired sidelobe parameter with the linear relationship

$$\sigma \approx p_1 S + p_0 . \tag{246}$$

where

$S$ = sidelobe level with respect to mainlobe peak in dBc, with $S < 0$. (247)

Frequency in Eq. (241) takes on the discrete values

$$f = \left(k/K\right) f_s , \quad \text{for } 0 \le k \le K-1 , \tag{248}$$

where for a unit-length aperture, we identify the sampling frequency as

$$f_s = N - 1. \tag{249}$$

Recall that we expect $K \ge N$. The scale factor to provide unit DC gain is calculated as

$$A = \left( C_{N-1}^{\alpha}\left(x_0\right)\right)^{-1} . \tag{250}$$

With $W_K\left(k\right)$ so identifies, the discrete-time window function may be therefrom calculated. See Appendix A. Deczky also offers a Matlab® program to generate ultraspherical window functions, albeit limited to odd *N*.

As previously stated, this window approaches a Dolph-Chebyshev window as $\alpha \to 0$. Bergen and Antoniou also relate this to a Saramäki window for $\alpha = 1$, and to a Legendre window for $\alpha = 1/2$. These will be discussed later.

Plots and characteristics for this window for various parameter combinations are given in Figure 92 through Figure 95.

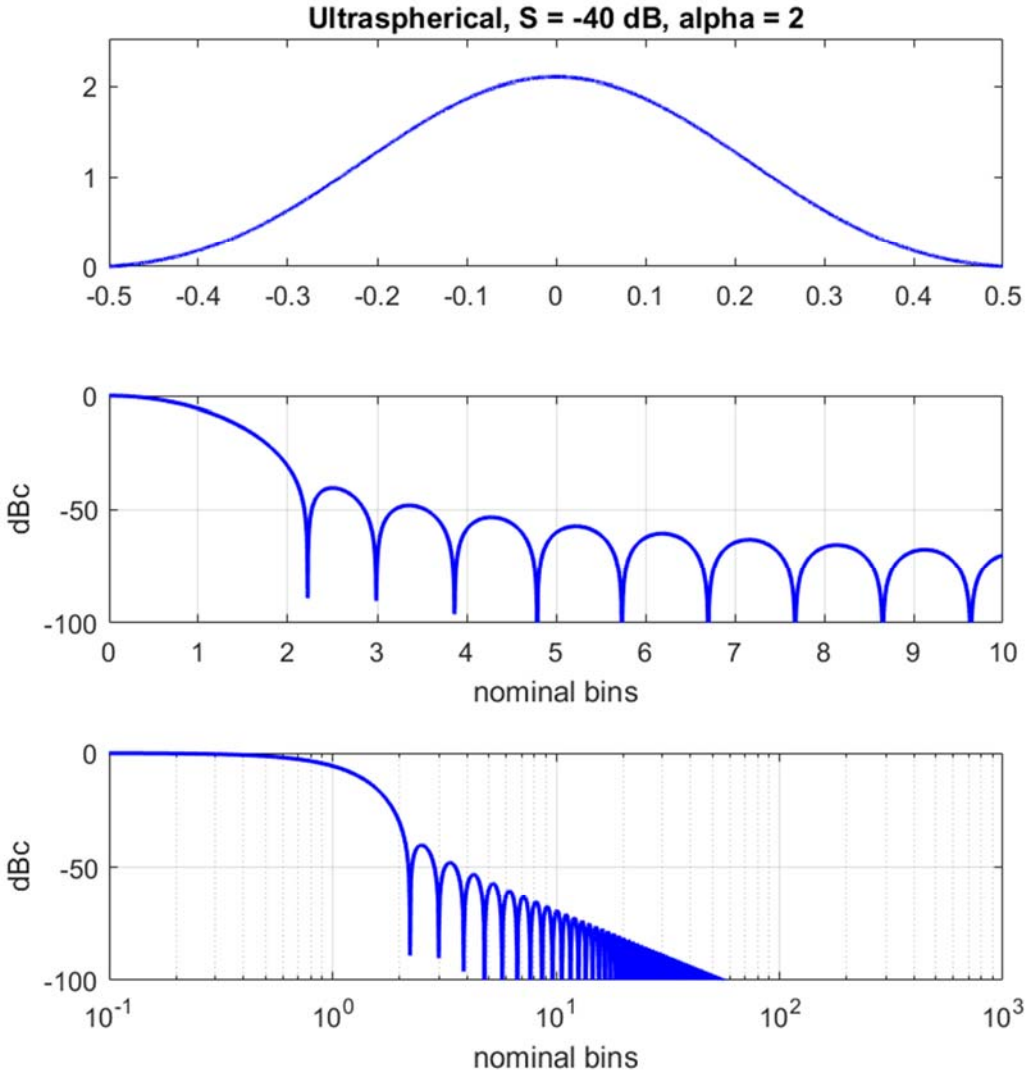


WINDOW SPECTRUM CHARACTERISTICS

half-power bandwidth = 1.4767 (normalized to 1/T)
-3 dB bandwidth = 1.4742 (normalized to 1/T)
-18 dB bandwidth = 3.3295 (normalized to 1/T)
noise bandwidth = 1.5438 (normalized to 1/T)
SNR loss = 1.886 dB
first null = 2.2227 (normalized to 1/T)
PSL = -40.3191 dBc
ISL = -42.2865 dBc from first null outward

**Figure 92.**

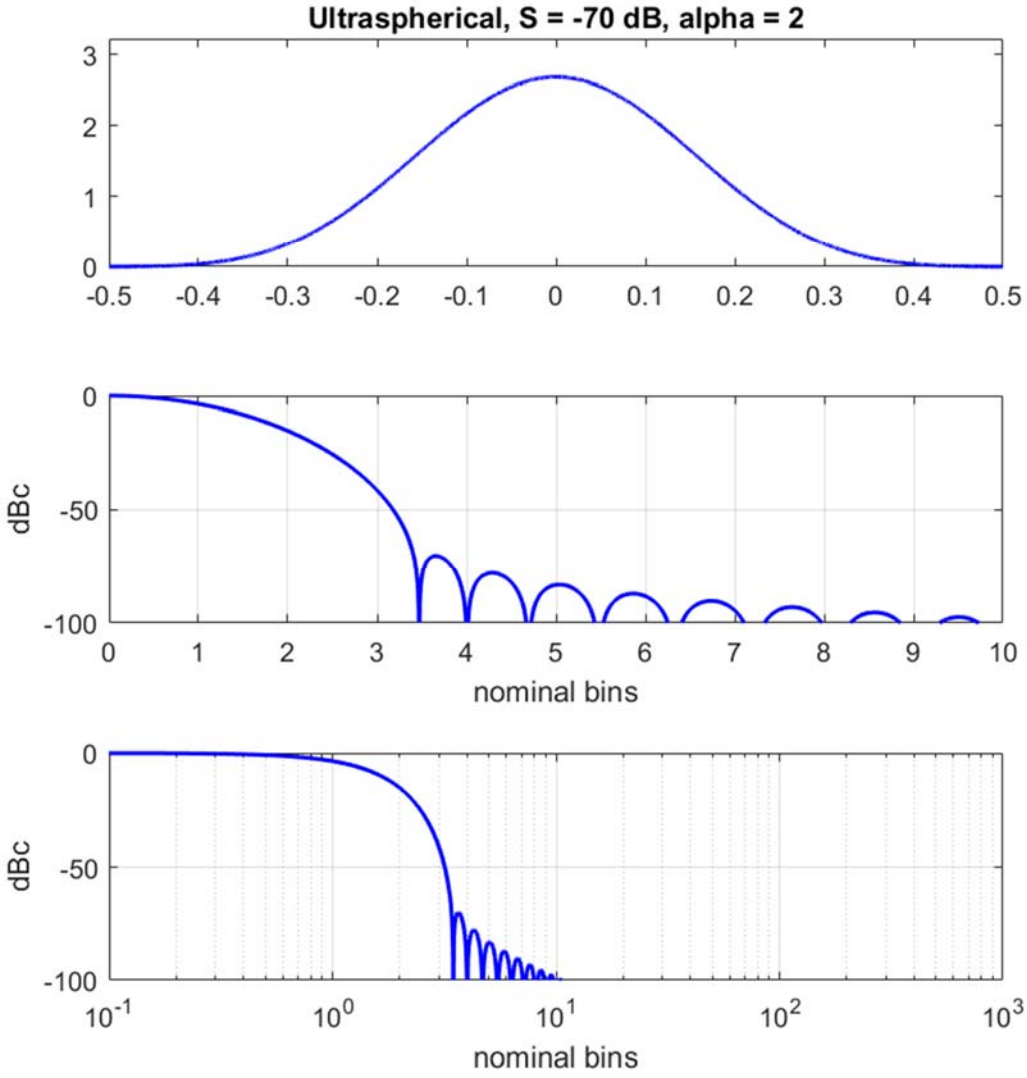


WINDOW SPECTRUM CHARACTERISTICS

half-power bandwidth = 1.8401 (normalized to 1/T)
-3 dB bandwidth = 1.837 (normalized to 1/T)
-18 dB bandwidth = 4.3004 (normalized to 1/T)
noise bandwidth = 1.9387 (normalized to 1/T)
SNR loss = 2.875 dB
first null = 3.4688 (normalized to 1/T)
PSL = -70.274 dBc
ISL = -74.647 dBc from first null outward

**Figure 93.**

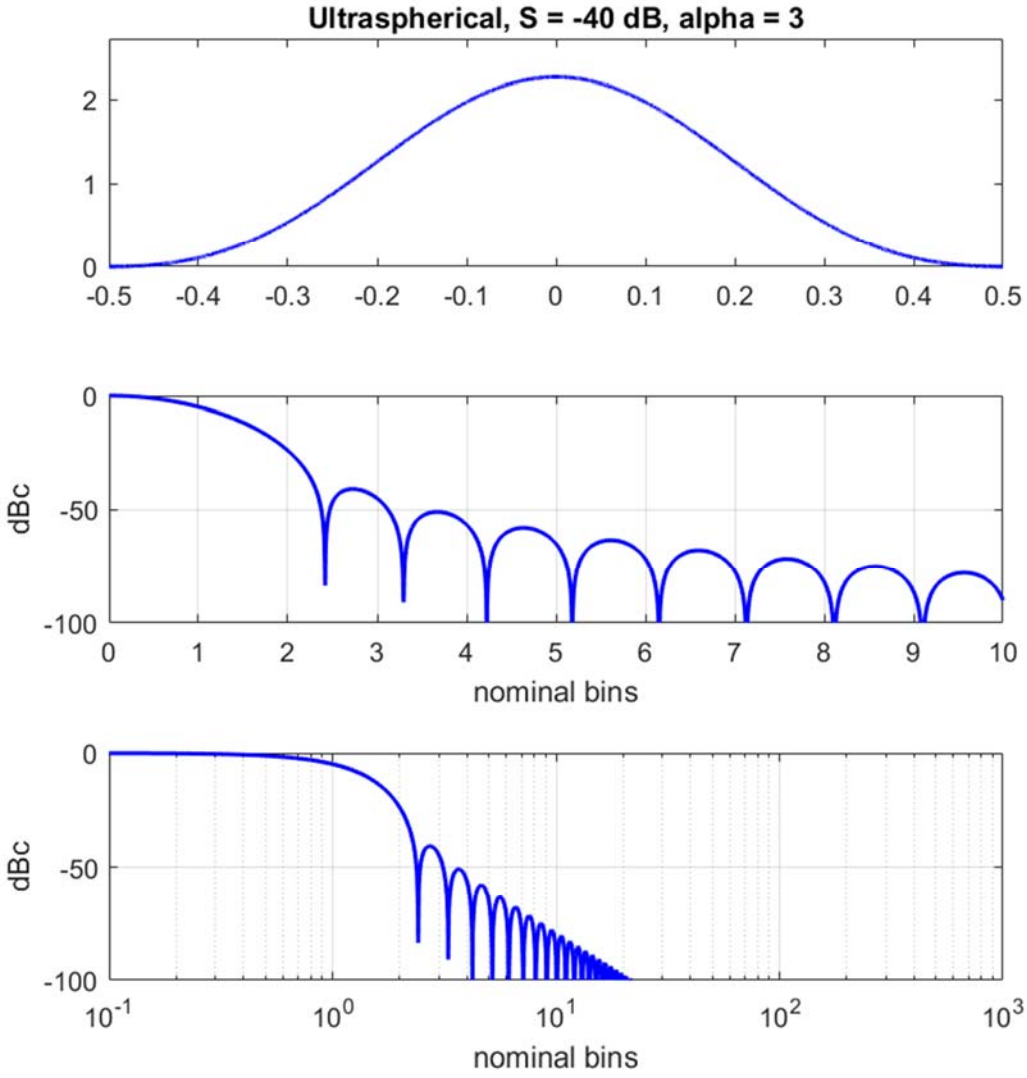


WINDOW SPECTRUM CHARACTERISTICS

half-power bandwidth = 1.5888 (normalized to 1/T)
-3 dB bandwidth = 1.5862 (normalized to 1/T)
-18 dB bandwidth = 3.5959 (normalized to 1/T)
noise bandwidth = 1.6625 (normalized to 1/T)
SNR loss = 2.208 dB
first null = 2.418 (normalized to 1/T)
PSL = -40.7809 dBc
ISL = -43.2127 dBc from first null outward

**Figure 94.**

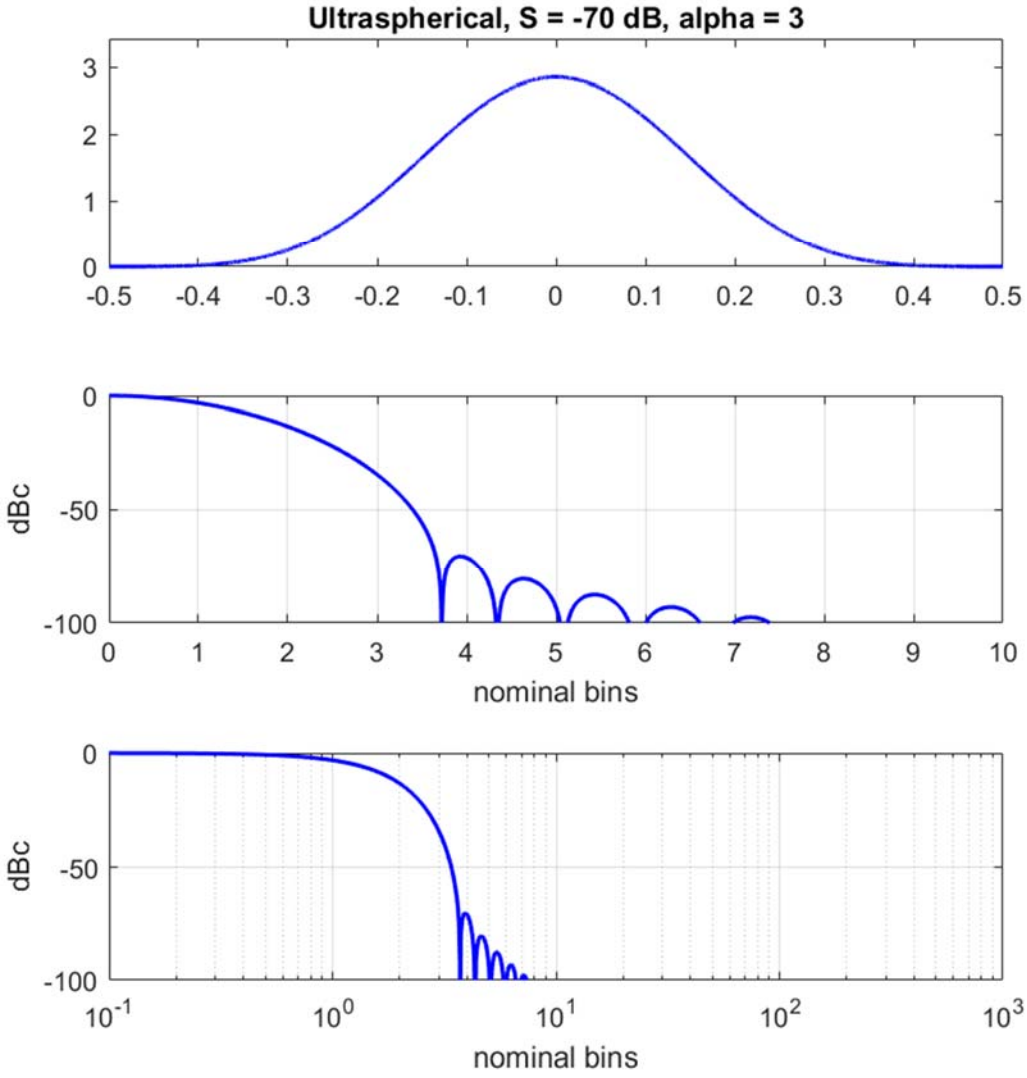


WINDOW SPECTRUM CHARACTERISTICS

half-power bandwidth = 1.9535 (normalized to 1/T)
-3 dB bandwidth = 1.9502 (normalized to 1/T)
-18 dB bandwidth = 4.5761 (normalized to 1/T)
noise bandwidth = 2.0593 (normalized to 1/T)
SNR loss = 3.137 dB
first null = 3.7227 (normalized to 1/T)
PSL = -70.4789 dBc
ISL = -75.3118 dBc from first null outward

**Figure 95.**

## 4.44 Saramäki

The Saramäki[48] window seeks to approximate the Kaiser window, but also with easier calculations.

Unlike more typical window taper functions, this window is also defined by its frequency response. The frequency response of the continuous time window taper function is calculated to be

$$W(f) = \frac{A\sin\left(\pi\sqrt{f^2+1-\beta^2}\right)}{\pi\sqrt{f^2+1-\beta^2}} = A\,\mathrm{sinc}\left(\sqrt{f^2+1-\beta^2}\right), \tag{251}$$

where

$$\beta = \text{distance of first null from mainlobe peak,} \tag{252}$$

and the scale factor to provide unit DC gain is

$$A = \left(\mathrm{sinc}\left(\sqrt{1-\beta^2}\right)\right)^{-1}. \tag{253}$$

We may approximately relate $\beta$ heuristically to the desired sidelobe level with

$$\beta \approx -0.0389\ S + 0.4509, \tag{254}$$

where

$$S = \text{sidelobe level with respect to mainlobe peak in dB, with } S < 0. \tag{255}$$

The actual window taper function itself is normally numerically calculated from the frequency response using an Inverse DFT. See Appendix A.

Plots and characteristics for this window for various sidelobe levels are given in Figure 96 and Figure 97.

***Original Formulation***

The origin of this window function is via a development by Saramäki that was performed using a discrete-frequency formulation.

Specifically, the discrete-frequency spectrum of the window taper function is developed directly to be

$$W_K(k) = N \frac{\sin\left(\frac{N}{2}\operatorname{acos}(x)\right)}{N\sin\left(\frac{1}{2}\operatorname{acos}(x)\right)}, \quad \text{for } 0 \le k \le K-1, \tag{256}$$

where

$$x = \gamma\cos\left(2\pi\frac{f}{f_s}\right) + \gamma - 1, \quad \text{for } x > -1\ , \tag{257}$$

and for this development, the sidelobe-level parameter is

$$\gamma = \frac{1+\cos\left(\frac{2\pi}{N}\right)}{1+\cos\left(\frac{2\pi\beta}{N}\right)}, \tag{258}$$

where $\beta$ is defined as in Eq. (252).

Frequency in Eq. (257) takes on the discrete values

$$f = \frac{k}{K} f_s, \quad \text{for } 0 \le k \le K-1, \tag{259}$$

where for a unit-length aperture, we identify the sampling frequency as

$$f_s = N - 1. \tag{260}$$

Recall that we expect $K \ge N$.

As *N* gets very large, with samples approaching the continuous case, we note that

$$\frac{\sin\left(\frac{N}{2}\operatorname{acos}(x)\right)}{N\sin\left(\frac{1}{2}\operatorname{acos}(x)\right)} \xrightarrow[N\to\infty]{} \frac{\sin\left(\pi\sqrt{f^2+1-\beta^2}\right)}{\pi\sqrt{f^2+1-\beta^2}}, \tag{261}$$

ultimately allowing the form given in Eq. (251).

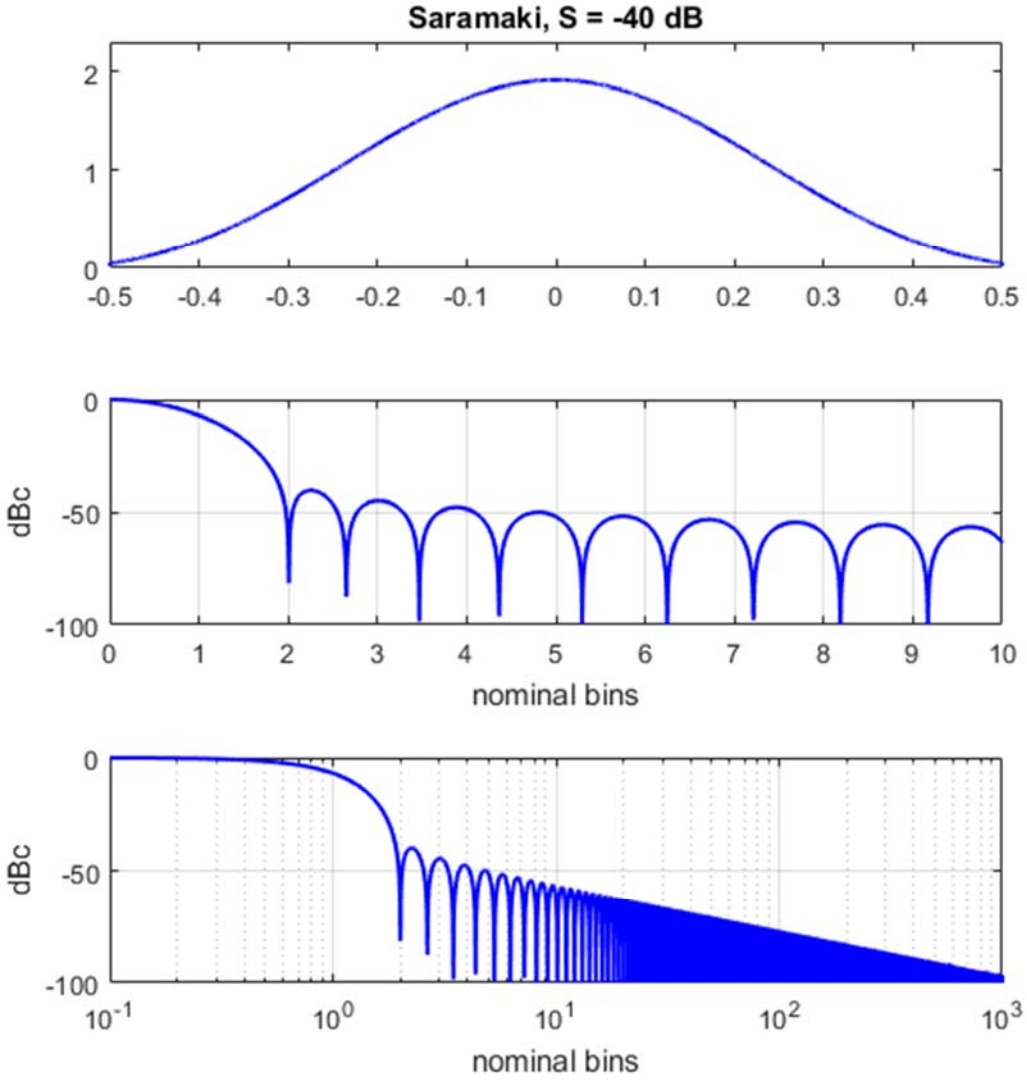


WINDOW SPECTRUM CHARACTERISTICS

half-power bandwidth = 1.35 (normalized to 1/T)
-3 dB bandwidth = 1.3478 (normalized to 1/T)
-18 dB bandwidth = 3.0297 (normalized to 1/T)
noise bandwidth = 1.41 (normalized to 1/T)
SNR loss = 1.492 dB
first null = 2.0078 (normalized to 1/T)
PSL = -39.9678 dBc
ISL = -39.4211 dBc from first null outward

**Figure 96.**

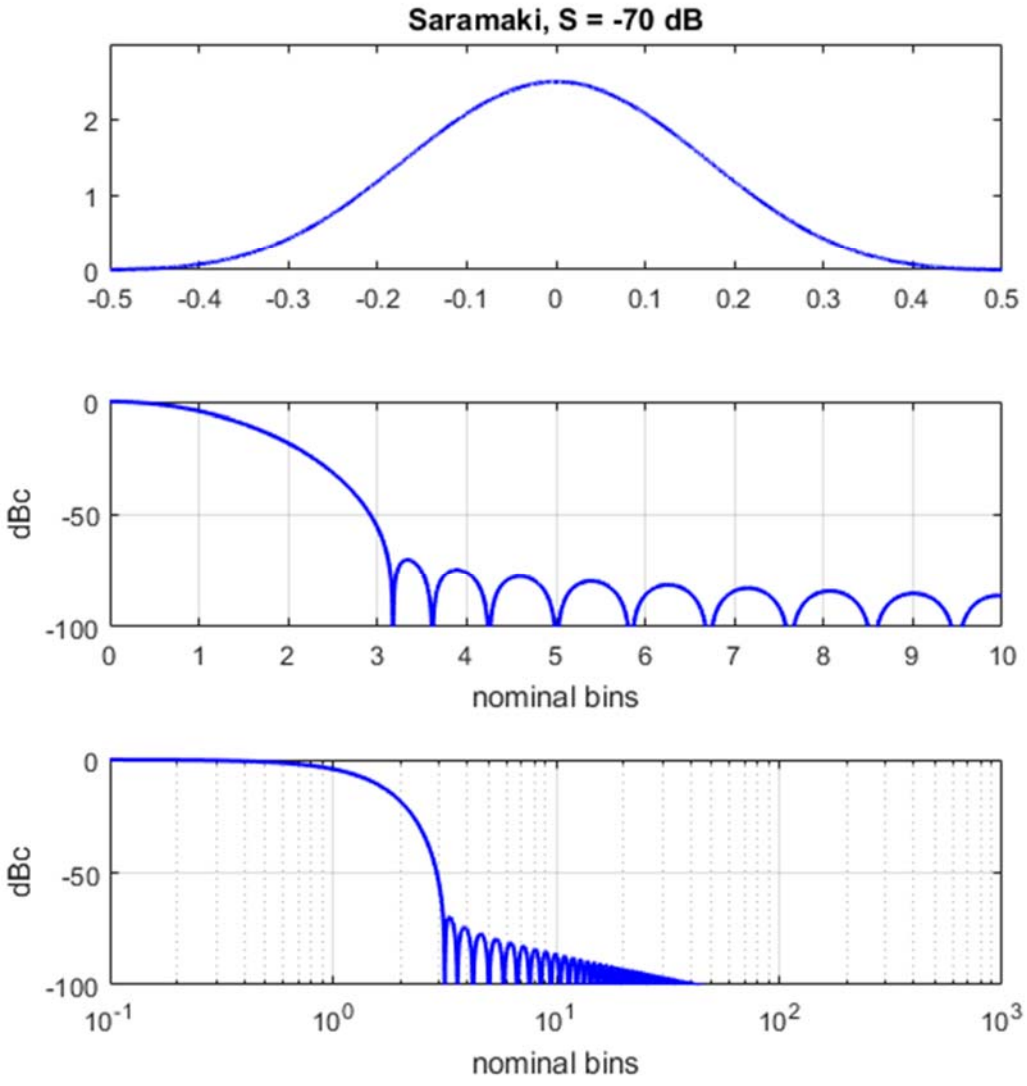


WINDOW SPECTRUM CHARACTERISTICS

half-power bandwidth = 1.7084 (normalized to 1/T)
-3 dB bandwidth = 1.7056 (normalized to 1/T)
-18 dB bandwidth = 3.9799 (normalized to 1/T)
noise bandwidth = 1.7987 (normalized to 1/T)
SNR loss = 2.55 dB
first null = 3.1758 (normalized to 1/T)
PSL = -69.9171 dBc
ISL = -71.3892 dBc from first null outward

**Figure 97.**

## 4.45 Legendre

Jaskula[49] presents a window taper function based on modified Legendre polynomials. Specifically, the discrete-frequency spectrum of the window taper function of length $N$ is developed directly to be

$$W_K(k) = N A P_{N-1}\left( x_0 \cos\left( \pi \frac{f}{f_s} \right) \right), \quad \text{for } 0 \le k \le K-1, \tag{262}$$

where the Legendre polynomial of degree $n$ is defined by the recurring relationships

$$P_0(x) = 1,$$
$$P_1(x) = x, \text{ and}$$
$$P_n(x) = \frac{1}{n}\left( x(2n-1) P_{n-1}(x) - (n-1) P_{n-2}(x) \right). \tag{263}$$

For this development, we further refine the parameter

$$x_0 = \cosh\left( \frac{1}{N-1} \operatorname{acosh}\left( 10^{-\sigma/20} \right) \right), \tag{264}$$

where

$$\sigma = \text{sidelobe parameter.} \tag{265}$$

We calculate the approximate desired sidelobe parameter with the heuristic linear relationship

$$\sigma \approx 1.0754\, S + 1.7388, \tag{266}$$

where

$$S = \text{sidelobe level with respect to mainlobe peak in dB, with } S < 0. \tag{267}$$

Frequency in Eq. (262) takes on the discrete values

$$f = \frac{k}{K} f_s, \quad \text{for } 0 \le k \le K-1, \tag{268}$$

where for a unit-length aperture, we identify the sampling frequency as

$$f_s = N - 1. \tag{269}$$

Recall that we expect $K \geq N$. The scale factor to provide unit DC gain is calculated as

$$A = \left( P_{N-1}\left( x_0 \right) \right)^{-1}. \tag{270}$$

With $W_K\left(k\right)$ so identified, the discrete-time window function may be therefrom calculated. See Appendix A. Jascula also offers a Matlab® program to generate Legendre window functions, albeit for odd *N*.

Spectral sidelobe roll-off rate is about $-10$ dB/decade.

Plots and characteristics for this window for various parameter combinations are given in Figure 98 and Figure 99.

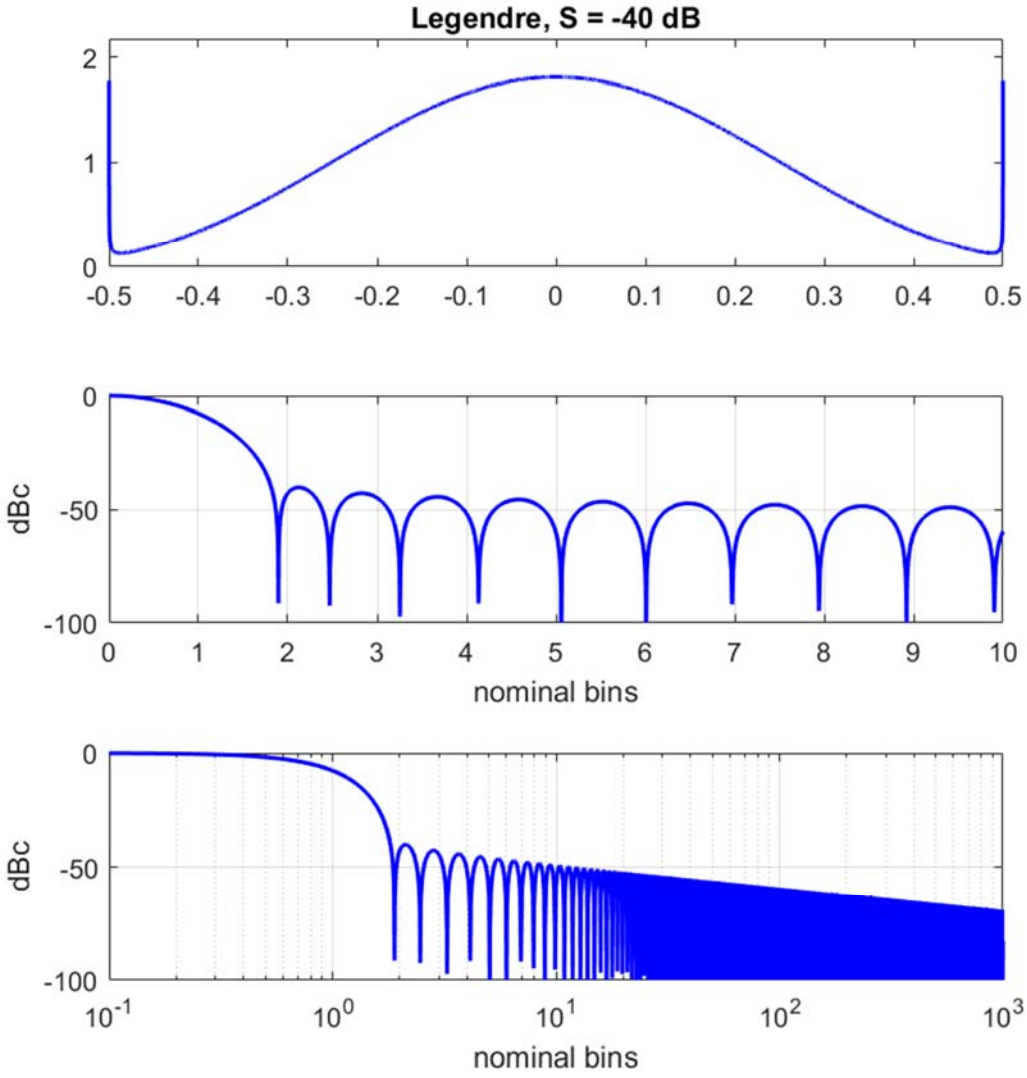


WINDOW SPECTRUM CHARACTERISTICS

half-power bandwidth = 1.2812 (normalized to 1/T)
-3 dB bandwidth = 1.2791 (normalized to 1/T)
-18 dB bandwidth = 2.8683 (normalized to 1/T)
noise bandwidth = Inf (normalized to 1/T)
SNR loss = Inf dB
first null = 1.8945 (normalized to 1/T)
PSL = -40.0794 dBc
ISL = Inf dBc from first null outward

**Figure 98.**

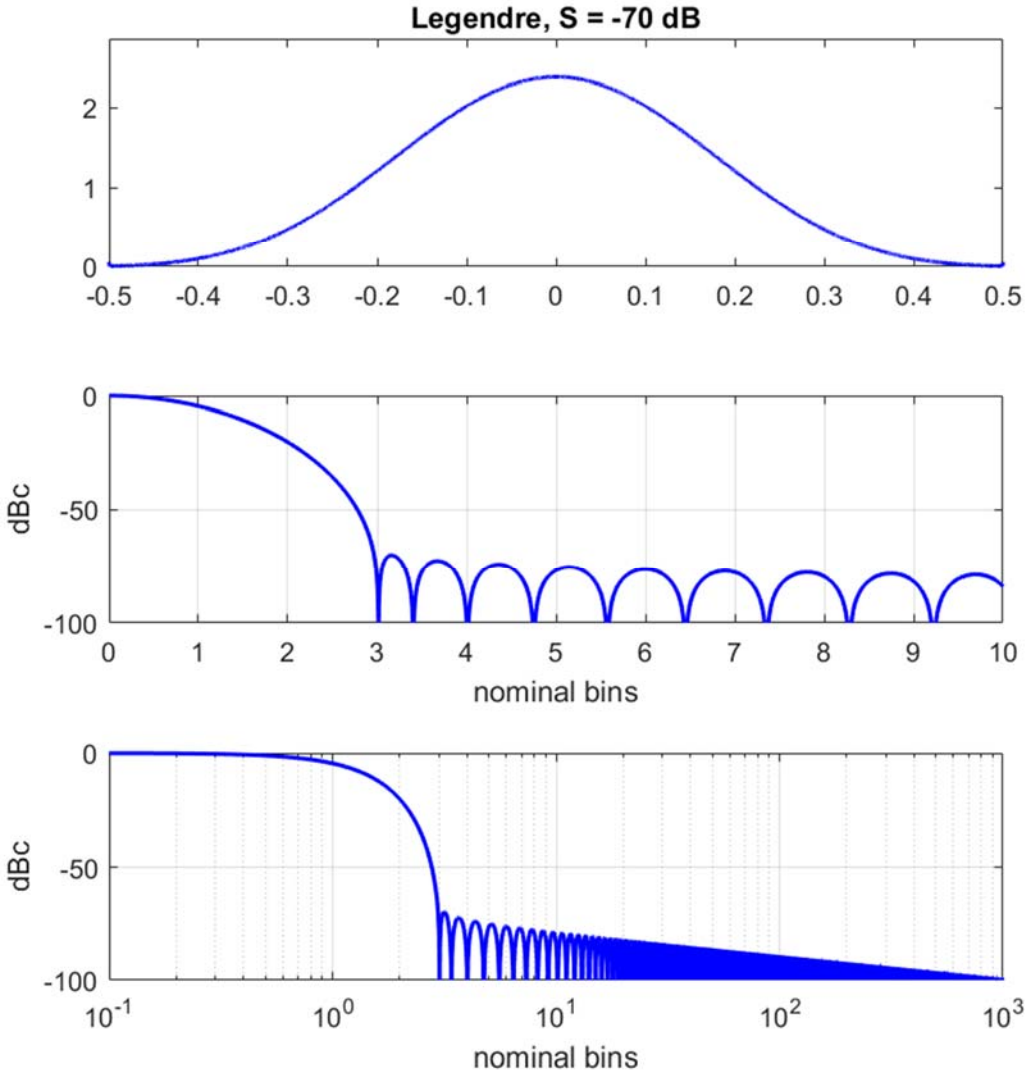


WINDOW SPECTRUM CHARACTERISTICS

half-power bandwidth = 1.6356 (normalized to 1/T)
-3 dB bandwidth = 1.6329 (normalized to 1/T)
-18 dB bandwidth = 3.8028 (normalized to 1/T)
noise bandwidth = Inf (normalized to 1/T)
SNR loss = Inf dB
first null = 3.0156 (normalized to 1/T)
PSL = -69.9865 dBc
ISL = Inf dBc from first null outward

**Figure 99.**

## 4.46 Modified First-Order Bessel (a.k.a. $I_1$-cosh)

Prabhu and Bagan[50] attribute this window to an unpublished Bell Laboratories memorandum by Kaiser in 1964. In contrast to the Kaiser-Bessel window taper function discussed in section 4.38, this window is now defined in terms of the first-order modified Bessel function of the first kind.

Accordingly, this window taper function family scaled for unit DC gain, is calculated as

$$w(t) = A \frac{I_1\left(\pi\alpha\sqrt{1-(2t)^2}\right)}{I_1(\pi\alpha)\sqrt{1-(2t)^2}} \operatorname{rect}(t), \tag{271}$$

where we identify the first-order modified Bessel function of the first kind as

$$I_1(x) = \sum_{k=0}^{\infty}\left[\frac{1}{k!(k+1)!}\left(\frac{x}{2}\right)^{2k+1}\right], \tag{272}$$

and we trade spectral sidelobe level against mainlobe width by selecting the parameter

$$\alpha > 0, \tag{273}$$

with the unit DC gain scale factor calculated to be

$$A = \frac{\pi\alpha\, I_1(\pi\alpha)}{\cosh(\pi\alpha) - 1}. \tag{274}$$

The Fourier Transform of the continuous time window taper function is calculated to be

$$W(f) = \frac{A\left(\cosh\left(\pi\alpha\sqrt{1-(f/\alpha)^2}\right) - \cos(\pi f)\right)}{\pi\alpha\, I_1(\pi\alpha)}. \tag{275}$$

Plots and characteristics for this window for several parameter combinations are given in Figure 100, Figure 101, and Figure 102.

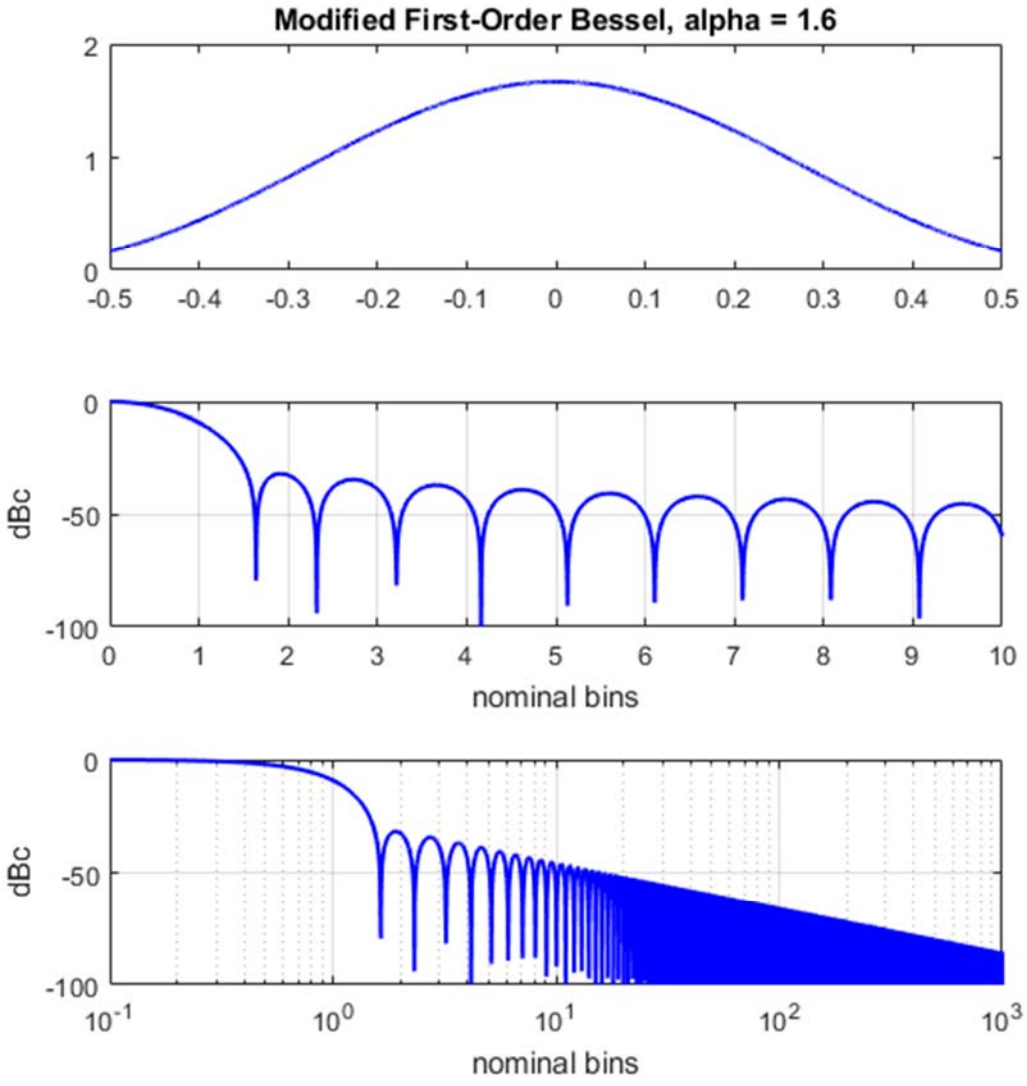


WINDOW SPECTRUM CHARACTERISTICS

half-power bandwidth = 1.1981 (normalized to 1/T)
-3 dB bandwidth = 1.1962 (normalized to 1/T)
-18 dB bandwidth = 2.624 (normalized to 1/T)
noise bandwidth = 1.2464 (normalized to 1/T)
SNR loss = 0.9565 dB
first null = 1.6406 (normalized to 1/T)
PSL = -31.7224 dBc
ISL = -28.7238 dBc from first null outward

**Figure 100.**

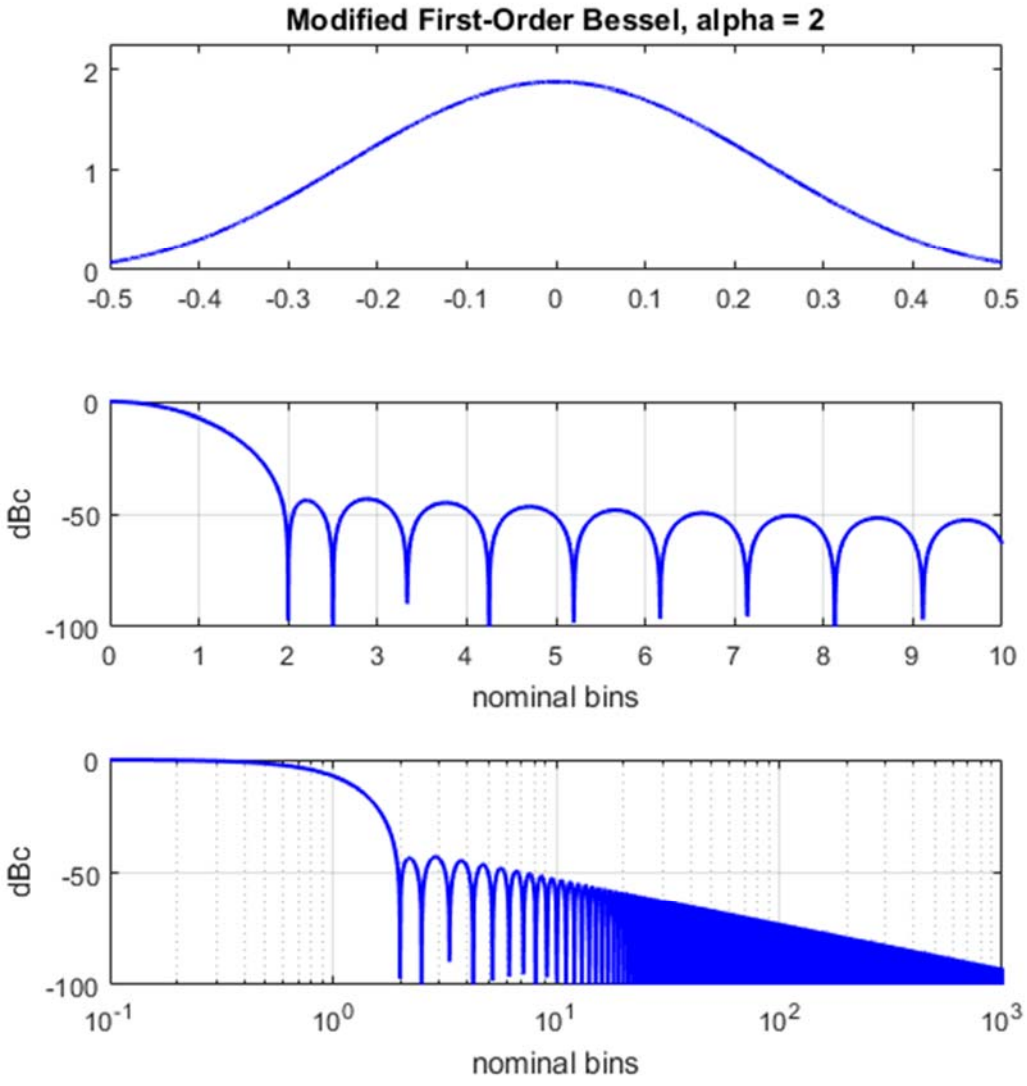


WINDOW SPECTRUM CHARACTERISTICS

half-power bandwidth = 1.3217 (normalized to 1/T)
-3 dB bandwidth = 1.3195 (normalized to 1/T)
-18 dB bandwidth = 2.972 (normalized to 1/T)
noise bandwidth = 1.381 (normalized to 1/T)
SNR loss = 1.4018 dB
first null = 2 (normalized to 1/T)
PSL = -42.9309 dBc
ISL = -37.9176 dBc from first null outward

**Figure 101.**

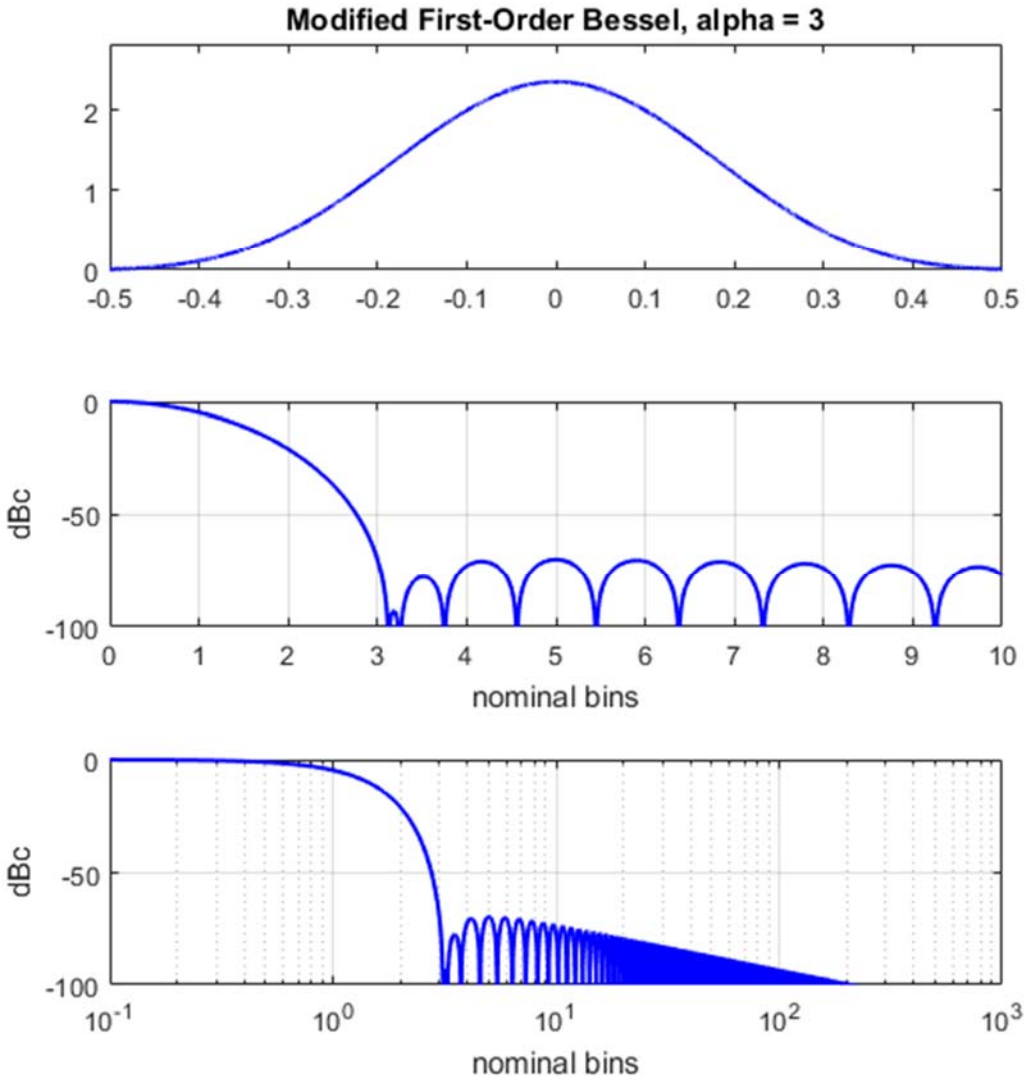


WINDOW SPECTRUM CHARACTERISTICS

half-power bandwidth = 1.613 (normalized to 1/T)
-3 dB bandwidth = 1.6103 (normalized to 1/T)
-18 dB bandwidth = 3.7532 (normalized to 1/T)
noise bandwidth = 1.6976 (normalized to 1/T)
SNR loss = 2.2985 dB
first null = 3.125 (normalized to 1/T)
PSL = -69.8318 dBc
ISL = -62.3458 dBc from first null outward

**Figure 102.**

## 4.47 Shayesteh-Kashtiban

Shayesteh and Mottaghi-Kashtiban[51] developed a window taper function by optimizing the coefficients of a Hamming window using an Extended Kalman Filter (EKF). It may be thought of as having features from both a Lanczos window and a Dolph-Chebyshev window.

This window is defined in the discrete-time domain as

$$w_N(n) = \begin{cases} A\left[0.02 + 0.001(N-1) + \dfrac{1}{2(N-1)+50}\right] & \text{for } n = 0,(N-1) \\ A\,\mathrm{sinc}^{2.5}\left(\dfrac{n-(N-1)/2}{0.654(N-1)}\right) & \text{for } 1 \le n \le (N-2), \\ 0 & \text{else} \end{cases} \quad (276)$$

where the DC gain scale factor is calculated to be

$$A = N\left[2\left(0.02 + 0.001(N-1) + \frac{1}{2(N-1)+50}\right) + \sum_{n=1}^{N-2} \mathrm{sinc}^{2.5}\left(\frac{n-(N-1)/2}{0.654(N-1)}\right)\right]^{-1}. \quad (277)$$

The spectrum of this window taper function is not readily calculated in closed-form. It may be numerically calculated for specific parameters, i.e. using a DFT on the discrete-time samples of the window function, as given in Eq. (276).

Note that for very large *N*, the endpoints of the window function itself become very impulse-like, much like the Dolph-Chebyshev window, and the spectrum itself becomes very Dolph-Chebyshev-like, albeit without the sidelobe-level control.

Plots and characteristics for this window for $N = 16384$ given in Figure 103.

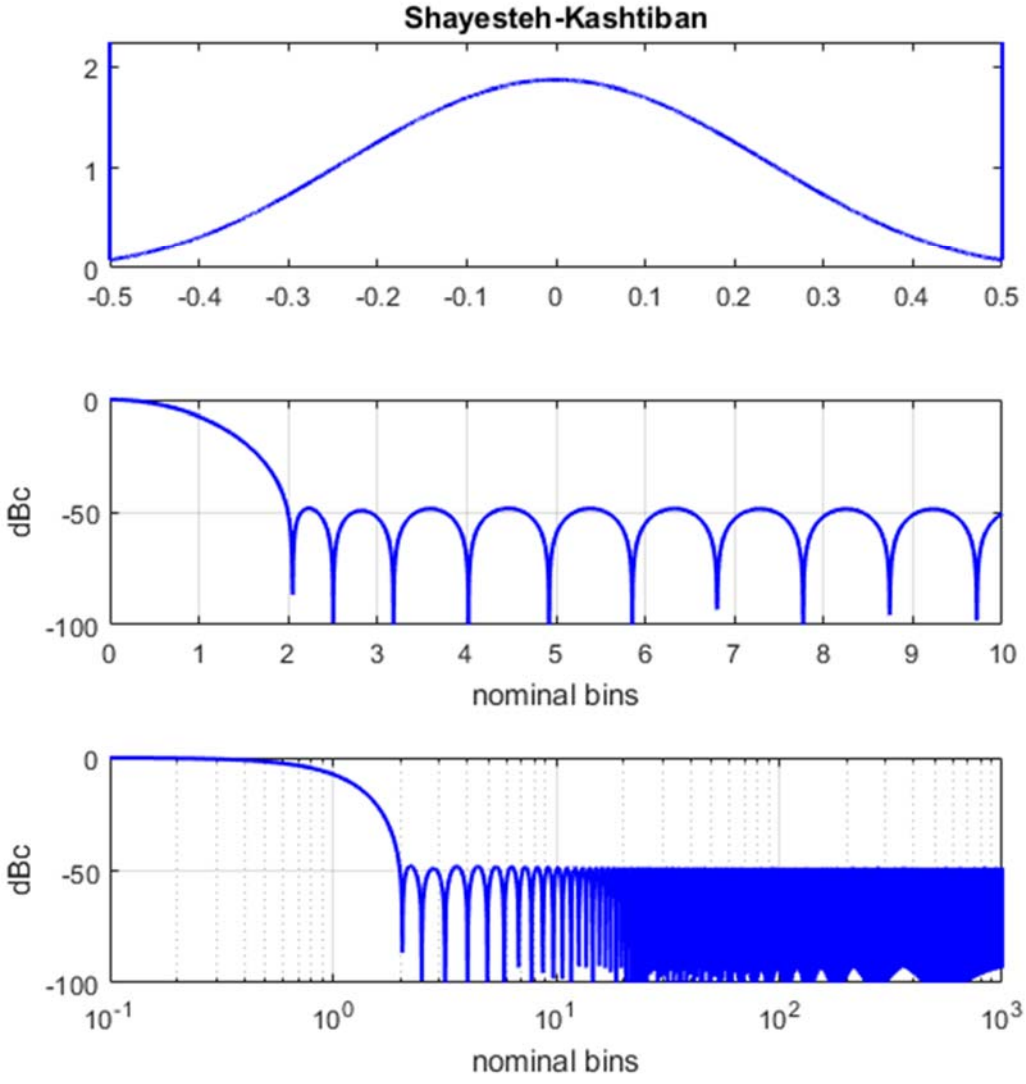


WINDOW SPECTRUM CHARACTERISTICS

half-power bandwidth = 1.307 (normalized to 1/T)
-3 dB bandwidth = 1.3048 (normalized to 1/T)
-18 dB bandwidth = 2.9605 (normalized to 1/T)
noise bandwidth = 1.4819 (normalized to 1/T)
SNR loss = 1.708 dB
first null = 2.0508 (normalized to 1/T)
PSL = -47.9131 dBc
ISL = -11.1273 dBc from first null outward

**Figure 103.**

## 4.48 Kaiser-Bessel-Derived (a.k.a. KBD, Dolby)

This window is derived from the Kaiser-Bessel window taper function described in section 4.38, where we recall, and re-designate the window function as

$$w_{KB}(t) = \frac{\pi\alpha}{\sinh(\pi\alpha)} I_0\left(\pi\alpha\sqrt{1-(2t)^2}\right)\mathrm{rect}(t). \tag{278}$$

This now becomes the kernel for the Kaiser–Bessel-Derived window taper function, which we calculate for continuous time as

$$w(t) = A\sqrt{\frac{\int_{-1/2}^{2|t|+1/2} w_{KB}(\tau)\,d\tau}{\int_{-1/2}^{1/2} w_{KB}(\tau)\,d\tau}}\,\mathrm{rect}(t). \tag{279}$$

Because we have defined the Kaiser-Bessel window kernel with unit DC gain, this reduces to

$$w(t) = A\left(\sqrt{\int_{-1/2}^{2|t|+1/2} w_{KB}(\tau)\,d\tau}\right)\mathrm{rect}(t). \tag{280}$$

For this new window to have unit DC gain, we calculate

$$A = \left[\int_{-1/2}^{1/2}\left(\sqrt{\int_{-1/2}^{2|t|+1/2} w_{KB}(\tau)\,d\tau}\right)dt\right]^{-1}. \tag{281}$$

We stipulate that more typically, discrete-time Kaiser-Bessel-Derived window tapers are calculated from discrete-time Kaiser-Bessel window functions. In fact, this is how they were originally derived. This, of course, turns all the integrations into summations. The Kaiser–Bessel-Derived window taper function enjoys particular popularity for audio encoding, and in fact was developed for this application to meet some unique required characteristics.[52]

The spectrum of this continuous window taper function is not readily calculated in closed-form. It may be numerically calculated for specific parameters, i.e. using a DFT on the discrete-time samples of the window function.

Examples are plotted in Figure 104, Figure 105, and Figure 106.

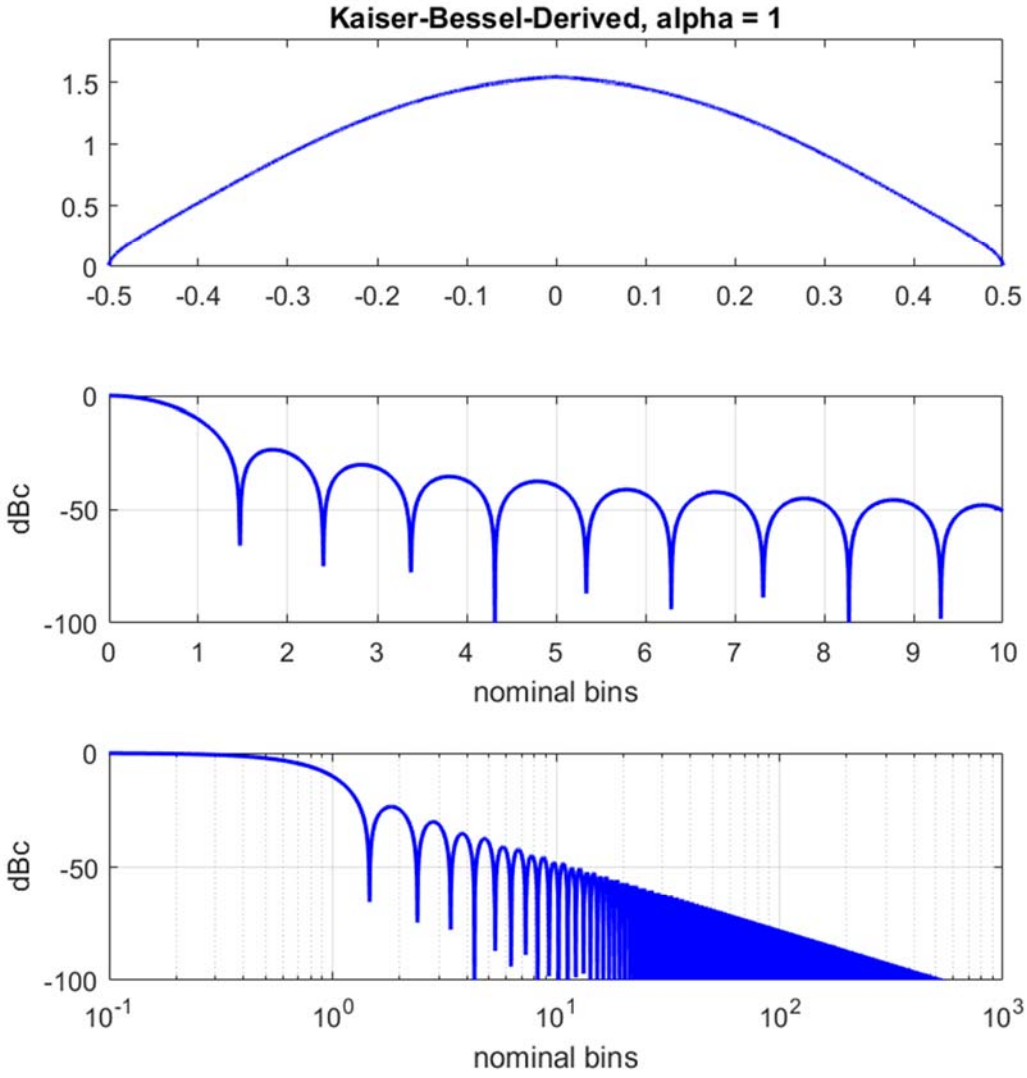


WINDOW SPECTRUM CHARACTERISTICS

half-power bandwidth = 1.1557 (normalized to 1/T)
-3 dB bandwidth = 1.1538 (normalized to 1/T)
-18 dB bandwidth = 2.4589 (normalized to 1/T)
noise bandwidth = 1.1993 (normalized to 1/T)
SNR loss = 0.789 dB
first null = 1.4648 (normalized to 1/T)
PSL = -23.5001 dBc
ISL = -23.1526 dBc from first null outward

**Figure 104.**

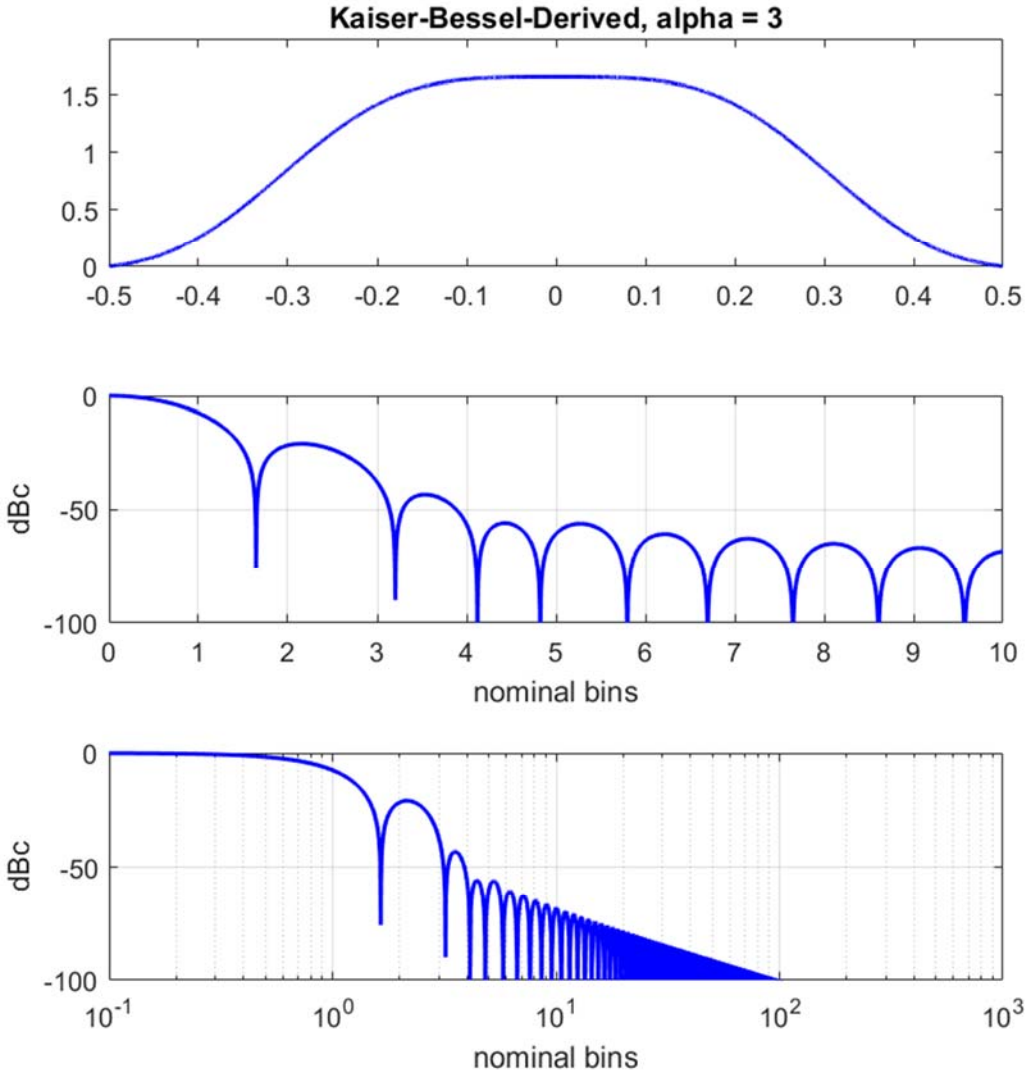


WINDOW SPECTRUM CHARACTERISTICS

half-power bandwidth = 1.3166 (normalized to 1/T)
-3 dB bandwidth = 1.3144 (normalized to 1/T)
-18 dB bandwidth = 2.7904 (normalized to 1/T)
noise bandwidth = 1.3699 (normalized to 1/T)
SNR loss = 1.367 dB
first null = 1.6445 (normalized to 1/T)
PSL = -20.8949 dBc
ISL = -20.917 dBc from first null outward

**Figure 105.**

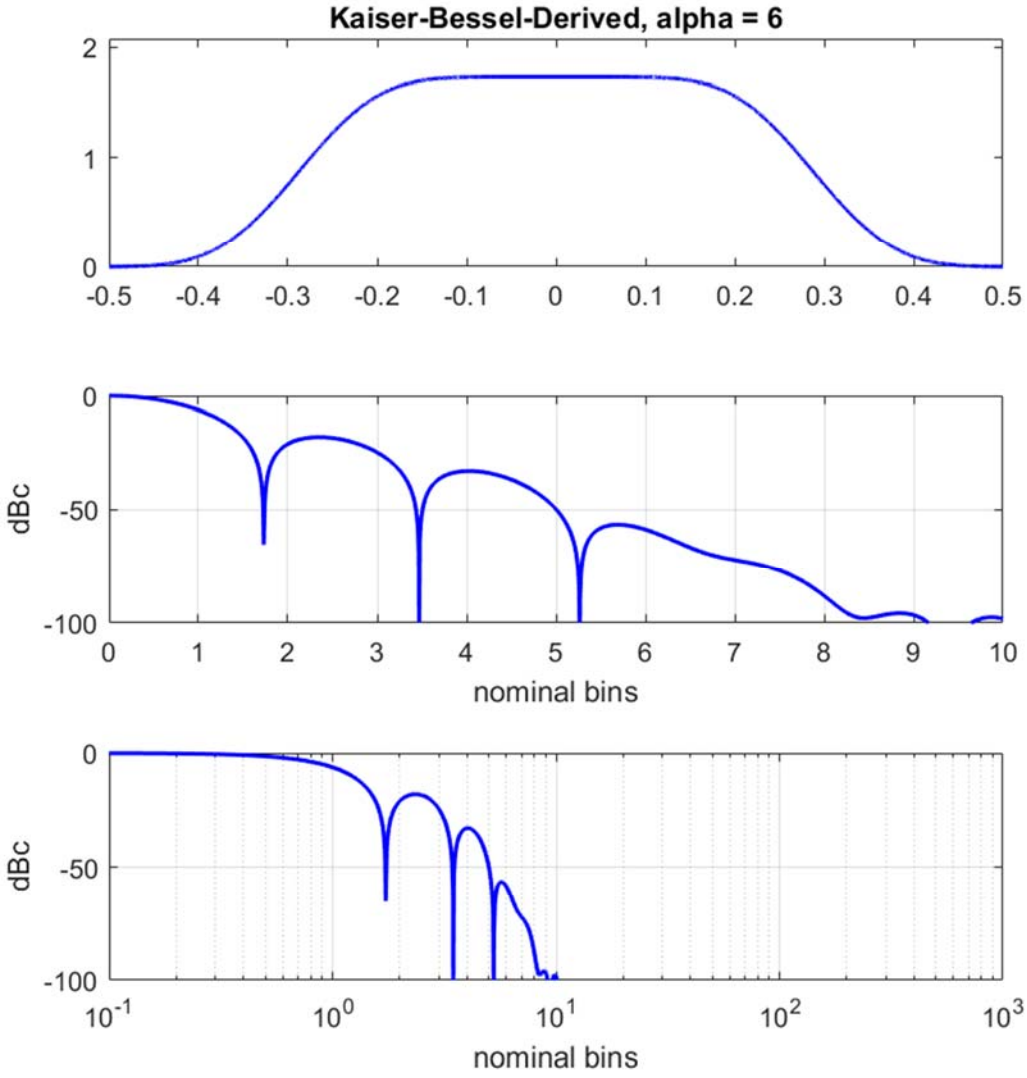


WINDOW SPECTRUM CHARACTERISTICS

half-power bandwidth = 1.4326 (normalized to 1/T)
-3 dB bandwidth = 1.4302 (normalized to 1/T)
-18 dB bandwidth = 2.9861 (normalized to 1/T)
noise bandwidth = 1.4993 (normalized to 1/T)
SNR loss = 1.759 dB
first null = 1.7305 (normalized to 1/T)
PSL = -18.0327 dBc
ISL = -17.6246 dBc from first null outward

**Figure 106.**

## 4.49 Vorbis (a.k.a. Ogg Vorbis)

This window also enjoys popularity for audio encoding.[53,54] This window taper function, scaled for unit DC gain, is calculated as

$$w(t) = A\sin\left(\frac{\pi}{2}\cos^2(\pi t)\right)\mathrm{rect}(t)\,. \tag{282}$$

For this new window to have unit DC gain, we calculate

$$A = \frac{\sqrt{2}}{J_0(\pi/4)} \approx 1.6606\,, \tag{283}$$

where

$$J_0(x) = \text{Bessel function of the first kind, order zero, of } x. \tag{284}$$

The spectrum of this continuous window taper function is not readily calculated in closed-form. It may be numerically calculated for specific parameters, i.e. using a DFT on the discrete-time samples of the window function.

Example plots are given in Figure 107.

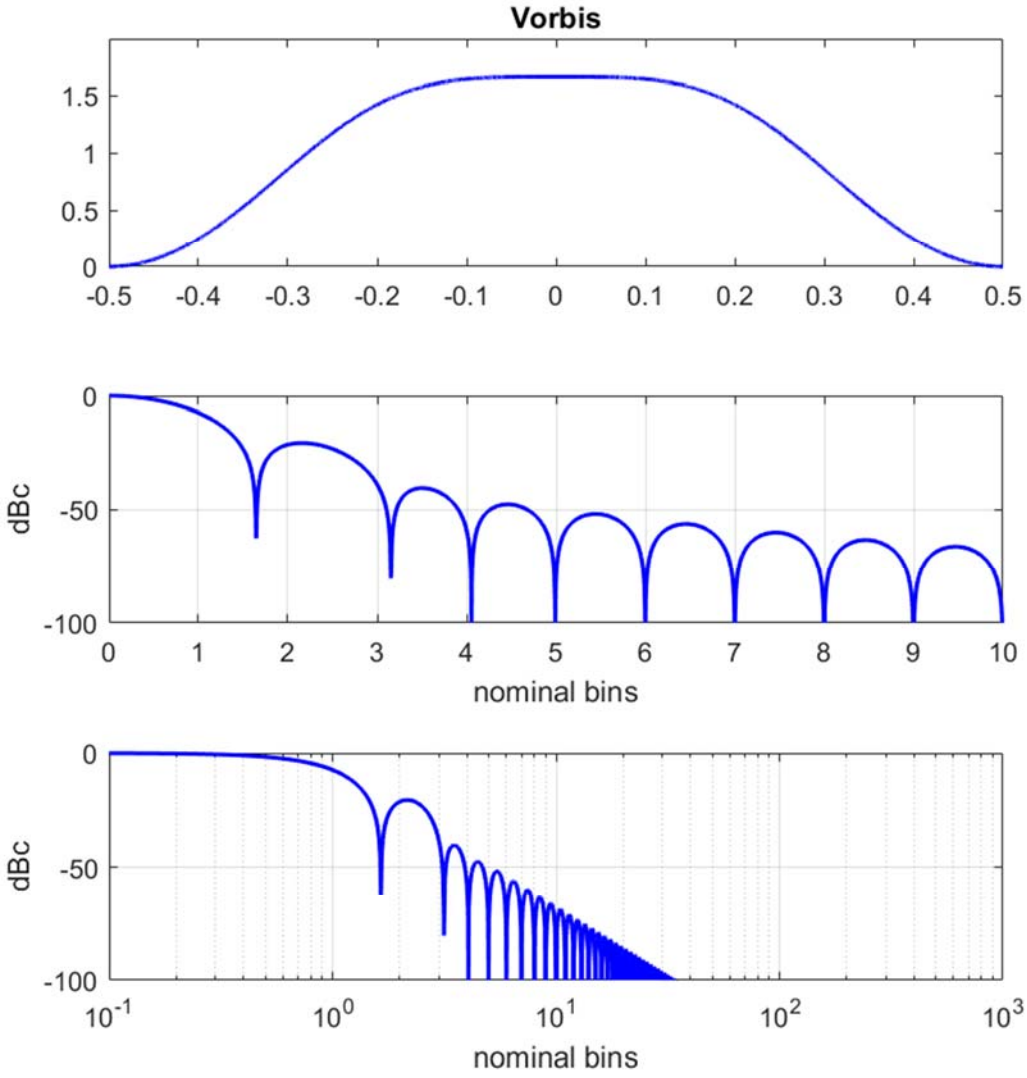


WINDOW SPECTRUM CHARACTERISTICS

half-power bandwidth = 1.3254 (normalized to 1/T)
-3 dB bandwidth = 1.3232 (normalized to 1/T)
-18 dB bandwidth = 2.8004 (normalized to 1/T)
noise bandwidth = 1.3789 (normalized to 1/T)
SNR loss = 1.395 dB
first null = 1.6484 (normalized to 1/T)
PSL = -20.5882 dBc
ISL = -20.6505 dBc from first null outward

**Figure 107.**

## 4.50 Flat-Top

This window enjoys popularity for instrumentation spectral analysis.[55,56] It is intended to have a spectrum that approaches a rectangle function. It is a specific member of the general Blackman-Harris family in that it is defined as a particular sum of cosine terms given by

$$w(t) = A\left(\sum_{l=0}^{L-1} \alpha_l \cos(2\pi l\, t)\right) \text{rect}(t), \tag{285}$$

where

$$\begin{aligned} &l = \text{coefficient index, } 0 \le l \le L-1, \\ &\alpha_l = \text{coefficient, and} \\ &A = 1/\alpha_0 = \text{scale factor used to force a unit DC gain.} \end{aligned} \tag{286}$$

The specific coefficients for $L = 5$ are

$$\begin{aligned} \alpha_0 &= 0.21557895, \\ \alpha_1 &= 0.41663158, \\ \alpha_2 &= 0.277263158, \\ \alpha_3 &= 0.083578947, \text{ and} \\ \alpha_4 &= 0.006947368. \end{aligned} \tag{287}$$

The Fourier Transform of this continuous time window taper function is calculated as

$$W(f) = \text{sinc}(f) + \frac{1}{2\alpha_0}\sum_{l=1}^{L-1}\left(\alpha_l \,\text{sinc}(f-l) + \alpha_l \,\text{sinc}(f+l)\right). \tag{288}$$

Example plots are given in Figure 108. An unusual feature of this window is that it in fact has negative values in $w(t)$.

The specific coefficients for $L = 3$ are given as

$$\begin{aligned} \alpha_0 &= 0.2811, \\ \alpha_1 &= 0.5209, \text{ and} \\ \alpha_2 &= 0.1980. \end{aligned} \tag{289}$$

Example plots for this window for $L = 3$ are given in Figure 109.

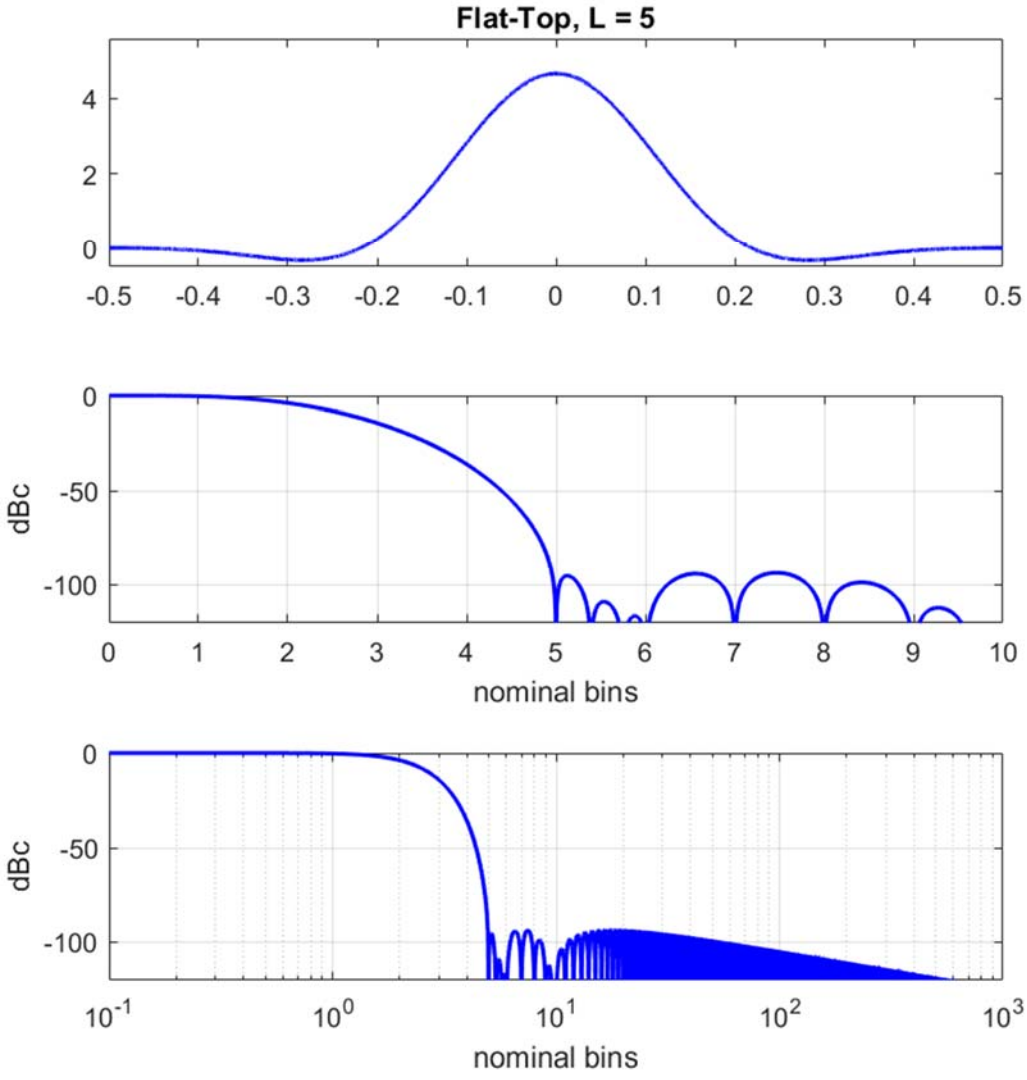


WINDOW SPECTRUM CHARACTERISTICS

half-power bandwidth = 3.7239 (normalized to 1/T)
-3 dB bandwidth = 3.7202 (normalized to 1/T)
-18 dB bandwidth = 6.4613 (normalized to 1/T)
noise bandwidth = 3.7705 (normalized to 1/T)
SNR loss = 5.764 dB
first null = 5 (normalized to 1/T)
PSL = -93.0291 dBc
ISL = -82.6393 dBc from first null outward

**Figure 108.**

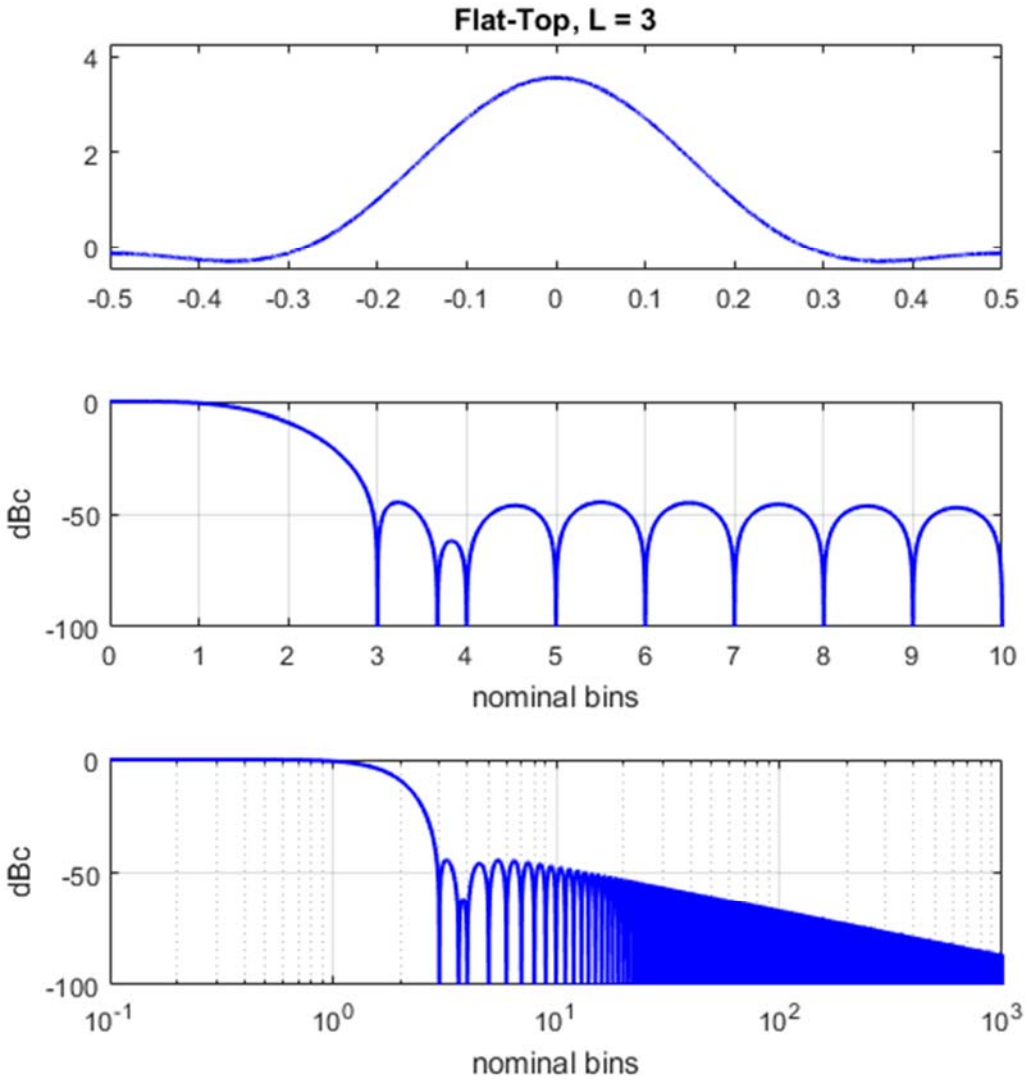


WINDOW SPECTRUM CHARACTERISTICS

half-power bandwidth = 2.9334 (normalized to 1/T)
-3 dB bandwidth = 2.9306 (normalized to 1/T)
-18 dB bandwidth = 4.8383 (normalized to 1/T)
noise bandwidth = 2.9653 (normalized to 1/T)
SNR loss = 4.721 dB
first null = 3 (normalized to 1/T)
PSL = -44.3662 dBc
ISL = -38.6079 dBc from first null outward

**Figure 109.**

# 5 Related Discussion

We now offer a number of disjoint comments and observations.

- Often, the mainlobe of the spectrum of some window taper function itself can be, and often is, used as a window taper function. An example is the mainlobe of a sinc function, where the sinc function is the spectral response of a Rectangle window function.

- Many other window functions can be derived from those presented here by combinations of adding, multiplying, or convolving windows (or their spectra) with themselves or any number of other window functions, in addition to varying parameters and/or scaling.

- Nonlinear combinations of tapered functions of the data may also be used to advantage, although they carry some baggage as well.[57]

- While we have presented window taper functions that provide real and even spectra, we stipulate that window taper functions can also be developed that yield different sidelobe responses on either side of the mainlobe. A reason for this might be foreknowledge that weak signals exist on just one side of a strong signal, such as radar ranging through a lossy medium.[58] Such window functions are necessarily complex-valued, as opposed to real-valued.

- Another application requiring an odd-symmetric window taper function is the difference channel of a monopulse radar antenna. Here, the desire is for minimum (or at least controlled) sidelobes in the difference between opposite halves of the aperture. Bayliss addressed optimizing such a window taper function for monopulse antennas.[59]

- In some applications, it is useful to process a larger aperture in terms of subapertures. This causes a coupling of effects from weighting within the subapertures, and then weighting across subapertures.[60] Furthermore, weighting the larger aperture before parsing into subapertures also has effects such as moving phase-centers in the subapertures, and imparting nonuniform subaperture gains.[61]

- While we have discussed herein using amplitude tapers to generate a precise spectral response, we note that we can often produce essentially equivalent spectral responses using phase-only filter functions.[62] This is quite common for generating Non-Linear FM chirp radar waveforms.[63]

- While this report discussed window taper functions for one-dimensional apertures of signals, imaging systems will often deal with two-dimensional apertures requiring two-dimensional windows. An example of this is Synthetic Aperture Radar.[64] These may be orthogonal applications of one-dimensional windows, or

bona fide two-dimensional windows. Another example is a non-rectangular antenna aperture or array. These concepts can also be extended to more than two dimensions.

- We note that especially for two-dimensional window taper functions, beamshaping for laser beams is very much related.[65]

- While we have herein dealt with tapering apertures to control sidelobes, we note that the same principles apply to controlling spectral leakage into "notches" inserted into a spectrum.[66]

## Other Techniques for Spectral Estimation

We briefly mention that other techniques have been explored over the years to mitigate effects of finite apertures, including mitigation of mainlobe-broadening while still suppressing sidelobes. These techniques often fall under the heading of "spectral estimation" techniques. We offer that many of these techniques are non-linear in nature, and often very sensitive to SNR of the input signal. Furthermore, we stipulate that the following are two entirely separate problems:

1. We are searching for a known number of sinusoids in the input data.

2. We are searching for an indeterminate number of general signals in the input data.

Techniques that might excel at the former, may in fact break down horribly for the latter. Nevertheless, the nature of the problem at hand might warrant a look at some of the techniques offered in this arena.

***Superresolution***

We further offer that it has been asked "With fine-enough resolution, do we really care about sidelobes?" This in turn leads to the notion of "How do we improve the resolution of a detected signal to something finer than the finite aperture-width might otherwise allow? That is, can we super-resolve the signal in which we are interested?"

Much effort and investment has been spent on superresolution techniques of various sorts over the years, with sometime extraordinary claims having been put forth. Except that to acknowledge that this area of study exists we will not discuss it further beyond to say that those techniques generally exhibit the same limitations as stated above for spectral estimation techniques generally.[67]

# 6 Conclusions

We reiterate the following key points.

- Finite apertures inherently generate sidelobes in the spectrum of the signal, mainly due to their edges.
- The spectra from finite apertures of a signal can be modified to reduce sidelobes by tapering, or windowing, the signal within the aperture.
- A plethora of window taper functions exist to optimize various aspects and trades in the characteristics of the spectrum of the signal.
- Proper selection of a window taper functions requires first understanding the trades in spectrum characteristics, and defining/acceptable limits and margins for those characteristics.

*"Forgive me my nonsense,*
*as I also forgive the nonsense of those that think they talk sense."*
*-- Robert Frost*

# Appendix A – Generating Window Functions from Their Spectra

Our task here is to begin with a window taper function that is defined by its spectrum, and calculate the discrete-time weights from it.

Accordingly, we borrow notation from section 2.6, and repeat some more relevant parameters here as

$$f_\Delta = \frac{f_s}{K} \text{ = frequency-sample spacing, and}$$

$$T_a = \frac{1}{f_\Delta} \text{ = time-interval represented by frequency-sample spacing.} \quad \text{(A1)}$$

For the desired window function itself,

$$T_\Delta = \frac{T}{(N-1)} \text{ = the time-sample spacing, and}$$

$$f_s = \frac{1}{T_\Delta} \text{ = the time-sampling frequency.} \quad \text{(A2)}$$

We recall that for a unit-width aperture, where $T = 1$, then *N* samples spread from end to end over this aperture implies that

$$f_s = N - 1 \text{ , for a unit-width aperture.} \quad \text{(A3)}$$

We furthermore recall that the spectrum of the continuous-time window is related to its sampled version by

$$W_K(k) \approx N\, W(f_\Delta k), \text{ for small } k. \quad \text{(A4)}$$

We will presume that this is essentially true for spectral regions with significant energy, which we assert includes the regions

$$|k| \le K/2, \quad \text{(A5)}$$

and especially for large *N*.

Recall that for sampled data, we expect repeated spectra, such that

$$W_K(k+K) = W_K(k), \text{ for small } k. \quad \text{(A6)}$$

We now define the Inverse Discrete-Frequency Fourier Transform (IDFT) conventionally as

$$w_K(n) = \frac{1}{K}\sum_{k=0}^{K-1} W_K(k) e^{j2\pi\frac{n}{K}k} . \tag{A7}$$

This yields a sequence of $K$ time samples covering the span

$$0 \le t \le (T_a - T_\Delta), \tag{A8}$$

stepping in increments of $T_\Delta$. For large $K$, i.e. small $T_\Delta$, this becomes effectively a span width of $T_a$.

However, this isn't quite the span we are seeking. Rather, we are seeking $N$ time samples over the span of time

$$-T/2 \le t \le T/2 , \tag{A9}$$

but still stepping in increments of $T_\Delta$.

This suggests that we wish to modify the IDFT to the following function

$$w_K(n) = \frac{1}{K}\sum_{k=0}^{K-1} W_K(k) e^{j2\pi\frac{\left(n-\frac{N-1}{2}\right)}{K}k} , \tag{A10}$$

which we may rewrite as

$$w_K(n) = \frac{1}{K}\sum_{k=0}^{K-1}\left[ W_K(k) e^{-j\pi\frac{(N-1)}{K}k} \right] e^{j2\pi\frac{n}{K}k} . \tag{A11}$$

This says that we must pre-multiply the window spectrum with a complex modulation before employing a standard conventional IDFT. Once accomplished, we may extract the $N$-length window taper function as the first $N$ samples of $w_K(n)$, namely

$$w_N(n) = w_K(n), \quad \text{for } 0 \le n \le N-1 . \tag{A12}$$

Note that this only contains the explicit sampled $t = 0$ term for odd values of $N$. Nevertheless, in the manner given, $w_N(n)$ may be calculated for all values of $N$, odd or even.

# References


[1] Emanuel Parzen, "On choosing an estimate of the spectral density function of a stationary time series," *The Annals of Mathematical Statistics*, Vol. 28, No. 4, pp. 921-932, 1957.

[2] M. S. Bartlett, "On the theoretical specification and sampling properties of auto- correlated time series," *Supplement to the Journal of the Royal Statistical Society*, Vol. 8, No. 1, pp. 27-41, 1946.

[3] Fredric J. Harris, Windows, *Harmonic Analysis, and the Discrete Fourier Transform,* Report NUC-TP-532, Undersea Surveillance Department, Naval Undersea Center, San Diego, CA, September 1976.

[4] Fredric J. Harris, "On the Use of Windows for Harmonic Analysis with the Discrete Fourier Transform," *Proceedings of the IEEE*, Vol. 66, No. 1, pp. 51-83, January 1978.

[5] K. M. M. Prabhu, *Window Functions and Their Applications in Signal Processing*, ISBN-13: 978-9814463089, CRC Press, Taylor & Francis Group LLC, 2014.

[6] Eric Anterrieu, Philippe Waldteufel, and André Lannes, "Apodization Functions for 2-D Hexagonally Sampled Synthetic Aperture Imaging Radiometers," *IEEE Transactions on Geoscience and Remote Sensing*, Vol. 40, No. 12, pp. 2531-2542, December 2002.

[7] R. B. Blackman, John Wilder Tukey. "The measurement of power spectra from the point of view of communications engineering—part I." *Bell System Technical Journal*, Vol. 37.1, pp. 185-282, 1958.

[8] R. B. Blackman, John Wilder Tukey, "The measurement of power spectra from the point of view of communications engineering—Part II." *Bell System Technical Journal*, Vol. 37.2, pp. 485-569, 1958.

[9] R. B. Blackman, J. W. Tukey, *The Measurement of Power Spectra from the Point of View of Communication Engineering*, Dover Publications, Inc., 1958.

[10] R. B. Blackman, *Linear Data-Smoothing and Prediction in Theory and Practice*, Addison Wesley Publishing Company, Inc., 1965.

[11] Alan V. Oppenheim, Ronald W. Schafer, *Digital Signal Processing*, ISBN 0-13-214635-5, Prentice-Hall, 1975.

[12] M. S. Bartlett, "Periodogram Analysis and Continuous Spectra," *Biometrika*, Vol. 37, pp. 1-16, 1950.

[13] Emanual Parzen, "Mathematical Considerations in the Estimation of Spectra," *Technometrics*, Vol. 3, No. 2, pp. 167-190, May 1961.

[14] Peter D. Welch, "The use of fast Fourier transform for the estimation of power spectra: A method based on time averaging over short, modified periodograms," *IEEE Transactions on Audio and Electroacoustics,* Vol. 15, No. 2, pp. 70-73, June 1967.

[15] Emanuel Parzen, "On Consistent Estimates of the Spectrum of a Stationary Time Series," *The Annals of Mathematical Statistics*, Vol. 28, No. 2, pp. 329–348, 1957.

[16] Puneet Singla, Tarunraj Singh, "Desired order continuous polynomial time window functions for harmonic analysis," *IEEE Transactions on Instrumentation and Measurement*, Vol. 59, No. 9, pp. 2475-2481, September 2010.

[17] N. K. Bary, *A Treatise on Trigonometric Series, Vol. I*, translated by Margaret F. Mullins, Pergamon Press, The Macmillan Company, 1964.

[18] N. I. Achieser, *Theory of Approximation*, translated by Charles J. Hyman, Frederick Ungar Publishing, Co., 1956.

[19] John G. Proakis, Dimitris G. Manolakis, *Digital Signal Processing – Principles, Algorithms, and Applications - fourth edition*, ISBN-13: 978-0131873742, Pearson, 2006.

[20] J. W. Tukey, R. W. Hamming, *Measuring Noise Color I*, Memorandum for File, MM-49-110-119, Bell Telephone Laboratories, December 1, 1949.

[21] R. J. Webster, "A generalized hamming window," *IEEE Transactions on Acoustics, Speech, and Signal Processing*, Vol. 26, No. 3, pp. 269-270, 1978.

[22] Charles Cook, Marvin Bernfeld, *Radar Signals an Introduction to Theory & Application*, ISBN-13: 978-0121867508, Academic Press, 1967.

[23] Harald Bohman, "Approximate Fourier analysis of distribution functions," *Arkiv Foer Matematik*, Vol. 4, Issue 2, pp. 99-157, April 1961.

[24] Athanasios Papoulis, "Minimum-bias windows for high-resolution spectral estimates," *IEEE Transactions on Information Theory*, Vol. 19, No. 1, pp. 9-12, January 1973.

[25] C. Bingham, M. Godfrey, J. Tukey, "Modern techniques of power spectrum estimation," *IEEE Transactions on Audio and Electroacoustics*, Vol. 15, No. 2, pp. 56-66, June 1967.

[26] D. C. Rife, G. A. Vincent, "Use of the Discrete Fourier Transform in the Measurement of Frequencies and Levels of Tones," *Bell System Technical Journal*, Vol. 49, pp. 197–228, 1970.

[27] Gregorio Andria, Mario Savino, Amerigo Trotta, "Windows and interpolation algorithms to improve electrical measurement accuracy," *IEEE Transactions on Instrumentation and Measurement*, Vol. 38, No. 4, pp. 856-863, 1989.

[28] Albert H. Nuttall, "Some Windows with Very Good Sidelobe Behavior," *IEEE Transactions on Acoustics, Speech, and Signal Processing*, Vol. ASSP-29, pp. 84–91, February 1981.

[29] M. Mottaghi-Kashtiban, M. G. Shayesteh. "New efficient window function, replacement for the Hamming window," *IET Signal Processing*, Vol. 5, No. 5, pp. 499-505, 2011.

[30] C. L. Dolph, "A Current Distribution for Broadside Arrays Which Optimizes the Relationship between Beam Width and Side-Lobe Level," in *Proceedings of the IRE*, vol. 34, no. 6, pp. 335-348, June 1946.

[31] Albert H. Nuttall, "Generation of Dolph-Chebyshev Weights via a Fast Fourier Transform," *Proceedings of the IEEE*, October 1974.

[32] T. T. Taylor, "Design of line-source antennas for narrow beamwidth and low side lobes," *Transactions of the IRE Professional Group on Antennas and Propagation*, Vol. 3, No. 1, pp. 16-28, Jan. 1955.

[33] Walter G. Carrara, Ron S. Goodman, Ronald M. Majewski, *Spotlight Synthetic Aperture Radar Signal Processing Algorithms*, ISBN 0-89006-728-7, Artech House, Inc., 1995.

[34] Armin W. Doerry, *Synthetic Aperture Radar Processing with Tiered Subapertures*, Ph.D. Dissertation, University of New Mexico, Albuquerque, New Mexico, May, 1995.

[35] D. Slepian and H. Pollak, "Prolate-spheroidal wave functions, Fourier analysis and uncertainty-I," *Bell System Technical Journal*, Vol. 40, pp. 43-64, Jan. 1961.

[36] H. Landau and H. Pollak, "Prolate-spheroidal wave functions, Fourier analysis and uncertainty-II," *Bell System Technical Journal*, Vol. 40, pp. 65-84, Jan. 1961.

[37] Fred M. Dickey, Louis A. Romero, Armin W. Doerry, "Window functions for imaging radar: a maximum energy approach to contiguous and notched spectrums," *Optical Engineering*, Vol. 42, No. 7, pp 2113-2128, July 2003.

[38] Franklin F. Kuo, James F. Kaiser, *System Analysis by Digital Computer*, John Wiley & Sons, Inc., 1966.

[39] Kemel Avci, Arif Nacaroglu, "Cosh window family and its application to FIR filter design," *International Journal of Electronic Communication (AEÜ)*, Vol. 63, pp. 907-916, 2009.

[40] Kemel Avci, Arif Nacaroglu, "Modification of Cosh Window Family," *Proceedings of the 2008 3rd International Conference on Information and Communication Technologies: From Theory to Applications*, pp. 1-5, Damascus, 2008.

[41] Maurizio Migliaccio, Ferdinando Nunziata, Felice Bruno, Francesco Casu, "Knab sampling window for InSAR data interpolation," *IEEE Geoscience and Remote Sensing Letters*, Vol 4, No. 3, pp. 397-400, 2007.

[42] John Knab, "The sampling window (Corresp.)," *IEEE Transactions on Information Theory*, Vol. 29, No. 1, pp. 157-159, 1983.

[43] K. Avci, A. Nacaroglu, "A new window based on exponential function," *2008 Ph.D. Research in Microelectronics and Electronics,* pp. 69-72, 2008.

[44] John Knab, "Interpolation of band-limited functions using the approximate prolate series (Corresp.)," *IEEE Transactions on Information Theory*, Vol. 25, No. 6, pp. 717-720, 1979.

[45] Victor Barcilon, Gabor C. Temes, "Optimum Impulse Response and the van der Maas Function," *IEEE Transactions on Circuit Theory*, Vol. CT-19, No. 4, pp. 336-342, July 1972.

[46] Andrew G. Deczky, "Unispherical windows." *Proceedings of the 2001 IEEE International Symposium on Circuits and Systems - ISCAS 2001*, Vol. 2, pp. 85-88, 2001.

[47] Stuart W. A. Bergen, Andreas Antoniou. "Design of ultraspherical window functions with prescribed spectral characteristics." *EURASIP Journal on Applied Signal Processing*, pp.2053-2065, 2004.

[48] Tapio Saramäki, "A class of window functions with nearly minimum sidelobe energy for designing FIR filters," *Proceedings of the IEEE International Symposium on Circuits and Systems*, pp. 359-362, 8 May 1989

[49] Marek Jascula, "New windows family based on modified Legendre polynomials", *Proceedings of the 19th IEEE Instrumentation and Measurement Technology Conference - IMTC/2002*, Vol. 1, pp. 553-556, 2002.

[50] K. M. M. Prabhu, K. Bhoopathy Bagan, "Variable parameter window families for digital spectral analysis," *IEEE Transactions on Acoustics, Speech, and Signal Processing*, Vol. 37, No. 6, pp. 946-949, 1989.

[51] Mahrokh G. Shayesteh, Mahdi Mottaghi-Kashtiban, "FIR filter design using a new window function," *Proceedings of the IEEE 16th International Conference on Digital Signal Processing*, pp. 1-6, July 2009.

[52] Fielder, Louis D., Marina Bosi, Grant Davidson, Mark Davis, Craig Todd, and Steve Vernon. "AC-2 and AC-3: Low-complexity transform-based audio coding." In *Audio Engineering Society Conference: Collected Papers on Digital Audio Bit-Rate Reduction*. Audio Engineering Society, pp. 54–72, 1996.

[53] Christian R. Helmrich, "On the Use of Sums of Sines in the Design of Signal Windows," *Proc. of the 13th Int. Conference on Digital Audio Effects (DAFx-10)*, Vol. 10, Graz, Austria, September 6-10, 2010.

[54] V. Arun Raj, M. Davidson Kamala Dhas, D. Gnanadurai, "An overview of MDCT for Time Domain Aliasing Cancellation," *Proceedings of the 2014 International Conference on Communication and Network Technologies (ICCNT)*, pp. 203-207, 2014.

[55] Gabriele D'Antona, A. Ferrero, *Digital Signal Processing for Measurement Systems – Theory and Applications*, ISBN-13: 978-0387-24966-7, Springer Science+Business Media, Inc., New York, 2006.

[56] Svend Gade, Henrik Herlufsen, "Use of Weighting Functions in DFT/FFT Analysis (Part I)," *Windows to FFT Analysis (Part I)*, Brüel & Kjær Technical Review, No. 3, 1987.

[57] H. C. Stankwitz, R. J. Dallaire, J. R. Fienup, "Nonlinear Apodization for Sidelobe Control in SAR Imagery," *IEEE Transactions on Aerospace and Electronic Systems*, Vol. 31, No. 1, pp. 267-279, Jan. 1995.

[58] Armin W. Doerry, *A Model for Forming Airborne Synthetic Aperture Radar Images of Underground Targets*, Sandia National Laboratories Report SAND94-0139, Unlimited Release, January 1994.

[59] Edward T. Bayliss, "Design of monopulse antenna difference patterns with low sidelobes," *Bell System Technical Journal*, Vol. 47, No. 5, pp. 623-650, 1968.

[60] Armin W. Doerry, *Window Taper Functions for Subaperture Processing*, Sandia National Laboratories Report SAND2013-10619, Unlimited Release, December 2013.

[61] Armin W. Doerry, Douglas L. Bickel, *Phase Centers of Subapertures in a Tapered Aperture Array*, Sandia National Laboratories Report SAND2015-9566, Unlimited Release, October 2015.

[62] Armin W. Doerry, *Simple Array Beam-Shaping Using Phase-Only Adjustments*, Sandia National Laboratories Report SAND2015-5538, Unlimited Release, July 2015.

[63] Armin W. Doerry, *Generating Nonlinear FM Chirp Waveforms for Radar*, Sandia National Laboratories Report SAND2006-5856, Unlimited Release, September 2006.

[64] Armin W. Doerry, *Anatomy of a SAR Impulse Response*, Sandia National Laboratories Report SAND2007-5042, Unlimited Release, August 2007,

[65] Fred M. Dickey (ed.), *Laser Beam Shaping – Theory and Techniques*, ISBN-13: 978-1-4665-6101-4 (eBook - PDF), CRC Press - Taylor & Francis Group, 2014.

[66] Armin W. Doerry, John M. Andrews, *Frequency-Dependent Blanking with Digital Linear Chirp Waveform Synthesis*, Sandia National Laboratories Report SAND2014-15907, Unlimited Release, July 2014.

[67] F. M. Dickey, L. A. Romero, J. M. DeLaurentis, A. W. Doerry, "Superresolution, Degrees of Freedom and Synthetic Aperture Radar," *IEE Proc.-Radar Sonar Navig.*, Vol. 150, No. 6, pp 419-429, December 2003.

*“The world is still a weird place, despite my efforts to make clear and perfect sense of it.”*
*-- Hunter S. Thompson*

# Distribution

Unlimited Release

| | | | | |
|---|---|---|---|---|
| 1 | MS 0519 | M. R. Lewis | 5349 | |
| 1 | MS 0519 | A. W. Doerry | 5349 | |
| 1 | MS 0519 | L. Klein | 5349 | |
| 1 | MS 0532 | S. P. Castillo | 5340 | |
| 1 | MS 0899 | Technical Library | 9536 | (electronic copy) |

Sandia National Laboratories